DEVELOPMENT OF A PILOT SCALE BLACK LIQUOR GASIFIER

By

VERNON ALASTAIR AVIDI

Submitted in fulfilment of the academic requirements for the degree Master of Science in Chemical Engineering to the School of Chemical Engineering, University of Kwa-Zulu Natal, Durban, South Africa.

March 2005

Supervised by Professor Dave Arnold

PREFACE

The research work presented in this thesis was undertaken at the former University of Natal, Durban, South Africa from March 2000 to March 2002. The work was supervised by Professor Dave Arnold and co-supervised by John Hunt and Tony Leske.

This thesis is submitted as a full requirement for the degree of Master of Science in Chemical Engineering to the University of Kwa-Zulu Natal, Durban. All work presented in this thesis is original unless otherwise stated and has not been submitted in part or whole to any other university as part of a degree.

V.A. Avidi

March 2005

Date

ACKNOWLEDGMENTS

I would like to thank God for granting me the ability, endurance and patience to conduct this study. I would also like to acknowledge the following people for their invaluable assistance and contribution to this work:

- My supervisor Professor Dave Arnold and co-supervisors John Hunt and Tony Leske for their guidance and knowledge imparted to the project.
- Nelson Naidoo for his assistance with the software programming of the temperature logging program.
- The technical staff at the university, Kelly Robertson, Ken Jack, Dhavaraj Naidoo for their workmanship and patience during the procurement and construction phase of the pilot unit.
- Jon Buzzard for his assistance in leading the hazop study and general advice and coaching during the design stage.
- SAPPI for their financial support throughout the project.
- The engineers at SAPPI, Chris Davies, Clinton Clarence, Stephen Trickett and Rob Lax.
- Ron Thring from the University of Northern British Columbia for his role in the planning of the experimental program.
- Dr. Momtaz N. Mansour and Lee Rockvam from ThermoChem, Inc. for their input during the designing of the reactor.
- Ein from Natal Burner Services for his invaluable assistance with the operation and repairs of the gas burner.
- Afrox for the sponsorship of the LPG installation
- B.D. Ravno for the use of the school's bench scale fluidization test rig during the design of the bubble caps and allowing modifications to be made to the equipment.
- Professor B.K. Loveday for the use of the school's milling equipment for the preparation of the charcoal bed.
- Prathisha Devnarain for her assistance, encouragement and support during the project and with the compilation of this thesis.

ABSTRACT

The use of black liquor gasification as an alternative to conventional chemical and energy recovery systems for spent liquors is an area of particular interest to the pulp and paper industry.

The motivation to explore this technology is to improve the thermal efficiency of the recovery process by utilizing the energy content of the spent black liquor more effectively and provide chemical recovery for sodium and sulphur containing liquors for a local pulp and paper mill.

A study of the available gasification technologies showed that the steam reforming process marketed by ThermoChem Recovery International is particularly suited to the mill in that it can handle a change to a sulphite pulping chemistry and also handle silica removal which is an inherent problem with the bagasse raw material that the mill uses. However the technology required further development and confirmation of process suitability before implementation at the mill.

This aim of this project was to build and operate a gasifier based on the TRI concept to determine if this process is suitable for recovery of SASAQ black liquor from bagasse pulping. This included gaining an understanding of the process variables like the black liquor solids composition and the non-process element levels and required carrying out a mass balance on inorganic components across the reactor as well. The focus of this investigation was primarily on the front end of the project and entailed basic and detailed design of a pilot gasification unit.

The pilot unit was subsequently constructed, commissioned and operated to prove the unit met the design intent. Preliminary results showing the conceptual proof of the technology are presented as well as performance tests showing the unit capability of gasifying a 3.1 l/hr 60% solid content black liquor feed. Problematic areas that could influence the design of a scale-up unit were identified and highlighted for further development, with proposed solutions.

TABLE OF CONTENTS

LIST OF FIGURES

LIST OF TABLES

NOMENCLATURE

Unless otherwise stated specifically in the text, units shown below are to be used.

Symbol	Description	Units
A_r	Riser cross sectional area	m^2
C_d	Orifice discharge coefficient	-
C_{dr}	Drag co-efficient of the particle	-
C_{pg}	Specific heat capacity of the gas	kJ/kg°C
C_{ps}	Specific heat capacity of the solids	kJ/kg°C
$C_{p.i}$	Specific heat capacity of i	kJ/kg°C
D	Bed diameter	m
D_i	Reactor internal diameter	m
D_o	Reactor external diameter	m
ΔH	Heat of reaction	kJ/mol
ΔH_{H_2O}	Latent heat of vaporization of water.	kJ/kg
ΔH_{rxn}	Average heat of the gasification reactions.	kJ/kgBLS
d_i	Mean particle diameter in the size range	m
d_{or}	Orifice diameter	m
$d_{or,eq}$	Diameter of a hole having the same area as the total number of orifices in the tuyere	m
d_p	Particle diameter	m
d_{sv}	Diameter of a sphere having the same surface area to volume ratio of the particle. i.e. $d_{sv} = d_p \times \phi_s$	m
d_t	Vessel or tube diameter	m
d_{ti}	Outer diameter of the horizontal immersed tube in the fluidised bed	m
f_{or}	Fraction of the total area of the distributor open to gas flow	-
g	Gravitational acceleration	m/s^2
H	Fluidized bed height	m

Symbol	Description	Units
h_p	Gas to particle heat transfer coefficient	$kW/m^2°C$
h_w	Heat transfer coefficient between the bed and wall surface	$kW/m^2°C$
K	Friction loss co-efficient	-
K''	Kozeny constant dependant on porosity and particle shape	-
K	Friction loss coefficent	-
K_d	Distributor flow factor	-
k_g	Thermal conductivity of the gas	kW/m°C
L	Bed depth	m
m_{BLS}	Mass of black liquor solids	kg
m	Mass flowrate	kg
m_{H_2O}	Mass of water	kg
Mr	Molar mass	g/mol
N	Number of tuyeres required per unit cross sectional area	-
N_t	Total number of tuyeres	-
Nu_p	Nusselt number for gas to particle heat transfer	-
q	Heat required	kW
Q	Volumetric flow rate	m^3/s
Q_{latent}	Latent heat to vaporize the water contained in the black liquor.	kJ
Q_{mf}	Steam volumetric flow rate at u_{mf}	m^3/s
Q_o	Steam volumetric flow rate at u_o	m^3/s
Q_{rxn}	Energy required for the gasification reactions.	kJ
$Q_{sensible}$	Energy required getting the black liquor from supply temperature to the boiling temperature.	kJ
Q_{total}	Total energy required to gasify the black liquor.	kJ
Re_{mf}	Reynolds number at u_{mf}	-
Re_o	Reynolds number at u_o	-
Re_{or}	Reynolds number at u_{or}	-
S	Cross sectional area of reactor or tube	m
T	Final temperature	°C
T_o	Initial temperature	°C
t	Distributor plate thickness	m
u	Fluid velocity	m/s
u_c	Superficial or "*empty tube*" gas velocity	m/s
u_{mb}	Minimum bubbling velocity	m/s

Symbol	Description	Units
u_{mf}	minimum fluidising velocity	m/s
u_o	Terminal falling velocity	m/s
u_{or}	Gas velocity through the orifice	m/s
u_r	Gas velocity in the riser	m/s
u_w	Superficial gas velocity in the windbox or plenum chamber	m/s
x_i	Mass percentage of particles in a certain size range	-
ΔP	Pressure gradient or pressure drop	Pa
ΔP_b	Pressure drop across the bed of solids	kPa
ΔP_d	Pressure drop across the distributor	kPa
ΔP_{max}	Maximum pressure drop across the bed	Pa
ΔT	Difference in temperature between the black liquor reactor entrance temperature and the boiling point	°C
ΔT_{LM}	Log mean temperature difference	°C
ε	Bed voidage	-
ε_m	Fixed bed stagnant voidage	-
ε_{mf}	Voidage of the bed at minimum fluidizing velocity	-
ϕ_s	Sphericity- the ratio of the surface area of a sphere to that of the particle of the same volume	-
μ	Fluid viscosity	Pa.s
ρ	Fluid density	kg/m^3
ρ_s	Density of the solid bed material	kg/m^3
ρ_w	Gas density in the wind box or plenum chamber	kg/m^3

GLOSSARY

Abbreviation	Description
BL	Black liquor
BLG	Black liquor gasification
BLGCC	Black liquor gasifiers in a combined cycle
BLS	Black liquor solids
DS	Dissolved solids
GC	Gas chromatograph
HHV	Higher heating value
LHV	Lower heating value
LPG	Liquid petroleum gas
MTCI	Manufacturing Technology and Conversion International Incorporated
NPE	Non process elements
NSSC	Neutral sulphite semi chemical
PFD	Process flow diagram
SASAQ	Semi alkaline sulphite anthraquinone
TDH	Transport disengaging height
TRI	ThermoChem Recovery International

CHAPTER 1

INTRODUCTION

The world today has evolved into an electronic age where most contracts, information, and even organizations exist in a cyber world that remains void of unnecessary paperwork. But even in this age, however advanced we may seem with our online banking and Internet shopping abilities, we still have the persistent need to write down the shopping list on a scrap of paper, to sign our name on a cheque, to capture an artists thoughts on a canvas, to teach our children to scribble the newly learnt letters of the alphabet on a piece of paper or to conclude of a multi billion dollar deal with the signing of a contract printed on paper. To be able to realize all this, is the task of having to produce a product made from the natural resources of this earth through a process that is technically possible, minimizes detrimental effects to the environment, and is economically feasible.

The Groundwood Process was the first process whereby wood fibres were used on a large scale for the manufacture of paper [www.cartonboard.com.au]. Like most mechanical processes it produced a pulp of low strength properties and premature discoloration of products.

The first chemical as opposed to mechanical process to be developed was the Soda Process (1854) [www.cartonboard.com.au] whereby wood chips and other raw materials like bagasse or bamboo were treated with caustic soda (NaOH) to yield a strong pulp which could be chemically bleached for production of white writing papers.

Chemical pulping was developed over the years to yield several variations of the technology and today the Kraft or sulphate process, is by far the most predominant pulping process used in the world [Consonni et al, 1997]. It was developed in 1884 from the Soda Process when sodium sulphate was added to the waste liquor prior to combustion as a makeup source of sodium. The

result was cooking liquor that contained sodium sulphide which markedly accelerated delignification and produced the strongest pulp used in papermaking.

As opposed to the alkaline sulphate Kraft process, the sulphite pulping process which was first industrialized in 1866 is based on an acid cooking liquor process. It produces a pulp that can be easily bleached with hydrogen peroxide and fills the demand for chlorine free products and is best suited for specialty pulps.

Several variations of the sulphite pulping processes exist today, Acid Sulphite pulping, Neutral Sulphite Semi Chemical (NSSC) Pulping and Semi Alkaline Sulphite Anthraquinone (SASAQ) Pulping to name a few.

Sulphite pulping in the alkaline field was not investigated till the late 1960's and semi alkaline sulphite pulping is a more recent development [Richard *et al*, 1998]. The SASAQ pulping method is more selective than the Kraft process and removes more lignin and less cellulose for both softwoods and hardwoods. The SASAQ pulp therefore has a greater yield than the Kraft pulp for the same lignin content [Howard, 1996].

With all of the chemical pulping processes, wood material (lignin) is chemically removed and hence the yield is lower than the mechanical processes. Consequently the cost of pulping is higher than the mechanical processes. In addition a waste material is generated which must be treated or recovered. As such it is fundamental to the economic success of any chemical process that the inorganic chemicals are recovered from the spent liquor, termed 'black liquor'. Unless such inorganic chemicals are regenerated without considerable loss, the cost of the operation will increase proportionally to the makeup chemicals.

Although chemicals were recovered from the beginning, the modern soda furnace was not introduced until the 1930's [www.cartonboard.com.au]. The recovery boiler is an important part of the chemical pulping process. It is not only used for the recovery and regeneration of the cooking chemicals but at the same time it also uses the substantial amount of heat liberated during the combustion of the organic matter in the black liquor to produce steam. Excess steam is expanded in a turbine for power generation. It is one of the most expensive units in the pulping process but is also responsible for making the plant almost self sufficient in terms of the primary energy supply.

Black liquor of between 50-75% solids content is sprayed into the recovery boiler. Combustion air is blown into the furnace and during combustion the water in the liquor is evaporated and the

organic matter burns. The inorganic chemicals react and form a bed at the bottom of the furnace where further reactions occur and result in the formation of a smelt. The smelt is then discharged and dissolved in water to form a weak wash known as 'green liquor'. The green liquor is further treated in a causticising plant to reconstitute the cooking chemicals used in the pulping process.

Improvements in technology will allow mills to operate more efficiently and with less impact on the environment. Gasification of black liquor is one promising alternative for recovery systems. The rate of the development of the technology is such that the gasification option is more likely to be chosen as time goes on [Cantrell, 2001; Grace, 1996; Frederick, 1999].

In black liquor gasification (BLG) the carbon in the black liquor is converted to a hydrogen rich gas stream by reaction with water vapour and carbon dioxide by the water-gas shift reactions:

$$C(s) + H_2O(g) + heat \rightarrow CO(g) + H_2(g) \qquad [\Delta H = +121.42 \text{ kJ/mol}] \qquad \textbf{(1.1)}$$

$$CO(g) + H_2O(g) \Leftrightarrow CO_2(g) + H_2(g) + heat \qquad [\Delta H = -41.84 \text{ kJ/mol in the} \rightarrow \text{direction}] \textbf{(1.2)}$$

$$C(s) + CO_2(g) + heat \rightarrow 2CO(g) \qquad [\Delta H = +163.29 \text{ kJ/mol}] \qquad \textbf{(1.3)}$$

The gases can then be burned in a gas turbine. It is shown in the literature [Larson; Kreutz *et al*, 1998; Larson *et al*, 2000; Berglin *et al*, 1996; Kreutz *et al*, 1998; Comsonni *et al*, 1997] that the generated power can be up to twice that of a conventional plant with an electrical efficiency of 30% and a total efficiency of 77% based on higher heating values.

Apart from the energy benefits of BLG, several other advantages exist including [Finchem, 1995; Larson *et al*, 1997;]:

- Less complicated process unit – less expensive equipment
- Flexibility of chemical recovery system – smelt or solid phase processes
- Eliminated smelt water explosion risk due to no need for internal cooling coils
- Modular expansion is possible making production increases easier
- Flexibility of power and heat generation – gas can be used in an advanced gas turbine cycle or a simple gas fired boiler

- Reduced emissions – with fuel gas cleaning after the gasifier the flue gas rate is much smaller than the corresponding flue gases in a conventional recovery boiler.

BLG can be broadly classified into two types according to the operating temperatures, or by the physical state of the inorganic components leaving the reactor. High temperature gasifiers operate at about 1000°C and produce a molten smelt whilst low temperature gasifiers operate below 700°C to ensure that the inorganics leave as dry solids.

This work investigated the application of the low temperature gasification technology to a local pulp and paper manufacturer as an alternative to their existing Copeland bubbling fluidised bed combustion of the black liquor. The technology replacement was aligned with the long term view of replacing their aging chemical recovery furnace. At the same time, the change to a newer pulping method offering substantial yield improvements was under consideration.

1.1 Sappi Stanger's operation

The Sappi mill at Stanger, S.A. produces tissue and wood-free fine paper from bagasse pulp. The mill used the Soda pulping chemistry.

The Soda pulping process at the mill produced black liquor that contains no sulphur since the cooking chemical is only caustic. The black liquor from this process is burned in the mill's Copeland recovery system which produces a sodium carbonate solid product. The dry soda ash bed material is sold as a byproduct. The mill has no chemical and energy recovery system. Caustic soda costs were a major contributor to the mills variable production costs and only a small percentage of these costs were recovered by the sale of the byproduct soda ash.

The mill also experienced shortages of bagasse supply during drought cycles. During these periods, bagasse had to be imported from mills further afield than the neighboring sugar mill and this increased the raw material cost significantly. By increasing the pulping yield, the problem of fiber shortage during the drought periods could be mitigated.

The mill was planning to change the cooking chemistry to semi-alkaline sulfite anthraquinone (SASAQ) pulping to increase the pulp yield significantly and decrease

bleaching chemical costs. This new pulping chemistry showed potential of increasing the pulp yield by as much as 25%.

With the new proposed SASAQ chemistry that the mill was investigating, it meant the introduction of sulphur into the pulping chemistry and consequently the recovery system would have had to be able to treat this new sulphur containing black liquor. With their Copeland recovery process the sulphur would be oxidized or exit the process as sulphates mixed with sodium carbonate. In order for the sulphur to be recycled to the pulping process it is required in the form of sodium sulphite (Na_2SO_3) and sodium sulphide (Na_2S), hydrogen sulphide (H_2S) or sulphur dioxide (SO_2).

It was thus necessary to investigate a new recovery system that will be able to recovery the sulphur in this reusable form if the mill was to change its pulping chemistry to SASAQ in an effort of increasing their pulp yields. Installing a new recovery system will also allow the mill an opportunity to gain the advantage of energy recovery from the spent liquor stream as well.

The mill produces 500 metric tons per day of black liquor solids.

One of the recovery systems available that would be able to produce the sulphur in the form suitable for recyling with relatively few treatment steps is the gasification of the black liquor. In this process, the sulphur can be removed in the form of H_2S gas in the syn gas produced or in a smelt containing Na_2S, Na_2SO_3 and sodium carbonate (Na_2CO_3) depending on the operating temperature of the gasification.

In the syn gas case, the gas is then burnt to form sulphur dioxide which is used in the process to reconstitute the cooking chemicals. The production of a clean syn gas also meant increased energy recovery potential by not only recovering the sensible heat of the syn gas, but also by combustion of the gas and recovery of the heat generated thereof for meeting process steam requirements.

This recovery system option required further investigation and one of the gasification systems identified as suitable was the low temperature steam reforming system by TRI. The TRI technology eliminated the formation of a smelt and the explosion risks associated thereof. This project involved further investigation into the TRI process and it's applicability to the new SASAQ black liquor by designing, building and operating a pilot plant based on the TRI technology.

A 3kg/hr black liquor solids (BLS) pilot plant was designed, built, commissioned and its operation demonstrated. The pilot plant's ability to treat 3kg/hr black liquor was verified and a pathway for further development of the pilot plant was mapped out.

The next chapter looks at the history of recovery systems and the development of black liquor gasification technologies as well as the current status of the technology as it is available today. CHAPTER 3 recaps some basic fluidized bed reactor fundamentals and theoretical principles used in the design of the reactor and sets the design basis for this work. CHAPTER 4 presents the core design and commissioning approach used for the plant. Preliminary results are presented and discussed in CHAPTER 5 with the conclusions of this research work and proposed recommendations captured in CHAPTER 6.

CHAPTER 2

BLG TECHNOLOGY DEVELOPMENT

This chapter attempts to capture the development of the gasification technologies and the current state of the technology options that are available for a mill's recovery system. In understanding these technologies, it is important to have a brief overview on the pulping process itself and understand where in a mill's process the recovery system fits in. Conventional recovery systems are discussed before the several gasification options and the energy optimization of these gasification systems are presented. A few commercially available technologies are then reviewed.

2.1. Chemical pulping processes – a brief overview

The Soda process was the first chemical process to be developed. In the Soda pulping process, the wood chips or non-wood based raw material is treated with an aqueous solution of sodium hydroxide alone. This is a simple process and is sulphur free. The process yields a strong pulp that can be chemically bleached for the production of white papers.

As discussed in the previous chapter, the Soda process was developed into newer pulping processes by the addition of sulphur to the cooking chemicals. The introduction of sulphur into the system added a new constraint to the chemical recovery system. Broadly speaking, these new chemical pulping processes using sulphur developed into primarily two main forms which can be classified as:

- Sulphate pulping – e.g. Kraft, rapid displacement heating, superbatch-Sunds
- Sulphite pulping – e.g. Acid sulphite pulping, NSSC, SASAQ

2.1.1 Kraft Pulping

The sulphate or Kraft process developed by the addition of sodium sulphate to the cooking chemicals as a make-up source of sodium for the Soda process. The result was cooking liquor that contained sodium sulphide.

In Kraft pulping, wood chips are treated with an aqueous solution of sodium hydroxide (NaOH) and sodium sulphide (Na_2S) at about 170°C.During the pulping process about 50% of the wood which is constituted of mostly cellulose and a high percentage of lignin and some carbohydrates, is dissolved in the cooking chemicals. The spent pulping liquor is termed 'black liquor' and is rich in carbon [Li and Heiningen, 1995]. A schematic of the Kraft pulping process is shown in figure 2.1 below:

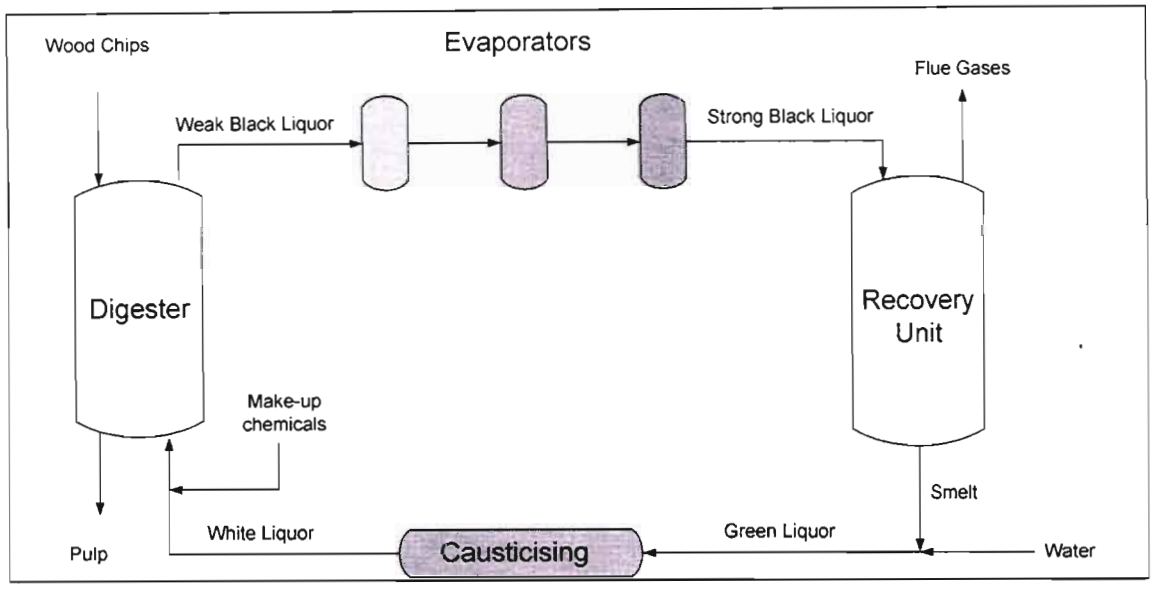

Figure 2.1: Schematic description of the Kraft pulping process

The weak black liquor has a solids content of approximately 15% by weight which is far too low for combustion. To raise the solids content in the liquor, it is evaporated in a series of evaporators to produce a resulting strong liquor of around 50-75% solids content.

Bagasse pulps produce weaker black liquor with a solids content of around 40-45%. When a Copeland recovery system is used, this figure drops even further to around 25% as the black liquor is concentrated in a venture scrubber and cyclone system to 45% before it enters the reactor. This is discussed further later in this chapter.

In the recovery unit the chemical energy of the black liquor is converted by full combustion (conventional recovery) or by partial combustion (gasification technologies) to yield an inorganic smelt and gases depending on the type of recovery technology that is used. Most of the chemicals that leave the recovery unit are fed back into the pulping process as white liquor after further treatment.

2.1.2 Sulphite Pulping

Sulphite pulping developed around the same time as the sulphate process, and was driven primarily by the low cost of its raw materials [McDonald, 1998]. It was for a long period the leading pulping process in the world due to this cost advantage.

The raw materials which were sulphur and calcium carbonate, though the calcium carbonate base could be substituted with magnesium carbonate, ammonium carbonate or sodium carbonate, was cheaply available and with the pollution laws being less stringent at that time, the mills could afford to dispose of the waste liquors into waterways due to the low toxicity and high biodegradability of sulphite liquors.

The process comprises of a sulphur dioxide (SO_2) manufacture stage, a SO_2 absorption stage, the digester and the chemical recovery stages. Figure 2.2 below is a block flow diagram of the sulphite pulping process.

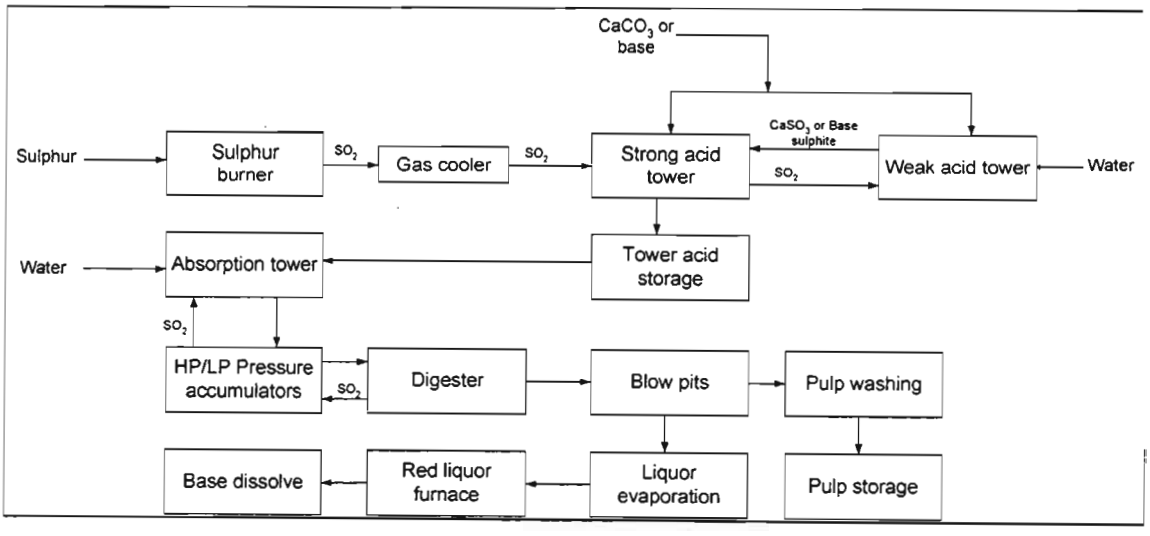

Figure 2.2: Block flow diagram of sulphite pulping process [McDonald, 1998]

SO_2 is produced by burning sulphur. SO_3 formation is prevented by controlling the air to the burning process and by cooling the product SO_2 to minimize conversion to SO_3. The SO_2 gas is absorbed into a solution of the base carbonate. Sulphurous acid is formed (H_2SO_3) which reacts with the base carbonate to form the corresponding sulphite and some quantities of bisulphate, calcium sulphite ($CaSO_3$) and calcium bisulphate ($CaHSO_3$) in the case of calcium. SO_2 gas that is released from the digesters is contacted with the sulphite solution. These reactions are shown below [McDonald,1999] with X representing either Ca, Mg, $(NH_4)_2$ or Na_2:

$$S + O_2 \rightarrow SO_2 \quad \textbf{(2.1a)}$$

$$SO_2 + H_2O \rightarrow H_2SO_3 \quad \textbf{(2.1b)}$$

$$H_2SO_3 + XCO_3 \rightarrow XSO_3 + H_2O + CO_2 \quad \textbf{(2.1c)}$$

$$H_2SO_3 + XCO_3 \rightarrow XHSO_3 + H_2O + CO_2 \quad \textbf{(2.1d)}$$

$$XSO_3 + H_2O + SO_2 \rightarrow X(HSO_3)_2 \quad \textbf{(2.1e)}$$

The acidity of the cooking chemicals is sometimes based on the solubility of the base component. In the case of calcium, this dictates a low pH of around 1-2 and a high amount of sulphurous acid is present in the cooking liquor. Modified processes using more advanced bases dictate that the medium can be maintained at neutral to alkaline conditions as well.

The cooking temperature is lower than the Kraft process at around 140-170°C and the cooking time has to be extended to compensate for the reduced reaction rates [McDonald, 1998; Braunstein, 2004]. This means larger digesters are required for the sulphite process. The digesters are operated under pressure due to the insolubility of the SO_2 at high temperatures.

The pulp is discharged into blow pits where it is washed before being sent to storage. The spent liquor, which is also known as red liquor in the case of sulphite pulping is concentrated in evaporators before being sent for chemical recovery. The pulps produced by the sulphite process, and in particular when an acidic medium is used, are weaker in strength than those of the Kraft process.

Sulphite pulping has been on a decline as the environmental legislations on mill effluents have become more stringent. This has forced the mills to move away from the

calcium based carbonates towards more advanced bases. This however raises the capital investment required for these mills and the Kraft process then becomes more attractive with the added benefit of producing a pulp with higher strength.

2.1.2.1 SASAQ Pulping

The SASAQ process is a variation of sulphite pulping that involves the addition of anthraquinone to the cooking chemicals. The process is operated under semi-alkaline conditions in the cooking chemicals. The anthraquinone aids the cooking chemicals in removing more lignin and less cellulose from the raw material and helps lower the alkali requirments. This pulping chemistry thus produces a greater yield than the Kraft process.

Anthraquinone is usually added as 0.1 – 0.15% on the fibre content of the pulp. Na_2CO_3 is also added to the chemical mix in the ratio of 0.2 - 0.25 times that of Na_2SO_3 in the cook. SASAQ pulping time is considerable longer than the Kraft process, a factor of 2-5 times longer. The increased yield of around 5% higher remains essentially intact through the process [McDonald, 1998].

SAPPI Ltd has patented a three step process that involves pre-hydrolysis, SASAQ digestion and extraction. Sodium carbonate is used as the base carbonate. Up to a 25% increase in yield was seen in laboratory SASAQ trials on bagasse pulps performed by Sappi [Richard *et al*, 1998].

By maintaining a semi-alkaline medium, the pulp strength is not compromised and shows strength properties similar to Kraft pulps [McDonald, 1998]. Non process elements which need to be removed from the process by the recovery system take the form of NaCl, K_2SO_3 and Na_2SiO_3 [Braunstein, 2004].

Several other variations of these chemical pulping processes exit today but the Kraft process is by far the dominant pulping chemistry used in the paper and pulp industry.

When sulphur is present in the cooking chemicals, the black liquor recovery process must be able to conserve or regenerate the sulphur in the sodium sulphide, sodium sulphite or H_2S form for reuse as cooking chemicals in sulphur based pulping processes.

2.2 Types of black liquor

Of interest to this study is the black liquor and it is important at this stage to consider a few properties of black liquor. Chemically black liquor from any pulping process is a mixture of several basic elements with the largest fractions being carbon, oxygen, and residue inorganic cooking chemicals. The organic solids are composed mainly of degraded lignin and polysacharides (hemicelluloses and cellulose) degradation products (aliphatic carboxylic acids), together with a minor fraction of extractives. [Gea *et al*, 2003]

A typical Kraft black liquor analysis is shown below in Table 2.1a [Berglin *et al*, 1996, 1998] and Table 2.1b shows the typical analysis from a Soda pulping process[Gea *et al*, 2003] for straw. Table 2.1c shows results of a preliminary elemental analysis for the Soda black liquor from Sappi Stanger's mill. The unclassified components of 0.45% are typically silica, potassium and chlorine. Table 2.1d shows a typical analysis of sulphite black liquor from a hardwood pulp.

The black liquor properties are also dependant on the raw material that is used in the pulping process. The general distinction is those pulping processes based on wood and those that use non-wood raw materials like bagasse, straw and bamboo. There are many advantages of non-wood based pulping [Hunt, 2001], including:

- Short growth seasons for crops – crops return profits quicker
- Use of waste material – crop residues like bagasse (sugar industry) and straw (wheat cereal grain industry)
- Low cooking and refining energy – non-wood fibres have weaker inter-fibre lignin deposits
- Low cooking and bleaching chemical requirements – lower cooking energy required

The marked distinction between black liquors from non-wood based processes and those from wood based processes is the high concentrations of non-process elements. These non-process elements like silica, potassium and chlorine enter the system with the raw materials and work their way through the pulping process eventually exiting in the black liquor. This can be seen by the higher concentrations of silica, potassium and chlorine in the soda straw liquor analysis shown in Table 2.1b when compared to the wood based black liquors of the Kraft and sulphite liquors.

Some of these non-process elements like potassium and chlorine are removed using electrostatic precipitators on the recovery boiler stacks [http://archive.greenpeace.org/toxics/reports/zerodisch.pdf]. Since the non process elements for non-wood based black liquors are higher than for wood based black liquors, the recovery system used for treating non-wood based black liquors must be able to remove these non-process elements effectively before recycling of sulphur and sodium to the cooking chemicals.

The heating value of the black liquor varies depending on the cooking yield and the carbon content of the black liquor. Generally the higher the solids content of the black liquor, the more heat can be generated in the recovery boiler due to less water to evaporate. All black liquors typically have higher heating values in the range of 13.09-14.4 MJ/kg dissolved solids [Verrill, *et al*, 1998]. Comparing this to natural gas which has a HHV of 52.2MJ/kg, one can begin to understand the potential energy available for recovery. For a global black liquor generation rate of 0.5 million tonnes per day this translates in terms of energy into 85000MW_{fuel} per day [Consonni, Larson, and Berglin, 1997].

Table 2.1a : Typical Kraft wood based black liquor analysis [Berglin *et al*, 1996, 1998]. LHV corrected for hydrogen and sulphur content

Black liquor solids component	**Mass percentage of DS**
Carbon	35.2
Hydrogen	3.4
Sodium	19.2
Potassium	2.6
Sulphur	5.4
Oxygen	34.1
MJ/kg dissolved solids	14.2 (HHV)*
MJ/kg dissolved solids	11.7 (LHV)*

* HHV – higher heating value, LHV – lower heating value

Table 2.1b : Typical liquor analysis for a Straw Soda black liquor [Gea *et al*, 2003]

Black liquor solids component	Mass percentage of DS
Carbon	39.05
Hydrogen	4.54
Sodium	8.83
Potassium	4.10
Sulphur	0.78
Oxygen	37.97
Nitrogen	1.00
Chlorine	3.50
Silica	0.23

Table 2.1c : Black liquor analysis for a Sappi Stanger Soda black liquor

Black liquor solids component	Mass percentage of DS
Carbon	37.54
Hydrogen	4.97
Sodium	16.90
Oxygen	40.14
Others	0.45

Table 2.1d : Typical liquor analysis for a Sulphite hardwood black liquor [Whitty *et al*, 1997]

Black liquor solids component	Mass percentage of DS
Carbon	33.5
Hydrogen	4.0
Sodium	13.2
Potassium	1.1
Sulphur	7.6
Oxygen	40.0
Nitrogen	0.2
Chlorine	0.4

2.3. Current technologies in use for chemical and energy recovery

The recovery processes today are primarily geared towards chemical recovery. Currently the main recovery processes in use are the conventional recovery process in a Tomlinson boiler for the sulphate process and the Lurgi and Tampella processes for the sulphite pulping process. The use of fluidized beds for combustion of the black liquor is also practiced, though this is recovery system is unsuited to sulphur based processes.

2.3.1. Conventional Kraft recovery

Today the industry burns Kraft black liquor in Tomlinson boilers that feed back pressure steam turbine cogeneration systems supplying process steam and electricity to the mills. [Larson; McDonald *et al*, 1998].

The black liquor is sprayed into the recovery boiler and is combusted in the presence of air. The sulphur and sodium in the black liquor forms sodium sulphide (Na_2S), but side reactions also result in the formations of sodium sulphate (Na_2SO_4). Typical sulphur reduction efficiencies are about 95%. The sodium in the black liquor that is not reacted with the sulphur forms sodium carbonate (Na_2CO_3). The smelt that leaves the recovery boiler contains mainly sodium sulphide (Na_2S), sodium carbonate (Na_2CO_3) and sodium sulphate (Na_2SO_4).

The hot flue gases during combustion are in the region of 1000-1200 °C. This heat is recovered in the boiler section of the recovery boiler to produce high-pressure superheated steam. Some of this heat is also used in direct contact evaporators to concentrate up the black liquor to 65%. About 60% of the higher heating value of black liquor can be transferred into high-pressure steam, 65% in the absence of a direct contact evaporator. To relate this in terms of steam production, it is between 3 to 3.3 kg steam/kg dissolved solids.

The high pressure steam is normally passed through a steam turbine to generate electricity. The energy generated is currently one of the most important sources of energy from biomass, and supplies the major share of the energy used in the production of chemical Kraft pulp. In terms if global production of energy from biomass, it is estimated to be of the order of 3000 PJ that is generated annually by the pulp industry [Berglin and Bernston, 1998]. In 1993, the total global energy production was 324 873

PJ [Energy Statistics Yearbook: 1993, http://www.ieer.org/ensec/no-1/glbnrg.html]. Globally this translates into about 1% of worldwide energy production.

The furnace section of the recovery boiler can be divided into a reducing section, a drying section and an oxidizing section [Hupa *et al*, 1987] as shown in Figure 2.3 below.

The primary air contributes only 35-45% of the total combustion air. This allows for optimal conditions in the reducing section for the reduction of sulphur:

$$Na_2SO_4 + 2C \rightarrow Na_2S + 2CO_2 \qquad \textbf{(2.2)}$$

In the drying section the black liquor drops are evaporated to 100% dryness:

$$R - Na \rightarrow Na_2CO_3 + H + C \qquad \textbf{(2.3)}$$

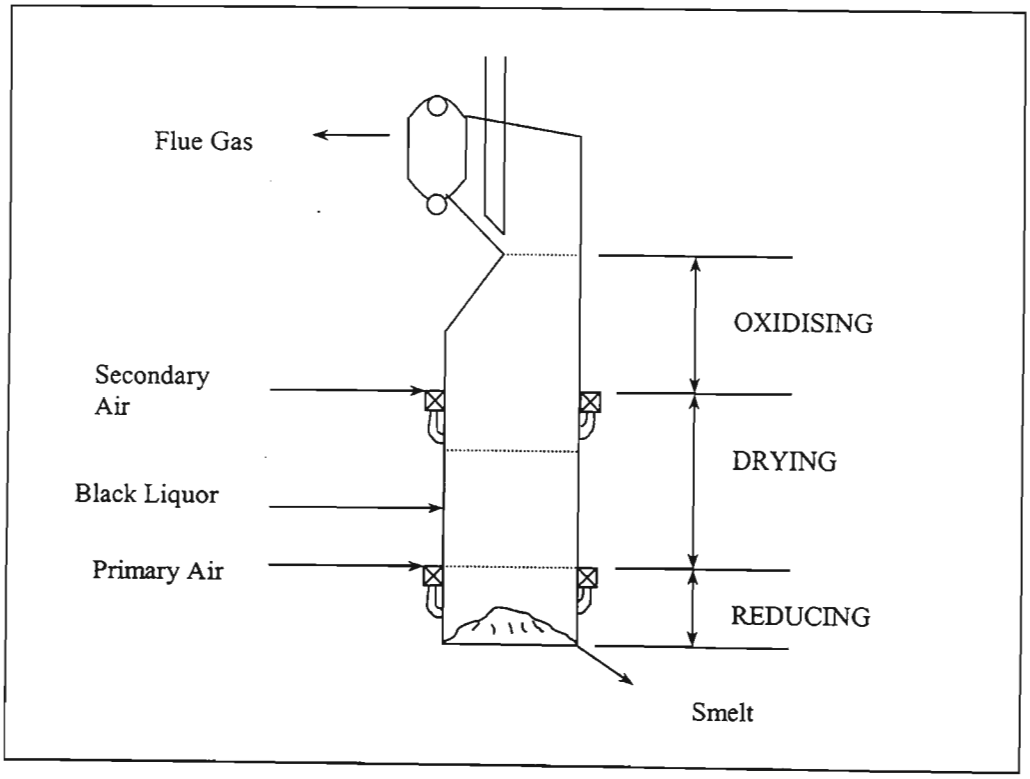

Figure 2.3: Reaction sections in recovery furnace

In the oxidising section the combustion is made as complete as possible. This requires a surplus air supply which is provided by the secondary air supply. A good distribution of the secondary air is essential to facilitate complete combustion.

$$4H + O_2 \rightarrow 2H_2O$$
$$2CO + O_2 \rightarrow 2CO_2 \quad \textbf{(2.4)}$$

Essentially all of the inorganic pulping chemicals are recovered as a smelt of sodium sulphide and sodium carbonate which is dissolved in water to form "Green Liquor". Green liquor is delivered from the recovery system to the causticizing area of the mill where it is reacted with calcium hydroxide [$Ca(OH)_2$] formed by mixing calcium oxide (CaO) with water in a causticizer. The reaction converts the sodium carbonate in the smelt to sodium hydroxide (NaOH), thereby regenerating the pulping chemical, a mix of sodium sulphide (Na_2S) and sodium hydroxide (NaOH). The calcium carbonate ($CaCO_3$) precipitates from the causticizer is heated in a lime kiln to regenerate calcium oxide (CaO).

The reactions in the furnace are in reality much more complex. The above equations are merely a simplification of these.

To understand the changes a black liquor droplet undergoes, it is necessary to examine an individual drop behavior upon entering the furnace. As early as 1963, Monaghan [1963] filmed the combustion of calcium sulphite liquor droplets and identified that the liquor burned in stages. Much later Hupa *et al* [1987] studied the burning of Kraft black liquor with a similar technique and labeled the burning stages as:

i. Drying
ii. Devolatilization or pyrolysis
iii. Char burning

These stages are illustrated in figure 2.4 below. Hupa *et al* [1987] explained the stages as follows.

Drying involves evaporation of water from the droplet and occurs within a fraction of a second. As soon as the droplet comes into contact with the hot gas, the droplet expands a slight bit. A shell is formed around the droplet that prevents boiling. The expansion is followed by the bursting of the shell and a steam enclosed bubble many times larger than the original droplet is formed.

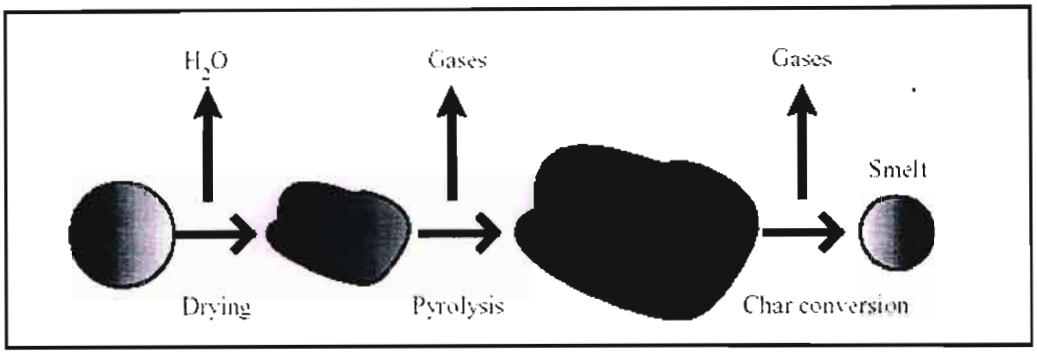

Figure 2.4: Conversion stages of a black liquor droplet [Markland (ETC), 2002]

This is when hot water and other volatile matter starts to boil and the droplet is now in the second stage of burning. During devolatilization volatile components in the liquor are released into the gas phase, as well as some inorganic material is released. When boiling is completed, the particle is solidified into a porous particle which is followed by rapid shrinkage during which the major portion of the carbon and hydrogen contained in it, volatilizes [Wessel *et al*, 1997].

The solid char or carbon that remains is combusted or gasified in the final stage, char burning. The main factors influencing the combustion are:

- combustion air supply and distribution
- black liquor physical and chemical properties
- black liquor distribution and droplet size inside the furnace

The burning stages are not isolated and overlap to varying degrees. De-volatilization begins before the particle is totally dry and char burning commences before completion of the de-volatilization stage.

Whitty *et al* [1997] studied the behaviour of fifteen black liquors over a wide range of temperatures and pressures to measure burning properties like swelling, volatiles yields, burning stage durations and black liquids solids reactivity, and offered correlations between the different burning properties.

The main advantages of the conventional Tomlinson recovery boiler are its high thermal efficiencies and chemical recoveries. The drawbacks are the high capital costs and the complicated operation. It also has the inherent potential of a smelt-water explosion.

2.3.2 Sulphite pulping recovery processes

The recovery of calcium red liquor was not done due to the low cost of the raw materials as was mentioned earlier above. When magnesium is used as the base carbonate, the magnesium liquor is concentrated in an evaporator and then combusted in a furnace to produce SO_2 with some SO_3, CO_2, CO, water vapor and magnesium oxide (MgO). These are separated from the exhaust gases and the magnesium oxide is slurried with water for re-absorption of the SO_2 gas [McDonald, 1998].

When sodium carbonate is used as the base, as is the case with Sappi Stanger's proposed SASAQ pulping process, the soda liquor is recovered in a furnace similar to the conventional Tomlinson furnace discussed above. The furnace produces a smelt with a high sulphidity which can then be treated in a few processes for reuse of the cooking chemicals.

2.3.2.1 Lurgi Process

In the Lurgi process the high sulphidity smelt, or green liquor as it is called is reacted with CO_2 from the process as follows [McDonald, 1998]:

$$Na_2CO_3 + Na_2S + 3CO_2 + 3H_2O \rightarrow 4NaHCO_3 + H_2S \qquad \textbf{(2.5)}$$

The bicarbonate ($NaHCO_3$) is thermally split to produce CO_2 for the reaction shown by equation 2.5 above and Na_2CO_3 for the cooking liquor. The H_2S from reaction 2.5 is combusted to produce SO_2 which is reused in the process and together with the Na_2CO_3 they reconstitute the cooking chemicals.

2.3.2.2 Tampella Process

In this process the green liquor is partially carbonated to produce bicarbonate and sodium hydrogen sulphide (NaHS). These products are steam stripped at low pressures to produce H_2S and Na_2CO_3 which is then treated in a similar process to the Lurgi process for reuse in the cooking chemicals. These reactions are shown below in equations 2.6a and 2.6b [McDonald, 1998]:

$$Na_2CO_3 + Na_2S + 2CO_2 + 2H_2O \rightarrow 3NaHCO_3 + NaHS \qquad \textbf{(2.6a)}$$

$$NaHS + NaHCO_3 \rightarrow H_2S + Na_2CO_3 \quad \textbf{(2.6b)}$$

2.3.2.3 Fluidised bed combustion

This process is used to treat the liquor from the pulping process but it does not allow for reuse of the chemicals for the sulphite pulping process. The liquor particles are combusted in a fluidized bed with air and the systems is kept below the melting point of the sodium carbonate. This recovery process is not suitable for recovery of sulphur containing chemicals as it produces a product that consists of both sodium carbonate and sodium sulphate. This product is usually sold and was formally used when there was a cheap source of sulphur and a market for the combined sodium carbonate and sodium sulphate product.

2.3.3. Fluidised bed reactor - recovery system suitable for non-wood based mills

For smaller agricultural or non-wood based paper and pulp mills such as straw and bagasse mills, there are three main recovery systems which are used in the industry [Sharma *et al*, 1998]:

- The roaster and smelter system
- The Conventional Tomlinson recovery boiler
- The fluidised bed reactor

With non-wood based pulp systems the silica content in the black liquor is high, and at high solids concentrations high viscosity becomes a problem. The recovery plant must be able to handle a highly viscous feed, or alternatively accept a less concentrated feed. In the latter case this would indicate that the recovery boilers for agro systems would need to be larger to be able to accommodate the same capacity of black liquor solids when compared to a wood based black liquor.

Black liquor is burnt in a roaster with the help of auxiliary fuel. The burnt ash is incinerated in a smelter and dissolved in a weak wash to give green liquor. This is then converted to white liquor in a recausticizer using lime. Although this method is simple and requires low investment costs, one of its main drawbacks is its continuous need for auxiliary fuel. It also has a low chemical recovery rate and if the fuel gases are used for

generating steam, they tend to leave deposits on the boiler tubes which are a major problem.

The Copeland fluidised bed chemical recovery process was developed in the 1960's [Marshall and Ropers, 1995] and is illustrated in figure 2.5 below. The fluidized bed reactor system accepts a much lower concentration of black liquor, 22-25% from a multiple effect evaporator and concentrates it further to 45% with the help of the hot reactor flue gases at 450°C in a venturi scrubber and cyclone system. This aspect can provide incremental throughput increases to an existing plant without requiring any additions to the evaporator capacity. Bed temperatures are maintained at approximately 710°C and the freeboard temperature at approximately 450°C.

As the solids content is low in the multiple effect evaporator, the chances of silica scale deposition in the evaporator tubes is reduced and the need for regular cleaning is reduced. Steam or air is used to atomise the black liquor as it enters the top of the fluidized bed reactor to a droplet size of between 2.4mm – 4mm [Sharma *et al*, 1998].

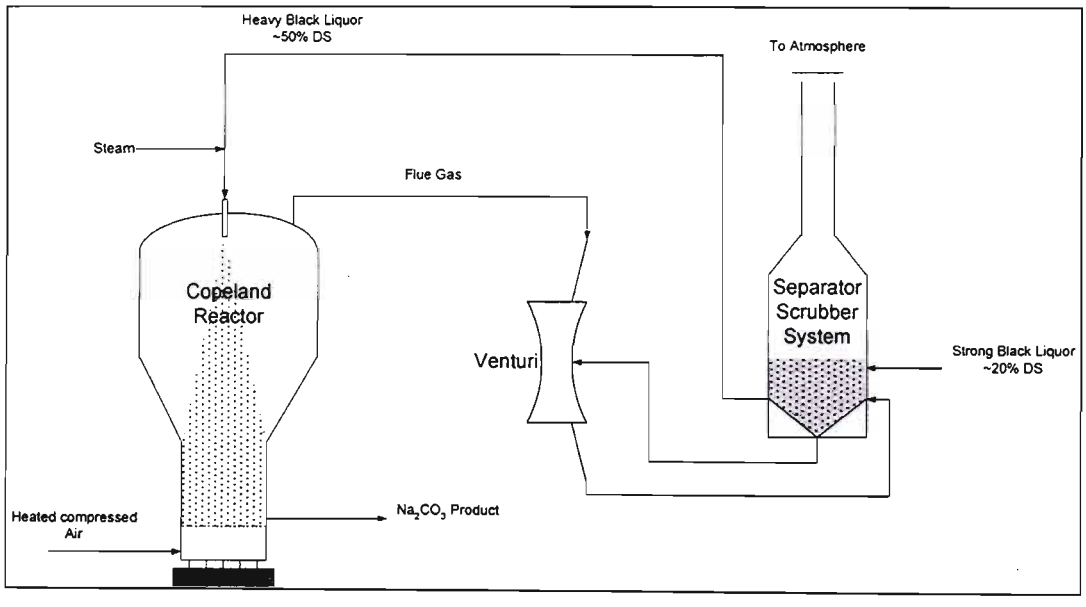

Figure 2.5 : Schematic of Copeland fluidised bed soda recovery system

The hot flue gas in the reactor freeboard heats the soda liquor and dries it to form char solids. These particles then move into the hot bed where combustion takes place. The char solids burn to form pellets of sodium carbonate and sodium sulphates and are discharged continuously from the reactor. The reactor bed is fluidized by compressed air. The fluidity of the bed ensures that the bed is completely mixed to avoid hot spots.

The particles grow larger as further combustion takes place and tend to gravitate to the bottom of the bed.

In the case of sulphur free black liquors there is no causticizer plant attached and the sodium carbonate pellets produced by the process are sold as a byproduct. However the price of the make-up caustic is considerably higher than the price obtained for the soda ash by-product.

The advantages of this system include:

- Low capital investment – only 7-8% the cost of a new recovery boiler [based on 1ktpd production – Marshall and Ropers, 1995].
- Safe operation without the hazards of smelt formation
- Can be used on all cellulosic raw materials, except those with a high chloride and potassium content. Their levels need to be brought down through wet cleaning first.
- It is not essential to install a recausticizer plant
- Easy to operate

The disadvantage of the process is that generally the process is energy inefficient due largely to the evaporation stage taking place in the venturi scrubber. This does not have the efficiency of a multiple effect evaporator. In addition, the fluidizing air absorbs a large portion of the electrical energy.

The presence of chlorides is always a negative factor for any combustion technology including the Copeland recovery. The technology can be applied to softwood, hardwood, and bagasse pulps made using a Soda, Sulphite or Kraft process. However with the latter two methods, the sulphur is oxidized and hence cannot be recycled to use as pulping chemicals directly without further treatment. The sulphur is required in the form of Na_2S or Na_2SO_3 or H_2S. As mentioned earlier, this process also produces the sulphur in the form of sulphates, but the drawback is that it is mixed with Na_2CO_3 as well and cannot be separated from the sulphates. The pulping process requires the ration of Na:S to be controlled and the Copeland recovery system is thus not an option for the Sappi Stanger mill if they wish to change to a sulphur based mill and recycle their cooking chemicals.

Being a low cost investment, this system is especially suited to the economics of a small and medium size pulp and paper mill. Generally the process is energy inefficient.

This is largely due to the evaporation stage in the venturi scrubber which does not have the energy efficiency of a multiple effect evaporator. In addition the fluidizing air absorbs a large portion of electrical energy. However it has been the most viable option for an agro based mill which is plagued with problems of solids deposition on the evaporator tubes due to the high silica content of its black liquor.

2.4 Gasification as a recovery process

Gasification of solid and liquid fuel stocks is not a new idea. It's been successfully applied since World War One [Harriz, 1999]. However its application to the pulp and paper industry is relatively new. Gasification is an alternative to the current recovery process and is under intense development because it offers potential advantages in both the chemical recovery function and to a much larger extent in the energy recovery and generation role. In addition potential environmental benefits exist when used in a combined cycle by reduced CO_2 generation. This is by offsets as a result of reduced fossil fuel usage to generate the additional electricity.

The main drivers for black liquor gasification and in particular for black liquor gasification in a combined energy recovery cycle are:

- High thermal efficiency in an integrated cycle. Currently the SAPPI mill has no heat recovery, Using gasification in an integrated cycle improves the mills thermal efficiency.
- High power yield in an integrated cycle.
- Superior environmental performance – net greenhouse gas emissions are reduced. Electricity generated from black liquor gasification in a combined cycle reduces the electricity required from the grid, and thus the greenhouse gases produced by the electricity supplier are reduced. For SAPPI, this is a positive reflection on the company's image on their environmental stance and a significant contribution to reducing their effect on the environment.
- Compatibility with biomass gasification. As with many paper mills, there exists parts of the raw materials that are unsuitable for papermaking. In the case of wood pulps, this would include parts of the tree such as bark. However this is not the case for Sappi Stanger. For SAPPI Stanger, their benefit would be that during high yield sugar cane seasons, the mill has access to excess amounts of bagasse which could be used in a gasification application.

- Flexibility in recovered chemicals composition. This is particularly relevant to SAPPI Stanger as the gasification option would allow the mill to initiate this recovery system with the current pulping chemistry, but also allow the possibility of a change in the pulping method to the SASAQ pulping and recover the sulphur based chemicals for reuse in the cooking process as well.
- Limited risk of smelt water explosions depending on the gasification technology.

As mentioned earlier in CHAPTER 1 two basic gasification processes exist:

- the smelt phase process which operates at approximately 950°C
- the solid phase process which operates at lower temperatures, 620 – 700°C.

The fluidizing medium for both processes can be either purely steam, in which case an additional source of heat is needed in the bed, or compressed air or oxygen mixed with steam. With the latter fluidizing medium the air or oxygen is added in controlled amounts to utilize the exothermic energy of combustion of a portion of the feed to provide the energy for the gasification of the rest of the feed. For the smelt process, the latter method is selected due to the higher energy requirements of the process.

The sulphur recovery systems also vary depending on the pulping chemistry [Frederick, 1999]. For instance, the standard Kraft process requires 100% sulphur recovered available as sodium sulphide to generate pulping liquors, as opposed to the SASAQ and Alkaline Sulphite Anthraquinone (ASAQ) process which requires 100% of the sulphur recovered as H_2S that can be converted to SO_2 and then sodium sulphite.

2.4.1. High temperature gasification – smelt phase process

This process is based on gasification at temperatures in the smelt formation regime. It entails partial combustion in short residence time entrained flow reactors that operate at temperatures in the region of 900 - 1000°C and pressures of 2-4 MPa [Stigsson, 1998]. Figure 2.6 below is a simplified flow diagram of the pressurized gasification process.

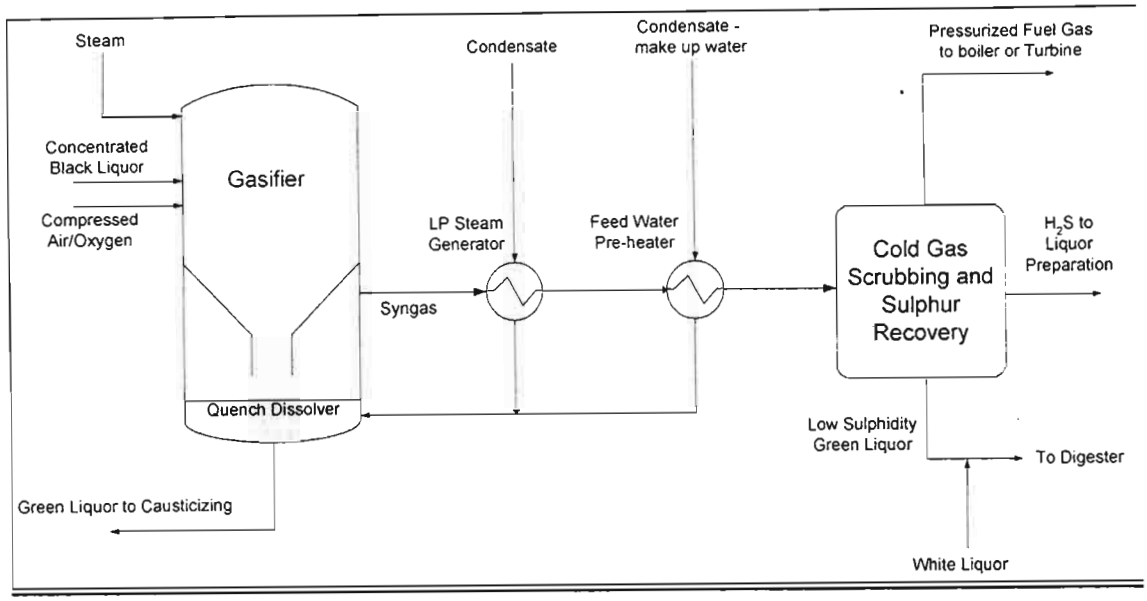

Figure 2.6: The pressurized black liquor gasification process [Näsholm and Westermark, 1997]

The oxygen or air blown black liquor gasification process features an entrained flow gasifier with refractory lining or a cooling screen to encase the partial oxidation process. Oxygen is used sometimes in place of air, permitting higher reactor temperatures to be reached, and the use of smaller-capacity equipment. The net power output is up to 12% higher for oxygen blown systems [Berglin and Berntsson, 1998].

The concentrated black liquor (60-85%) is injected into the upper part of the reactor together with the atomizing media (steam or air) and the oxidant. The black liquor is decomposed and partially oxidized to form a combustible syn-gas and an inorganic salt smelt.

The inorganic salts exit the system in the liquid phase. After the gasification the reaction mix, gas and smelt is directed into a quench cooler where it is cooled rapidly. The reduced cooking chemicals are dissolved and green liquor is produced. The green liquor is then sent to a causticizing operation and raw gas leaves the quench cooler system saturated with water vapour at a temperature of approximately 200°C. The sensible heat of the syn-gas is recovered to produce low pressure steam for use in the pulp and paper mill.

Finally the raw gas is recovered in a gas cleaning system which essentially recovers hydrogen sulphide (H_2S) from the stream and separates out the highly corrosive alkali compounds. Unlike the conventional process which produces green liquor with a fixed

sulphur composition, the gasification process has a more flexible chemical recovery system. The liquor composition ranges from sulphur saturated liquor to sulphur free liquor [Stigsson, 1994].

At the higher temperature the reaction rates are much higher; therefore the reactor can be a smaller entrained flow gasifier with a shorter residence time. Needless to say this reduces the capital cost of the gasifier unit to a certain degree. Just as in the conventional recovery boilers for the sulphate and sulphite processes, extra care is needed to facilitate the corrosive nature of the molten salt. This in itself is a challenge and both the equipment and refractory technology requires much development. There is certainly a need by the industry for an improved knowledge of refractory as it is in contact with molten sodium at 1000-1200 °C. There is a refractory that works, but requires constant replacement. The first Tomlinson unit was built in 1937 [Oscarsson, 1999] and it is still undergoing improvements and modifications after 65 yrs. Many more advances in the technology are expected to be made in the next 20 years.

2.4.2. Low temperature gasification – solid phase process

The solid phase process is based on gasification in a fluidised bed operating at or near atmospheric pressure and an operating temperature well below the smelt formation temperature. The gasifiers typically operate in the range between 600°C to 700°C. Two general processes are currently under development, the low temperature process with partial combustion of the black liquor and the steam reforming process using an indirectly heated fluidized bed.

2.4.2.1. Partial combustion low temperature process

Black liquor is partially combusted in a fluidized bed consisting of sodium carbonate (Na_2CO_3) and sodium sulphide (Na_2S) particles formed from the gasified black liquor illustrated in figure 2.7 below. The process is analogous in principle to the Copeland reactor except that the oxidation is partial and gasification is the predominant reaction mechanism whereas with the Copeland reactor the black liquor is totally combusted. In the Copeland rector pre-heated compressed air serves as the fluidizing media and for temperature control as well. The solid product is removed from the bottom of the bed whilst the gas exits overhead via a cyclone which returns fines back to the bed. The gas

leaves at the reactor temperature and is used to preheat the air to approximately 350°C in a direct contact exchanger and for high-pressure steam generation.

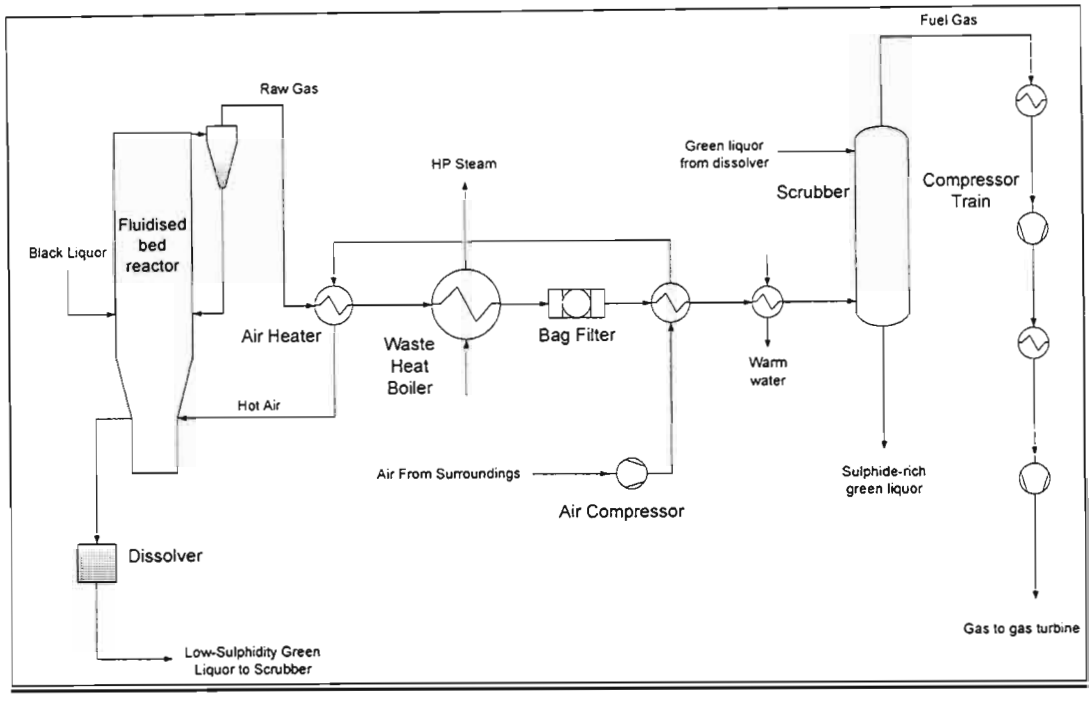

Figure 2.7: Flow sheet of the partial combustion solid phase process [Berglin, 1996]

From an energy perspective, this is an advantage of the solid phase process when compared to the thermodynamically unfavorable quenching of the gas in the smelt phase process. After the gas coolers, the gas is cleaned in a filter house to remove any additional solids carried over and then onto a hydrogen sulphide scrubber. The gas is further cooled before compression to condense most of the water.

This form of the low temperature gasification process offers several advantages over that of the high temperature process:

- Minimal alkali vaporization simplifies gas clean up train.
- Operation at lower temperature requires less consumption of black liquor heating value to drive the endothermic gasification reactions. In the high temperature gasification process this energy comes direct from the combustion of the black liquor [Grace and Timmer, 1995].
- Lower air requirement reduces product gas dilution and sensible heat losses.
- Absence of smelt formation increases metal and refractory life and eliminates the hazards associated with a smelt-water explosion.

However these advantages come at a cost of slower kinetics, which amount to longer residence times and sometimes incomplete carbon conversion and sulphur reduction. Another disadvantage is the formation of tars and higher molecular weight sulphur compounds both of which are undesirable and could result in troublesome operation of downstream equipment [Verrill *et al*, 1998]

Since the reactor doesn't operate under pressure, there is less to be gained from bleeding air from the gas turbine. Normally with black liquor gasification in an integrated combined cycle, the gas turbine and gasifier are intimately integrated in the air blown system because the gasification air is bled from the gas turbine compressor. A probable future development for the process is pressurized operation. This will reduce equipment size and cost and would then make it an advantageous for the gas turbine to supply the gasifier with bleed air [Berglin *et al*, 1996, Berglin and Berntsson, 1998].

2.4.2.2. Steam reforming in indirectly heated fluidized beds

This technology utilises indirect heating of a steam fluidised bed of sodium carbonate solids. Unlike the low temperature air or oxygen process, the heat required to achieve reactor operating temperature and for the endothermic gasification reactions is provided by an external heat source. This is usually heat exchangers immersed in the bed. Figure 2.8 below is an example of this process marketed by ThermoChem Recovery International.

Black liquor is injected directly into bubbling fluidised bed of sodium carbonate which is produced by the gasification reactions. The liquor droplets uniformly coat the bed solids resulting in high rates of heating, pyrolysis and steam reforming [Aghamohammadi *et al*, 1995]

The fluidising medium consists of steam, which also serves as a reactant for the gasification reactions. Recycled process gas is also be used to satisfy fluidisation requirements if needed. The gasifier operates in the temperature range of 580°C to 650°C which is substantially lower than the smelt formation temperature. In the absence of oxygen, steam reacts endothermically with the black liquor and char to produce a product gas rich in hydrogen. Due to the absence of combustion, the product gas is absent of the conventional products of combustion and nitrogen diluent.

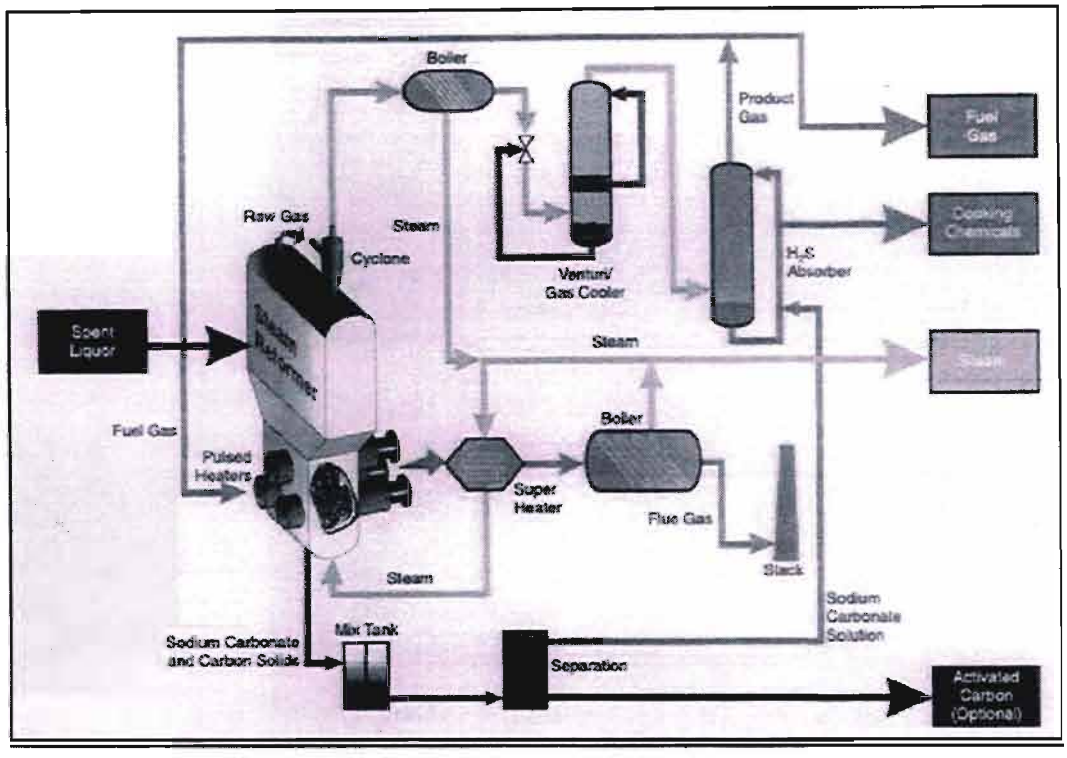

Figure 2.8 : ThermoChem Recovery International steam reformer flow diagram [http://www.tri-inc.net/TRI%20Attachment%201%20(White%20Paper).pdf]

The processes occuring in the gasifier are all endothermic, so the only location where an inorganic smelt can occur is directly on the heat exchanger surface since this is the hottest point in the reactor [Grace and Timmer, 1995]. This is a key technical issue in order to achieve acceptable gasification with minimal tar formation. The reactor temperature must be sufficiently below the bed fusion temperature to avoid fouling the heat exchanger surfaces causing bed defluidisation. This necessitates keeping the heat exchange surfaces sufficiently below the smelt formation temperature to avoid slagging on the heater surface yet still maintain a large enough temperature gradient between the exchanger surface and the bed to give acceptable transfer rates. This sometimes forces the bed temperatures of indirectly heated beds to be lower than those that are attainable with fluidised beds heated by partial combustion.

If present, the sulphur in the liquor is temporarily reduced to sodium sulphide. Sodium sulphide is unstable in the reformer environment and decomposes rapidly to form gaseous hydrogen sulphide and solid sodium carbonate [http://www.tri-inc.net/TRI%20Attachment%201%20(White%20Paper).pdf]. At these low temperatures, more than 90% of the sulphur in the black liquor is converted to hydrogen sulphide in the gas. The product gas is normaly scrubbed with a caustic solution to produce green liquor for re-use in the sulphate pulping cycle or combusted

to produce SO_2 for the sulphite process. The caustic solution is produced by dissolving sodium carbonate obtained from the fluidised bed and recausticizing it. Non-process elements like silica are removed by filtration of the caustic solution.

There is no advantage to pressurising an indirectly heated gasifier since the capacity is determined by the rate of heat transfer into the bed and this is essentially independent of the operating pressure. It's also important to note that the use of gasification as a recovery processs does not jeoperdize the production of process steam for the mill. It maintians the same 60-70% thermal recovery as steam that the conventional recovery processes exhibit [McKeough, 1993, Larson, McDonald *et al* 1998, http://www.tri-inc.net/EvolutionSR.pdf].

This process is particularly suited to Sappi Stanger's proposed SASAQ pulping chemistry as it seperates the sulphur from the alkali thus allowing a recovery of the cooking chemicals. It produces a sulohur free sodium carbonate bed which is recyled to the pulping process closing the sodium recovery loop and the sulphur is recovered as H_2S which can be combusted to produce SO_2 and recyled to the pulping process thus closing the sulphur recover loop. Soluble silicate groups (SIO_3^{2-})are reduced in the reformer to insoluble silica (SiO_2) that is removed in the filtration step after the sodium carbonate is dissolved and thus purged from the system.

2.4.3. Process comparison – high temperature vs low temperature gasification

The black liquor gasification processes can be broken down into two further sub divisions each, the gasification step itself and the gas cooling/cleaning and green liquor forming process. Grace and Timmer [1995] related the effectiveness of the different processes in terms of converting the higher heating value of the black liquor into a fuel value in the net product gas from the gasifiers for a base case set of conditions.Their results are useful for comparative purposes only due to the assumptions of their models. They compared several commercially available gasification processes using the following base conditions :

- a Kraft black liquor feed at 70% solids at 105°C
- a reduction efficiency of 90%
- a carbon conversion efficiency of 98%

- no heat losses from the gasifiers
- in all cases where heat had to be supplied by burning fuel, a portion of the gross gas production was assumed to be burned to supply the heat needed. This "parasitic" gas consumption was deducted from the gross production to give the net product gas.

Table 2.2 : Results of energy comparisons by Thomas and Timmer [1995] : Figures based on an original black liquor heating value of 14.65 MJ/kg

Process	**Gasifier Temp /°C**	**HHV in nett gas % of original**	**Reduced sulphur as hydrogen sulphide (H_2S)**
Smelt phase	954.4	55.9	50%
Partial combustion	676.7	70.4	70%
Steam reforming	648.9	49.0	99%

The results from their study are presented in table 2.2 above and it is clear the partial combustion gasifier demonstrates a far more efficient conversion of the the black liquor heating value to that of the net product gas. This is probably due to the lower gasifier operating temperatures that requires less air for partial combustion. This reduces the total amount of gas produced and hence raises the heating value per unit volume of product gas. Less gas produced also lowers the sensible heat loss and requires less gas consumption to heat the air.

Conversion efficiencies are lower in the higher temperature smelt phase gasifier and this could be explained by the fact that more air is required than partial combustion to achieve the higher reactor temperatures. An important contributing factor as well is the ability to recover additional heat from the hot gases as steam in a waste heat boiler. For instance, quenching of the gas and smelt in the green liquor, as is the case for the smelt phase process, leaves no opportunity to supply the heat for the feed air with internal process heat. This only leads to having a large amount of poor quality heat that needs to be removed from the green liquor. If the smelt phase process is pressurised, there exists the possibility of recovering some or all of the quench heat as low pressure steam since the elevated pressure would raise the boiling point of the green liquor to a point where a temperature driving force for a steam generator can be obtained.

The conversion efficiencies for the low temperature gasifiers are the lowest and this is largely due to the inefficiencies involved with indirect heating of the bed. If the process gas is used to generate this heat as was the assumption made in Thomas and Timmer's

study [1995], then it is clear that the low conversion efficiency is a direct consequence of the use of the product gas in the heat exchangers. The syngas would have to be burnt to generate a flue gas that leaves the heat exchangers at a temperature sufficiently higher than the gasifier operating temperature in order for heat transfer to occur. As a result, there is still a large amount of heat that remains in the exiting flue gases. Although this heat can be used to supply the energy in the steam used for gasification and maybe even possibly for additional process heat demands, the result is that the amount of nett syngas produced is sacrificed to generate this excess heat in another form. Another major heat loss is the excess steam used in the gasifier as the fluidising medium. This steam is condensed in the gas scrubbers and contributes to the scrubber heat removal requirements.

All gasification processes will benefit from a higher black liquor solids concentration. The benefits are greater than the case of the conventional recovery boiler because the reduced heat load on the gasifier reduces gross syngas consumption as well as the general heat loss associated with evaporating the excess water.

The steam reforming process is much more efficient in sulphur reduction and this can be primarily attributed to the instability of the sodium sulphide in the reforming environment. This finding is also reported by Aghamohammadi *et al* [1995] who achieved greater than 80% sulphur reduction even at low bed operating temperatures on their large scale pilot testing facilities. By separating the sodium and sulphur elements effectively, this provides flexibility in recovered chemical streams and therefore offers an economic and efficient means of recovering process chemicals for a broad range of spent pulping streams.

Table 2.3 below lists the component distributions for the product gases from the gasifiers. The syn-gas analysis for the steam reformer is taken after the excess steam has been condensed out in the venturi gas coolers, and due to the absence of combustion, it is absent of the conventional products of combusiton and nitrogen diluent. The values reported also illustrate the superior sulphur reduction capabilities of the steam reforming process over the smelt phase and partial combustion processes.

Table 2.3 : Gasification product gas compositions [Berglin *et al*, 1996; Aghamohammadi, 1995]

Gas component from gasifier (vol/vol)	Smelt phase process (%)	Solid phase partial combustion (%)	Solid phase steam reforming (%)
CO	8.24	8.66	5.3
CO_2	11.81	13.19	16.0
CH_4	1.23	0.99	8.7
C_2H_6 and C_3H_8	0	0	2.3
H_2	10.65	19.68	59.9
N_2	44.63	37.56	0
H_2S	0.77	1.08	7.8
H_2O	22.67	18.84	0
TOTAL	100	100	100

The high quality syngas is reported to have higher heating values in the range of 12.3 to 16.6 MJ/Nm^3 depending on the dry solids content in the black liquor and the temperature of the process. This is equivalent to 24 to 32% of the HHV of natural gas [Salmenoja, 1993 ; Nashölm and Westermark, 1997].

2.5 Optimising energy recovery

If the product gas from a black liquor gasifier is simply burned in a power boiler for steam generation, the energy recovery will not be as good as with a modern recovery boiler [Grace and Timmer, 1995]. However if the gas from the gasifier can be burned in a gas turbine for combined-cycle power and steam generation, the electrical power production is significantly greater than with a conventional recovery boiler.

The pulp and paper industry is faced with the need to retire many of its black liquor recovery systems, within the next 5-15 years due to the age of the existing units [Consonni *et al*, 1998; Larson and Raymond, 1997]. This presents an opportunity to replace the current steam turbine cogeneration systems with gas turbine based co–generation systems. The development of the technology is underway by several companies around the world and is reaching commercial status with several existing piloting and operational units in existence today. This opportunity presents itself to Sappi Stanger as it allows the mill to take advantage of the energy recovery

options when selecting a new recovery system for the proposed SASAQ pulping. The replacement of the recovery units will depend on many factors:

- performance
- process efficiency – energy and chemical
- reliability
- cost – capital and operating
- customer acceptance
- operating risks
- environmental impact

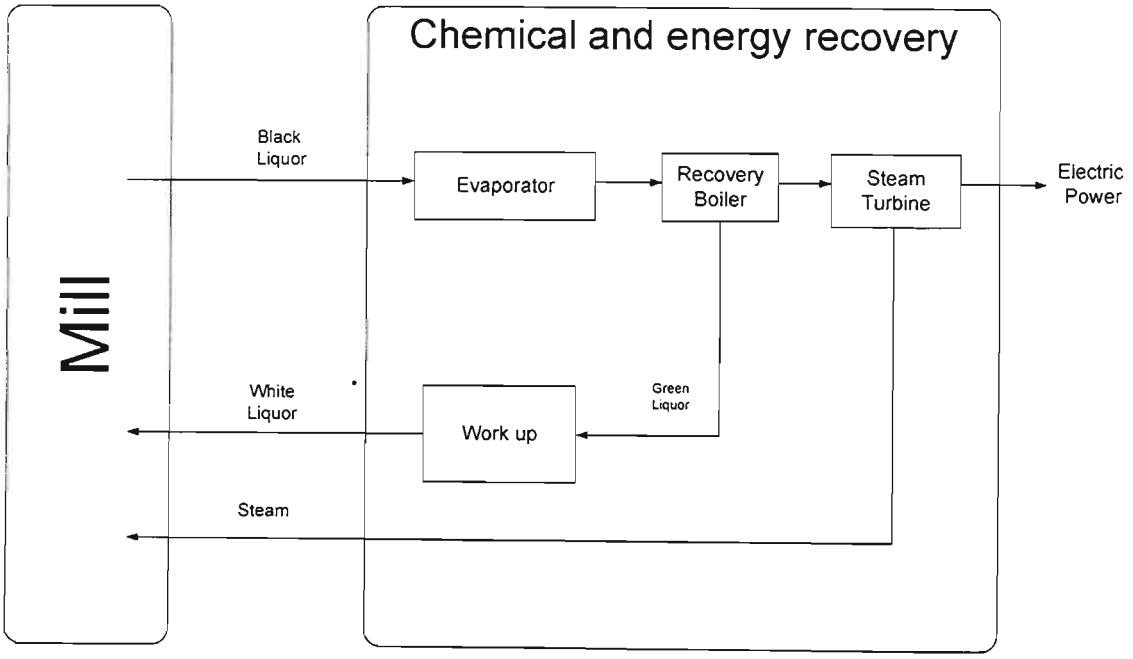

Fig. 2.9 (a) : Simplified schematic representation of a mill with conventional recovery, Berglin *et al* [1998]

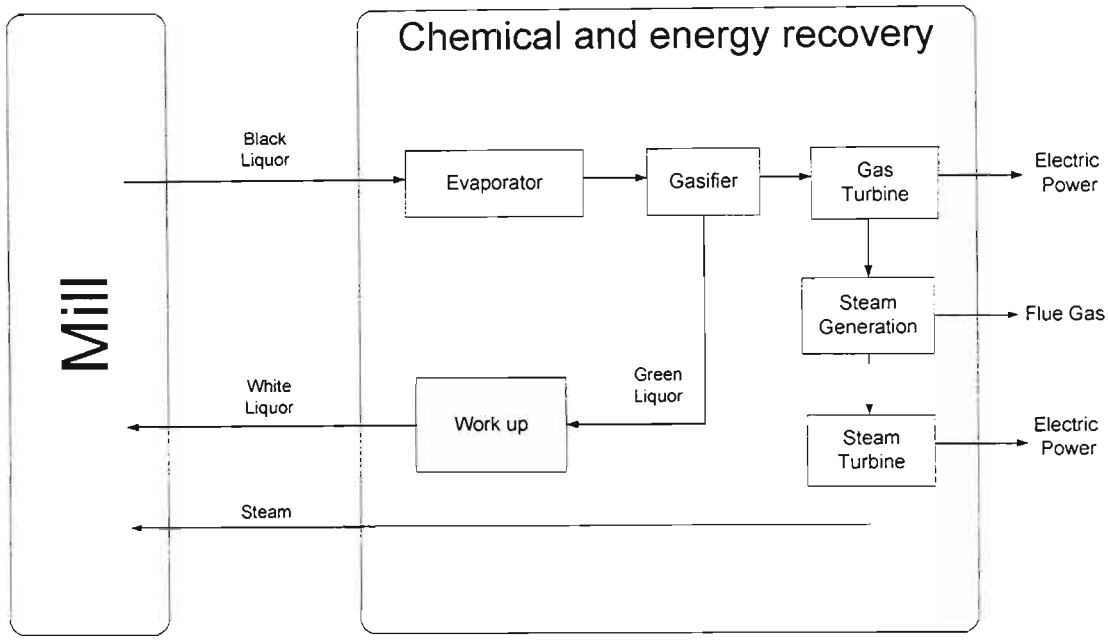

Fig. 2.9(b): Simplified schematic representation of a mill with a gasification based system, Berglin [1998].

Frederick [1999] compared black liquor gasification in an integrated combined cycle, illustrated in figure 2.9 (b), with the Tomlinson steam power cycle illustrated in figure 2.9 (a) and showed that the former technology would enable a modern mill to double electricity energy generation. Larson *et al* [1998] results from performance modeling of integrated black liquor gasification systems showed an increase of 100% to 175% greater electric power generation with black liquor gasification in a combined cycle is possible. Although the study utilizes a Tomlinson steam power cycle, the recovery furnace used in the sulphite recovery process is very similar to the operation of the Tomlinson furnace as mentioned earlier.

Their results are in accordance with other studies [Fogelholm and McKeogh, 1991; Consonni *et al*, 1997; Ahlroth and Svedberg, 1998; Ihren and Svedberg, 1994] which also confirm that the ultimate potential for power generation is up to 2.5 times that of the conventional recovery system and the steam generation remains the same.

The incorporation of black liquor gasification in an integrated combined cycle can result in a paper and pulp mill becoming an exporter of electricity. Knowing the present and future costs for biomass and black liquor fuels, this may place pulp mills in a favorable position to negotiate long term contracts for electricity sales. The guarantee of the long time price stability and the environmental "greenness" of the power might even command premium prices in a de-regulated market or a market having government imposed greenhouse gas emissions mitigations.

Because the black liquor energy resource is derived from a renewable resource, the use of this energy source contributes little or no net emissions to the atmosphere of carbon dioxide. Carbon dioxide released in utilizing this resource in power and heat generation is reabsorbed by new plant growth. If any power generated in excess of the process needs is exported to a utility grid, it eliminates the need to generate an equivalent amount of power from natural gas or from coal. The greater amount of power generated from biomass enables larger amounts of fossil derived utility power to be eliminated, leading to a global reduction in carbon emissions. The economics however will be driven largely by the relative cost of purchased fuels and value of electricity sales and by relative capital investments for competing systems.

Full replacement of the boiler and steam turbine systems with black liquor gasifiers in a combined cycle (BLGCC) will involve a fundamental change in the technology for the pulp industry, from steam turbines to gas turbines. Conventionally, the recovery system for a mill is determined by the expected liquor throughput, the boiler unit is sized accordingly, and the steam turbine is sized to handle the steam generated in the boiler. With the design of a black liquor gasifier in a combined cycle recovery system, the focus will change in that it requires the selection of a particular gas turbine model, within a fixed set of output ranges determined by original design decisions regarding gas turbines for aircraft applications. To identify a perfect match will be rare because black liquor availability is determined by considerations related to the pulp and paper production methods whereas the design of the gas turbine is determined by the few specific size ranges in the market [Kreutz, 1998].

To compare gasification based systems and Tomlinson boiler co-generation systems consistently; Larson, Consonni and Kreutz [1998] modeled the Tomlinson technology to a comparable level of detail. They modeled the preliminary economics of a $100MW_e$[†] integrated black liquor gasifier in a combined cycle for four different technology options based on detailed full load performance modeling :

- Tomlinson boiler
- High temperature oxygen blown gasification (HT-Oxygen)
- High temperature air blown gasification (HT-Air)
- Low temperature steam reforming (LT-Steam)

The overall performance and costs for the four alternative black liquor co-generation systems are summarized in Table 2.4 below. We can expect the sulphite recovery boiler to be similar to the Tomlinson boiler as discussed earlier.

[†] W_e – Net electricity generating capacity

Table 2.4 : Capital, operating and calculated electricity costs for 100MW$_e$ BLGCC system [Larson, Consonni *et al*, 1998]

		BLGCC		
	Tomlinson	HT- Oxygen	HT - Air	LT - Steam
Performance parameters				
Black liquor, tds/day	2158	2294	2281	2462
Nett power output, MW$_e$	46.8	135.4	101.4	129
Electricity, 10^6 kWh/yr	373.1	1079	808.3	1028
Process Steam, GJ/hour	842	893	890	961
Cost parameters				
Total capital ($10^6$$)	166.5	186.9	146.4	180.3
Unit capital costs				
$/kg BLS/day	72	76	60	68
$/nett kW$_e$	3302	1281	1339	1297
Operation and maintenance, ($10^6$$/yr)	6.56	11.51	10.56	6.13
Lifecycle cost, c/kWh				
Capital Recovery Rate of 20%	11.7	5.4	5.5	5.0

The higher net power output for the gasifier combined cycles is due to the higher electricity to process steam production ratio for a combined cycle cogeneration system. Larson showed that although all systems are roughly equivalent capital wise, the BLGCC system's cost per kW$_e$ is substantially lower than for the Tomlinson system because of the much higher energy output. Thus it can be concluded that strictly as power generators, the BLGCC systems have a considerable capital cost advantage over the Tomlinson system. We can expect the results to be similar for the sulphite recovery furnace as its operation is closely related to the Tomlinson system.

It is important to note that the steam generation remains almost the same for all of the systems, and this is confirmed by studies done by Näsholm and Westermark [1997]. Thus a BLGCC system will also produce adequate process steam for the mill as is indicated in Table 2.4 above as well.

The replacement of the recovery technology with the BLGCC systems will depend primarily on the ability of the BLGCC system to deliver an equivalent or better chemical recovery function than that of the conventional technology. The question that arises is what additional capital can be expended on this replacement technology to insure its chemical recovery function before the total life cycle cost of the system is equivalent to that of the existing technologies available?

Larson's analysis shows that the capital costs for the BLGCC systems could double easily before such a situation is attained. This certainly leaves much room for uncertainties that is still being resolved by the industry, as well as additional capital costs for suitable chemical recovery system suited to the mills requirements.

The ability to burn the gas in a gas turbine is dependant on the ability to produce a suitably clean gas. Larson and McDonald *et al* [1998] estimated the capital costs for new installations of a gasifier with a combined cycle system for oxygen or air blown gasification with several alternative hydrogen sulphide recovery systems:

A. Oxygen blown gasification, hydrogen sulphide recovery by scrubbing with green liquor
B. Oxygen blown gasification, selective hydrogen sulphide scrubbing with full recycle of hydrogen sulphide to the gasifier
C. Oxygen blown gasification; sulphur recovery and polysulphide and anthraquinone [†] pulping
D. Air blown gasification ; recycle of hydrogen sulphide to the gasifier

All cases were based on high temperature, pressurized, entrained flow gasification for a recovery plant that treated 2294 tons BLS/day. Their results, shown in figure 2.10 below, shows that with essentially the same capital costs as a Tomlinson furnace, a BLGCC system will generate nett operating savings of US$12-US$17 million per annum due to the twofold increase in power production. The lowest cost option was that of air blow gasification with recycling of the hydrogen sulphide to the gasifier with a capital cost advantage of US$20 million over the Tomlinson furnace.

In summary, it can be stated that BLGCC is comparable to the Tomlinson system with the benefit of the total cost of power generation from a BLGCC powerhouse being substantially lower than from a Tomlinson powerhouse. Although the annual total cost including, capital, operation and maintenance, fuel, etc. is higher for BLGCC systems than for a Tomlinson systems in some cases, the value of the electricity produced far outweighs the added costs.

[†] Polysulphide is produced by the capture of hydrogen sulphide from the scrubber, conversion to elemental sulphur in a Claus plant, and remixing with the white liquor. Use of polysulfide is said to increase pulp yields by 1-2%. Anthraquinone reduces the active alkali requirement and hence causticizing load

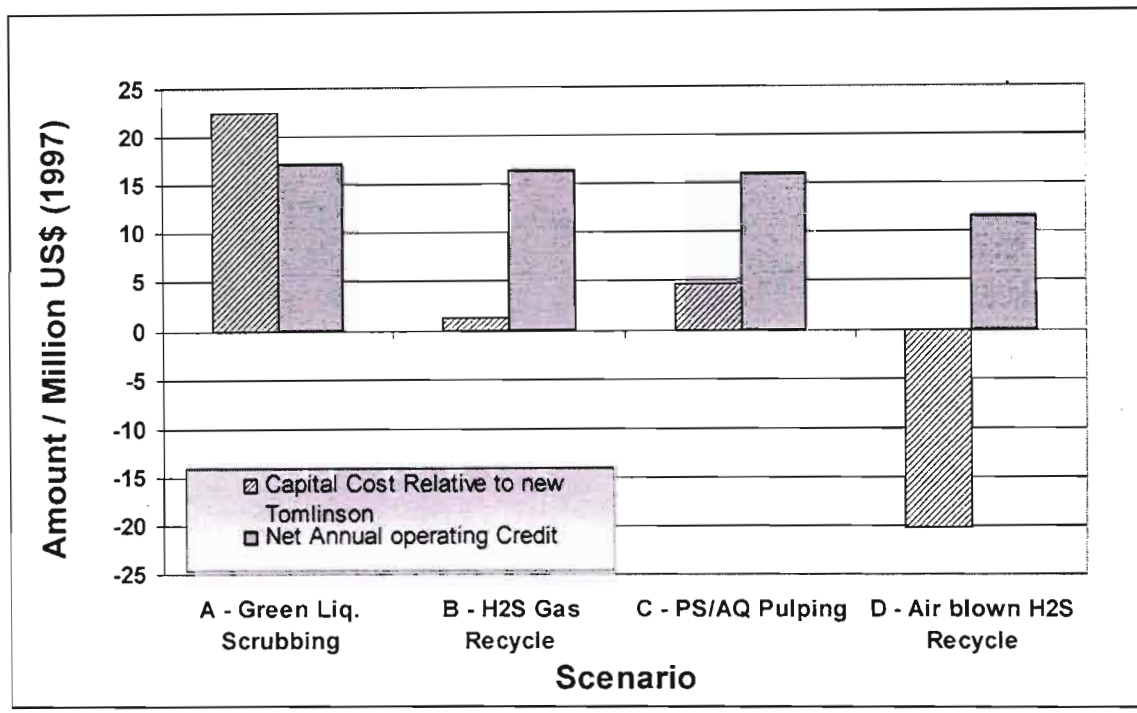

Figure 2.10 : Difference in installed capital cost between black liquor gasification combined cycle (BLGCC) scenarios and the Tomlinson powerhouse and the differences in annual operating credit as studied by Larson *et al* [1998]

The technology is under intense development and is clear that in time, the economics will be optimized further when the level of the gas turbine technology has taken into consideration the pulp and paper mill's requirements of having a gas turbine sized specifically to match the mills black liquor throughput. The gas turbine is insensitive to the fact that the gas is generated from black liquor, it's just a matter of designing for and maintaining the energy content of the gas. There are various techniques one can use to manipulate the gas coming to the turbine, including diluting, compensating and handling, in order to achieve an optimum cycle. It is simply a matter of carrying out a cycle optimization and discovering the correct and most efficient way to operate the cycle.

2. 6 Black liquor injection – a common point of interest

The delivery of black liquor into the boiler is crucial to the optimization of the recovery process. Black liquor is injected into the recovery boiler through a set of nozzles. The nozzles are usually of the splash plate type as shown in figure 2.11 below, but several designs are available commercially.

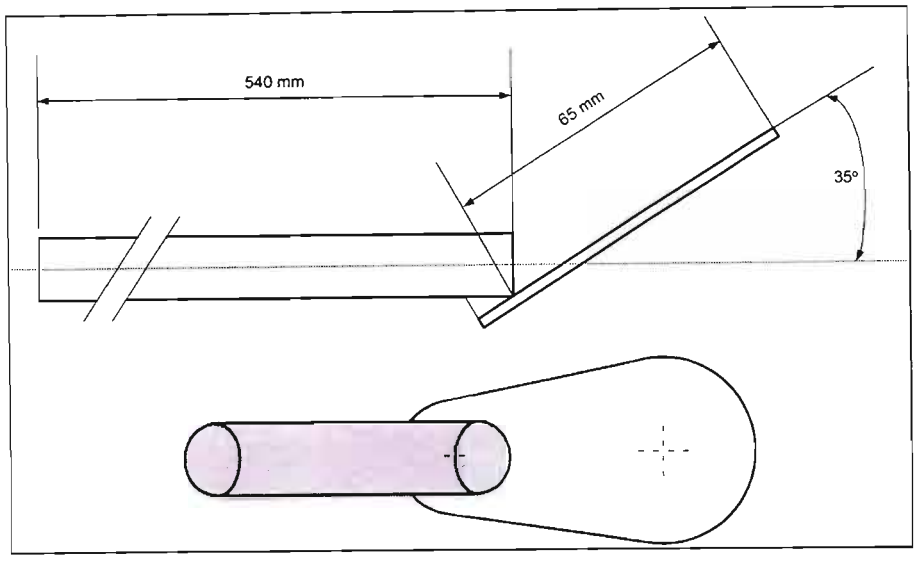

Figure 2.11: 15mm Splash plate nozzle design used by Helpio *et al*, [1996]

Upon exiting the nozzle, the liquid sheet formed by the nozzle is broken up into droplets. The ideal size of the drops is approximately 2-3 mm [Helpio *et al*, 1996]. The smaller the droplet, the greater the surface area per unit mass of black liquor and hence the greater the rates of heat and mass transfer. However too small drops cause increased carryover. Drops that are too large decrease the bed temperature and lead to unstable operation of the recovery furnace. Hence for black liquor throughput to be increased in a mill that is limited by its recovery boiler, it's not merely a matter of controlling the droplet size, but also the controlling the width of the size distribution that needs to be improved.

The performance of spray nozzles for several black liquors has been the subject of several investigations [Bennington and Kerekes, 1985; Galtung and Williams, 1975]. Empie *et al* [1995] studied the droplet size distribution of black liquors when sprayed through the standard splash plate, V-Jet and swirl cone nozzles in a spray chamber. His results showed that the droplet diameter decreased smoothly as liquor temperature was increased past its boiling point.

However Galtung and Willaims [1975] claimed that a change of a few degrees in liquor temperature can change a coarse spray into a fine mist. Helpio and Kankkunen [1996] was also in agreement with this theory and showed that flash boiling of liquor in the nozzle flow tube decreases the mean drop size of the spray. Flashing accelerates the flow in the flow tube thus increasing the initial drop velocity and it is also responsible for changes in the spray direction. A nett decrease of 23% in mass mean diameter was observed as the liquor temperature increased from 112 – 125°C. Empie *et al* also found that the size distribution for each nozzle was very similar, in agreement with Spielbauer [1989] and that the size distribution of the droplets followed the square root normal distribution curve.

The delivery of black liquor is an important criterion for the effective and efficient operation of the bed. Whether the delivery is into a conventional Tomlinson recovery boiler or a gasifier, the delivery into the bed involves almost identical technology with respect to mean droplet size distribution and an even distribution system within the bed.

2.7. Commercially available black liquor gasification technologies

Several technologies are available commercially for the gasification of black liquor. They are all a variation of those discussed earlier in this chapter and many of the licensors offer guaranteed performance of their units. In this section we will look at a few of these technologies that are available to the paper and pulp industry as well as some of the key players in the development of the technology.

2.7.1. Kvaerner Chemrec™ process

The Chemrec™ process uses an entrained flow gasifier with an integrated quench dissolver. It is classified as the high temperature smelt process discussed earlier. The Chemrec process is the first black liquor gasification process to be in commercial operation. The first unit was installed at AssiDomän's Frövifors mill in 1991 with a capacity of treating 75 metric tons of black liquor solids (BLS) per day. The unit was designed to add an incremental capacity to the mills existing recovery system.

It is an air blown black liquor gasification system that operates at a reactor operating temperature of about 955°C at atmospheric pressure. Concentrated black liquor is gasified under reducing conditions by reacting it with a stoichiometric amount of air pre-heated to about 500°C. The reduction efficiency is reported to be greater than 95% and the carbon conversion is reported to be greater than 98% [Stigsson, 1998]. The heating value of the gas is typically 2.79- 3.60 MJ/m^3 depending on the black liquor composition and air stoichiometric factor. The operation was straight forward and the process was found easy to control [Grace and Timmer, 1995]. The operating experience and design of the gasification system at Frövifors served as the basis for their second unit in commercial operation.

The second much larger (330 ton BLS/day) atmospheric capacity unit was installed at the Weyerhauser New Bern mill in North Carolina and began commercial operation in

early 1997. This gasification reactor was a geometric scale up of the Frövifors reactor, but changes to the black liquor injection system and air pre-heater systems were made. The unit demonstrated the ability to run at 90% of its design capacity and produced good quality green liquor. At the January 2000 maintenance stop, small cracks in the reactor vessel were detected and classified as stress corrosion cracks. The New Bern booster has remained out of operation while the cause of the cracks has been analyzed and remedial actions have been identified. The reactor vessel at New Bern was being re-engineered and the plant was expected to restart in July 2003.

Encouraged by the significant interest in black liquor gasification, the company advanced its commercialization efforts towards full scale oxygen blown black liquor gasification in combined cycle schemes and erected the first pressurized pilot plant gasifier and gas clean up system at a Swedish Kraft mill in 1994. Experiences and data from the pilot plant showed that the pressurized oxygen blown gasification process could deliver a gas with an adequate energy value greater than 7.45 MJ/m^3 required for reliable operation of gas turbines. The unit demonstrated carbon conversion efficiencies of greater than 99%. This led to the development of a full scale 300 to 550 tons BLS/day oxygen blown black liquor gasifier in an integrated combined cycle at the AssiDomän Kraftliner mill in Piteå, Sweden. The plant is currently Chemrec's latest design and was planned to be in operation by August 2003. The gasifier operates at temperatures of 950-1000°C and pressures between 3 to 3.5 MPa [Stigsson, 1998; http://www.chemrec.se/]

The Chemrec process was developed and is marketed by Kvaerner Pulping. Their atmospheric process has proven to be commercially viable and with ongoing development of their pressurized oxygen blown unit, they claim to be the leading developer for high temperature gasification processes.

2.7.2 Noell gasifier

The Noell gasifier is similar to the Chemrec™ gasifier in that it uses partial combustion in an entrained flow reactor with an internal quench as well. However the gasifier is pressurized and uses only oxygen instead of air. It is also a lined, water cooled reactor instead of the refractory-lined, uncooled Chemrec™ reactor. Although Noell has no experience with gasifying black liquor, they do have technologies for commercial scale

brown coal gasifiers and hope to develop the black liquor technology based on their expertise in this field [Grace, 1996].

2.7.3 Tampella

Tampella Power Inc. has been working on black liquor gasification since 1989. A 3 ton BLS/day pilot scale unit was developed at the Sunila Kraft pulping mill in Kotka and started trial testing in early 1991. Black liquor is gasified by partial combustion in an entrained flow reactor operating at 900-1000°C temperature range in an un-pressurized reactor. The process differs from the Chemrec™ process in that it includes concentration of the black liquor up to 80% BLS and the incorporation of a novel and efficient method for alkali removal from the vapour phase through the use of a smelt cyclone that separates the smelt from the product gas. The alkali fines are recycled to the gasifier or into the dissolver. They claim that this eliminates the serious fouling and corrosion problems that arise as a result of the condensation of large amounts of alkalis produced in black liquor gasification on the cold surfaces [Salmenoja, 1993].

The pilot unit was operated for about 3 yrs during which it produced reduction efficiencies of 50-70% and a syn-gas with a LHV of 1.5-2.0 MJ/Nm^3. The low heating values were consistent with the high stoichiometric air ratios used and thought to be due to the relatively high heat losses from a physically small unit. A commercial unit is expected to operate at lower stoichiometric air ratios and produce a higher fuel value gas [Grace and Timmer, 1995].

The main advantage of the Tampella process lies in the hot smelt separation and hot gas clean up but whilst pilot tests have been run, these have to yet to be proved on the commercial scale.

Tampella has since put a hold on all experimental development and has limited their research activities now to basic fundamental research studies.

2.7.4 Ahlstrom Kamyr

The Ahlstrom approach used the high temperature smelt phase process. No details of the process are currently available apart from the fact that the company completed its

gasification research towards the end of 1991. Their pilot plant demonstration unit was operated at the Aänekoski mill for a period equivalent to 4 days of gasification time. They concluded that gasification was feasible, but that the pilot system demonstrated no improved energy efficiency over the traditional Tomlinson Recovery boiler in combination with the back pressure Rankine steam turbine cycle power generation. It also required major changes to the chemical recovery section to achieve a clean enough product fuel gas to be used in a gas-fired turbine generator. Their theoretical models show that up to three times greater amount of electricity can be generated through use of the gasification technology in a combined cycle but the company's plan employed since is to be a follower in the technology. They feel they have learned what is necessary and are concentrating on other black liquor technologies in the short term.

2.7.5 Babcock and Wilcox

The Babcock and Wilcox process uses a bubbling fluidized bed gasifier operating at the low temperature level. The bed consists of solid sodium carbonate particles, generated by the gasification reactions, fluidized with stoichiometric amounts of steam and pre-heated air. The bed product is dissolved in water whilst the fuel gas is cooled in a heat recovery boiler to a temperature appropriate for hydrogen sulphide recovery. The carbonate solution is used to reabsorb the hydrogen sulphide in the chemical recovery system.

Babcock and Wilcox have developed a BLG system that they claim to work but have not built neither a demonstration nor a commercial facility. Their focus remains on black liquor recovery boilers and choose to be a follower in the technology [Finchem, 1995].

2.7.6 ABB-CE (Sweden)

The ABB-CE gasification process uses a circulating fluidized bed that operates at 700°C. Black liquor is gasified by partial combustion to produce a solid bed product of sodium carbonate and sodium sulphate particles. The bed is fluidized by preheated compressed air which also serves as the temperature control mechanism. The syn-gas is cooled in a gas cooler, treated in a bag house for additional solids removal and then scrubbed to remove hydrogen sulphide. The process separates sodium sulphide from

sodium carbonate by allowing the system to produce separate white liquor streams of differing sulphidity. The first pilot unit was operated in November 1991 at the company's research facility with a capacity of treating 2-4 tons BLS/day. The system experienced no problem with tar formations and outperformed the conventional recovery boilers in terms of carbon conversion by obtaining 0.1 – 0.2% carbon in the ash as opposed to 1% carbon in the ash obtained from a recovery boiler. Grace and Timmer [1995] reported carbon efficiencies of the order of 70% were obtained from their pilot testing facilities.

The company reports that the process is being developed for both the Rankine- and combined cycle power generation systems but their core focus area is on developing an atmospheric system that provides Rankine cycle steam for power production and power heating. They do expect their next generation of gasifier to develop to a pressurized system, integrated with gas fired turbines and steam generators for improved power production and plant heating.

2.7.7 ThermoChem/MTCI process

In 1987 Manufacturing Technology and Conversion International Incorporated (MTCI) began development work on steam reforming of black liquor. They together with ThermoChem Recovery International (TRI) developed a technology that uses steam gasification in an indirectly heated bubbling fluidized bed. It utilizes indirect pulsed heating of a steam fluidized bed of sodium carbonate solids. The black liquor is sprayed directly onto the bed which operates at temperatures in the region of 600 to 650°C and at pressures near atmospheric. The process is patented under the name PulseEnhanced™ Steam Reforming and Recovery by MTCI [US Patent No. 5637192; US Patent No. 5059404]. StoneChem, a subdivision of TRI and Stone and Webster, are the exclusive license holders.

Bed temperatures are well below the smelt formation temperatures. The heat exchangers consist of bundles of pulse combustor resonance tubes. A portion of the syn-gas can be burned in these pulse combustion heaters to supply the necessary heat. The pulsations give a gas-side heat transfer coefficient in the heat exchanger which is 3 to 5 times greater than in a conventional fire–tube heater. This effectively reduces the size of the heat exchangers needed and also allows a more effective transfer of heat into the bed. In light of maintaining exchanger surface temperatures below the smelt

formation temperatures, yet sufficiently high enough to maintain a temperature driving force for heat transfer the pulsed combustor design works well.

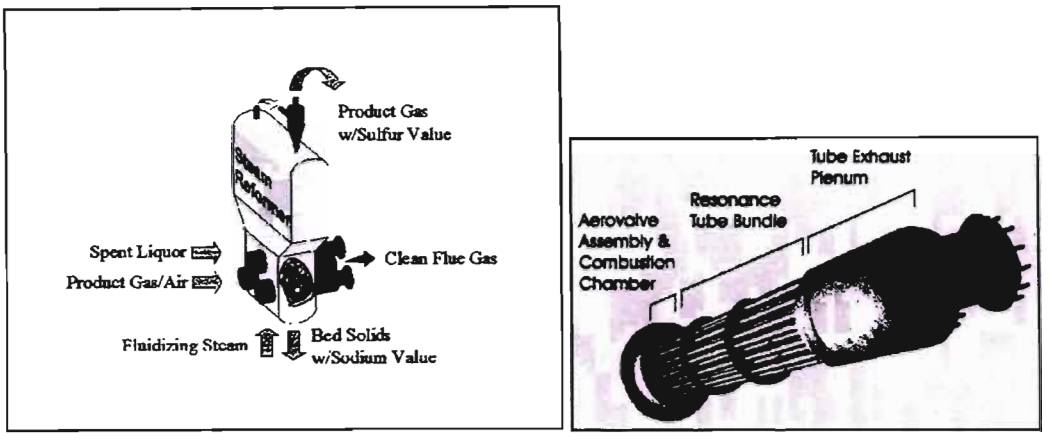

Figure 2.12: TRI/MTCI steam reformer (left) and pulsed heater module (right) [http://www.tri-inc.net/TRI%20Attachment%201%20(White%20Paper).pdf]

The heater units each have a capability of gasifying 3-4 ton BLS/hr and a modular approach is used to meeting the requirements of larger systems. The process produces a high quality syn-gas with a higher heating value of 12 to13.3 MJ/m^3 that is free of the conventional combustions products and nitrogen diluents. The gas contains 73% hydrogen, 14% carbon dioxide, 5 % carbon monoxide, 5% methane and 3% higher hydrocarbons on a volume to volume basis [Rockvam and Tenore, 1996]. The hot gas exiting the reformer is used to generate steam in a steam generating unit before passing to a wet venturi scrubber that removes fine particulates. The gas then enters a gas cooler where the excess water vapour is condensed out before passing on to a hydrogen recovery system if required by the chemistry of the recovery process.

Pilot plant studies were carried out in a 55-100 tons BLS/day pilot unit installed at the Weyerhaeuser New Bern Mill, North Carolina in 1994. Their data collected indicated carbon conversion figures of greater than 90% even at temperatures as low as 620°C. Two commercial scale units are currently being installed, a 115 tons BLS/day unit at Norampac's Trenton Mill in Canada and a 182 tons BLS/day unit at Georgia-Pacific's mill in Virginia. [http://www.energysolutionscenter.org]

The company is looking for additional commercial units with further development in the areas of fuel cells, auto caustization, supersulphidity and polysulphide pulping techniques.

Kvaerner Pulping, ABB-CE and Babcock and Wilcox also manufacture conventional recovery boilers. The two newer players Noell and Stonechem are more likely to have a beneficial impact on black liquor gasification development since they do not have any long standing investments in traditional recovery boiler technologies. They may move more quickly with their development and spur the traditional recovery boilers to speed up their development efforts as well.

2.8 Scope of project

Sappi Stanger was actively exploring the possibility of using a black liqour gasification technology for their chemical recovery system. The mill produces bagasse pulps using the Soda pulping method. The mill was considering changing the pulping chemistry to Semi-Alkaline Sulphite Anthraquinone pulping (SASAQ) in an effort to increase their pulp yields. The change in pulping chemistry meant a new chemical recovery system was needed due to the introduction of sulphur into the pulping process. The milled used a Copeland recovery process and the drawback of this recovery system with sulphur containing black liquors has been highlighted earlier. The mill explored several BLG technologies available and found that the most suitable technology available for their needs is that offered by the joint venture between Thermochem Recovery International (TRI) and Manufacturing Technology & Conversion International Inc. (MTCI). The mill had entered into discussions with the technology vendor and realized that the technology had to be developed further to clarify process variable issues such as:

- Bed temperature.
- Black liquor composition effects.
- Non process elements (NPE) levels (silica,chlorine).
- Conversion efficiencies of carbon and sulphate.

The route taken to evaluate these variables was to construct a pilot gasifier to evaluate the various reactions and factors affecting gasifier performance. The design, construction and operation of a pilot unit formed the basis of this work. Co-operation on the design and process evaluation was available from TRI/MTCI. TRI/MTCI had already constructed a smaller lab scale gasifier (4 inch diameter) and their proposal was that a larger scale reactor, between 8-12 inches diameter, be constructed for preliminary testing of the process which will also assist in addressing any scale up issues that may arise.

2.8.1 Reactor chemistry

The primary reactions that were considered were the water gas shift reactions given by equation 1.1 to equation 1.3. Reduction of sulphate in the system occurs by the following reactions [Wessel *et al*, 1997 and Li *et al*, 1995]:

Sodium sulphate reduction:

$$8C + 3Na_2SO_4 \rightarrow 3Na_2S + 4CO + 4CO_2 \qquad \textbf{(2.7)}$$

Sulphur emission:

$$Na_2S + H_2O + CO_2 \rightarrow Na_2CO_3 + H_2S \qquad \textbf{(2.8)}$$

Silicate reduction occurs by:

$$SiO_3^{2-} + C \rightarrow SiO_2 + CO \qquad \textbf{(2.9a)}$$

and

$$SiO_3^{2-} + CO \rightarrow SiO_2 + CO_2 \qquad \textbf{(2.9b)}$$

The next chapter reviews fluidized bed reactor design fundamentals and presents the background and design basis for this work.

CHAPTER 3

FLUIDIZED BED REACTOR FUNDAMENTALS

The theory on fluidisation technology is well established with several books dedicated entirely to the subject alone. This chapter hopes to capture the bare essentials necessary for the design of a fluidised bed reactor, and presents the methodology used in the design of the pilot plant fluidised bed reactor used in this work. This work centres on a gas-solid fluidised system and hence the review on fluidised systems will be more focused towards gas-solid systems.

3.1. Nature of gas-solid fluidised beds

A fluidised bed is formed by passing a fluid, liquid or gas, upwards through a bed of solid particles supported on a distributor. The pressure drop across the bed is directly proportional to the rate of fluid flow when the fluid flow rates are low. At high fluid flow rates this relationship no longer stands and the pressure drop increases exponentially with the fluid flow rate. When the frictional drag on the particles becomes equal to the apparent weight (actual weight less buoyancy) of the particles, the particles rearrange themselves to offer less resistance to the flow and the bed expands. If the velocity is increased such that the total frictional force on the bed particles is balanced by the weight of the particles, the bed particles become suspended in the upward flowing gas or liquid. At this point the pressure drop through any section of the bed equals the weight of the fluid and particles in that section. The section behaves like a liquid having a density equal to the bulk density of the bed particles. At this point the bed is said to be just fluidised and the velocity of the fluid is said to be the minimum fluidising velocity (u_{mf}).

The voidage of the bed at the minimum fluidising condition (ε_{mf}) is not known accurately, but is approximately 0.4 [Coulson & Richardon, 1997]. Leva [1959] reported experimental values of ε_{mf} for several particles of different sphericity. Sphericity (ϕ_s) is defined as the ratio of the surface area of a sphere to that of the particle of the same volume.

Up to this stage there is no differentiation between a liquid-solid system and a gas-solid system. However at higher velocities there is a distinct difference between the two. With a liquid system the bed continues to expand uniformly and this smooth fluidisation is termed 'particulate fluidisation'. With gas solid systems, particulate fluidisation only occurs at low fluid velocities and the bed level changes little as the fluidising velocity is increased.

Gas-solid systems exhibit large instabilities as the fluidising velocity is increased further than the minimum fluidising velocity. Two separate phases form, a continuous phase called the "dense" or "emulsion" phase, and a discontinuous phase called the 'lean' or 'bubble' phase. A fluidised system in this state is termed 'aggregative fluidisation' and closely resembles a boiling liquid. If the bed is sufficiently deep, coalescence of the bubbles takes place as well as channelling of the gas and formation of gas slugs. Slugging also occurs when the gas velocity is sufficiently high such that the bubble size approaches the diameter of the bed. The bed then moves into the slug flow regime.

At a sufficiently high fluid flow rate the frictional drag forces overcome the terminal falling velocity of the bed particles and the solids are carried out with the fluid. Figure 3.1 below is an illustration of the different fluidisation regimes:

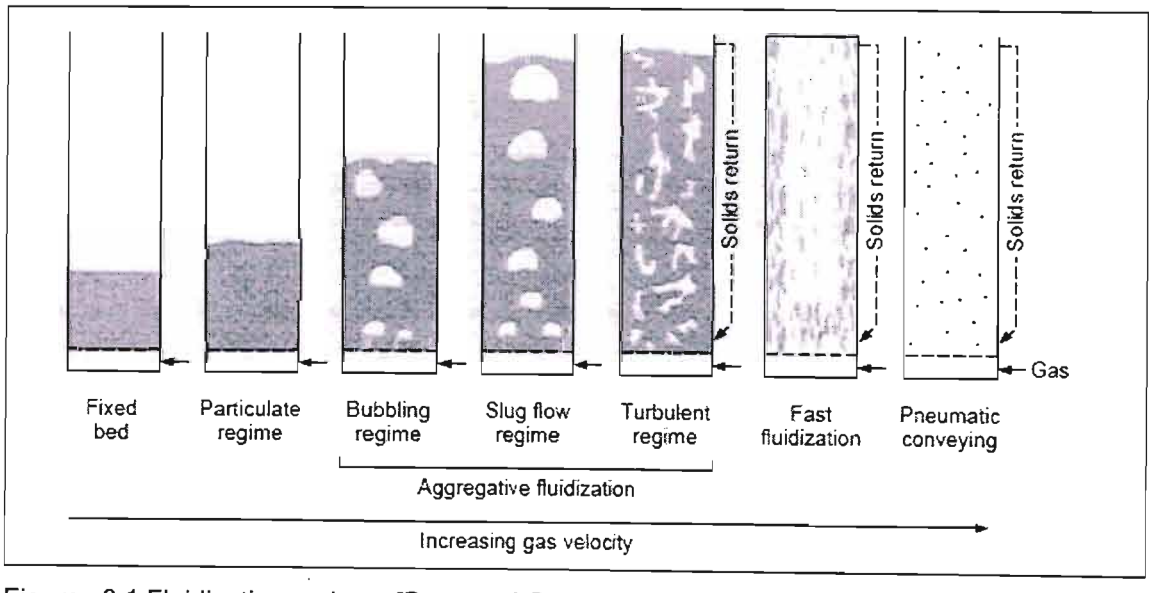

Figure : 3.1 Fluidisation regimes [Perry and Green, 1999, Chapter 17]

The criterion for determining the type of fluidisation is given by the Froude Number (Fr), Geldart [1971] :

$$Fr = \frac{u_{mf}^2}{g d_p} \tag{3.1}$$

where u_{mf} is the minimum fluidising velocity [m/s]
d_p is the particle diameter [m]
g is gravitational acceleration [m/s^2]

If the Fr number is less than 1, then smooth or particulate fluidisation occurs. If the Froude number is greater than 1, then bubbling or aggregative fluidisation occurs.

In gas-solid fluidised systems the bubble phase makes a relatively small contribution to the bed expansion. Systems with fine particles do tend to expand considerably before bubbling occurs, but once it does the bed collapses. This lower limit of the gas velocity at which bubbling begins to occur is termed the 'minimum bubbling velocity' (u_{mb}). u_{mb} is determined by many factors including the distributor design, the presence of any obstructions in the bed, bed geometry, vessel internals and the nature of the bed particles themselves. The ratio of u_{mf}: u_{mb} gives an indication of the degree of bed expansion possible for the system. Fine light particles tend to have a high value whilst large dense particles generally have low values.

3.2 Characterisation of fluidised powders

The properties of a particle determine the ease with which it can be fluidised. Fine low density particles fluidise more easily than large dense particles. The more spherical the particles are, the better they fluidise. The presence of a small proportion of fines is said to aid fluidisation of the coarser particles by coating them with a lubricating layer.

Powders with a wide size distribution show more stable fluidisation than a powder having a narrow size range. It was often thought that this characteristic can be attributed to the smaller bubble sizes that are generated by a powder with a wide size distribution, but Geldart (1971) showed that the size distribution of the powder had no effect on the bubble sizes at all. This led him to the idea of classifying powders into specific groups characterised by their approximate density and particle size shown in figure 3.2 below [Geldart, 1986]. Table 3.1 below summarises the properties of the various Geldart group powders.

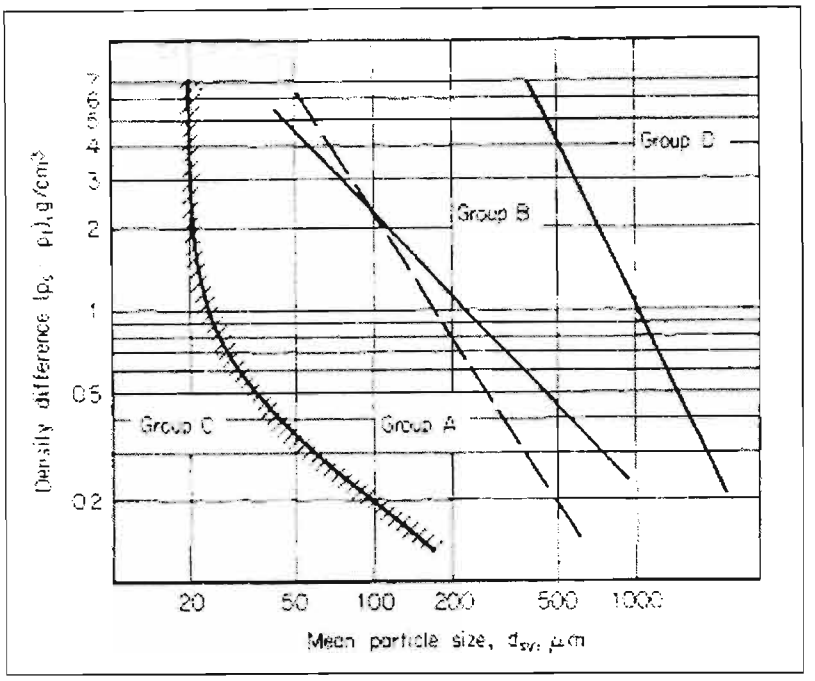

Figure 3.2 : Geldart powder classification diagram for fluidisation by air at ambient conditions [Perry and Green, 1999]

Table 3.1 Summary of Geldart powder group properties [compiled from Geldart, 1986 and Coulson & Richardson, 1997]

	Particle size / (μm)	**Fluidisation characteristic**	**Example**
Group A	30-100	Mainly particulate fluidisation – bubble free range of fluidisation	Cracking catalyst
Group B	100-800	Starts bubbling at just above u_{mf}	Building sand, table salt
Group C	20	Cohesive powders, difficult to fluidise. Readily forms channels.	Flour, cement, fine silica
Group D	1000	Coarse dense solids, can be made to form spouted beds.	Coffee beans, wheat, crushed limestone

His classification took into account three major effects:

i. Bed expansion with increasing gas velocity before bubbling occurs. This is the ratio of $u_{mb} : u_{mf}$ as discussed above.

ii. Rising velocity of bubbles being greater or less than interstitial gas velocity.

iii. Effect of adhesive forces between particles on tendency of the bed to channel rather than fluidise.

Geldart's concept of the four broad groups of powders each possessing distinctive fluidisation characteristics is now widely accepted in the fluidisation field.

3.3. Effect of fluidising velocity on bed pressure drop

For relatively low gas flow rates in a packed bed, a linear relationship exists between the pressure gradient across the bed (ΔP) and the superficial or "*empty tube*" gas velocity (u_c) as indicated in figure 3.3 below:

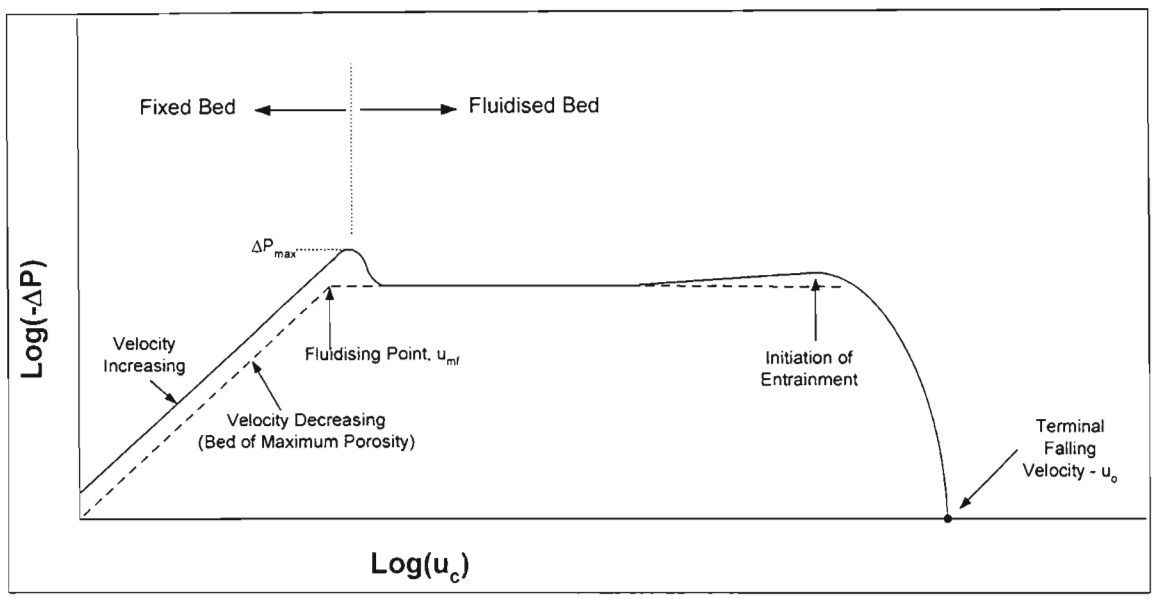

Figure 3.3: Pressure drop over fixed and fluidised beds [adapted from Kunii & Levenspiel, 1969]

As the gas velocity is increased, it passes through a maximum value (ΔP_{max}) that is slightly higher than the static pressure of the bed. The bed "unlocks" when the frictional forces between the particles are overcome. The bed rearranges itself such that the voidage increases from the fixed bed stagnant voidage (ε_m) to ε_{mf} resulting in the pressure drop falling slightly. The pressure drop then maintains an approximately constant value for increasing gas velocities despite the non-homogeneity of the bed arising from the formation of gas bubbles. This pressure value is approximately equivalent to the buoyant weight per unit area of the bed, but in practice it may fluctuate as a result of channelling in the bed [Kunii & Levenspiel, 1969].

If the velocity is now decreased, the bed contracts until the particles are just in touch with each other. At this point the bed has the maximum porosity for a fixed bed, and will remain in this condition if the velocity is decreased further provided that the bed is not shaken. If the gas velocity is increased again, it is expected then that the dashed curve in figure 3.3 above will be

retraced, however this is difficult to produce since the bed tends to consolidate again as it is difficult to keep the bed free of vibrations.

A pressure drop diagram like figure 3.3 is useful as an indication of the quality of fluidisation especially when the bed cannot be viewed during operation. Fluctuations of the curve in the fluidised region indicate a slugging bed. An absence of the sharp change in slope at the fluidising point coupled with an unusually low pressure drop thereafter indicates incomplete contacting, with particles only partly fluidised.

As stated earlier in a fluidised bed, the total pressure drop must be equal to the effective weight of the bed. Thus it can be written that for a given bed of depth L and voidage ε [Coulson, Vol 2, 1997]:

$$\frac{-\Delta P}{L} = (1-\varepsilon)(\rho_s - \rho)g \tag{3.2}$$

where: $-\Delta P$ is the pressure drop across the bed

ε is the porosity or fraction voids in the bed

ρ_s is the density of the solid bed material

ρ is the fluid density

L is the height of the bed when fluidized

g is the acceleration due to gravity

Equation 3.2 is valid from the onset of fluidization until solid entrainment occurs. For conditions below this region, the bed is a normal packed bed and the pressure drop is given by the Carmen-Kozeny correlation (equation 3.3). This correlation is valid for laminar flow with Reynolds numbers (Re) less than about 1. The Ergun correlation (equation 3.4) is valid for both the laminar and turbulent regimes.

$$\frac{-\Delta P}{L} = \frac{36K''\mu}{d_{sv}^2}\frac{(1-\varepsilon)^2}{\varepsilon^3}u_c \tag{3.3}$$

where: K'' is a the Kozeny constant dependant on porosity and particle shape

μ is the fluid viscosity

d_{sv} is the diameter of a sphere having the same surface area to volume ratio of the particle. i.e. $d_{sv} = d_p \times \phi_s$ where d_p is the particle diameter

K'' is generally assumed to be 5, though this value is used for voidages between 0.4 and 0.5. The experimental data in this field is limited and the constant 5 is normally used with its possible inaccuracies [Coulson, Vol 2, 1997].

$$\frac{-\Delta P}{L} = 150\frac{(1-\varepsilon)}{\varepsilon^3}\frac{\mu u_c}{d_{sv}^2} + 1.75\frac{(1-\varepsilon)}{\varepsilon^3}\frac{\rho u_c^2}{d_{sv}} \tag{3.4}$$

Substitution of equation 3.2 into equation 3.3 yields the relationship between u_c and ε under laminar conditions. Assuming K'' is equal to 5 this gives:

$$u_c = \frac{1}{180}\frac{\varepsilon^3}{(1-\varepsilon)}\frac{d_{sv}^2(\rho_s-\rho)g}{\mu} \tag{3.5}$$

Similarly substitution of equation 3.2 into equation 3.4 which covers both the laminar and turbulent regimes, and with a little manipulation gives:

$$\frac{\rho(\rho_s-\rho)gd_{sv}^3}{\mu^2} = 150\frac{1-\varepsilon}{\varepsilon^3}\frac{u_c d_{sv}\rho}{\mu} + \frac{1.75}{\varepsilon^3}\left(\frac{u_c d_{sv}\rho}{\mu}\right)^2 \tag{3.6}$$

In equation 3.6:

$\frac{\rho(\rho_s-\rho)gd_{sv}^3}{\mu^2}$ is defined as the Galileo number, *Ga* and the term $\frac{u_c d_{sv}\rho}{\mu}$ is a form of the Reynolds number, *Re*. Thus equation 3.6 can be expressed as [Coulson Vol 2, 1997]:

$$Ga = 150\frac{1-\varepsilon}{\varepsilon^3}\mathrm{Re} + \frac{1.75}{\varepsilon^3}(\mathrm{Re})^2 \tag{3.7}$$

The voidage in a packed bed is related to the sphericity of the particles. For smaller diameter columns, the wall effect plays a prominent role and influences the bed voidage. Reliable voidage predictions are scarce and since it is a relatively simple quantity to measure, it is often determined experimentally.

3.4. Minimum fluidising, minimum bubbling and terminal falling velocities

There are two boundaries to the gas flow rate through a fluidized bed. On the lower end is the minimum fluidizing velocity u_{mf}, which determines the onset of fluidization and on the top end

of the scale is the point of solids entrainment of particles out of the bed. This upper limit of the gas flow rate is approximated by the terminal falling velocity or free-fall velocity of the particles, u_o. For gas-solid fluidized systems, another more important point on the fluidization curve is the minimum bubbling velocity u_{mb}, the gas velocity at which the first small bubbles begin to appear.

3.4.1 Minimum fluidizing velocity, u_{mf}

Equations 3.5 and 3.6 are only valid for packed beds since the fluidised bed curve breaks away from the Ergun and Carmen-Kozeny equations at velocities above the minimum fluidising point u_{mf} as shown in figure 3.4 below. However the equations are valid up to an including the fluidising point, u_{mf}.

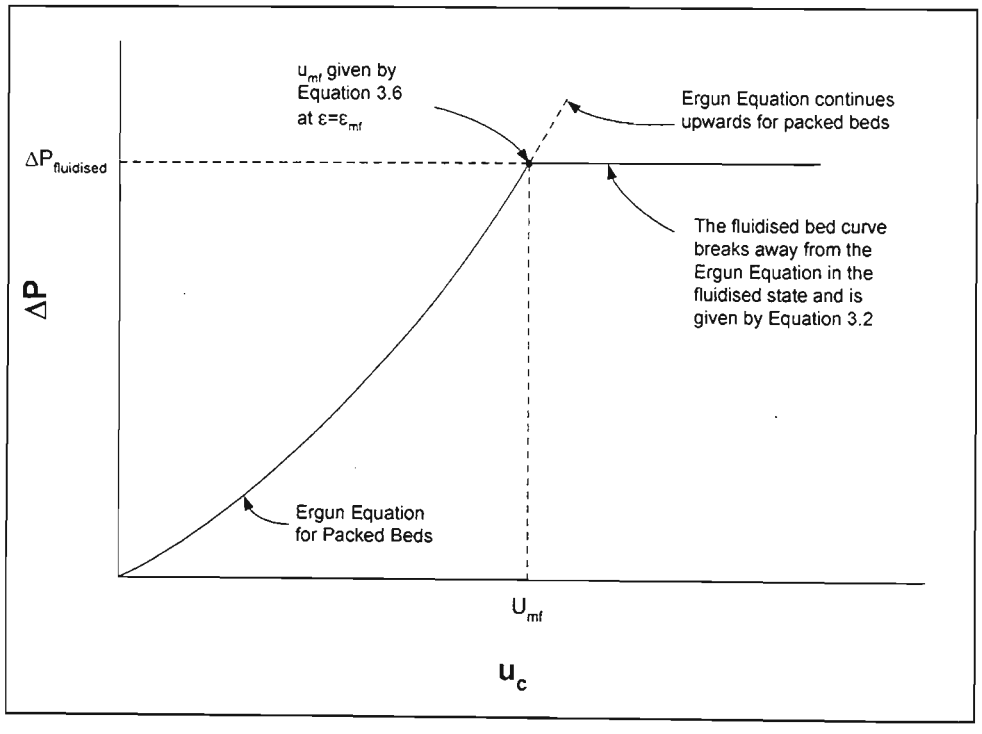

Figure 3.4: Illustration of pressure drop in the packed bed and in the fluidised bed [Adapted from Geldart, 1986].

In order to calculate u_{mf}, the voidage at the minimum fluidizing point (ε_{mf}) is required. As mentioned before, there are some reported values of ε_{mf} for several particles but the experimental evidence is limited and a typical value of 0.4 is used for ε_{mf} [Coulson, Vol2, 1997]. Using this value gives us the following equations for u_{mf}:

using equation 3.5 which is valid for laminar flow :

$$\left(u_{mf}\right)_{\varepsilon_{mf}=0.4} = 5.93\times10^{4}\,\frac{d_{sv}^{2}\left(\rho_s-\rho\right)g}{\mu} \tag{3.8}$$

and from equation 3.7 with some mathematical manipulation :

$$\left(\mathrm{Re}_{mf}\right)_{\varepsilon_{mf}=0.4} = 25.7\left(\sqrt{1+5.53\times10^{-5}\,Ga}-1\right) \tag{3.9}$$

u_{mf} is then calculated from the definition of Re_{mf}, which is the Reynolds number at u_{mf}. It is probable that the Ergun and Carmen-Kozeny equations over predicts the pressure drop for fluidised systems at the fluidizing point, but in the absence of any experimental evidence to alter the coefficients, the above equations can be used within their predictive errors [Kunni and Levenspiel, 1969].

Wen and Yu [1966] studied the experimental data from a variety of systems and found that at the minimum fluidizing point the following conditions existed for the relevant groups in the Ergun equation:

$$\frac{1}{\phi_s\varepsilon_{mf}^{3}} \cong 14 \tag{3.10}$$

$$\frac{1-\varepsilon_{mf}}{\phi_s^{2}\varepsilon_{mf}^{3}} \cong 11 \tag{3.11}$$

Using this information in equation 3.4 and substituting $d_{sv} = d_p\phi_s$ the following equation, which is valid for the whole range of Re numbers at u_{mf}, can be derived by carrying an identical process as used in the derivation of equation 3.7:

$$\left(\frac{\mathrm{Re}_{mf}}{\phi_s}\right) = \sqrt{(33.7)^{2}+0.0408\left(\frac{Ga}{\phi_s^{3}}\right)}-33.7 \tag{3.12}$$

Equation 3.12 has been found to predict u_{mf} to within a standard deviation of $\pm$ 34% [Kunni and Levenspiel, 1969]. If information on ε_{mf} and ϕ_s is available, then equation 3.7 is expected to give a more reliable prediction of u_{mf}.

3.4.2 Minimum bubbling velocity, u_{mb}

Coarse powders generally tend to start bubbling just above u_{mf}. Fine powders on the other hand behave differently. They are able to be fluidized at velocities greater than u_{mf} without the formation of bubbles. The bed expands uniformly up to a certain limit where small bubbles begin to appear at the surface of the bed. Beyond this limit, relatively large bubbles form periodically and the bed height begins to oscillate between a certain height range as the large bubbles burst through the bed surface periodically. The average of the velocities at which the bubbles appear and disappear is called the minimum bubbling velocity, u_{mb}. This generally is the point of the maximum bed height that can be achieved within the fluidized bed. A poor distributor design or disturbances in the bed can also result in pre-mature bubbling.

The minimum bubbling velocity u_{mb} was correlated by Abrahamsen and Geldart [1980] who studied 48 gas-solid systems and found that u_{mb} is a function of the density and viscosity of the fluidizing gas, the mean sieve size of the powder and the fraction of fines less than 45 μm. It is not dependant on particle density.

$$u_{mb} = 2.07e^{0.716F}\frac{d_p\rho^{0.06}}{\mu^{0.347}} \tag{3.13}$$

Where F is the fraction of fines less than 45μm and all units are SI.

Equation 3.13 is only valid for fine powders, less than 100μm mean size, which have u_{mf} values less than u_{mb}.

From equation 3.13 it can be seen that u_{mb} increases with pressure and an increase in temperature reduces u_{mb}. The former is as a result of the gas density term and the latter as a result of the gas viscosity terms.

3.4.3 Terminal falling velocity, u_o

The upper limit to gas flow rate is approximated by the terminal falling velocity of the particles. When entrainment occurs, the solids removed must be recycled or replaced to the bed in order to maintain steady-state operation. The terminal falling velocity can be

estimated by fluid mechanics using the following equation [Kunni and Levenspiel, 1969]:

$$u_o = \sqrt{\frac{4gd_p(\rho_s - \rho)}{3\rho C_{dr}}} \tag{3.14}$$

Where C_{dr} is the drag co-efficient determined experimentally.

Several correlations are available in the literature for the calculation of C_d which is a function of the particle's Reynolds number at the terminal falling velocity, Re_o. A more common correlation used is that formulated by Khan & Richardson [1989] for spherical particles given by equation 3.15:

$$\mathrm{Re}_o = \frac{\rho u_o d_{sv}}{\mu} = \left(2.33Ga^{0.018} - 1.53Ga^{-0.016}\right)^{13.3} \tag{3.15}$$

Equation 3.15 is valid only when the particle's motion is unaffected by the walls of the reactor.

To avoid solids carryover a gas velocity between u_{mf} and u_o must be used for fluidized operations. In calculating u_{mf}, a mean particle diameter is used, whilst in calculating u_o, it is important to use the smallest size particle present in an appreciable amount. The ratio $\frac{u_o}{u_{mf}}$ is usually between 10 and 90 and gives an indication of the flexibility of the operation. The ratio is smaller for large sized particles indicating a narrow range of operation than with smaller particles. The range of operation is further determined by the degree of channeling and slugging, and this is a serious concern when dealing with large uniformly sized particles where it is often difficult to fluidize the bed at all.

3.5. Hydrodynamics of bubbling fluidised beds

As stated earlier, in gas solid systems only a limited uniform expansion of the bed occurs as the gas velocity is increased. At high gas flow rates, much of the gas passes through the bed in the form of bubbles and makes small contribution to the expansion of the bed. It is essential to distinguish between the two phases present in a bubbling bed, the bubble or lean phase and the

particulate or dense phase. The bubble phase is the gas voids that move upwards within the bed and they contain virtually no bed particles. The dense phase consists of the particles fluidized by the relatively slow moving interstitial gases. A bubbling bed is usually defined by the dispersed bubble phase and the continuous dense phase. The bubbles are the main source of solids mixing in a bubbling bed and also contribute to the temperature uniformity and high bed heat transfer coefficients characteristic of fluidised beds.

The gas in a bubble is not in direct contact with the bed particles, and thus cannot take part in any reactions between the gas and solid bed particles. It is for this reason that bubbling in a fluidised bed reactor is undesirable. The interchange between interstitial gas and gas in the bubbles can thus determine the performance of fluidised bed reactors. Several models are presented in the literature on bubble behaviour and the interaction of these bubbles. Postulations and studies have been done on individual bubble behaviour and the theory on bubble formation, bubble shape and dispersion models are well documented in the literature [Geldart, 1971, 1986].

The incorporation of baffles in a fluidised bed of coarse solids substantially eliminates fluctuations within the bed. The arrangement of the baffles is crucial and down facing horizontal surfaces are avoided as they cause areas within the bed to de-fluidise. It is for this reason that vertical tubes are more favourable over horizontal tubes when used in a heat transfer application. The horizontal tubes exhibit low heat transfer rates due to the localised partial de-fluidization that occurs.

Stirring can also be another effective means of improving the quality of fluidisation. In some instances, stirring need only be used to initiate fluidisation and once fluidisation has been established, the stirrer could be stopped.

When there is a wide range of particle sizes in the bed material, a bed which is tapered offers more stable fluidisation by providing the minimum cross sectional area at the bottom. Coarse particles accumulate at the bottom of the bed and tend to be fluidized and assist in the distribution of the gas. At the same time, the reduced velocity at the top of the bed reduces the carryover of fines. A tapered bed is particularly useful as well if the pressure drop across the bed is substantial, as in the case of very deep beds. The varying cross sectional area can be designed such that a constant velocity is maintained throughout the bed.

Gas solid beds are difficult to scale up because of the strong influence of the column diameter on the hydrodynamics. The primary cause of the scale dependence is the fact that the rising velocity of the bubbles is scale dependant. Existing scale up procedures in the literature are

largely empirical. Computational fluid dynamics (CFD) is a tool largely used in the scale up of fluidised beds [Krishna & van Baten, 2001].

Slugging fluidisation can occur in beds of small diameter and is therefore encountered often in laboratory and pilot plant units. The wall effects reduce the rise velocity of the bubbles and cause the bubbles to be more rounded. Bubbles formed at the distributor grow by coalescence until they reach the size of slugs, which is typically a bubble diameter greater than 0.6 times the bed diameter. When slugging occurs, the bed height oscillates widely. Each time a slug brakes through the top of the bed, the level drops sharply, and then rises again until the next slug breaks through.

3.6. Heat transfer in a fluidised bed

One of the most important features of a fluidised bed is its temperature uniformity which exists in both the radial and axial directions as a result of the bubble induced circulation of solids. This makes fluidised beds ideal in circumstances where good temperature control is required. Up to a one-hundred fold increase in the heat transfer co-efficient is achieved in a fluidised bed when compared to with just the gas alone. It is suggested [Coulson and Richardson, 1997] that this can be attributed mainly to two factors:

- solid particles having a high heat capacity serve as the heat transfer agents between the bed body and the heat transfer surface
- erosion of the laminar sub layer at the surface of the heat transfer surface by the particles

There is an extremely large area of solids exposed to the gas. Such a large area greatly facilitates solid to gas heat transfer properties. Due to the solids mixing that occurs within the bubbling gas fluidised bed, temperature gradients are reduced and the bed possesses a high effective thermal conductivity.

The heat transfer coefficients depend on many factors, the degree of fluidisation, system geometry, flow patterns within the bed, gas and solid properties and the conditions at minimum fluidisation. The one property that has negligible influence is the thermal conductivity of the solids.

There are two heat transfer mechanisms at work here in a fluidised bed that needs to be considered:

i) Heat transfer between particles to gas : Solid-gas heat transfer

ii) Heat transfer between the bulk bed and a heat transfer surface : Bed-surface heat transfer

Descriptive models of the mechanisms available in the literature are of limited use as they require knowledge of parameters usually not available.

3.6.1 Solid – gas heat transfer

Due to the large solids surface areas exposed to the gas, the particle to gas heat transfer is very rarely the limiting factor to the amount of heat that can be transferred to the bed. Correlations in the literature are based on one of two assumptions on the nature of the gas flow through the bed:

- Backmix flow of gas as indicated by the uniform bed temperatures
- Plug flow of the gas and the almost uniform temperature of the gas in the bed represents the flat tail of the exponential temperature decay for plug flow

Each assumption leads to different temperature driving forces and different heat transfer coefficients. Up to a thousand fold variation exists between different workers, [Kunni & Levenspiel, 1969].

The actual flow pattern of the gas fits neither of the two patterns perfectly. Results based on the plug flow assumption from various workers correlate well with each other, whereas results based on the back-mix assumption show considerable scatter. Kunni & Levenspiel [1969] pointed out that the most realistic model to use is the plug flow model and correlated the following equation in SI units for the heat transfer coefficient between the solids and gas valid for particle Reynold's numbers up to 50:

$$Nu_p = \frac{h_p d_{sv}}{k_g} = 0.03\,\mathrm{Re}^{1.3} \qquad \textbf{(3.16)}$$

where Nu_p is the Nusselt number for gas to particle heat transfer

h_p is the gas to particle heat transfer coefficient

k_g is the thermal conductivity of the gas

3.6.2 Bed – surface heat transfer

Several correlations are available in the literature for the heat transfer coefficient between the fluidised bed and the vessel walls or between the bed and immersed tubes. The equations however must be used with extreme caution as the heat transfer coefficient is highly dependant on the flow patterns of the gas and solids and the system geometry. Kunni and Levenspiel [1969] lists several correlations that can be found in the literature and suggested the most reliable correlation for heat transfer to the vessel walls to be that proposed by Dow & Jakob [1951] [SI units] :

$$\frac{h_w d_t}{k_g} = 0.55\left(\frac{d_t}{L}\right)^{0.65}\left(\frac{d_t}{d_{sv}}\right)^{0.17}\left(\frac{(1-\varepsilon)\rho_s C_{ps}}{\varepsilon\rho C_{pg}}\right)^{0.25}\left(\frac{u_c d_t \rho}{\mu}\right)^{0.8} \tag{3.17}$$

where h_w is the heat transfer coefficient between the bed and wall surface

d_t is the vessel or tube diameter

C_{ps} is the specific heat capacity of the solids

C_{pg} is the specific heat capacity of the gas

Vreedenberg [1952] studied the effect of several factors on the heat transfer coefficient on immersed tubes and recommended the following correlation in SI units for horizontal immersed tubes:

For $\frac{d_{ti}\rho u_c}{\mu} < 2000$:

$$\frac{h_w d_{ti}}{k_g} = 0.66\left(\frac{C_{pg}\mu}{k_g}\right)^{0.3}\left[\left(\frac{d_{ti}\rho u_c}{\mu}\right)\left(\frac{\rho_s}{\rho}\right)\left(\frac{1-\varepsilon}{\varepsilon}\right)\right]^{0.44} \tag{3.18}$$

where d_{ti} is the outer diameter of the horizontal immersed tube

For $\frac{d_{ti}\rho u_c}{\mu} > 2500$:

$$\frac{h_w d_{ti}}{k_g} = 420\left(\frac{C_{pg}\mu}{k_g}\right)^{0.3}\left[\left(\frac{d_{ti}\rho u_c}{\mu}\right)\left(\frac{\rho_s}{\rho}\right)\left(\frac{\mu^2}{d_{sv}^3\rho g}\right)\right]^{0.3} \tag{3.19}$$

3.7. Design of fluidised bed systems

A fluidized bed reactor normally consists of a more or less standardized system of equipment associated with just the fluidized bed reactor itself. The major parts of the system relevant are:

- Fluidization vessel
- Instrumentation
- Solids feed system
- Solids discharge system
- Solid-gas separator

Continuous systems require a solids feed and discharge system, and since this work focuses on a batch process, a discussion of these systems will be omitted. Small scale systems also omit the need for a solid-gas separation unit such as a cyclone, by using of a series of filters to limit the entrainment of solids in the gas. Entrained solids are returned to the bed in one of two main ways as illustrated in Figure 3.5 below and small scale systems often utilise settling as an effective means of returning the bed solids.

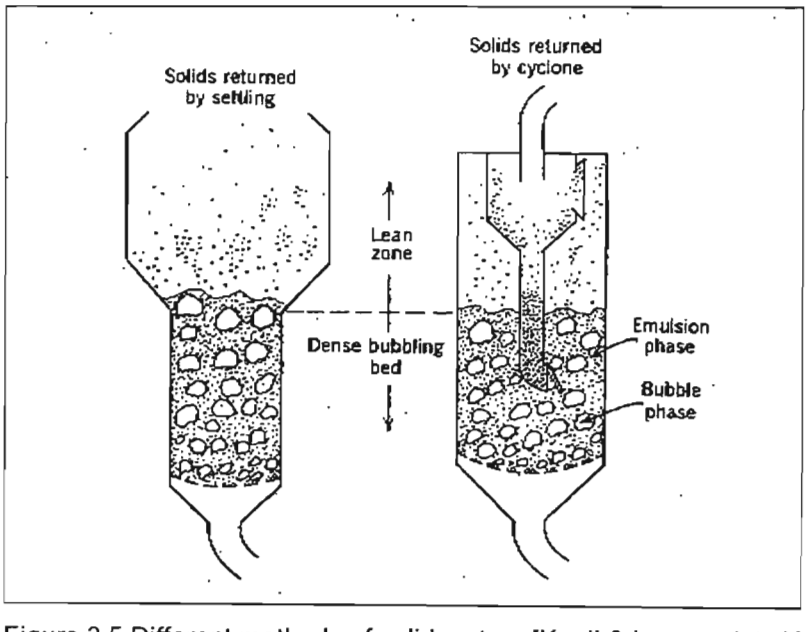

Figure 3.5 Different methods of solids return [Kunii & Levenspiel, 1969]

The fluidization vessel is broken down into three characteristic sections:

i) The fluidized bed section

ii) Freeboard area or disengaging space

iii) Gas distributor

The most common shape of the fluidisation vessel is a vertical cylinder although there is no real limitation on shape [Perry & Green, 1997]. On smaller scale units two dimensional columns of rectangular or square cross-section or semi cylindrical columns are common. For experimental purposes, column diameters less than 0.1m give misleading results. Smaller columns give rise to slugging and bridging effects are severe. As a general rule, the column diameter should never be less than the 100 times the particle diameter. The upper limit of the column diameters for laboratory scale is 0.6m. It is sufficiently large enough to produce meaningful results, yet small enough to avoid excessive costs [Geldart, 1986].

3.7.1 Bed section

Factors like gas-contact time, solids retention time and the space required for internal exchangers need to be considered when determining the required bed height. Bed heights are not less than 0.3m or more than 50m [Perry, 1997]. Beds operating at high temperatures make use of a refractory lined steel shell which insulates the shell from the high temperature and protects the shell from abrasion by the violently bubbling bed. Due to the motion of the bed, the reactor must be securely supported.

3.7.2 Freeboard area

Space must be provided above the bed for bed expansion and for disengaging entrained material as the bubbles burst on the surface of the bed. This distance between the top of the fluidised bed and the gas exit outlet is called the freeboard or disengaging area. Classification of solid particles occurs in the freeboard area. As the bubbles burst at the surface entraining some solid particles, the coarser more dense particles are returned to the bed whilst the finer and lighter particles are carried upwards. The finer particles have a greater rate of entrainment and the higher the concentration of the fines, the greater the entrainment. The distance above the bed at which the entrainment is constant is the transport disengaging height (*TDH*). Gas outlets and cyclones are usually located above this height if entrainment is undesirable.

Entrainment and carryover cannot be calculated from first principles and empirical correlations often give predictions that differ by a factor of 100 [Geldart, 1986]. Perry [1997, Fig 17-8] presented a reliable correlation of TDH as a function of gas velocity and bed diameter.

3.7.3 Gas distributors

The gas distributor strongly influences the quality of fluidization obtained in the bed. To summarize its importance, a high pressure drop across the distributor plate ensures good mixing and eliminates hot spots and gas channeling. An excessively high pressure drop is undesirable because of the wasted cost of pumping the fluidized gas. Hence a compromise in between the two extremes must be met. Several workers have proposed suggestions in this area. Perry and Green [1997] suggest the pressure drop across the distributor (ΔP_d) should be between 0.5 kPa to 20kPa. Zenz [1968] proposed that ΔP_d should be at least 30 percent of the pressure drop across the bed of solids (ΔP_b). Argarwal *et al* [1962] suggest that ΔP_d should be between 0.1 to 0.3 times ΔP_b or 3.45 kPa, whichever is the greater.

Qureshi and Creasy [1979] concluded from their study of published information, that the ΔP_d required depends on the bed depth to diameter ratio and proposed that for satisfactory operation with a perforated plate distributor:

$$\frac{\Delta P_d}{\Delta P_b} = 0.01 + 0.2\left[1 - \exp\left(\frac{-D}{2L}\right)\right] \qquad \textbf{(3.20)}$$

where D is the bed diameter.

Equation 3.20 gives a maximum value of 0.21 for $\frac{\Delta P_d}{\Delta P_b}$ applicable for a shallow bed. Geldart [1986] advises that if the bed material is difficult to fluidize, that this value should be increased to 0.3. The distributor plate must not only be able to achieve this required ΔP_d, but it also has to prevent solids from falling through into the windbox or plenum area below the distributor plate. There are several available designs for distributors but the simplest case for a bench scale unit is the perforated plate. Geldart [1986] states that for a perforated plate, as long as the width of the holes is less than 10 particle diameters, little weeping of solids through the distributor can be expected.

A more classic type of a distributor designed to reduce, if not eliminate weeping of solids altogether, is the tuyere as shown in figure 3.6 below:

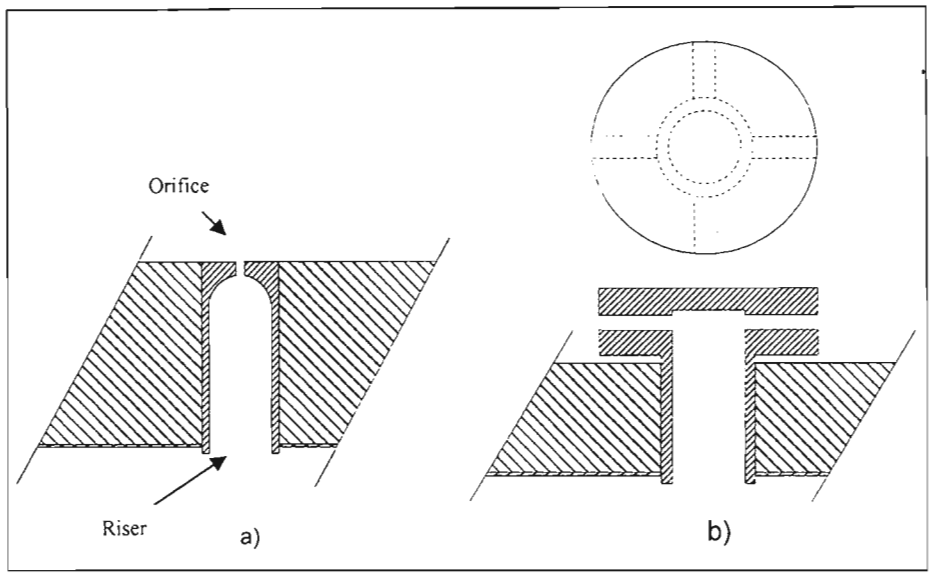

Figure 3.6: Tuyere gas distributors. a) Single hole tuyere b) Multiple hole tuyere (Adapted from Perry and Green [1999] and Coulson and Richardson [1997])

Tuyeres are widely used as they are well suited to high temperature applications by providing a protecting solids layer over the distributor plate in fluidized bed combustors. A bubble cap type tuyere is also commonly used.

The pressure drop in a tuyere is dominated by the velocity in the exit holes and account for more than 90% of the pressure drop across the distributor [Lombardi *et al*, 1997]. The number of holes in a multi-hole tuyere is selected to give the required ΔP_d. For design purposes the distributor plate is treated as a multiple-orifice distributor. The pressure drop across the distributor can then be expressed as in SI units:

$$\Delta P_d = \frac{u_{or}^2 \rho g}{2C_d^2} \tag{3.21}$$

$$u_{or} = \frac{u_w}{f_{or}} \tag{3.22}$$

where u_{or} is the gas velocity through the orifice given by equation 3.22
C_d is the orifice discharge coefficient
u_w is the superficial gas velocity in the windbox or plenum chamber
f_{or} is the fraction of the total area of the distributor open to gas flow

The orifice discharge coefficient is a function of the Reynolds number at the orifice (Re_{or}) and the orifice shape. For square edged circular orifices with a diameter (d_{or})

much larger than the plate thickness (t), (i.e. $t/d_{or}<1$) C_d is taken as 0.6 when fluidized solids are present [Lombardi *et al*, 1997]. For $t/d_{or}>0.09$, C_d can be estimated by a correlation given by Qureshi and Creasy [1979] in consistent units:

$$C_d = 0.82\left(\frac{t}{d_{or}}\right)^{0.13} \tag{3.23}$$

Lombardi *et al* [1997] showed that equation 3.23 overestimates C_d by approximately 32% for tuyere flow coefficients and 14% for perforated plates. He also showed that for tuyere distributors with riser cross sectional area A_r twice the head holes cross sectional area A_{or} (i.e. $A_r/A_{or} = 2$) and for Re_{or} in the range from 1800 – 22 000, C_d did not vary with Re_{or} and can be obtained as a function of d_{or} from equation 3.24 below:

$$C_d = 0.599 + 0.0324d_{or} - 0.00274d_{or}^2 \tag{3.24}$$

Geldart [1986] derived the following equation to estimate the pressure drop in a multiple hole tuyere:

$$\Delta P_d = \rho_w \frac{3u_r^2}{4}\left[1+\left(\frac{d_r}{d_{or,eq}}\right)^4\right] - \rho_w \frac{u_w^2}{2} \tag{3.25}$$

where ρ_w is the gas density in the windbox or plenum chamber

u_r is the gas velocity in the riser

$d_{or,eq}$ is the diameter of a hole having the same area as the total number of orifices in the tuyere

To determine the number of tuyeres required per unit cross sectional area (N) is then given by [SI units]:

$$N = \frac{u_w}{A_r u_r} \tag{3.26}$$

where N is the number of tuyeres required per unit cross sectional area

A_r is the cross sectional area of the riser

The gas velocity entering the bed should be limited to less than 70m/s to minimize attrition of the bed particles [Perry & Green, 1997]. Whitehead and Dent [1967] and Whitehead *et al* [1970] studied the pressure and flow maldistribution at the distributor level of a number of fluidized beds and determined the minimum superficial gas velocity u_{min} for continuous operation of all tuyeres. Their correlation, valid for beds with cross sectional areas between $0.09m^2$ and $5.9m^2$ is given by equation 3.27 below:

$$\frac{u_{\min}}{u_{mf}} = 0.7 + \sqrt{0.49 + \frac{3.23\times10^{-7} N_T^{0.22} K_d \rho_s H}{u_{mf}^2}} \qquad (3.27)$$

where u_{min} and u_{mf} is in ft/s

N_t is the total number of tuyeres

K_d is the distributor flow factor, $60u\sqrt{\Delta P_d}$, u in ft/s and ΔP_d in lb/ft^2

H is the fluidized bed height in ft

ρ_s is in lb/ft^3

For complicated tuyere designs, it is advised in the literature to determine the pressure drop in a pilot plant or "cold model" so that the u_{or} can be selected to give the required pressure drop under operating conditions [Geldart, 1986].

The usual scale up or scale down procedure for experimental fluidized beds is to keep the height fixed while varying the diameter and hence the aspect ratio. This means the distributor of the small column should be identical to the full scale one, in other words it should be a portion of the full scale unit rather than a scaled down replica [Geldart, 1986]

3.7.4 Instrumentation

3.7.4.1 Temperature

Temperature is usually measured very simply by standard temperature sensing elements like thermocouples. Due to the high abrasion wear associated with horizontal tubes in the bed, it is common practice to use vertical tubes in the bed. For high temperatures optical pyrometry can be used.

To determine the gas-to-solids heat transfer co-efficient it is required that the gas and solids temperatures be determined individually. For this purposes micro-thermocouples are often used to measure the solids temperatures and the gas temperature is measured using high pressure drop suction thermocouples.

To determine the bed-to-surface heat transfer co-efficient, measurements of wall temperature and the bulk bed temperature is required and both are measured by means of thermocouples.

3.7.4.2 Pressure

Pressure taps are positioned at regular intervals up the side of the fluidized bed reactor vessel. There must always be a pressure tap installed in the windbox below the distributor plate. Pressure taps just above and below the distributor plate can indicate whether the distributor holes become blocked or changes in the distributor performance occurs. The bed height is normally controlled by an overflow at a given point in the bed. In the absence of this provision, pressure measurements taken at various heights in the bed are used to determine bed levels.

3.7.4.3 Flow measurement

Although the pressure drop across the distributor plate is an indicator of the gas flow rate, it is advisable to measure the gas flow rate by another method. Measurement of flow rates of clean gasses usually is very simply and taken upstream by using a rotameter or an orifice plate. Flow measurement of dirty gases is avoided. Solids feed rate is measured by a weigh belt or using load cells on a hopper feeding the bed. Gas composition is measured by the use of sampling tubes within the bed, freeboard and gas outlet points. Solids samples are analyzed after removal from the bed through the use of exit ports or a sample grabber.

This concludes the basic theory needed for the design of a fluidized bed reactor. We have captured the core knowledge required to proceed with the design of a fluidized bed reactor. The following chapter presents the core design details of the pilot plant built for this work and discusses some of the commissioning experiences that contributed to design changes during the startup of the unit.

CHAPTER 4

EQUIPMENT DESIGN AND OPERATION

This chapter focuses on the equipment design and operation of the pilot plant built for this work. It also discusses the approach used for the design and construction of the reactor and the downstream and upstream processes.

4.1 Design basis

4.1.1 Reaction information

An overall heat of reaction requirement of 3.489 MJ/kg of BLS (endothermic) was used for design calculations as supplied by TRI/MTCI based on their experimental findings. The specific heat capacity of 60% BLS content black liquor is between 2.5-2.9 kJ/kg.°C as supplied by the Sappi Stanger mill.

4.1.2 Pilot unit capacity and source of heating

- This pilot unit is based on the test work done by TRI/MTCI on their 4" reactor unit. It's a larger scale capacity unit than the TRI/MTCI unit and the design of the unit was independent of the TRI/MTCI design and a fresh approach to the design was used. The need for a larger scale unit was identified by TRI/MTCI and proposed by them to Sappi.
- The amount of heat that is provided for the heat of reaction is proportional to the amount of black liquor solids that can be gasified. It was assumed that this heat will be provided by an internal electrical heater, as this method was tried and proven by TRI/MTCI in their 4 inch diameter unit. Based on the amount of

thermal energy that enters the bed, it automatically sets the capacity of the unit, and upstream equipment was designed on this basis.

- The heat required for maintaining the bed at operating temperature was provided by the superheated steam.
- An additional source of heat was designed to provide the energy to maintain the reactor and its associated equipment at operating temperatures. TRI/MTCI used external heaters on their test unit.

4.1.3 Feed specifications

- Soda black liquor was supplied in a 40-45 wt% solids solution from the Sappi mill. The dissolved solids tend to settle out when left standing for long periods of time. The black liquor is almost solid at room temperature and was heated to 80-90 °C before use.
- Initial start up and make-up bed material consisting of sodium carbonate particles was provided by Sappi from their Copeland unit.
- Saturated steam was available at 6 bar (g) and needed to be let down and superheated for use in the reactor.
- Although the black liquor was supplied at 40-45%, the design was based on a 60% feed with the intention that the black liquor feed would be concentrated in a feed preparation stage. However the actual solids content of the black liquor feed used was constrained to 45% by the poor operation of the black liquor injection tube and spray nozzle and is discussed later in this chapter. Hence the black liquor injection tube would be the next bottleneck when up-rating of the unit is considered.
- SASAQ bagasse based black liquor was synthesized in the laboratory using the Soda bagasse based black liquor as a base. The feed is unique liquor for this application. This involved the addition of potassium chloride (KCl), potassium sulphate (K_2SO_4), sodium sulphate (Na_2SO_4) and silica to the black liquor. 50ml of a water solution containing:
  - 5.8 g/l KCL
  - 20.4 g/l K_2SO_4
  - 47.6 g/l Na_2SO_4
  - 254.4 g/l $Na_2SiO_3.5H_2O$

  was added per kg of black liquor.

4.1.4 Materials of construction

- All reactor material was a suitable grade of stainless steel due to the highly caustic nature of the black liquor as well as the high operating temperatures.
- Normal carbon steel was used where the application permitted.

4.1.5 Utilities

- Saturated steam was available at 6 bar (g).
- Mains water was available at 650 kpa (g).
- Instrument air was available at 4 bar (g).

4.2 Characterization of the sodium carbonate bed material

A particle size analysis of the bed material supplied from Sappi's Copeland unit was carried out by means of sieves and the results are shown in table 4.1 below:

Table 4.1: Size distribution of starting bed material - 9 October 2001

Size Range / μm	Mass % x_i
+1000	0.0
1000/710	28.6
710/500	54.5
500/355	11.5
355/250	4.1
250/150	1.0
-150	0.2
Total	100

The Sauter Mean Diameter of the particles is given by [Coulson & Richardson, 1996]:

$$d_p = \frac{1}{\sum \frac{x_i}{d_i}} \qquad \textbf{(4.4)}$$

where x_i is the mass % of particles in a certain size range

d_i is the mean particle diameter in the size range

From figure 3.2 for a particle mean diameter of 583 μm, the bed material is classified as a Geldart type B powder. This means we can expect bubbling to occur at just past u_{mf} with no limit on bubble size.

The particles were assumed to be spherical which was evident from a visual inspection of the bed particles. Using equations 3.12 and equation 3.9, u_{mf} was predicted to be in the range of 28 to 32 m/s respectively. The upper end of fluidization given by the terminal falling velocity of the particles was calculated from equation 3.15 to be 1.9 m/s.

4.3 Process flow diagram (PFD) and process description

The pilot plant is divided into the following sections as shown in Figure 4.1below:

- S100 – Black liquor storage and feed prep
- S200 – Gasification
- S300 – Gas sampling
- S400 – LPG Storage

A complete set of process flow diagrams can be found in Appendix A. Figure 4.2 below shows an overall PFD of the pilot plant.

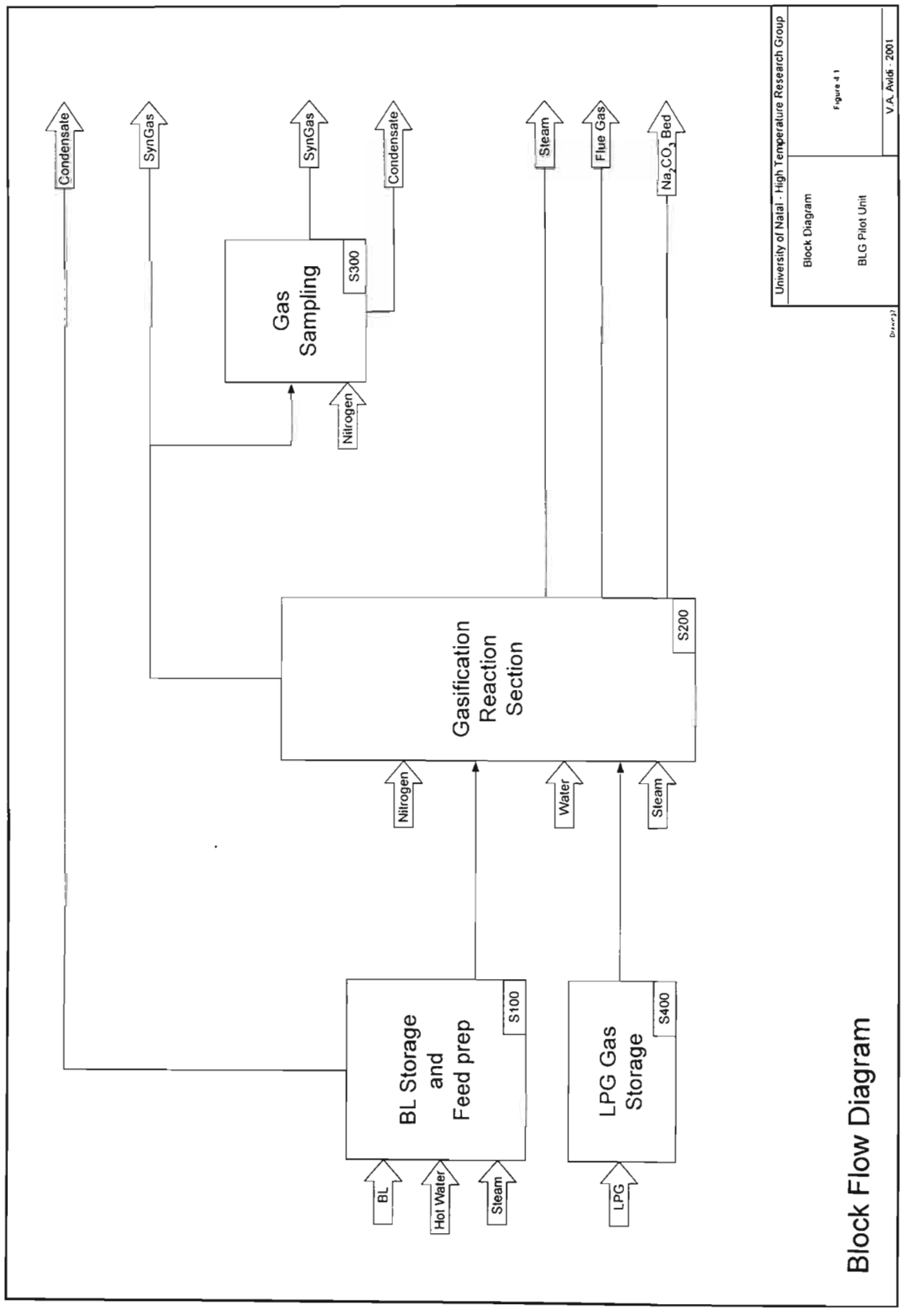

Figure 4.1: Block flow diagram of pilot unit

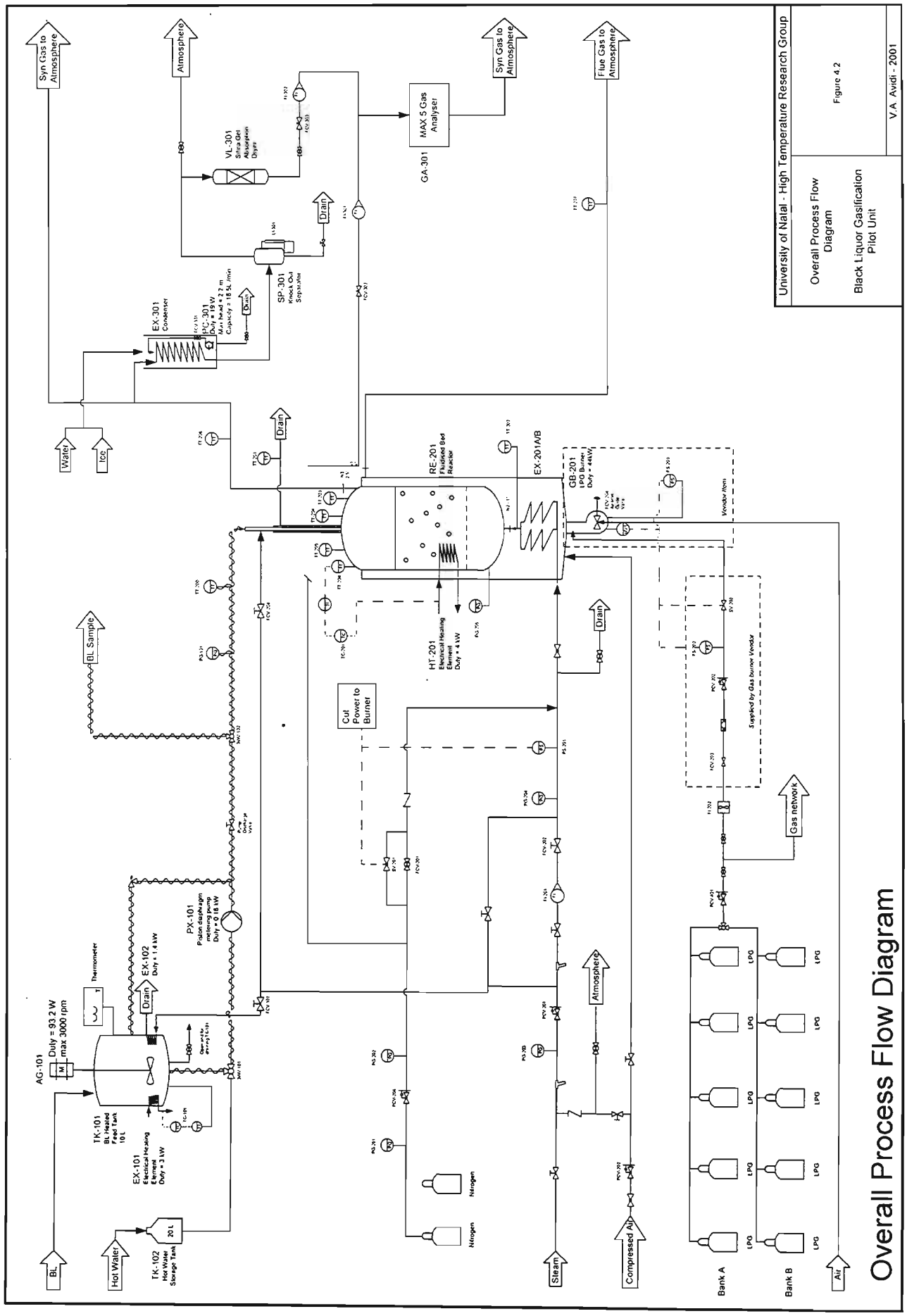

Figure 4.2: Overall process flow diagram of pilot unit

Black liquor was stored in polypropylene containers at a temperature of 5°C in a refrigerated room. In preparation for a run, a 50 L stainless steel drum containing the black liquor was placed overnight in an oven maintained at 90°C. The hot black liquor was then transferred manually to the black liquor heated feed tank TK-101. The tank was fitted with an immersed agitator AG-101 to prevent the formation of a skin layer on the liquid surface and the settling out of the solids. The black liquor was maintained at 85-90°C by an internal electrical heating element EX-101 and an immersed steam coil EX-102.

The black liquor was pumped by PX-101 into the reactor via a steam jacketed black liquor injection tube. The black liquor feed line was electrically heat traced to prevent the black liquor from cooling and solidifying in the lines.

In the reactor the black liquor undergoes the gasification reactions with the fluidizing steam at a temperature of approximately 620°C and atmospheric pressure to form solid sodium carbonate bed particles and a hydrogen rich syn-gas. The sodium carbonate accumulates in the bed and the mixture of syn-gas and excess fluidizing steam passes overhead to the atmosphere via a vent pipe.

A sample stream from the syn-gas vent line was withdrawn for use in the gas sampling system to analyze for CO, CO_2, and a combined combustible group composition. Gas is drawn through the condenser EX-301, the knock out separator SP-301 and an absorption dryer VL-301, by a vacuum pump included in the MAX 5 gas analyzer. EX-301 was fitted with a submerged pump to circulate ice water at 0°C to the top of the condenser to prevent the formation of a skin layer around the immersed sample tube. Ice is added to the shell side periodically to maintain the submerged coil at 0°C, and the level maintained by draining the contents through a drain valve fitted at the bottom of EX-301. The cooled gas and condensed liquids pass into SP-301 where the gas is separated out from the condensed liquids and passes through to VL-301 where entrained moisture is removed. The dry gas is diluted with nitrogen before passing into the MAX 5 for analysis.

The solid bed material was removed at the end of the run using a vacuum cleaner and a sample of the bed material was taken for analysis of carbon, silicate, sodium and sulphur content to determine reduction efficiencies. A sieve analysis was done on the bed material to obtain particle size distributions to establish natural particle degradation patterns.

4.4 S100 – Black liquor storage and feed preparation

The primary function of this section is to store and deliver the black liquor safely and under controlled conditions to facilitate process requirements. The original scope of the project was to treat a 60% solids black liquor stream and consequently most of the data used for sizing the equipment was evaluated at a solids content of 60%. Viscosity data was measured at Sappi Stanger's laboratory facility. The solids content of the black liquor was measured by drying samples in a drying oven set at 105°C for a period of 5 days. The results of these tests are shown in Table 4.2 and 4.3 below. Density of the 42% black liquor at 85°C was evaluated in the lab and found to be 1237 kg/m^3.

Table 4.2: Results of weight % solids tests on black liquor samples - 14 January 2001

Sample No.	Wt% solids
1	43
2	41
3	42

Table 4.3: Viscosity as a function of solids content

20 °C		85 °C	
BLS %	**Viscosity mPa.s**	**BLS %**	**Viscosity mPa.s**
53	160	20	2
55	260	37	18
57	430	45	43
58	630	46	65
59	800	51	185
60	1010	52	160
61	1300	59	501
61	1600	60	556

4.4.1 TK-101 – Black liquor storage tank

At room temperatures the 42% black liquor solution is almost solid and needs to be stored at elevated temperatures when in use. An industry practice is to keep the black liquor at a temperature between 60 – 80 °C. The storage tank needed to be fitted with internal heating and a stirrer to prevent settling out of the solids from solution. Due to

the caustic nature of the black liquor, pH between 12 and 13, the material of construction had to be of a suitable grade stainless steel.

An 8L stainless steel tea urn was modified to fulfill the role of the black liquor storage tank, TK-101. The internal 3 kW electric heating element with its own temperature control proved to be sufficient to heat up the tank contents to 85°C. An additional steam coil EX-102 was installed to allow for quicker and more even temperature distribution throughout the tank and as a standby heat source should the element fail during use. The steam coil was constructed out of ¼" stainless steel tubing into a 140mm diameter coil with a total coil height of 10 cm on a 6 mm pitch. Using 1 bar(g) steam as the heat source, a calculated additional duty of 1.4 kW was added to the tank. This is based on an average overall heat transfer co-efficient of 306 $W/m^2.°C$ [*Perry & Green*, 1997, Table 11-2].

A drain valve was installed at the base of the tank for draining purposes. The product off take point was located 30mm from the tank base to protect the electrical element should the tank be accidentally emptied during operation. The lid of the urn was cut to facilitate the stirrer. Figure 4.3 below shows a photo of the tank and its internals. A 93.2W stirrer motor by Voss Instruments was used with a custom made paddle to provide mixing (AG-101). The lid is also fitted with a thermowell to house a thermometer for measurement of the tank temperature.

Figure 4.3: Photo of TK-101 showing tank internals.

4.4.2 PX-101 – Black liquor delivery pump

The delivery rate of black liquor is connected to the treatment capacity of the gasifier. Thus they were designed concurrently. A 4kW electrical resistive heating element was procured for the gasifier, and this duty set the boundary limit for the amount of black liquor that the reactor would be able to gasify. Based on the overall heat of reaction of 1500 BTU/lb of BLS, a 60% black liquor feed stream, equation 4.5a and 4.5b were derived based on negligible heat transfer resistances [SI units]. Calculations showed that the reactor would be able to treat up to 3.1 L/hr of a 60% BLS content black liquor. Future upgrade plans for the internal heating element included a second 4kW heating element translating into a probable gasification treatment rate of 6.2 L/hr.

$$Q_{total} = Q_{sensible} + Q_{latent} + Q_{rxn} \quad \textbf{(4.5a)}$$

$$= m_{H_2O} C_{p.H_2O} (\Delta T) + m_{H_2O} \Delta H_{H_2O} + m_{BLS} \Delta H_{rxn} \quad \textbf{(4.5b)}$$

where Q_{total} is the total energy required to gasify the black liquor.

$Q_{sensible}$ is the energy required to get the black liquor from supply temperature to the boiling temperature.

Q_{latent} is the latent heat to vaporize the water contained in the black liquor.

Q_{rxn} is the energy required for the gasification reactions.

m_{H_2O} is the mass of water.

m_{BLS} is the mass of black liquor solids.

ΔH_{H_2O} is the latent heat of vaporization of water.

ΔH_{rxn} is the average heat of the gasification reactions.

ΔT is the difference in temperature between the black liquor reactor entrance temperature and the boiling point.

Figure 4.4 below shows the plot of Equation 4.5b :

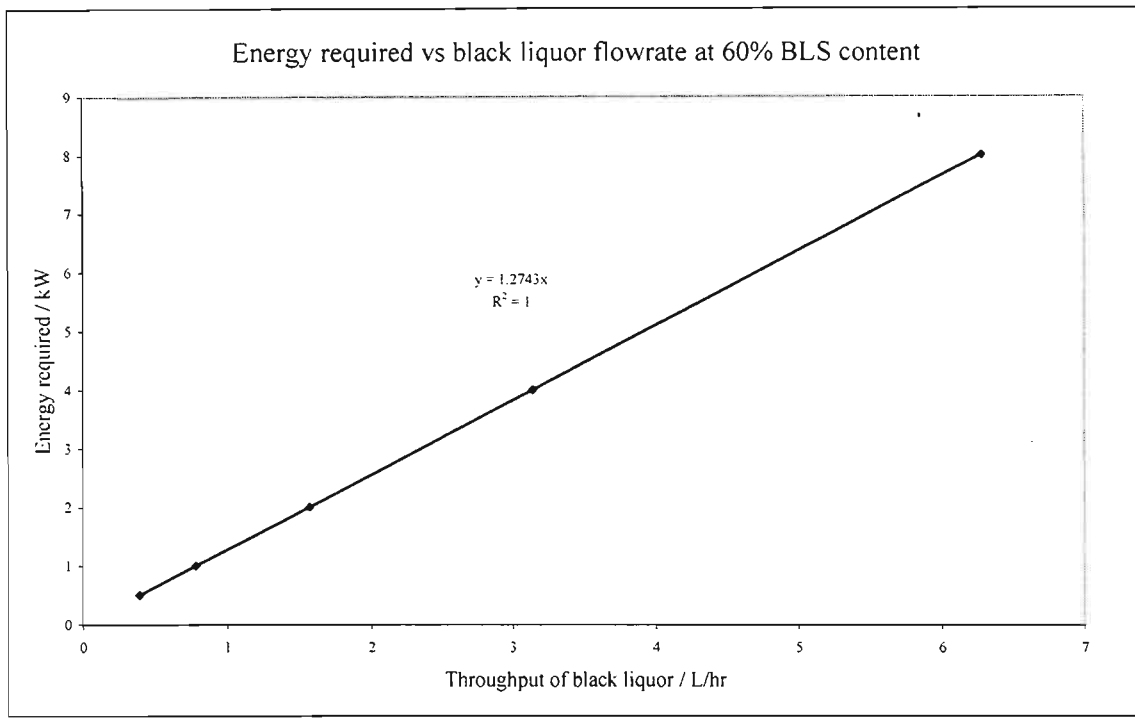

Figure 4.4: Plot of gasification heating requirement as a function of a 60% BLS black liquor throughput.

The pump discharge pressure was determined by the line and black liquor nozzle pressure drop. The results of calculations for the injection tube pressure drop are represented in figure 4.5 below for a 1 meter ¼" black liquor injection tube fitted with a nozzle consisting of three 1mm holes.

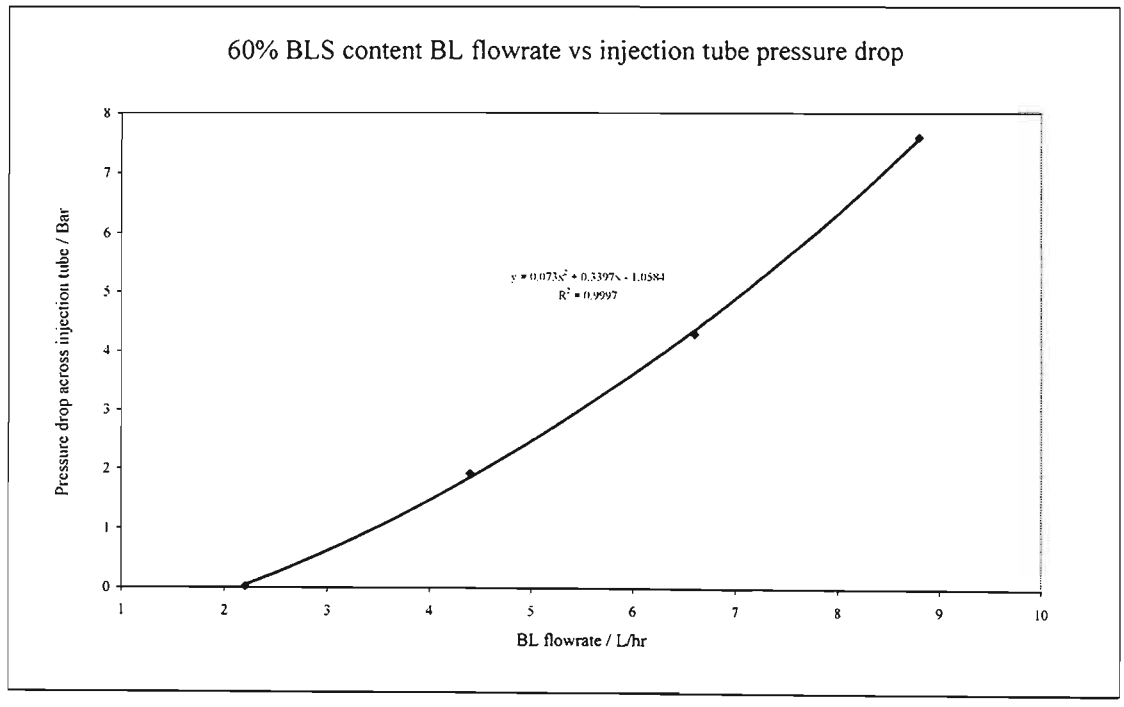

Figure 4.5: Results of pressure drop calculations for a 1m ¼" BL injection tube fitted with a nozzle consisting of three 1mm holes.

The pump delivery pressure included over design to cater for the future upgraded gasification capacity of the reactor to 6.2 L/hr.

These calculations were verified in the lab by quick trial experiments to make certain that a 7 bar delivery pressure would be sufficient to push the black liquor through the tube and the approximate 6 bar pressure drop across the nozzle would be sufficient to create a satisfactory spray pattern from the nozzle. The tube was filled with a sample of molasses diluted with water such that the viscosity was equivalent to that of 60% black liquor at 112°C. A jet of air was injected into the tube and the spray pattern from the nozzle observed. Air pressures were varied from 2 bar(g) up to 7 bar(g). A delivery pressure of 7 bar(g) produced the best spray pattern and consequently a pump delivery pressure of 7 bar(g) was selected. A 30% design safety factor was included to specify the pump delivery pressure as 9.1 bar(g).

Given the pump requirements, figure 4.6 from *Perry & Green (1997)* below was used to select the type of pump.

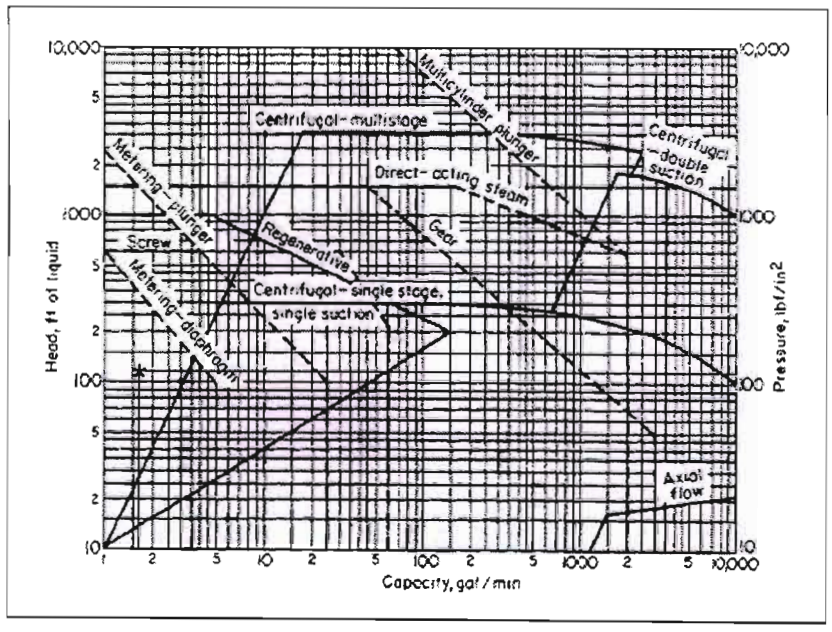

Figure 4.6 : Pump coverage chart based on normal ranges of operation of commercially available types. Solid lines: use left ordinate (head scale). Broken lines: use right ordinate (pressure scale). [Perry & Green, 1997]

A Sera piston diaphragm dosing pump (model number R 409.1 – 8.5 KM/14) was procured from Datatrol Systems (Pty) LTD in Sandton. The drive for the unit was provided by a 3-phase motor with a power output of 0.18 kW. The pump data sheet and test certificate is shown in Appendix B1. The pump can deliver flow in the range from

0 up to 8.5L/hr and at a maximum discharge pressure of 10 bar(g). The pump was calibrated with water using a stopwatch and a volumetric measuring cylinder. The calibration curve is shown in Figure 4.7 below.

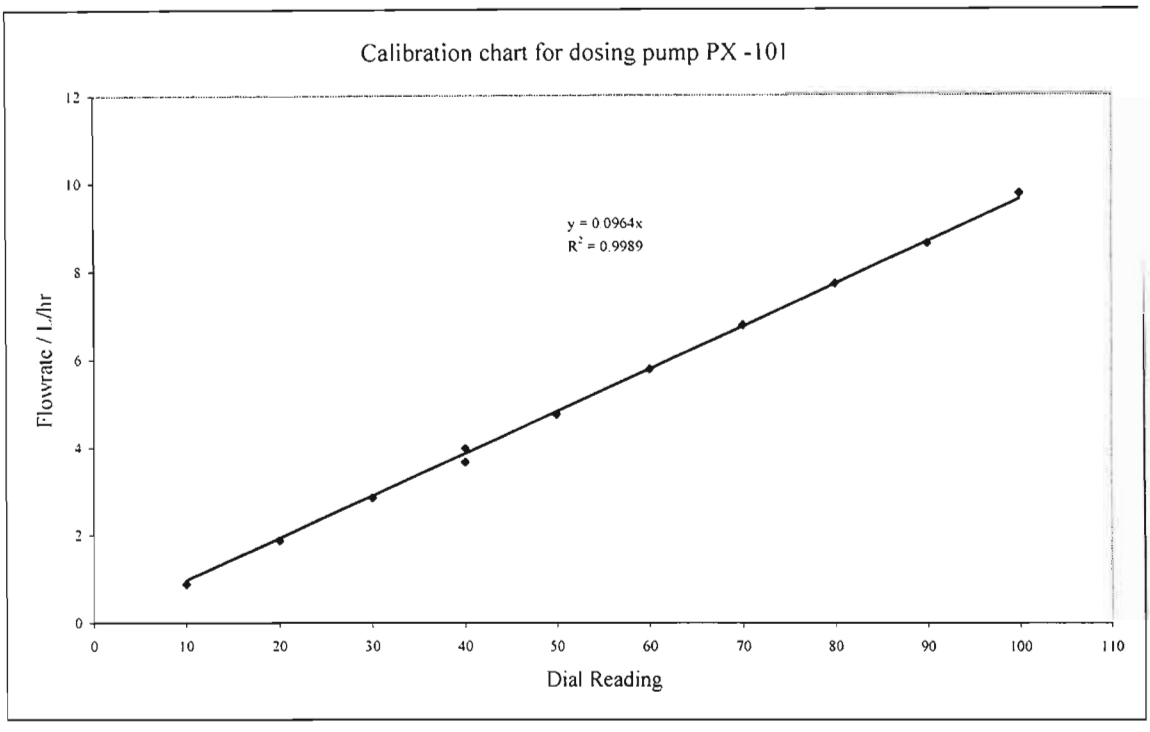

Figure 4.7: Calibration curve for PX-101

An option of using a centrifugal pump with a varying spillback to regulate flow to the reactor was also investigated. This option also facilitated using a separate flow measurement device to record black liquor flow. Quotes were obtained for a variety of black liquor flowmeters (VSE spur gear meter, magnetic and integral orifice flowmeters) but the economics of a centrifugal pump and a separate flowmeter proved not feasible with a total cost almost double that of a metering pump. A picture of PX-101 is shown in figure 4.8 below. A peristaltic pump was also considered but no suitable material for the tube was found at the time.

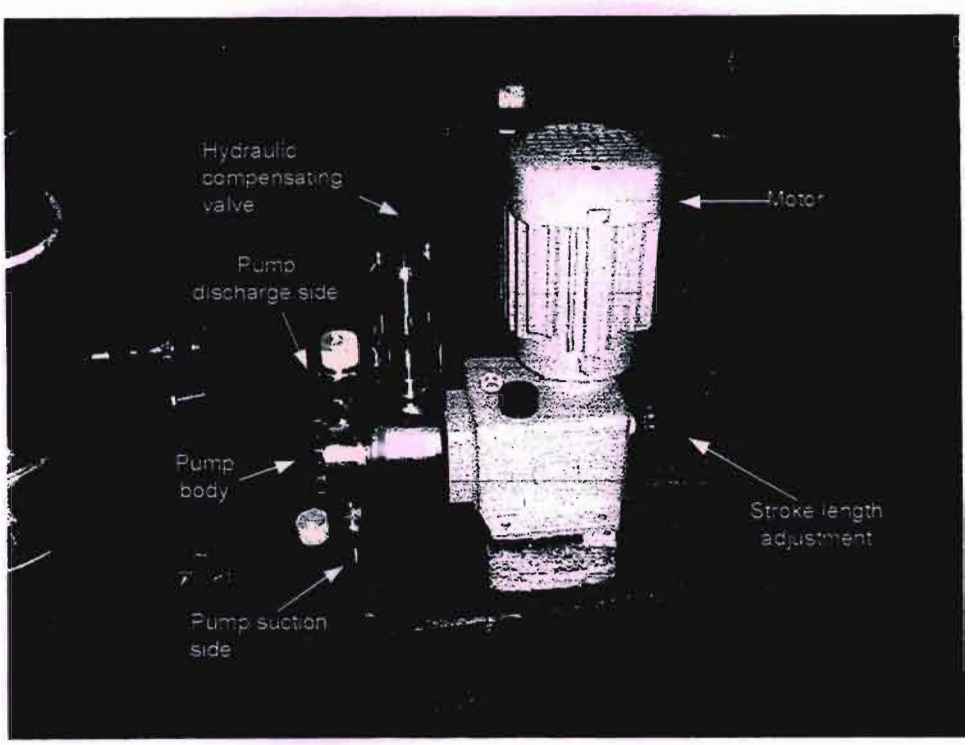

Figure 4.8: Photo of piston diagraphm pump PX-101

4.4.3 Other process equipment

The pump discharge line was fitted with a Birkeet pressure relief valve PSV-101 set to relieve at 900 kpag to protect the pump from over pressure in the event of the discharge line experiencing blockage. The safety valve was procured from DLM and a copy of the pressure testing certificate can be found in Appendix B2.

Hot water is needed during startup and shutdown of the plant to heat up the pump and also flush the lines clean at shutdown. The hot water storage tank TK-102 was a 20L polypropylene water storage container. The tank was filled with hot water at the beginning of a run and was not fitted with any temperature control.

The lines carrying black liquor from TK-101 to the reactor was heat traced using nickel ribbon wire. Current was supplied to the tracing by a variac. Voltage was regulated at ± 35V.

4.5 S200 – Gasification reaction section

4.5.1 Reactor vessel

The design of the reactor incorporated a novel approach that saw the combination of the steam super heater and the fluidized bed reactor in one compete unit, similar in design to a fired heater. Figure 4.9 below is a sketch of the reactor with the incorporated steam superheater and illustrates some important dimensions. The reactor is a 10-inch SS304L shell that expands to 12-inch diameter at the top. The reactor unit is housed in a 340 mm inside diameter (id) carbon steel shell. This inner shell is encased in a 640 mm (id) carbon steel shell. The annular region between the two carbon steel shells is filled with mineral wool insulation.

4.5.2 Steam super heater

Attached to the base of the reactor is the steam superheating coils. The steam super heater is composed of an inner coil encased within an outer coil both connected in parallel to a 1" steam supply socket. It discharges to a 1"header manifold that feeds into the reactor. Both coils are constructed from ½" 304L SS tubing. Steam enters the coil at the top and turns around at the base of the coils to enter the steam header manifold attached to the base of the reactor vessel. The manifold is fitted with a thermowell that houses a thermocouple which measures the fluidizing steam temperature just before it enters the reactor plenum. Figure 4.10 below is a sketch of the two coils showing their dimensions and the piping that connects them to the steam header.

The coils were sized based on the steam requirements for fluidization. The minimum and maximum steam requirements for fluidization were given by u_{mf} and u_o and were 1.3 and 79 kg/hr respectively based on the cross sectional area of the 10" reactor shell. To produce 79kg/hr of 1 bar(g) steam at 700°C and including a 30% factor for losses requires 37kW of energy. To heat up the steel and the bed (6kg) in 1 hr up to 700°C, a further 8kW was calculated to be required based on 30% heat losses as well.

Assuming a flame temperature of 1200°C and incorporating a design that facilitated the steam coils being located in the radiant section of the fired heater Coulson & Richardson [1999] recommend a heat flux of 30kW/m^2 for design purposes. A tube area of 1.2m^2 was calculated to be required at u_o conditions. This equated into a length of 18m of ½" tubing.

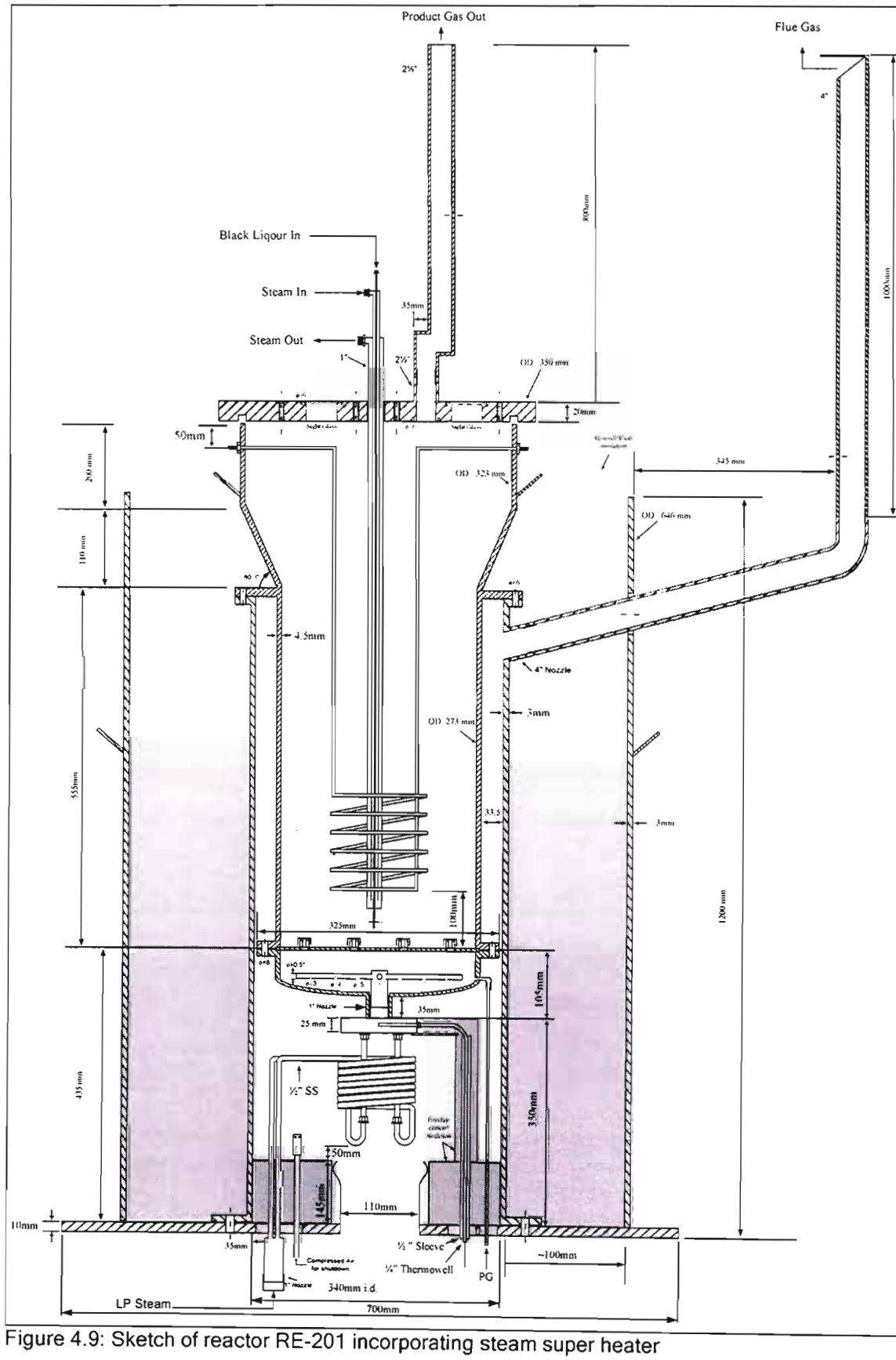

Figure 4.9: Sketch of reactor RE-201 incorporating steam super heater

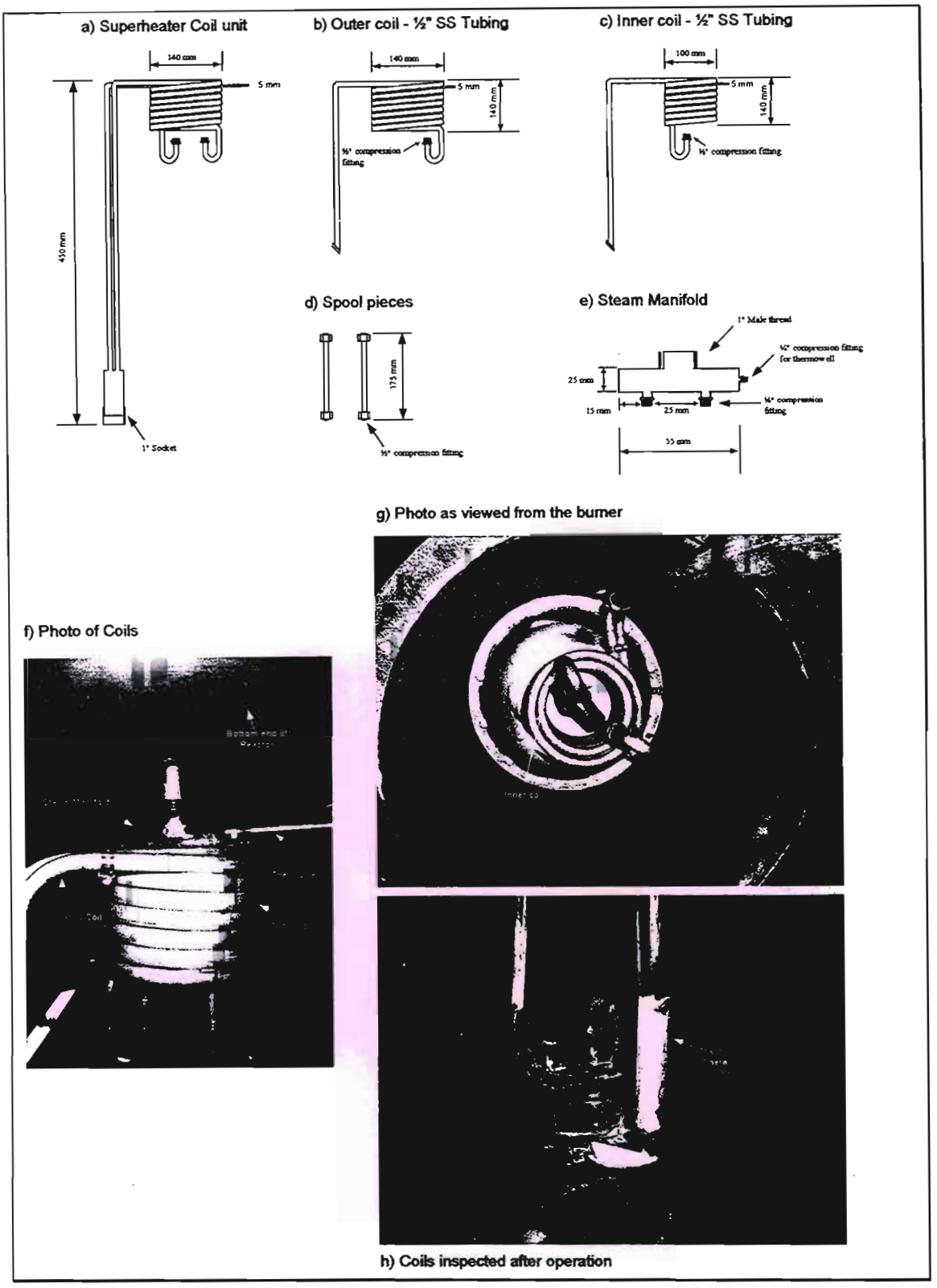

Figure 4.10: Sketch of steam super heater EX-201 A/B coils and associated photos

Seeing as it was unlikely that the unit would be operated near the point of u_o, the design was modified to produce 12.6kW of heat to the steam coils, which equates to a tube length of 6.3m, and a steam flow rate of 27kg/hr. The coil was split into an inner and

outer coil to facilitate both the volume flow through the pipe and for ease of construction.

4.5.3 Gas burner GB-201

A used 22-44kW type KL 20.1 aG Klöckner forced draft gas burner was procured from a local textile plant. The burner uses a liquid petroleum gas feed and features a Satronic MMG 810 Mod .33 control box that controls the startup and operation of the burner. As the burner was acquired second hand, no operating manuals or wiring diagrams were supplied. The burner manufacturer was traced to Germany and the necessary documentation acquired to wire the burner for use. The burner unit was supplied with a feed gas valve train as indicated in Drawing no. 02 in Appendix A. Figure 4.11 below shows photos of the burner during commissioning and as installed.

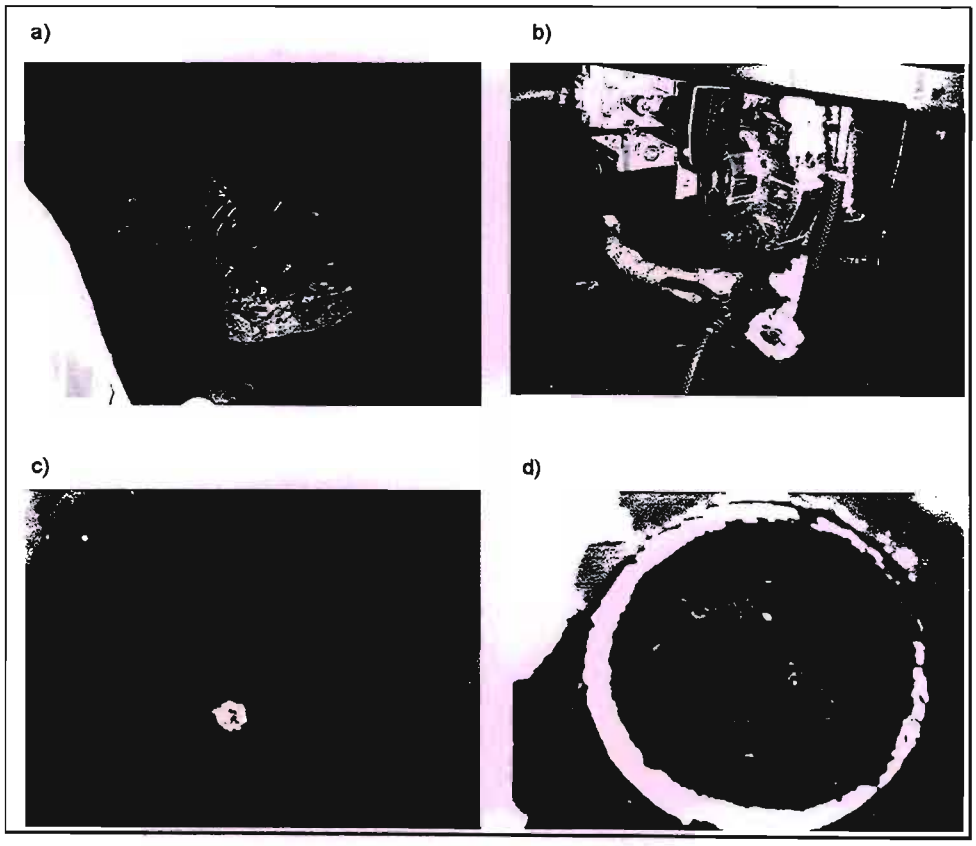

Figure 4.11 : Associated photos of gas burner GB-201. a) Bench testing of burner. b) Gas burner as installed at the base of the reactor housing. c) Testing of burner in housing. d) View of steam coils and reactor from view of gas burner.

The control box features several interlocks before the burner can be started up. It's is fitted with a pressure switches on both the LPG and air fan discharge lines. The loss of

flame is detected by a UV sensor that feeds a signal to the control box which shuts off the LPG supply to the burner by shutting the solenoid valve SV-202 on the LPG feed gas train.

Initially radiation through the base of the housing posed a problem and resulted in several of the burner cables experiencing damage. This action consequently led to a 145mm layer of refractory cement being installed at the base of the housing.

4.5.4 Black liquor injection tube

The design of the black liquor tube required a novel solution to a relatively difficult problem. The aim was to inject the black liquor as low into the bed as possible so as to increase the residence time of the particles in the reactor. In hindsight this may not have been the best approach due to problems discussed in the next chapter. The task at hand was to design a means of injecting the black liquor at a sufficiently high enough pressure through a nozzle of some sort so as to produce a reasonable distribution of droplets in the size range of 1-2mm. The splash plate nozzle design as discussed in CHAPTER 2 is well suited for large flow rates of black liquor and would not work on the smaller scale we were working with in the lab.

A second more important challenge of the injector design was to inject the black liquor which boils at 113°C into a bed at temperatures between 620 to 700°C without boiling the black liquor in the tube. Should the black liquor boil in the tube, the water will evaporate and leave through the nozzle leaving behind the charred black liquor solids in the tube and thus block the injector tube.

Figure 4.12 below shows a sketch of the black liquor injection tube and details of the nozzle design utilized. The nozzle was constructed with a 3mm riser and three 1.5mm orifices separated by 120°. The ¼" tube delivering the black liquor into the reactor is steam jacketed with low pressure steam. Steam flows down the annular region between the outside of the ¼" tube and the inside of the ½" tube till it gets to the nozzle end of the injection tube. It then turns around and flows in the annular area between the outside of the ½" tube, and the inside of the 1" pipe. This flow pattern means the ¼" tube is protected from the 620-700°C reactor environment by a double steam layer.

Initial designs for the jacket featured the use of cold water as the cooling medium with the intent of using the latent heat of vaporization as the heat sink. However, setting the cooling water flow rate under operating conditions proved extremely difficult and often resulted in overcooling of the black liquor and subsequent tube blockage. The colder tube surfaces also showed a drop in bed temperatures towards the centre of the reactor. The steam jacketed design proved to be much more reliable.

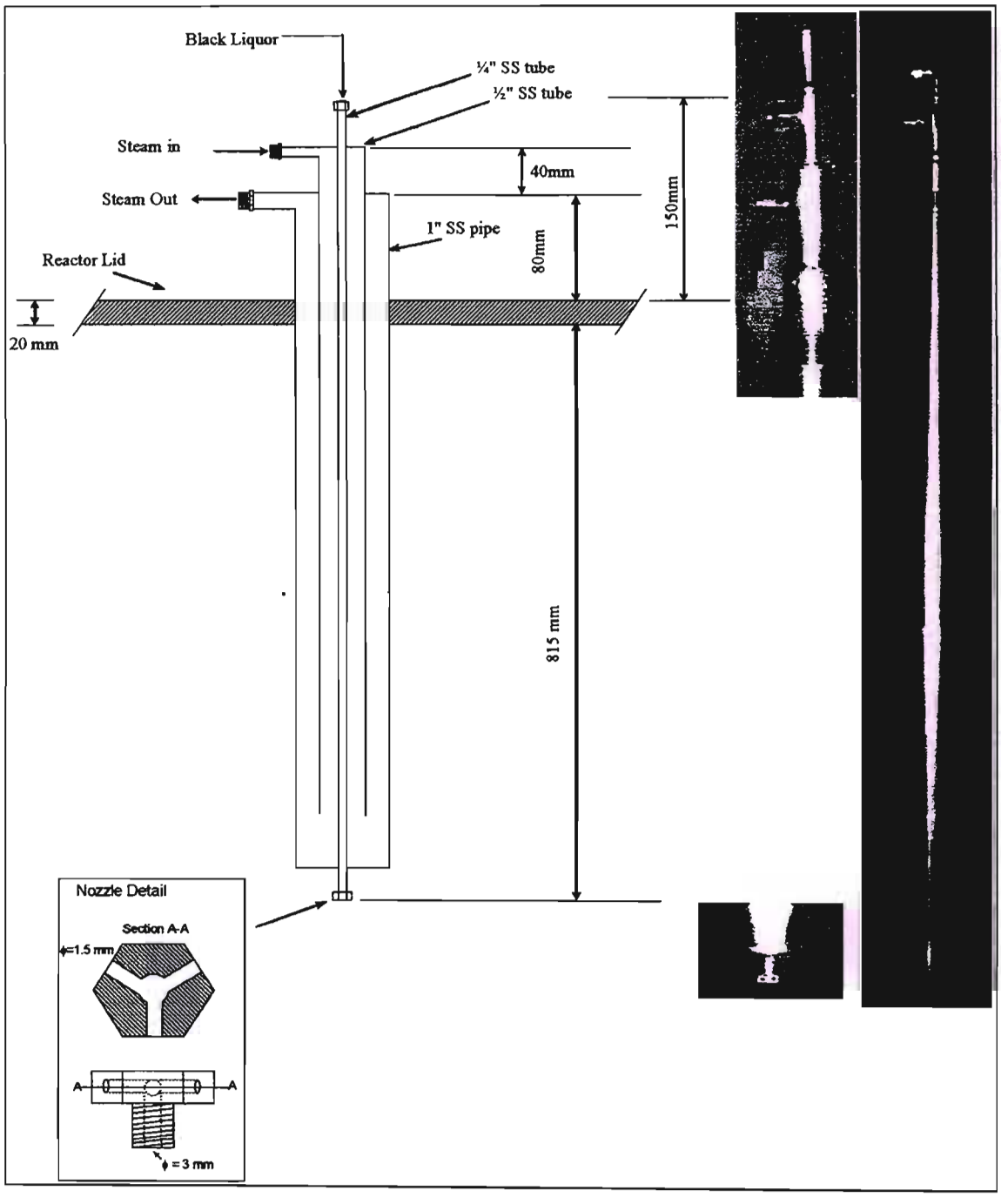

Figure : 4.12. Sketch and photos of the black liquor injection tube showing the important nozzle dimensions

4.5.5 Internal electrical heating element HT-201

The energy provided by the gas burner was originally designed just to provide the energy required by the steam superheater to produce 27 kg/hr of superheated steam at 700°C, and for heating up and maintaining the reactor and it's housing at operating temperatures. The design basis was to include an internal electrical heater to provide the energy for the heat of reaction directly into the bed. This would be the bottleneck in determining the capacity of the reactor to gasify black liquor. As the burner control is a very rough manual control mechanism, the use of an internal heater element on its own dedicated PID control loop proved a better control method for the reactor temperature.

A further advantage of using a heat source in the bed is that energy required by the reaction is made available where it is required, in the bed. Attempting to provide the heat at the reactor walls creates a temperature profile across the bed diameter with local hotspots on the reactor walls that will lead to localized smelt formation.

This is in theory, a similar concept to the internal pulsed heater bundles of the MTCI/Stonechem design. Figure 4.13 below is a sketch of the internal element and associated photos.

The element is a resistive heating element and was procured from GM Heating Elements. The maximum duty per coil that could be supplied was 4kW as the limit to the element length was 6m. The element is constructed from a 6mm diameter stainless steel sheath that encases the resistive heating element. The stainless steel construction is resistant to the abrasive environment of the fluidized bed.

The element is attached to the top of the reactor and extends into the bed. The two tube lengths that extend from the top of the reactor down to and from the coil itself is cold sleeved, i.e. the resistive element is contained only in the coil itself.

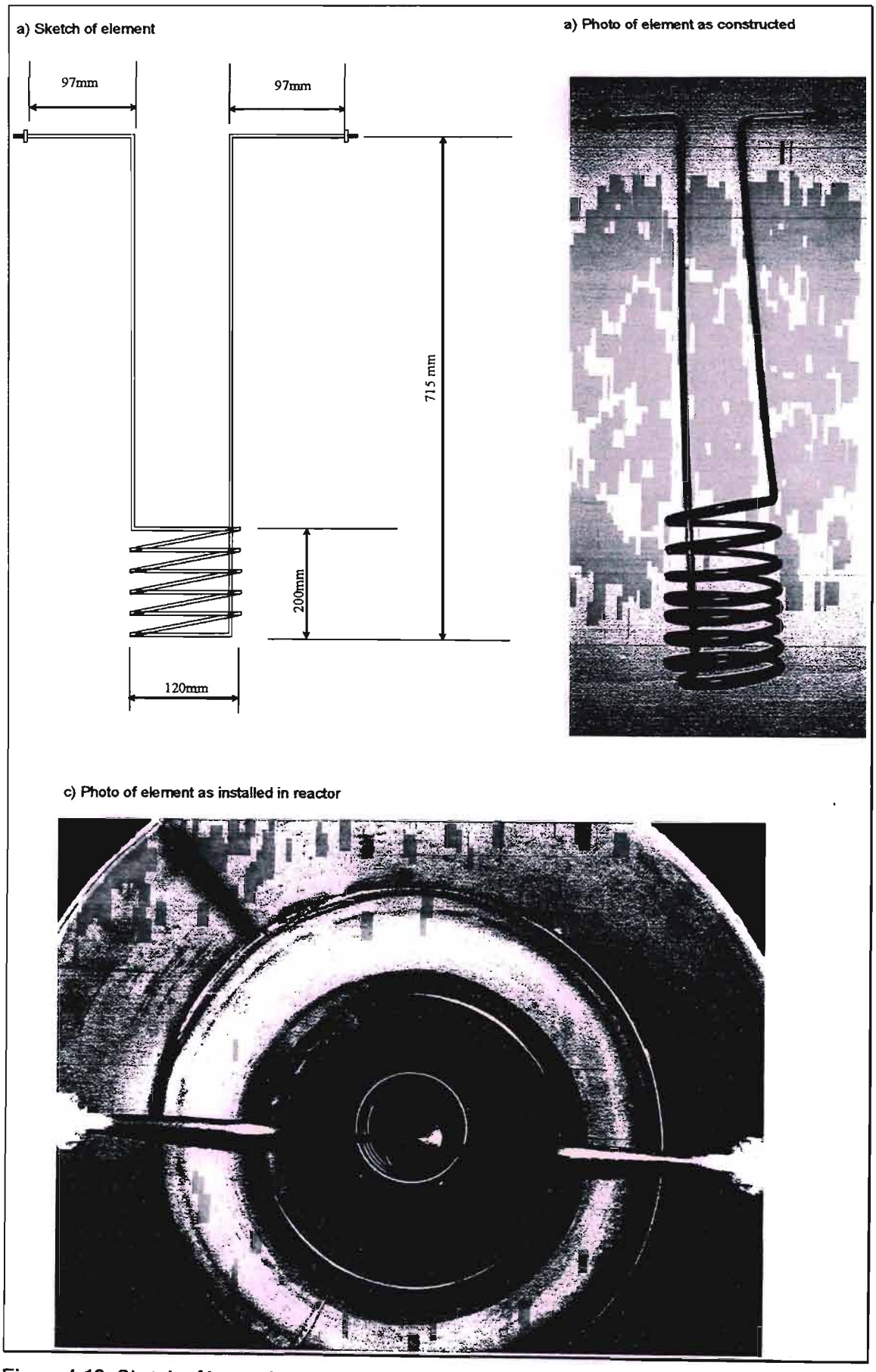

Figure 4.13: Sketch of internal heating element HT -201 and associated photos.

4.5.6 Air cooling tube for shutdown & steam drain system

To assist with the cooling down of the reactor at shutdown, a ½" tube fitted with a 6 hole nozzle was installed through the base of the reactor housing to deliver cold compressed air to the shell side of the reactor. The nozzle consisted of six 3mm holes drilled into the side of the tube so that the air exits into the housing in a radial direction and then moves up the outer sides of the reactor. It is important to cool down the reactor as quickly as possible at the end of a run. This is to stop the gasification reactions to prevent further reaction of any un-reacted carbon in the bed that could lead to erroneous carbon conversion efficiencies and mass balance errors.

At the start of a run the bed is cleaned up with compressed air and any residual carbon in the bed is burned off during the reactor heating up stage using compressed air as the fluidizing medium. By cleaning the bed sufficiently of any residual carbon, the assumption can be made that the initial carbon content is zero. The bed needed to be heated with air before steam can be introduced.

Once the bed has been sufficiently cleaned and the reactor is at operating temperature, steam is ready to be introduced into the system and a changeover from compressed air to steam needs to be made. The condensate produced by the heating up of the piping and instrumentation to the reactor inlet during this transition needs to be drained before it enters the steam super heater. Failure to do so would result in a thermal shock to the steam super heater which could result in cracking of the super heater tubes and subsequent failure of the super heater. This operation can also result in introducing condensate into the reactor and dissolve the bed material. To prevent this from occurring, a condensate drain line was installed just before the entrance to the reactor through which condensate is drained during the heating up of the pipe work.

4.5.7 Nitrogen purge system

During the shutdown of the reactor, it is necessary to stop the gasification reactions as explained earlier. In addition to the rapid cooling down of the reactor, it is also beneficial to evacuate the system of steam thereby removing one of the reactants and ending the reactions. To prevent air entering the system, the reactor is purged with nitrogen. Low pressure nitrogen is supplied from bottled cylinders at a pressures of 0.5 – 0.8 bar(g). At shutdown the system is operated manually, but in the event of a loss of

steam pressure, pressure switch PS-201 is used to detect the loss of pressure and opens the solenoid valve SV-201 automatically to purge the system with nitrogen.

4.5.8 Distributor plate design

Crucial to any fluidized bed design is the even distribution of the fluidizing medium. Uneven distribution of the fluidizing medium promotes pre-mature bubbling, slugging and channeling. Not only does this create hot spots within the bed, but it also leads to poor heat and mass transfer within the bed and eventually loss of fluidization.

As mentioned in chapter three, the use of a sieve plate distributor for lab scale tests is common. Initial trials with a stainless steel wire mesh (75μm) was unsuccessful. The mesh screen distributor can be seen in Figure 4.13 c) above. During fluidization, attrition of the bed particles produced particles less than 75 μm which fell through into the plenum chamber.

During cold testing of the reactor with air, it was observed that due to the proximity of the steam inlet nozzle to the distributor plate it resulted in a channel of air passing through the centre of the reactor creating dead zones at the reactor walls. This was observed by fluidising a cold bed of sodium carbonate with the air.

A steam nozzle was looked at for distributing the steam across the entire cross sectional area of the distributor plate, but the minimum distance for such a nozzle was 500mm and hence was deemed unsuitable for this application. A conventional vortex breaker design as shown in figure 4.14 below was used to construct a vortex breaker at the steam entrance port. The vortex breaker can be seen in figure 4.13 c) above.

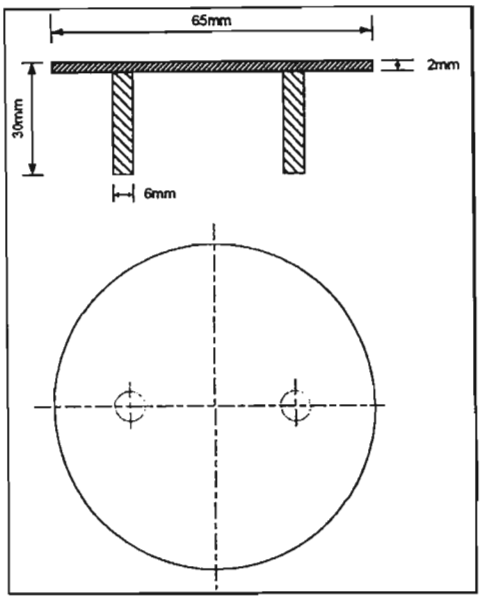

Figure 4.14: Sketch of vortex breaker

This design also proved to be unacceptable as it resulted in a dead zone in the centre of the reactor, once again detected by a visual observation of a fluidised sodium carbonate bed with cold air. The design shown in figure 4.15 below was adopted and cold run trials with air showed that it provided even distribution of the incoming steam.

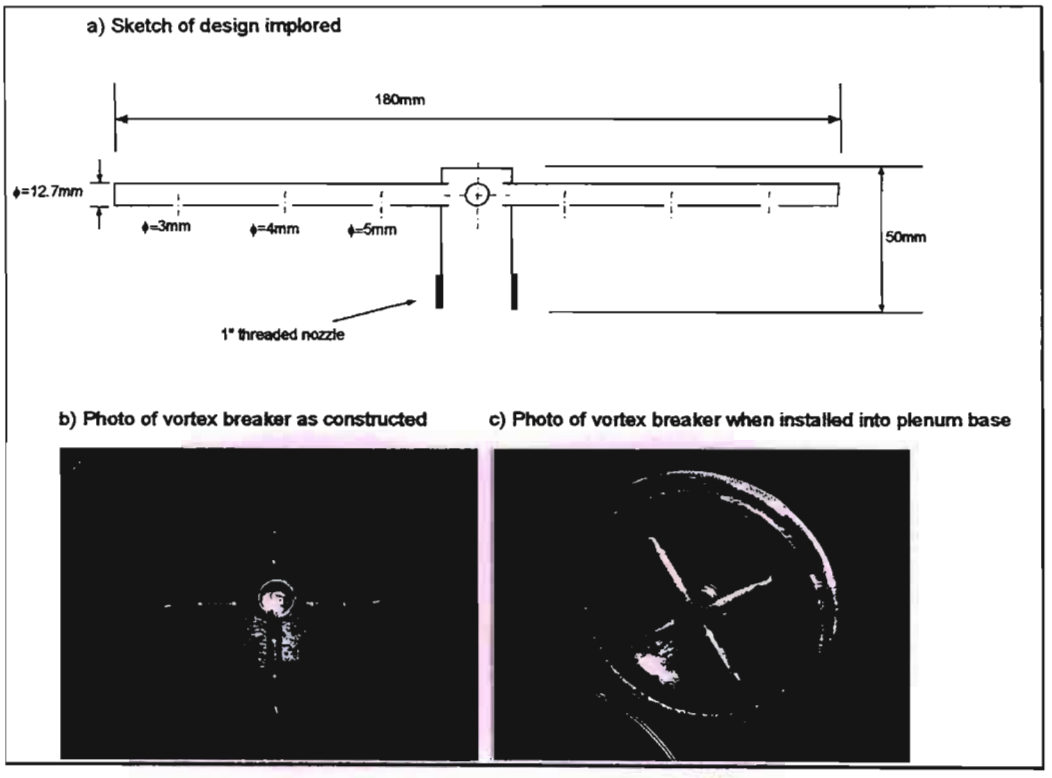

Figure 4.15: Sketch and associated photos of vortex breaker

Due to the poor operation of the mesh wire distributor attributed to weeping, a sieve plate distributor was designed and constructed from perforated plate. The plate was designed based on a flow rate of 30kg/hr and 700°C steam at 0.6 barg. Perry & Green (1999) recommend a pressure drop of between 0.5 – 20 kPa, with a pressure drop of at least one third that of the bed weight. With a 20% bed height, a bed mass of 6kg equates to a pressure of 0.36 kPa exerted by the bed itself. Calculations showed that for a 0.5mm thick plate punched with 1.5mm holes with a hole density of 10.6 holes/cm^2, a pressure drop of 0.84 kPa can be expected. Given that this would prove sufficient a pressure drop to ensure that all the holes would be in operation, a distributor plate was constructed, as shown in figure 4.16 below.

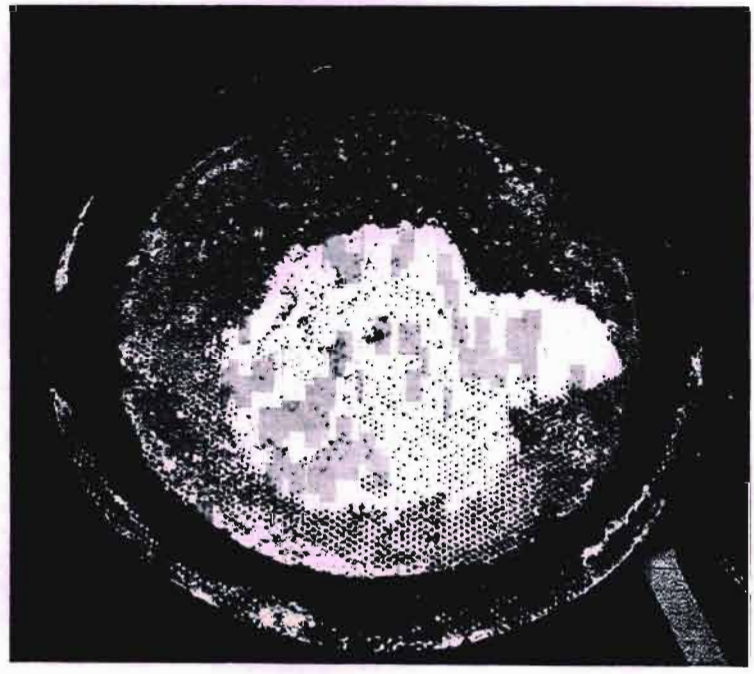

Figure 4.16: Photo of the sieve plate distributor

It was expected that natural bridging of the particles would prevent the bed material falling through into the plenum chamber, but this assumption proved to be wrong as weeping still continued to be evident. Due to the presence of particles in the plenum chamber, localized hotspots were formed in the bed due to the poor distribution of the steam. This resulted in smelt formation which caused blockage of some of the distributor holes. The design of the distributor plate was revisited and several options were looked at. These included the two more proven designs of bubble caps and tuyeres. These types of distributors have been shown to be well suited to a high temperature environment.

A tuyere design was initially considered but it was felt that due to the possible formation of a smelt, it could lead to premature blocking of the tuyere holes. The tuyere design also results in an insulating layer of bed material forming on the distributor plate itself. This is sometimes advantageous, as in the case of a fluidized bed incinerator, in that it offers some heat protection to the plate. However in this application, it presents a situation where a layer of smelt can form from this insulating layer and this is undesirable. The use of bubble caps would not only shield the entrance of the holes from direct contact with the bed particles, but also project the steam flow downwards towards the plate itself thus dispersing any material collected on the plate. The design methods for tuyeres and bubble caps are identical.

The main factors that influence the design of a tuyere are the riser diameter, the number of orifices per tuyere, the orifice diameter, the total gas flow rate and the total orifice area. The main contributing factors to the pressure drop across a tuyere are the exit losses from the orifices and to a much lesser extent the effect of the riser diameter. Three models were used to predict the pressure drop for the tuyere design, that given by Lombardi *et al* (1997), Geldart (1986) and Kunii & Levenspiel (1969). The predictions made by these models are presented in Figure 4.17 below. The details of these models are not presented here, and the original references should be referred to for the calculation procedures.

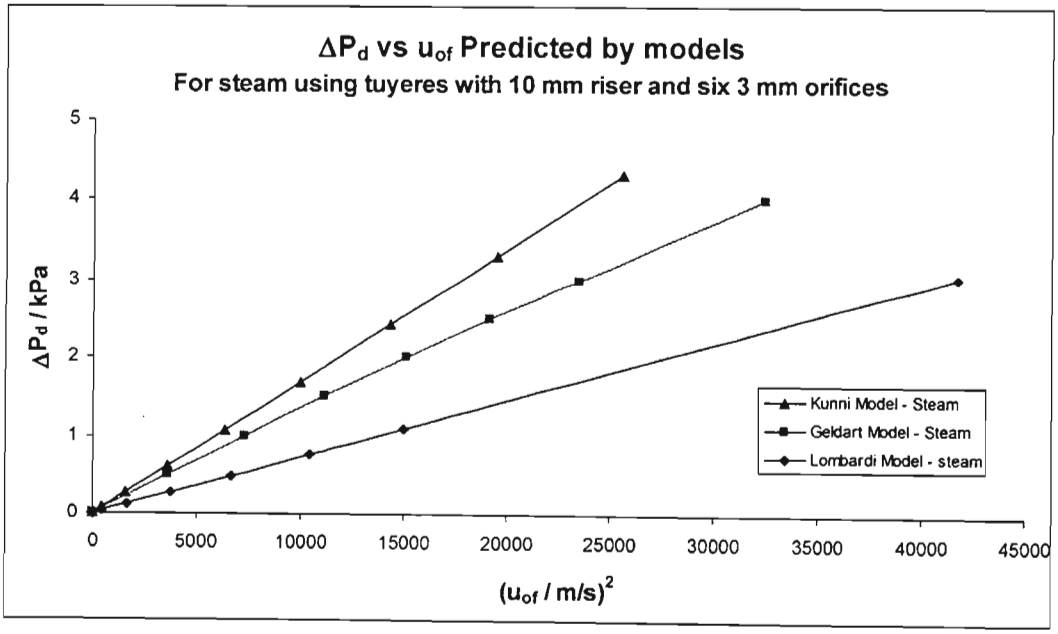

Figure 4.17: Tuyere performance predicted by models of Kunii & Levenspiel, Geldart and Lombardi

Due to the variation in performance predicted by the three models, it was felt necessary to verify these models with bench scale tests. Figure 4.18 below is a sketch of the test rig used to carry out these tests.

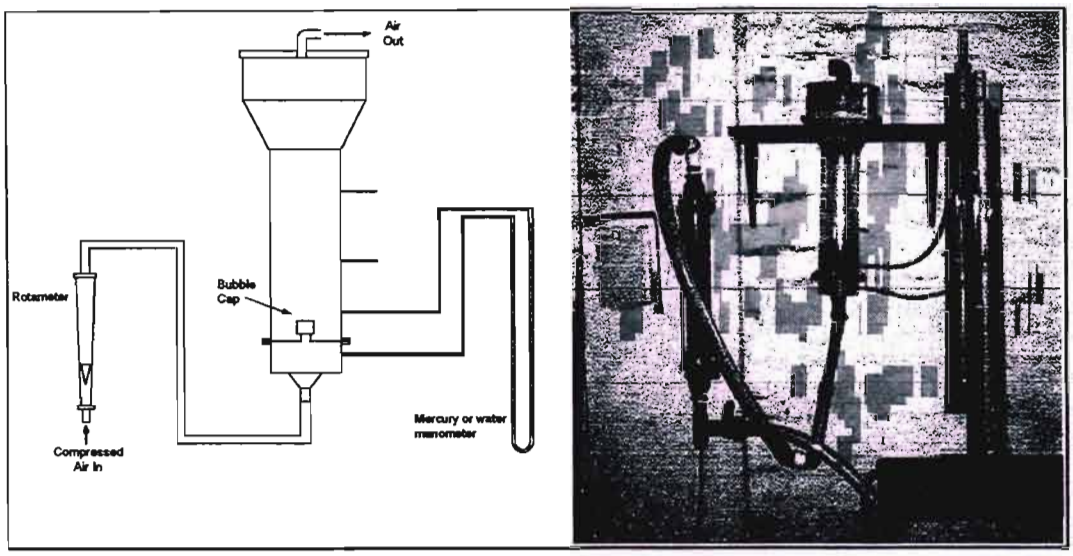

Figure 4.18: Sketch of test rig for bench scale testing of bubble cap design and photo of equipment.

Two types of bubble caps were tested and plots of u_{of} and ΔP_d were generated for each design. Both designs featured a riser diameter of 10mm and 3mm orifices. The first design was a 6-hole cap, and the second a 3-hole cap. Data was produced with air as the fluidizing medium and used to predict the expected pressure drop with steam at 0.6 bar(g) and 700°C.

This approach was used as there was no means of measuring the pressure drop with steam without having to construct a complete distributor with a full set of bubble caps. With the approach adopted, it simplified the task in that only a single cap needed to be constructed and measurement of pressure drop could be done by simple means of a water or mercury manometer depending on the pressure drop range.

Figure 4.19 and 4.20 below shows results from the bench tests and how they compare to those predicted for air using the models. Results from the test show that for low orifice velocities, the Lombardi model best predicts the pressure drop behavior, whilst for higher orifice velocities; the Geldart model is more suitable.

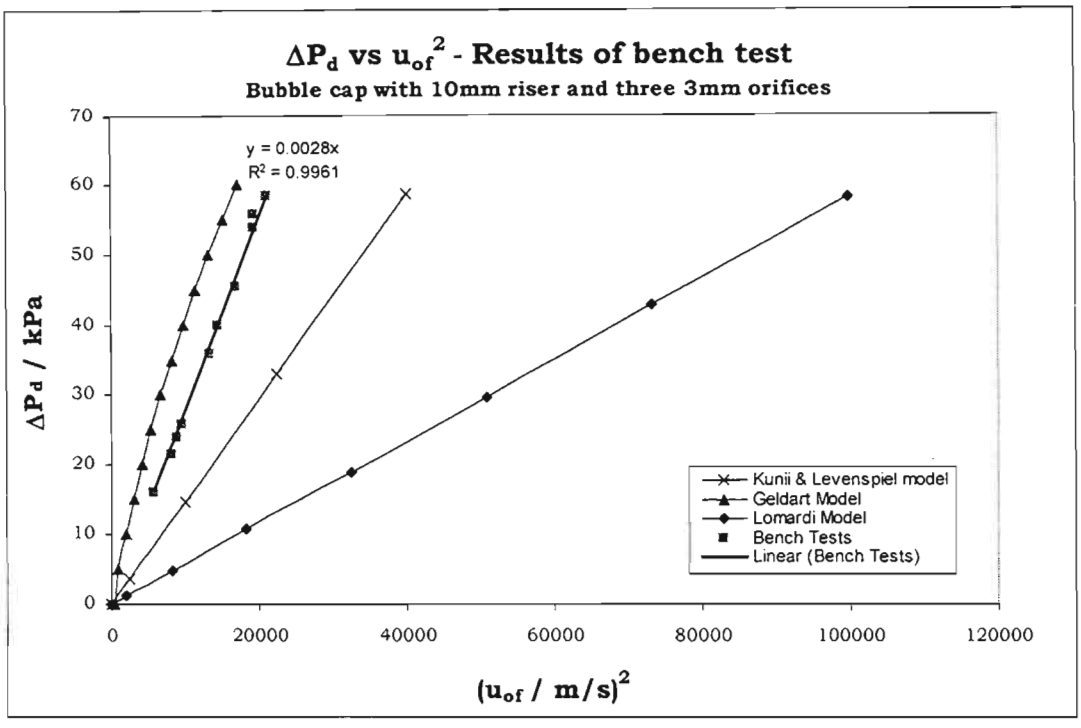

Figure 4.19: Results of bench tests compared to model data for 3 hole bubble cap

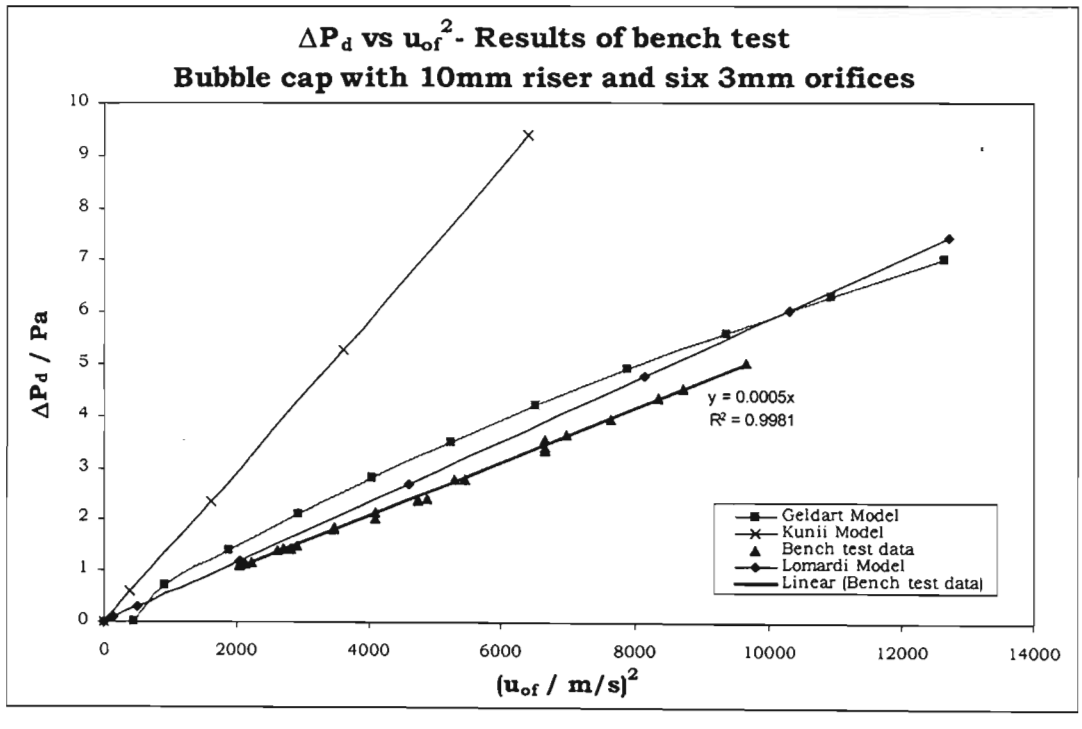

Figure 4.20 : Results of bench tests compared to model data for 6 hole bubble cap

The data from the bench tests were used to predict the pressure drop using steam at the above mentioned conditions. A general expression for pressure drop can be given by (*Perry and Green, 1997*):

$$\Delta P = K \frac{\rho u^2}{2} \tag{4.6}$$

where ΔP is pressure drop
K is a loss co-efficient
ρ is fluid density
u is the fluid velocity

Using the relationship that pressure drop is directly proportional to medium density, the bench scale data was used to predict the expected pressure drop using steam at 700°C and 0.6 bar(g) as the fluidizing medium. This method was adopted merely as an approximation to give an order of magnitude difference between the 3-hole and 6-hole designs. The result of this analysis is presented in figure 4.21 below.

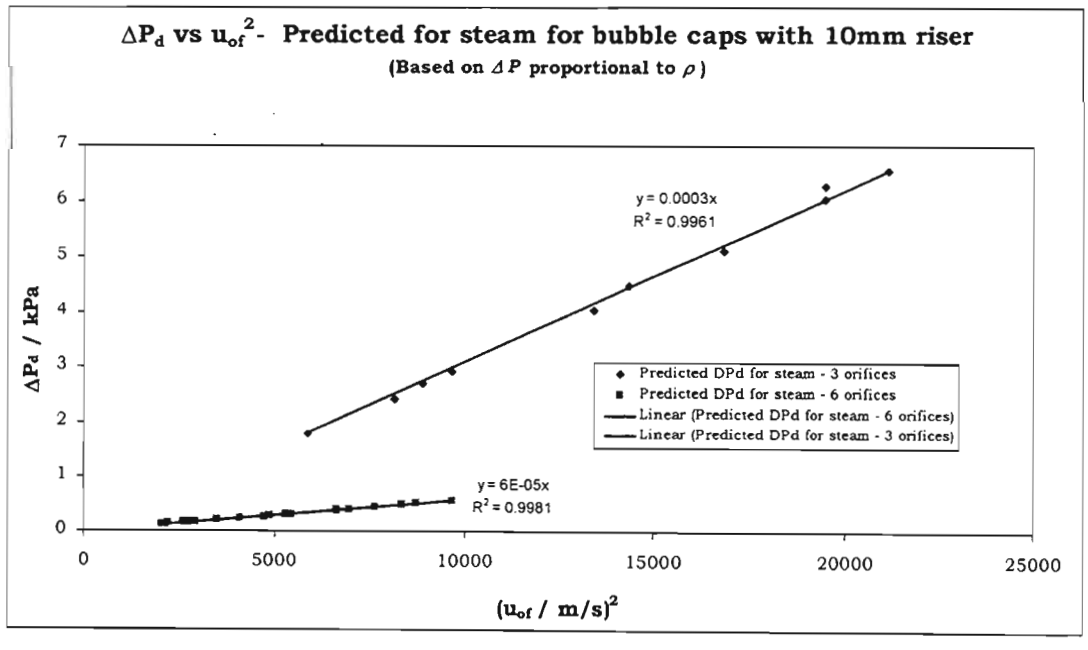

Figure 4.21: Bubble cap behavior with steam predicted using bench scale data.

As a comparison of this approach to those predicted by the models as shown in figure 4.17 for a 6 hole bubble cap, the Lombardi model once again proved to provide the closest fit at lower orifice velocities as shown in figure 4.22 below:

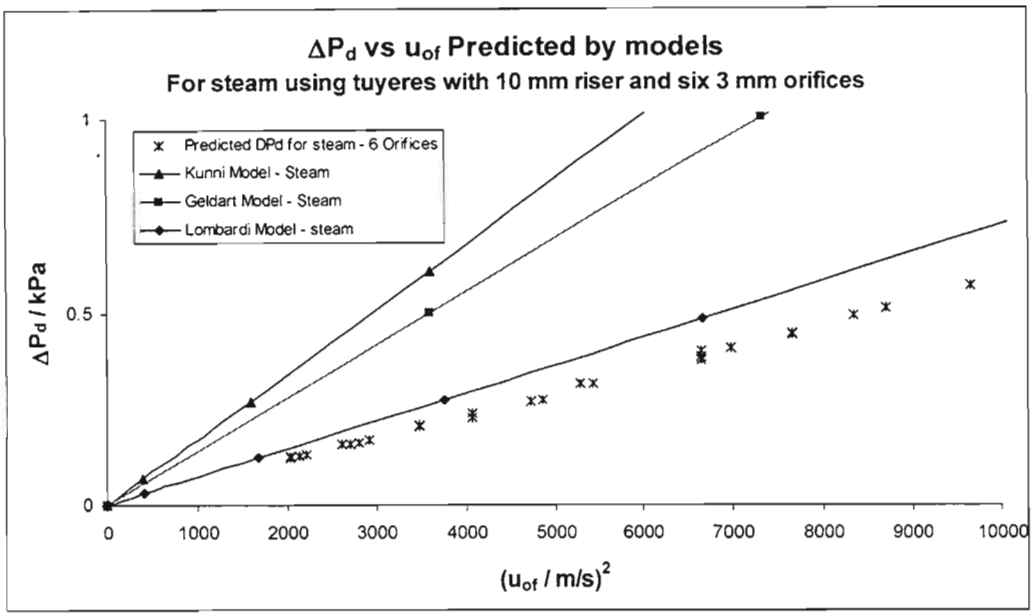

Figure 4.22: Prediction of pressure drop behavior with steam using bench scale tests analysis compared to those predicted by the models.

From the above analysis it was clear that a bubble cap with a 10mm riser and three 3mm orifices would provide adequate pressure drop for efficient operation of the distributor plate. Since the riser diameter contributes to the overall pressure drop across the bubble cap to a much lesser extent, the riser diameter was increased to 12mm to facilitate ease of construction for the machining of the 3 orifices in the head of the tuyere. Figure 4.23 below is a sketch of the bubble caps as constructed showing the relevant dimensions.

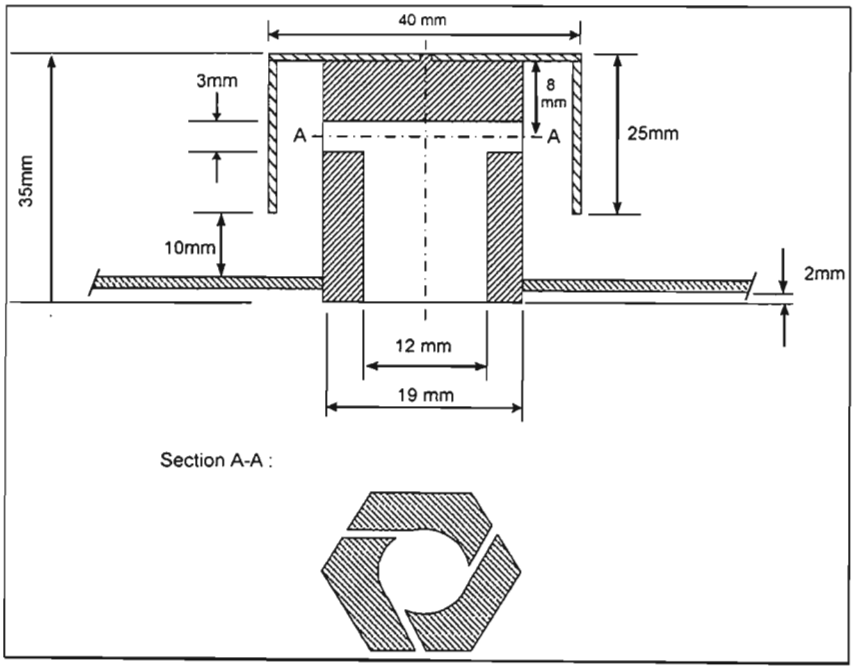

Figure 4.23: Sketch of Bubble caps

The cyclonic design of the bubble caps was adopted from Eleftheriades (1981) who showed that the cyclonic design could be treated in the same way as any other type of distributor even though the design tends to produce better mixing in the bed. He attributed the superior mixing qualities to the spiral nature in which the fluidizing fluid moves up the bed resulting in longer residence times within the bed as compared to a direct vertical pathway up the bed.

Figure 4.24 below is a sketch of the distributor plate as constructed consisting of twelve bubble caps and a photo of the plate as installed in the reactor. The plate was constructed out of 3mm 316L stainless steel.

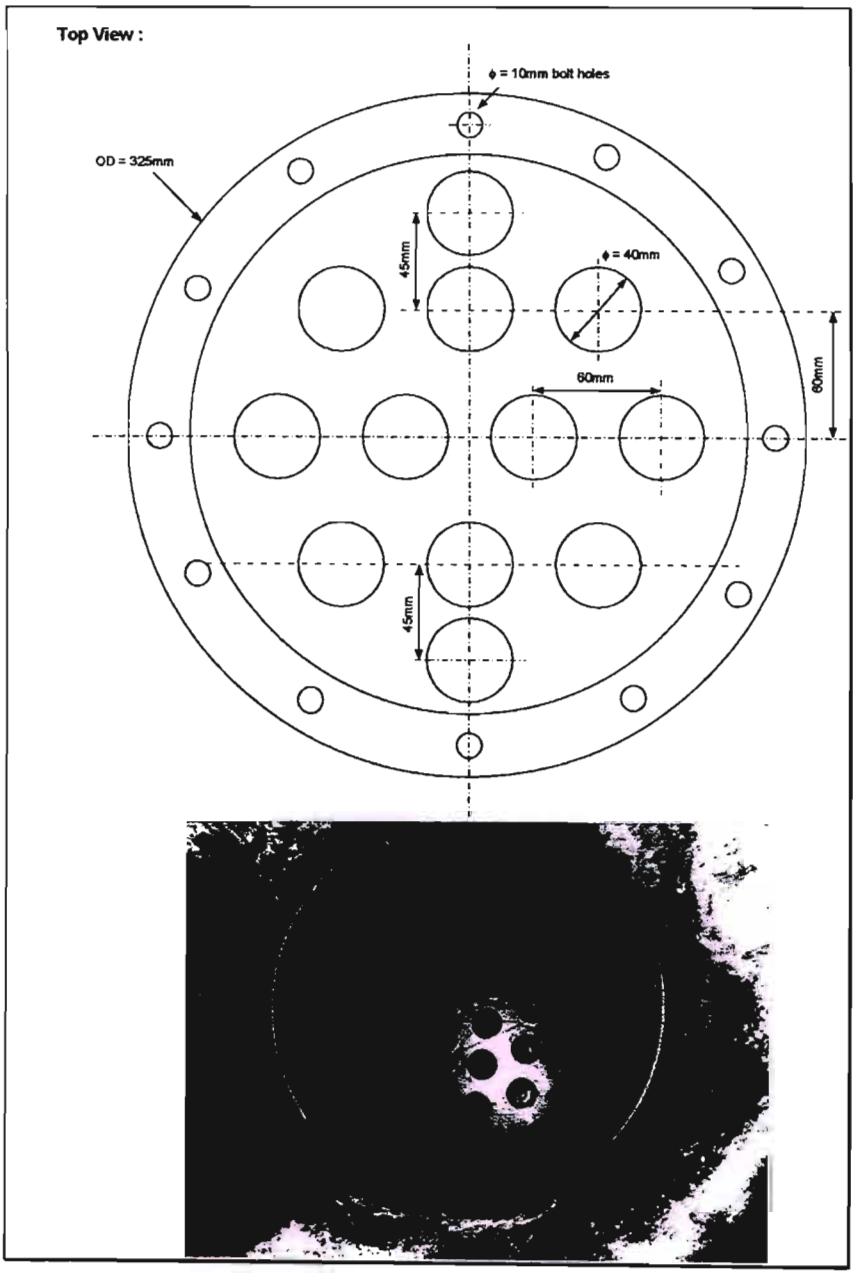

Figure 4.24: Sketch of distributor plate and photo of plate as installed in reactor.

After installation of the distributor plate, pressure drop data was generated in the reactor with air as the fluidizing medium. As mentioned earlier, the data could not be generated for steam due to pressure drop measurement restrictions given the fluidizing medium and temperature. Figure 4.25 below presents the data from these tests, with prediction of expected pressure drop using steam at 700°C as the fluidizing medium.

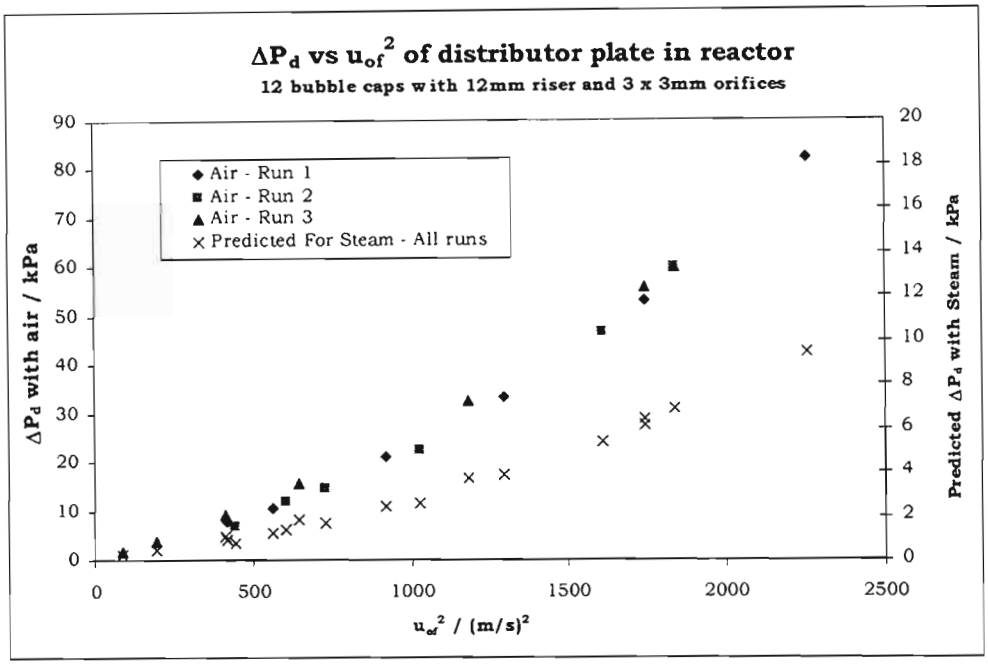

Figure 4.25: Results of pressure drop testing of distributor plate as installed in rector.

During operation with steam, the distributor plate displayed satisfactory behavior of pressure drop with values in the range of 5-7 kpa during normal operating conditions and is presented in CHAPTER 5.

4.6 S300 – Gas Sampling

The need for gas analysis is necessary to determine if the reaction is in fact occurring, and for characterization of the gasification operation for energy efficiencies and mass balance calculations. The level to which this analysis is done, will determine the extent to which the operation of the reactor can be quantified in terms of actual numbers, its behavior modeled and the operation optimized.

Ideally an on-line gas chromatograph (GC) would prove to be a most useful tool in analyzing and interpretation of syn-gas compositions for varying operating conditions. In all of the literature related to laboratory testing facilities of lab-scale gasifiers studied to date, the syn-gas

was always analyzed by some means of gas chromatography. However, given the early stages of development of this testing facility at the University of Natal, it became clear after some in depth investigations and vendor consultations, that the purchase of such a unit was beyond the budget of the initial phase of this project and it was decided that it would be postponed to a later stage in the overall development of the testing facility. The focus for this project in terms of gas analysis was thus to merely gain an indication that the gasification reactions were indeed occurring and a combustible gas was being produced.

The MAX5 portable combustion efficiency monitor was made available to the project by Sappi Stanger. The MAX5 directly measures oxygen, carbon monoxide and combustibles. The carbon monoxide concentration is measured by a solid state electrochemical sensor whilst the combined combustibles are measured by a low temperature catalytic bead type transducer in a constant current-excited Wheatstone Bridge circuit. It calculates levels of carbon dioxide and combustion efficiency based on these measurements. The MAX5 has a limited range of operation as it is designed for combustion efficiency monitoring in systems such as boilers and fired furnaces. It measures carbon monoxide up to 2.5% and grouped combustibles up to 5% based on volume.

Since the MAX5 was designed primarily for combustion efficiency monitoring, the gas sample that is fed to the analyzer must be water free and at or slightly above atmospheric pressure. The MAX5 features a built in vacuum pump that draws in the sample gas at a slight vacuum. The gas analysis system was designed around these requirements and the limitations of the MAX5.

The main features of the analysis train are a gas sample condenser EX-301, the knock out separator SP-301 and the dryer VL-301 as shown in Figure 4.26 below.

The sample condenser was constructed from a perspex shell, 200mm in diameter and 465mm in height. The inner (SS316L) stainless steel coil was constructed from ¼" tubing and rolled into a 150mm diameter coil with a 30mm pitch. The total coil height is 300mm with an overall surface area of 330 cm^2. The cooling medium used in the condenser is a mixture of ice and water to form an ice-water slurry at 0°C.

The shell side is circulated by a submerged centrifugal pump PC-301 which transfers the slurry mixture from the bottom of the condenser to the top. This helps promote heat transfer by effective mixing of the cooling medium. PC-301 is a RENA type C40 turbo centrifugal pump with a max head of 2.2m and flowrate of 16.5L/min and uses 19W of power. In operation the shell side is periodically drained and topped up with ice as required.

The knock-out pot SP-301 was constructed from SS304L stainless steel and is 80mm in diameter and 115mm in length. The gas outlet is from the top of the pot to allow a level of liquid to collect in the pot which is indicated by the level gauge LI-301. During operation the pot is drained periodically as required.

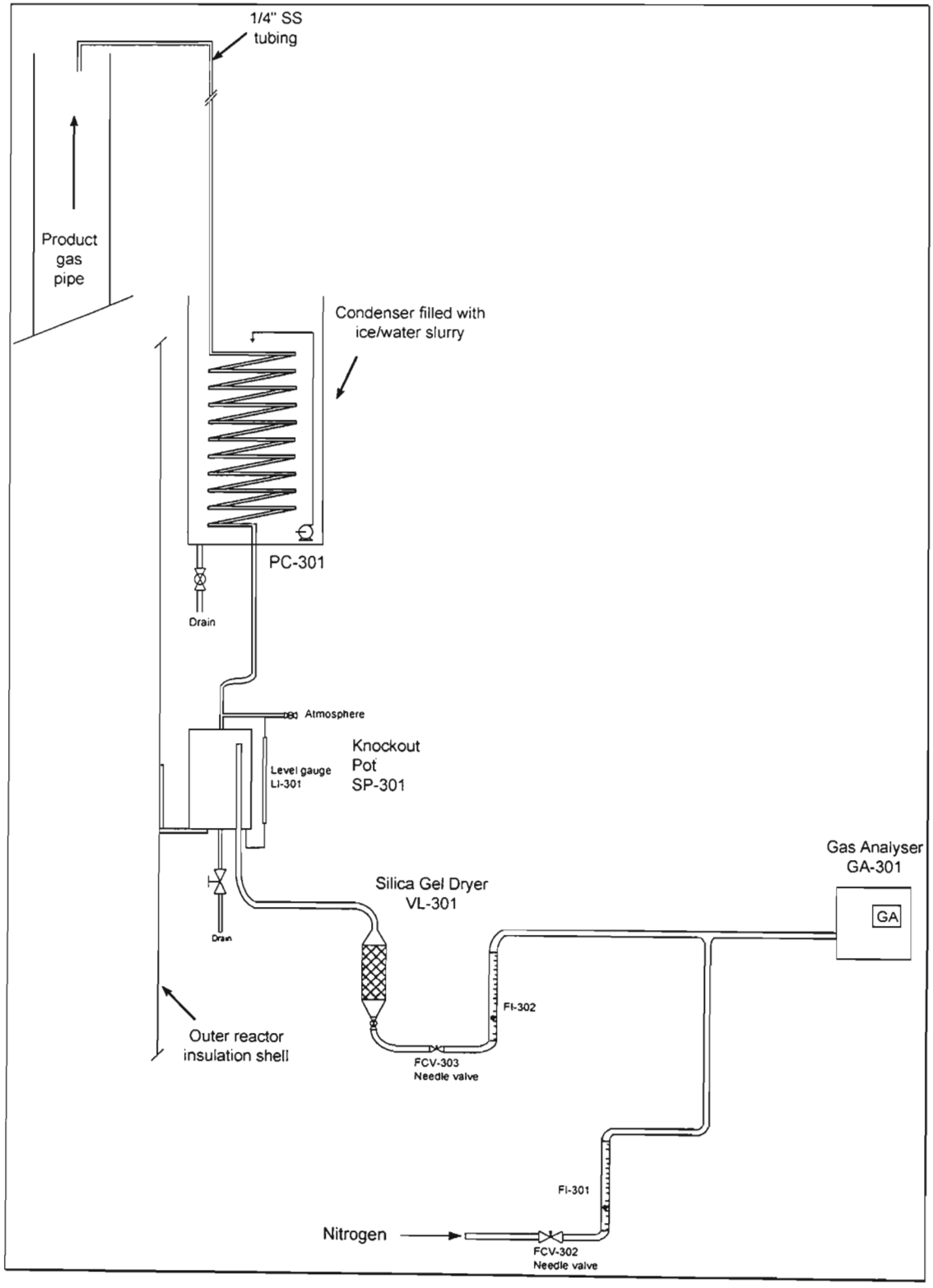

Figure 4.26: Sketch of gas sampling layout

Cold gas leaves through the bottom of SP-301 through a ½" tube that extends to the top of the pot internally as shown above in figure 4.26. It passes into the dryer VL-301 which is packed with silica gel crystals. A laboratory condenser was used for VL-301. The dry syn-gas is then mixed with nitrogen which acts as a diluent before proceeding to the MAX5 for analysis. The need for diluting the syngas with nitrogen was due to the analysis limitations of the MAX5 as mentioned earlier. Calibration curves were generated for FI-301 and FI-302 and can be found in Appendix E.

4.7 Instrumentation and data logging

The important process variables that need to be measured are flow and temperature. For the operation of the reactor it is vital that the temperature distribution within the reactor is observed, and needless to say, the flow rate of feed streams to the reactor is essential.

4.7.1 Temperature monitoring and data logging.

Due to the high temperatures in the reactor, type K thermocouples were used. Type K thermocouples span a temperature range from 0°C to 1260°C and they exhibit a standard tolerance of 2.2°C or 0.75%. Initially mineral insulated thermocouples were used but the mineral insulation broke down within the thermocouple at the high temperatures resulting in erroneous values. The thermocouples were subsequently changed to the ceramic type. The ceramic tube that housed the thermocouple wires proved to be much more resistant.

Temperature is measured at 4 points in the reactor. The four probes are mounted in the lid of the reactor, as shown in figure 4.27 below, and extend vertically to varying heights in the bed. The installation of the probes vertically in the bed is favored to the horizontal installation as it offers less resistance to the bed in a fluidized state.

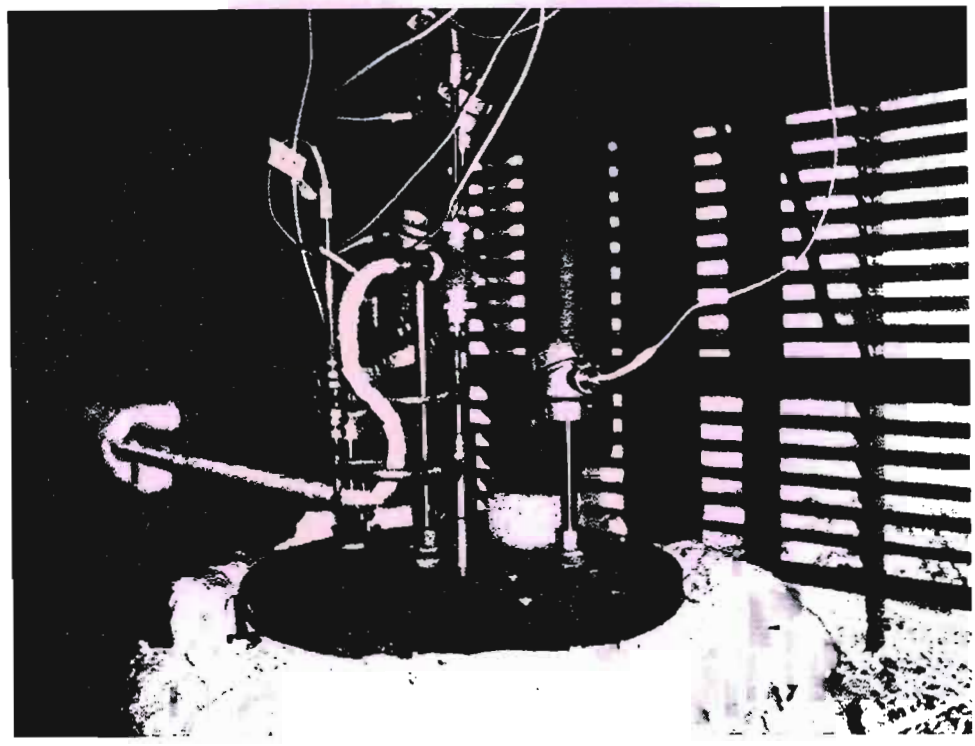

Figure 4.27: Photo of the reactor lid showing thermocouple installation

The first two probes were placed in the centre of the hot zone of the bed 85mm from the distributor plate. The first probe TT-203 is for temperature logging purposes, while the second probe TT-208 is used in TIC-201 for temperature control on the internal heating element. Since the hot zone is the zone most prone to smelt formation, having a second thermocouple installed at this point caters for the event of failure of a probe during operation. Two more probes, TT-204 and TT-205, are installed in the reactor at points 385mm and 585mm above the distributor plate respectively.

Additional temperature measurements were made at the following points:

- the exit syn-gas temperature – TT-206
- the black liquor inlet temperature – TT-200
- the steam inlet temperature just before it enters the plenum chamber – TT-202
- the black liquor tube steam jacket exit temperature – TT-201
- the exit LPG flue gas temperature – TT-207

TT-202 is housed in a 6mm thermowell and extends right into the steam manifold installed at the base of the reactor. The thermowell is shielded from the furnace environment by a ½" stainless steel sleeve. The sleeve is enclosed in a layer of fireclay cement. The fireclay insulation modification was implemented as a result of failure of the silicone insulation layer on the thermocouple during early testing. This particular

thermocouple was manufactured in the university workshop and was flexible so as to be installed in the thermowell.

The reactor's temperature was controlled by a CB100 digital temperature controller manufactured by RKC Instruments Inc. The controller used TT-208 to measure the temperature of the hot zone and used a PID controller to regulate temperature by sending a voltage pulse output of 12V to a Fotek 40amp solid state relay that switches the heating element on.

Temperature measurements were recorded on a desktop computer with the aid of an ISA PC-73-T PC board manufactured by Eagle Technologies. A program was written in Microsoft Visual Basic 5.0 to log the temperature measurements and display online temperature trends. This code for the program can be found in Appendix F. Table 4.4 below shows the channel allocation on the card.

Table 4.4: Channel allocation on the PC-73-T temperature card

Tag No.	Card Channel	Description of temperature measurement
TT-200	0	BL feed
TT-201	1	BL tube cooling
TT-202	2	Steam in
TT-205	3	Reactor top
TT-204	4	Reactor middle
TT-203	5	Reactor hot zone
TT-206	6	Exit product gas
TT-207	7	LPG flue gas

4.7.2 Flow measurements

The use of a dosing pump simplified the measurement of black liquor flow to the reactor. A calibration chart for the range of stroke settings was derived and used for flow measurements.

The steam flow rate was measured using a metal tube variable area flow meter manufactured by Tecfluid. The SC-250 model meter displayed a local reading only and for the operating flow of 20-30 kg/hr of steam at 0.6 barg the flow measurements was within an error of within 2.90%. The meter displayed a 0-100% reading and was

spanned by the manufacturer to read a maximum value of 100% at a flow of 52kg/hr of steam.

LPG flow to the burner was measured using a UGI domestic gas meter. The meter uses a diaphragm mechanism to record gas flows from 0.04 m^3/hr up to a maximum flowrate of 6m^3/hr.

Steam was let down from the available 6 bar(g) to 0.6 bar(g) by an IMI Bailey Birkett 470 pressure reducing valve.

Two sight glasses were installed in the reactor lid for visual observation of the bed behavior during fluidization. The glasses were made of quartz and were recessed into the reactor lid.

Figure 4.28 below is a photo of the complete unit and associated equipment. A hazop study on the unit was carried out and can be found in Appendix C. Start-up and shutdown procedures for operation of the pilot plant can be found in Appendix D.

Figure 4.28: Photo of the completed unit with associated equipment.

The next chapter presents the results of tests carried out and discusses the problems that arose from them and how they were overcome to achieve the project objectives.

CHAPTER 5

RESULTS AND DISCUSSION

As mentioned earlier in previous chapters, the core focus of this project was on the design and operability of the unit and to a much lesser extent the generation of operational data. The latter was purely to prove the functionality of the unit thus allowing the project to proceed into the next phase where with the addition of a more robust analysis train, the unit can be used to generate more meaningful data.

The experiments carried out demonstrated the unit's ability to gasify a viscous carbon rich liquid feed. Before proceeding to gasify such a feed it was necessary to verify the following factors:

- Basic fluidization mechanism
- Gasification of a solid fuel
- Verify operation of the designed liquid feed system
- Gasification of a liquid fuel
- Demonstrate the feed delivery system's ability to handle a viscous feed
- Gasify black liquor

For the gasification of a solid fuel which was charcoal, the duration of the experimental run was determined by observing the concentration of carbon monoxide and carbon dioxide generated in the product gas. A fall in the concentrations after a period of a prolonged concentration indicated a near total consumption of the solid fuel.

With a liquid feed, run durations were limited by the bed deposition rate based on the feed rate of the liquid fuel. Design calculations which can be found in Appendix G, show a maximum

bed (Na_2CO_3) deposition rate of 0.16 kg/hr with a feed of a 6% carbonate containing black liquor. This is based on the maximum feed rate of black liquor that a single 4kW internal heating element can handle i.e. 3.1l/hr. The run time must be sufficiently long for the reactor to reach a pseudo steady state, yet short enough to sufficiently prove the aims of the run, without jeopardizing the bed fluidization by contributing too much bed material.

A startup plan was devised for the reactor and it showed five distinct stages that can be summarized below:

- Dry run with steam to demonstrate the reactor and steam super heater's heating capability.
- Experiments with Na_2CO_3 bed fluidized with steam to determine nature of fluidization.
- Experiments gasifying a solid fuel to verify analysis train.
- Test involving the injection of BL in the absence of a bed, to verify the operation of the feed delivery system.
- Experiments with a steam fluidized Na_2CO_3 bed with continuous injection of black liquor.

During the commissioning stages numerous start-up attempts where made and the run had to be aborted due to failure of certain pieces of equipment. Design modifications were made at each phase of the start-up until a working design was achieved. The results presented in this chapter exclude these aborted runs but the causes of and solutions to these failures are discussed.

5.1 Heating ability of steam super heater and reactor

The aim of this phase of the commissioning was to determine the ability of the unit to produce steam at the required flow rate of 25-30kg/hr at approximately 700°C into the reactor. The thermal design of the unit was verified and modifications to the unit were implemented to meet the design basis. This was a first of a kind design at the University of Natal and necessitated several modifications and design effort before the unit was able to attain the specified design temperatures.

Figure 5.1 below shows the temperature trend with time of the steam inlet temperature into the reactor during a performance test run of the burner and steam super heater. The data collected during this stage then became the reference point during troubleshooting when the burner failed to achieve design capacity.

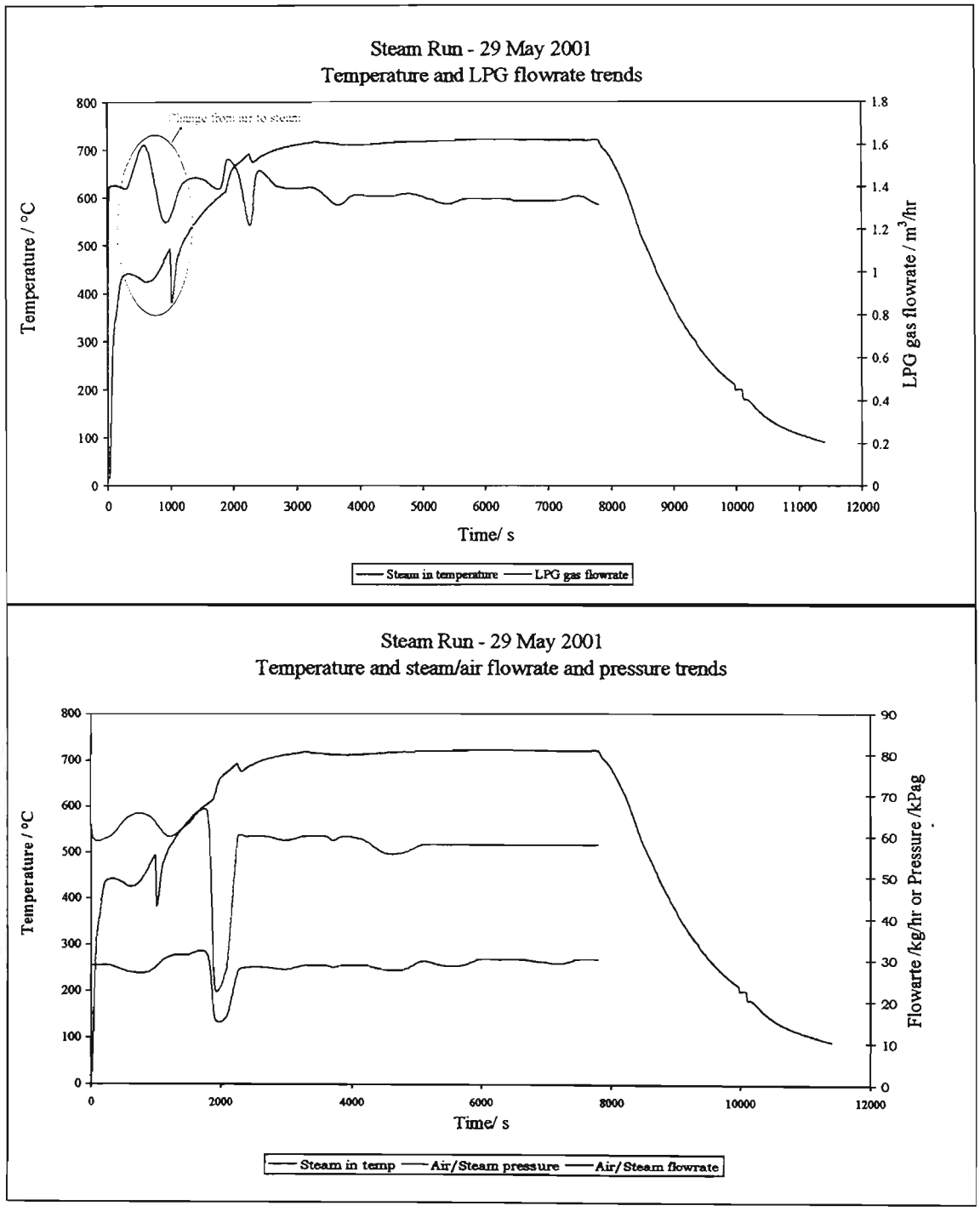

Figure 5.1 Reactor steam inlet temperatures and air/steam and LPG flow rates for dry run

As is evident in the above trends presented in figure 5.1 above, the reactor unit successfully achieved and sustained a steam inlet flow rate of 30kg/hr at a temperature of 700°C.

5.2 Demonstration of fluidization principles with a sodium carbonate bed

Once the reactor was proved capable of attaining design temperatures, the next step in the commissioning process was to establish the nature of fluidization with a sodium carbonate bed supplied from Sappi Stangers Copeland reactor with a size distribution shown in table 4.1. It was also necessary to observe the system behavior under automatic temperature control using the internal electrical heater HT-201. This stage of the commissioning involved extensive modifications to the distributor as was previously discussed in Chapter 4.

This step in the start-up plan was also necessary to verify the ability to transfer heat into the bed and maintain stable operating temperatures under fluidizing conditions. The nature of fluidization was verified by visual inspection through the sight glasses fitted onto the lid of the reactor. The wind box pressure was monitored for indication of blocking of the distributor plate which would cause misdistribution of the fluidizing steam.

Figure 5.2 a and b below show the temperature and flow trends for a trial run with a 4kg sodium carbonate bed. Subsequent testing was done with an increased bed load of 6kg. The longer time taken to achieve operating temperatures in comparison to Figure 5.1 above is attributed to the presence of the bed.

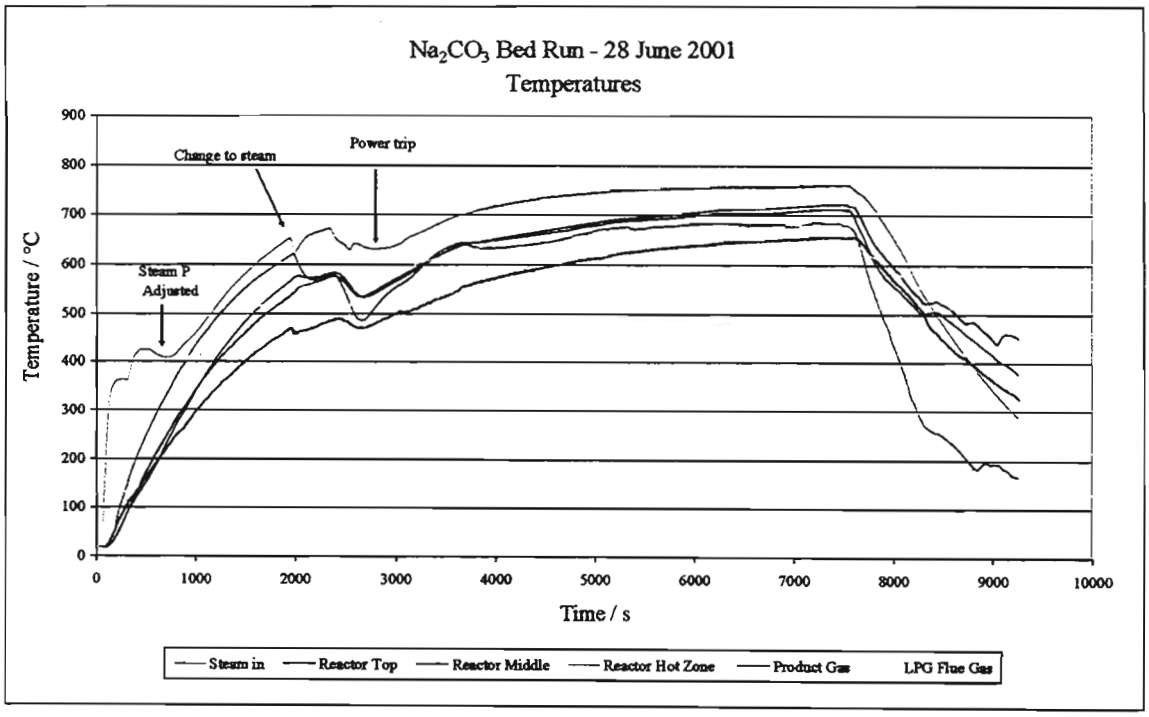

Figure 5.2a: Temperature profiles of reactor with a 4kg sodium carbonate bed.

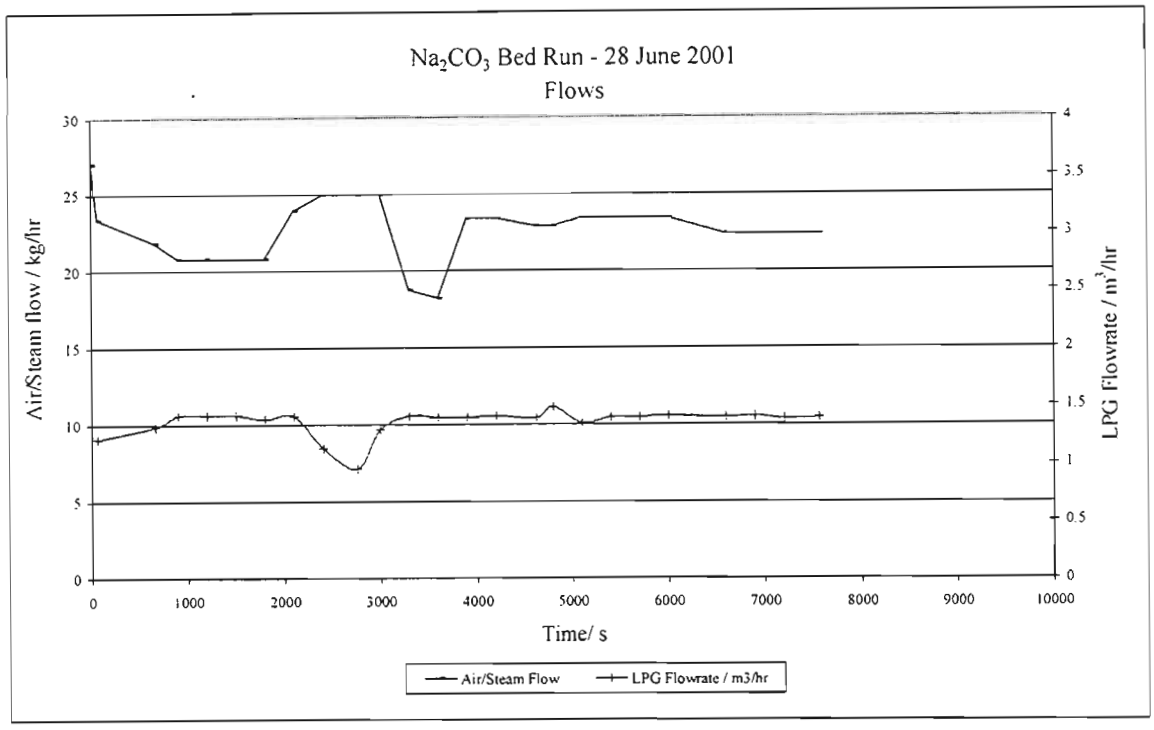

Figure 5.2b: Air, steam and LPG flow rates to the reactor during trial run with a 4kg sodium carbonate bed.

These series of tests showed that the reactor was successful in achieving bed temperatures up to 686°C in the hot zone. Fluidization was in agreement with Geldart's powder classification. The bed was classified as a Geldart type B powder and bubbling was experienced just past the minimum fluidizing velocity u_{mf} with no restrictions on the bubble size as the steam flow rate was increased.

One observation that stood out during these tests was that the reactor temperature increased with height up the reactor. This meant that the reactor hot zone was considerably lower in temperature than the top of the reactor, approximately 30°C lower. This was attributed to the additional heat that was transferred into the reactor by the exiting flue gases that passed on the shell side of the reactor.

This additional energy at the top would be absorbed to a certain extent by the steam jacket of the black liquor injection tube. It also pointed to future improvements in the design with respect to the point of injection of the black liquor. Having an additional source of energy at the top of the reactor would prove useful in flashing off the water in the black liquor as it is injected thus allowing the solid particles to drop into the hot zone of the reactor. This would also facilitate more energy being made available in the hot zone for the gasification reactions, thus increasing the treatment capacity of the reactor.

With the reactors ability to fluidize the sodium carbonate bed and reach and maintain stable operating temperatures up to 686°C established, the next step was to verify the operation of the analysis train and this was done by gasifying a solid carbon containing fuel source.

5.3 Analysis Techniques

i) Ash Content tests

The ash content of the bed samples was analyzed by burning the bed samples in a muffle furnace set at 750 – 800°C. The samples were left in the furnace overnight.

ii) Solids Content tests

The solids content of the black liquor was analyzed by drying samples of the black liquor in a drying oven set at 105°C overnight.

iii) Component Tests

These tests were carried out by Sappi's laboratory facilities. The analysis for the anions and cations were carried out using Ion Chromatography. Total sulphur content was analysed using a Sulphur analyzer. Sodium and potassium were analyzed using atomic absorption spectroscopy. Silica was measure gravimetrically by burning the sample in a furnace to remove the organics. The sample was then washed in hydrochloric acid to determine the amount of acid insolubles. It was thereafter washed with hydrofluoric acid to dissolve to determine the amount of soluble and insoluble silica in the sample.

The accuracy of these tests is greater than that of the sampling process.

5.4 Gasification of a solid fuel

The gasification of the solid fuel was further broken down into two sub sections:

- Gasification of a "pure" carbon rich fuel source like charcoal
- Gasification of a blend of the fuel source (charcoal) with sodium carbonate.

The reactor can not be heated up with fluidizing steam immediately but initially with compressed air until operating temperature is reached. Then only can a changeover in feed from

air to steam be done. Air is initially used to ensure sufficient heating of the steam super heater and the reactor thus preventing steam from condensing on the metal surfaces when fed into the reactor. This method has a further advantage in that the bed is cleaned of any carbonaceous material by combustion of it with air before a liquid feed is introduced into the reactor.

In the event of a solid batch feed this would not work as the carbon source will be combusted before steam can be introduced. It was thus necessary at this stage to heat up the empty reactor to operating conditions or a temperature sufficiently higher than the steam dew point temperature. When this point was reached, then only was the bed introduced into the reactor and the changeover of the fluidizing medium from air to steam done. The temperature difference between the superheated steam at approximately 700°C and the cold bed is more than adequately large enough to prevent steam from condensing on the bed particles.

5.4.1 Gasification of a "pure" carbon rich charcoal bed

Gasifying an almost pure carbon bed would increase the possibility of the gasification reactions occurring. It thus eliminated or reduced the probability of an uncertainty when the gas sampling system was commissioned.

Operations observed during this stage of the commissioning led to changes and modifications to the sampling system including a redesign of the original ½" copper tube condenser and the introduction of the diluent nitrogen for the syn gas being fed to the MAX5 gas analyzer. The reason for the latter is the concentration limitations of the MAX5 analyzer as discussed in Chapter 4.

Figure 5.3 below are the reactor temperature trends from a gasification run with a 200g charcoal bed. The charcoal was crushed in a ball mill into particles with a Sauter mean diameter of 1mm. Ash tests conducted at 750°C in a furnace showed the ash content of the charcoal to be an average 6.62%.

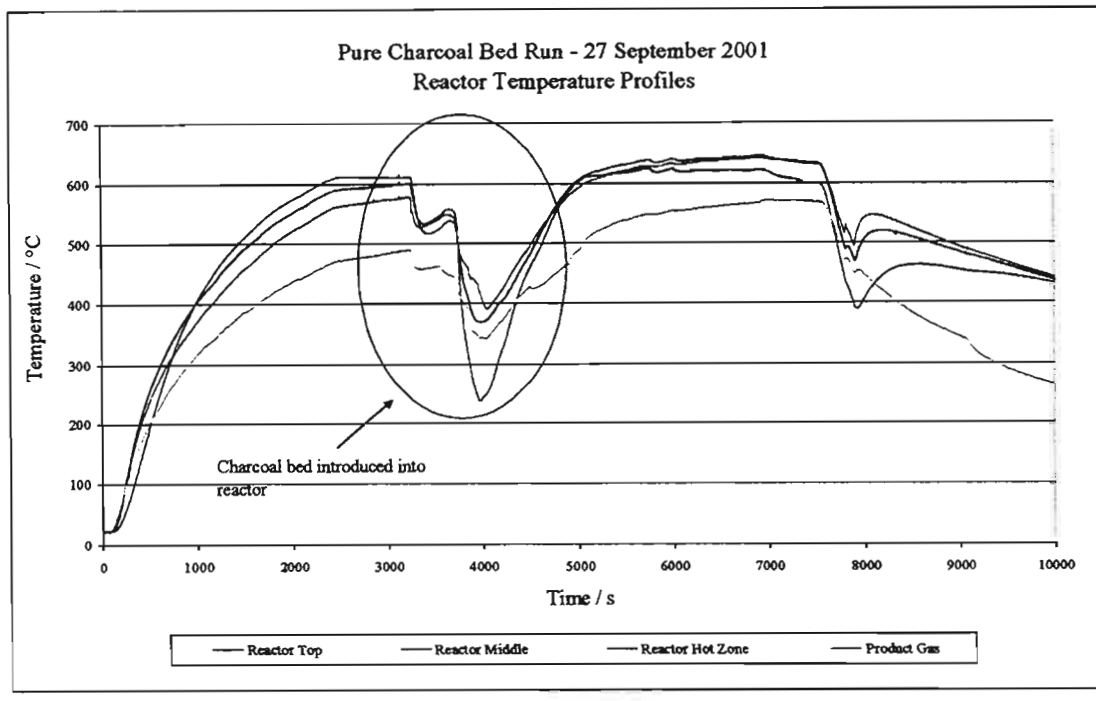

Figure 5.3: Reactor trends during gasification of a 200g charcoal bed at 620°C.

As indicated in Figure 5.3 above, the point of bed introduction occurs after the bulk of the equipment has been heated close to operating temperature with compressed air. A total of 40g of charcoal was gasified over the duration of this run.

Unfortunately due to the concentration limitation of maximum 5% combustibles and 2.5% carbon monoxide on the Max 5 gas analyzer, the syn gas produced during this run far exceeded these restrictions and the exact concentrations could not be analyzed. The nitrogen diluent system was also unable to cope with the concentrations due to the system design as explained below.

The Max 5 gas analyzer features a built-in vacuum pump that draws in the gas that is to be sampled at a set flow rate as discussed in Chapter 4. In order to sample the product gas stream from the reactor, the sample needs to be drawn through the condenser at a slight vacuum, which the Max 5 is able to do.

The problem arises when a diluent like nitrogen is added after the condenser and knockout pot. The nitrogen creates a backpressure on the reactor product gas sample line preventing flow from entering the condenser and knockout pot. Adjusting the nitrogen pressure to prevent this occurrence is not a simple task using the conventional needle valves employed in the design. The sampling system later proved to work considerably well in diluting the syn gas at lower concentrations, but not completely reliable or accurate. The importance of a gas chromatograph for the analysis of the

product gas stream cannot be overstated. With a gas chromatograph, the syn-gas sample need not be diluted at all and the current gas sampling system design would work well.

5.4.2 Gasification of a blended charcoal – sodium carbonate bed

A 100g sample of charcoal (6.62 wt% ash) was mixed with 7kg carbon free sodium carbonate (99.9wt% ash) and this mixture was gasified in the reactor. The aim of this approach was to produce a lower combustibles content syn-gas approaching that generated by the injection of black liquor. When black liquor is sprayed into the bed, the water flashes off and the carbonaceous solids drop into the sodium carbonate bed where it undergoes the gasification reactions. By providing the carbon source directly in the sodium carbonate bed, the bed environment during black liquor injection could be simulated on a batch scale.

Figure 5.4a and b below shows the reactor and flow trends during a run at 560°C.

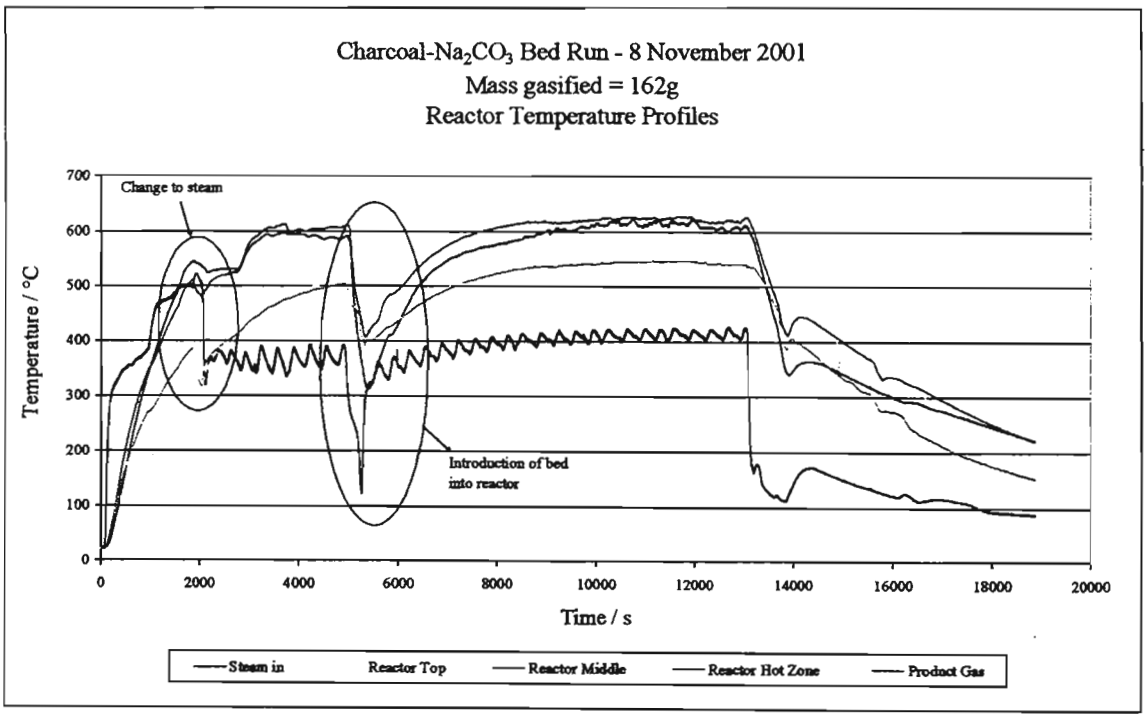

Figure 5.4a: Reactor profiles during gasification of charcoal-Na_2CO_3 at 560°C

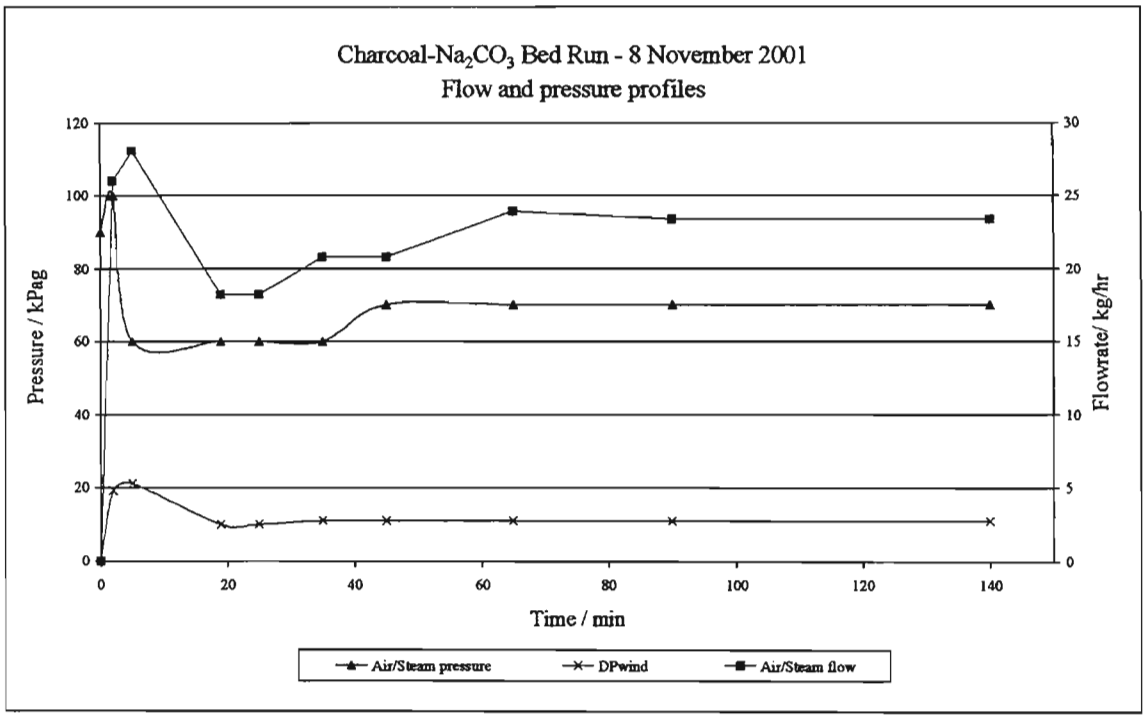

Figure 5.4b: Reactor profiles during gasification of Charcoal-Na_2CO_3 at 560°C

A similar run was performed at 600°C for an equivalent timeframe and the bed materials were analyzed for ash content. The bed material from the 560°C was used for the starting material for 600°C run. Figure 5.5 below shows the relationship between ash content and operating temperature.

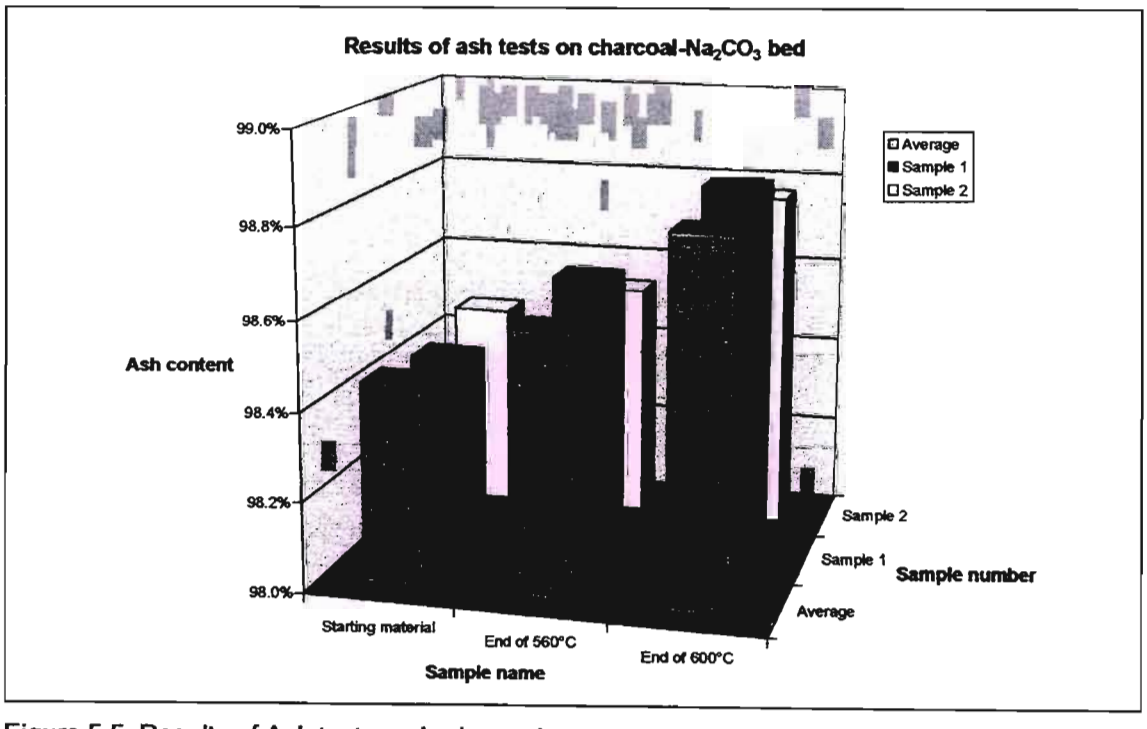

Figure 5.5: Results of Ash tests on bed samples

Using the average values and fitting a curve to the data as shown in figure 5.6 below, shows the almost exponential increase in the ash content with temperature. This is indicative of an almost exponential increase in the amount of carbon that is gasified. The less carbon that remains, the higher the ash content. This increase in ash content with temperature is attributed to the exponential increase in reaction rates with temperature in accordance with the Arrhenius equation for the rate constant dependency on temperature.

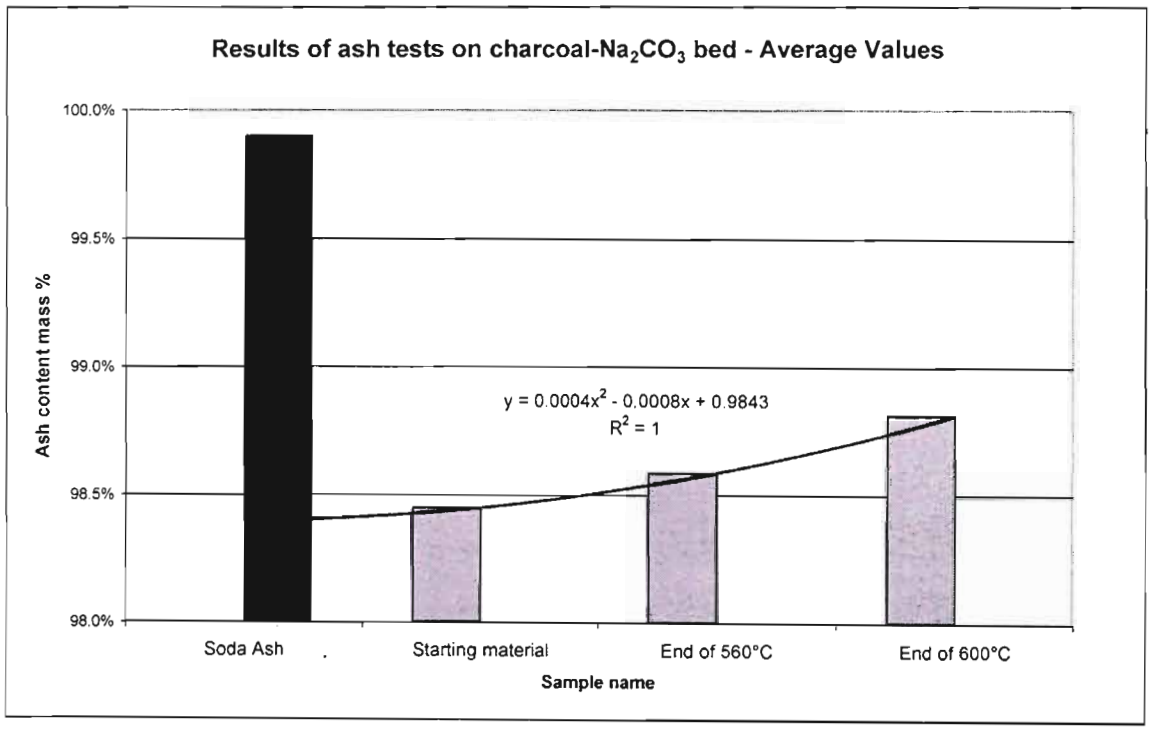

Figure 5.6: Average values of ash tests on charcoal-Na_2CO_3 bed material.

The above tests showed that the reactor successfully gasified a solid fuel and the next stage in the experimental program was to advance to injecting a liquid feed into the reactor under operating conditions.

Figure 5.4a above shows a deviation from normal operating conditions for the steam inlet temperature. This behavior was also seen in later runs with black liquor injection into the fluidized bed. The steam super heater failed to heat up the steam to operating temperature and the trend of the steam inlet temperature shows a cyclical deviation around a much lower temperature of approximately 400°C. Operating temperatures were still able to be attained due to the additional energy input from the internal heater. However, this reduces the gasification capacity of the reactor and the cause of the deviation was investigated.

The data collected during the performance test run of the thermal design was used to identify the root cause of the problem. From figure 5.7 below, the analysis pointed to a reduced LPG flow rate to the burner. After extensive investigations into the LPG distribution network the root cause was found to be blocked nozzles in the gas burner. The nozzles were cleaned and this immediately solved the problem. Figure 5.8 below shows the steam inlet temperature easily achieving 650°C after the burner nozzles were cleaned.

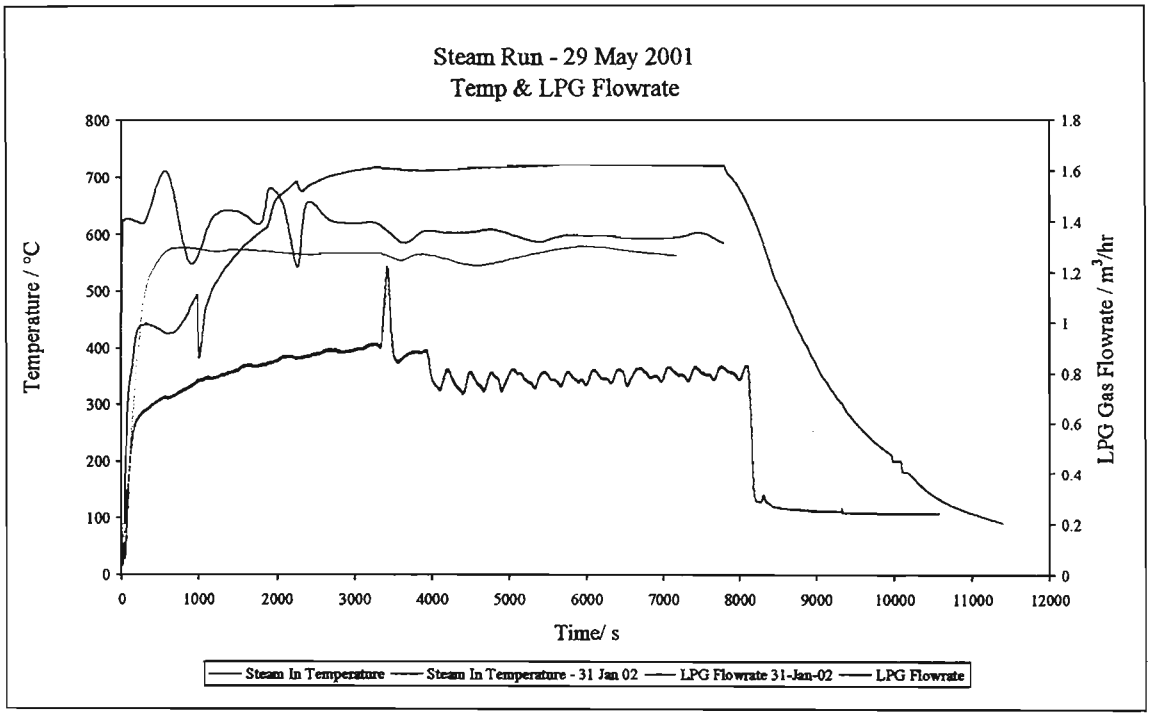

Figure 5.7: Comparative analysis of steam inlet temperatures and LPG flows during troubleshooting.

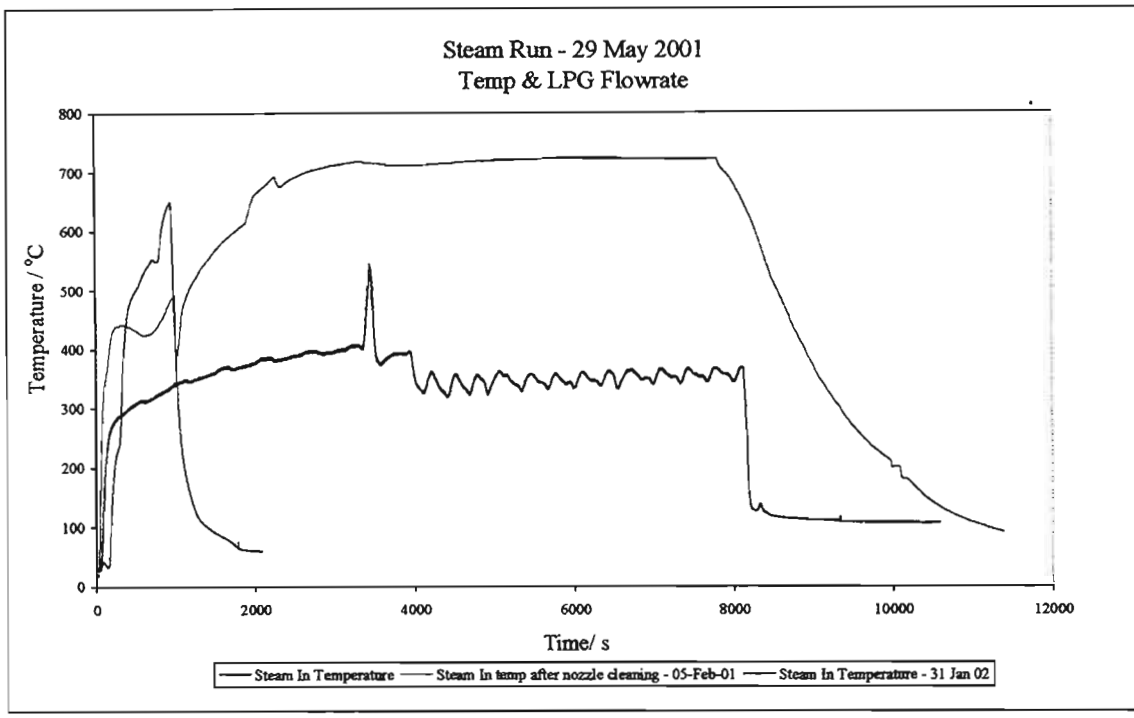

Figure 5.8: Design temperature attained easily after cleaning of nozzles as shown in temperature trends above.

Unfortunately due to the additional demand placed on the internal heater during the burner failure, the internal heating element failed and had to be replaced as well.

5.5. Introduction of a liquid feed into the reactor.

The next stage was to first introduce black liquor into an empty reactor at operating conditions and then proceed to normal operation with a sodium carbonate bed. By approaching the introduction of the feed in this two step approach, it would allow more attention to be focused on the feed delivery system.

5.5.1 Black liquor injection – no bed

The voltage on the nickel wire for the heated lines was set, as well as the steam flow rate to the black liquor steam jacket. It was during this stage that the change from a liquid phase water feed to the black liquor insulation jacket was made as discussed in Chapter 4. The original design intention was to feed the jacket with water and allow it to vaporize in the tube jacket. The control of this is not straight forward and often meant overcooling of the tube which had a twofold effect on the operation:

- unable to attain bed temperatures

- blockage of the black liquor tube by excessive cooling.

The steam jacket proved a much better insulation medium for the black liquor tube.

Numerous problems were experienced during this stage. Initial tests with a 60% black liquor solution caused blockages in the pump. The suction and discharge lines of the pump taper to a 3mm diameter inlet line in the pump casing. Integral to the pump casing is a double ball check valve as indicated in Figure 5.9 below. These valves feature two stainless steel ball bearings that prevent reverse flow. The cross sectional area that the fluid sees is much smaller than the ¾"suction and discharge screwed connections. It is for this reason that the pump manufacturers specify a solids free feed stream.

If the black liquor feed pump body is relatively cold during start-up and the hot black liquor feed is introduced into the pump, the solids precipitate out and cause blockages in the suction and discharge lines. This did occur often and required a time consuming manual stripping and cleaning of the suction and discharge check valves. As a result of this the black liquid solids content was reduced to 43-46%.

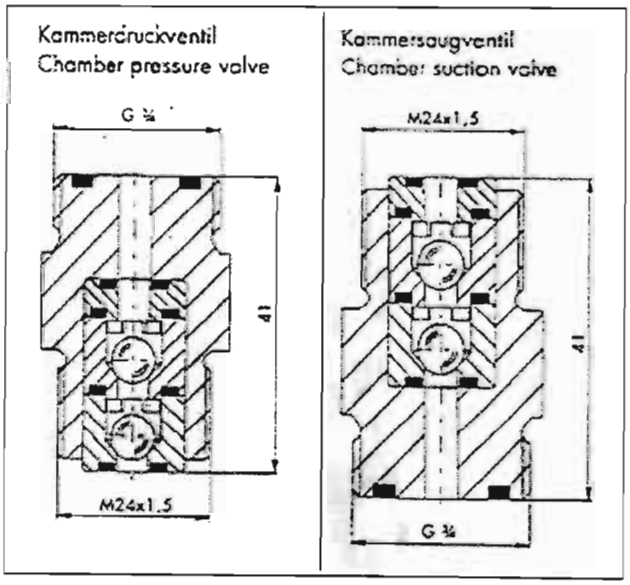

Figure 5.9: Sketch of suction and discharge check valves integral to black liquor pump PX-101 [adapted from the vendor's pump manual]

A change was made to the operating procedure as well (step 41, appendix D) to include a hot water wash through the pump to heat up the pump body prior to the introduction of black liquor into the system. Additional heat tracing was added to the pump body and the suction and discharge lines to counter any heat loss from these surfaces.

These additional precautions helped prevent blockage of the pump. In retrospect a piston diaphragm pump is not the best choice for this application. The better choice would probably be a Peristaltic pump. These pumps have no valves, seals or glands, and the fluid contacts only the bore of the hose or tube. The challenge in selecting such a pump would be in finding a suitable material for the hose or tube. This type of pump was considered during the pump selection stage, but a suitable material for the required temperature could not be procured at the time.

The high concentration of solids also led to problems of the black liquor tube blocking up as well. This was coupled with inadequate insulation from the reactor environment due to incorrect steam supply flow rates to the tube jacket. The tube blocked solid when this occurred. The tube had to be cleaned by drilling the blockage out through the use of a specially made long drill bit constructed from a welding rod.

With the current design, the ¼" stainless steel tube encased in the steam jacket, at most a 46% solids content black liquor feed can be pumped through without causing blockages. To cater for an increase in concentration, the steam supply to the tube would need to be up-rated. It is currently supplied via ¼" stainless steel tubing.

Solids entrained in the black liquor that had managed to pass through the pump blocked up the black liquor injection tube nozzle holes and consequently caused a blockage in the black liquor tube. A blocked tube was indicated by the lifting of the relief valve on the black liquor pump discharge line. During one such occurrence, the tube cracked internally as indicated in figure 5.10 below.

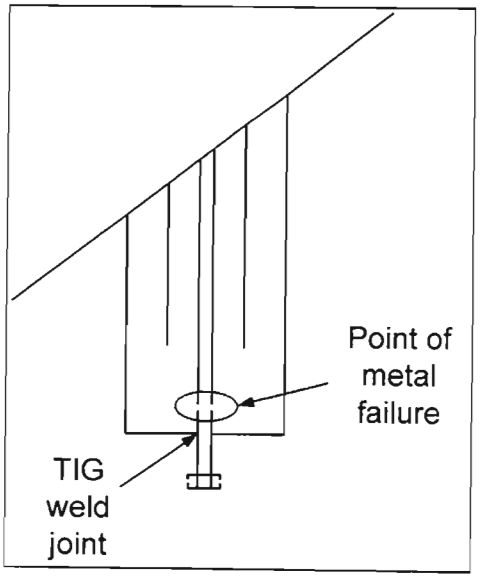

Figure 5.10: Sketch indicating point of failure of black liquor tube.

The cause of the tube failure was attributed to the TIG weld in close proximity of the crack. It is thought that due to possible improper welding techniques, the metal structure was de-natured during the welding process. A blocked tube leads to an increase in the tube pressure up to 9 bar(g) and this was sufficient to cause the metal fatigue at the weakened point. During the repair, more careful attention was paid to the welding procedure which prevented a reoccurrence of the failure.

The black liquor tube nozzle hole diameters were also increased from 0.6mm to 1mm which solved most of the problems.

With these problems solved, black liquor was introduced into the empty reactor. Figure 5.11 below shows the temperature profiles during a black liquor injection run without a bed.

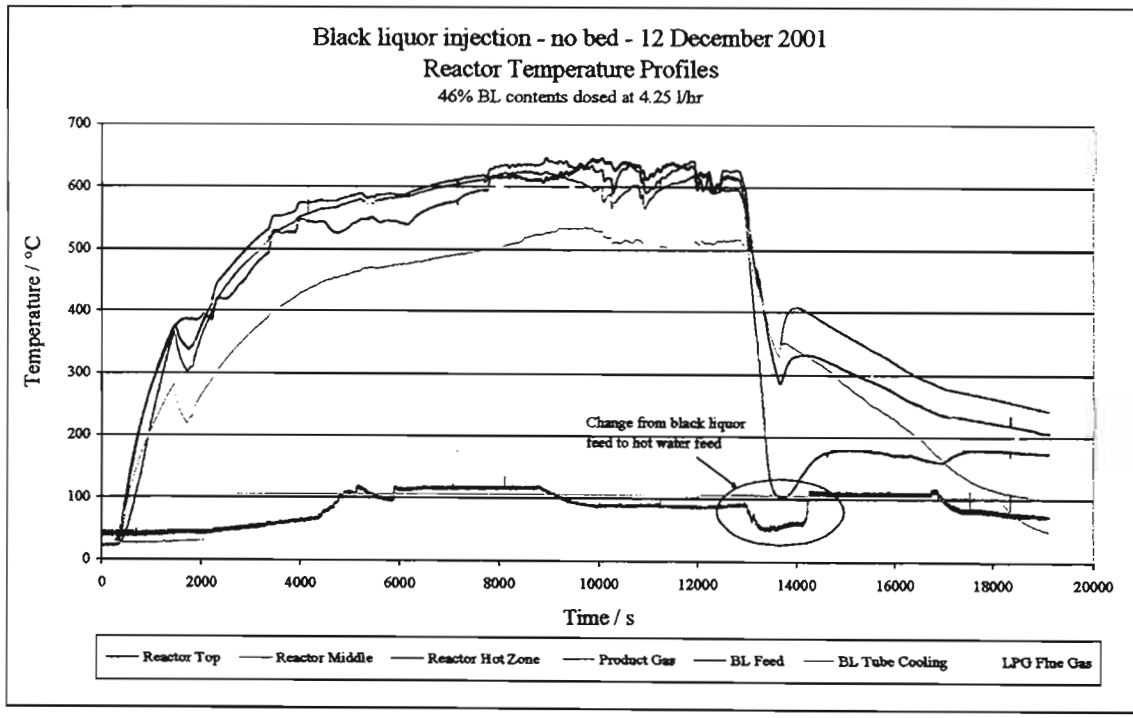

Figure 5.11: Temperature profiles during injection of black liquor at 620°C with no bed.

Indicated on the figure is the point at the end of the run when a change was made from black liquor to hot water in order to flush out the lines at shutdown. The rapid decrease in bed temperatures at shutdown is clearly seen with the injection of a liquid feed into the reactor as compared to previous runs without the liquid feed. It is clear as well that the reactor hot zone temperature drops much more rapidly than the middle and top zones of the reactor indicating two points of note:

- the liquid feed is being injected in the correct bed zone
- The gasification reactions are highest at this point in the bed as they consume most of the energy resulting in the sharp decrease in bed temperatures.

The final phase was to repeat the procedure with a sodium carbonate bed in fluidized state thus achieving the design intent of the pilot plant.

5.5.2 Black liquor injection into a fluidized sodium carbonate bed

A batch of SASAQ black liquor was simulated in the lab using soda black liquor as the base component. This involved the addition of a 50ml solution per kg of Soda black liquor as discussed in Chapter 4. The addition of this solution did not affect the viscosity of the synthesized SASAQ liquor as it is a relatively minor quantity that is added to the black liquor.

Table 5.1 below displays the analysis of the salt concentrations in the simulated black liquor.

Table 5.1: Results of salt analysis on simulated SASAQ black liquor prepared in the laboratory

Sample Label	wt% Cl anion	wt% SO_4 anion	wt% Acid insoluble	wt% Sodium	wt% Potassium	wt% Silica	wt% Ash
Run 1	0.25%	2.17%	1.65%	16.11%	0.125%	1.52%	44.6%
Run 2	0.27%	2.73%	1.66%	16.87%	0.134%	1.34%	46.7%
Run 3	0.27%	2.28%	1.49%	16.61%	0.107%	1.10%	46.1%
Run 4	0.27%	3.48%	1.60%	16.71%	0.122%	1.33%	48.6%

Four experimental runs were done at 620°C with increasing black liquor flow rates. An analysis of the bed material before and after each run was carried out to test for variables such as salt content, ash content and silica reduction.

Figure 5.12 below shows the hot zone temperatures for each run. Run 1 is considerably longer than the other runs due to the introduction of the bed into the reactor after heating up of the reactor as is seen by the drop in hot zone temperatures approximately 5000 seconds after the run commenced. This bed was consequently cleaned up before each run by combustion of any residual carbon deposited on the bed by fluidizing with

air. Any material lost by sampling was made up with additional bed material. The drop in temperatures around 2000-2500 seconds after the run commenced corresponds to the changeover in the fluidizing medium from air to steam.

With increasing feed rates, the black liquor storage tank emptied progressively quicker. Run 3 at a feed rate of 3.04 L/min was repeated in run 4 and allowed to continue for a longer duration by topping up the black liquor feed tank several times during the run. Figure 5.13 and 5.14 below show the temperature and flow trends for Run 4.

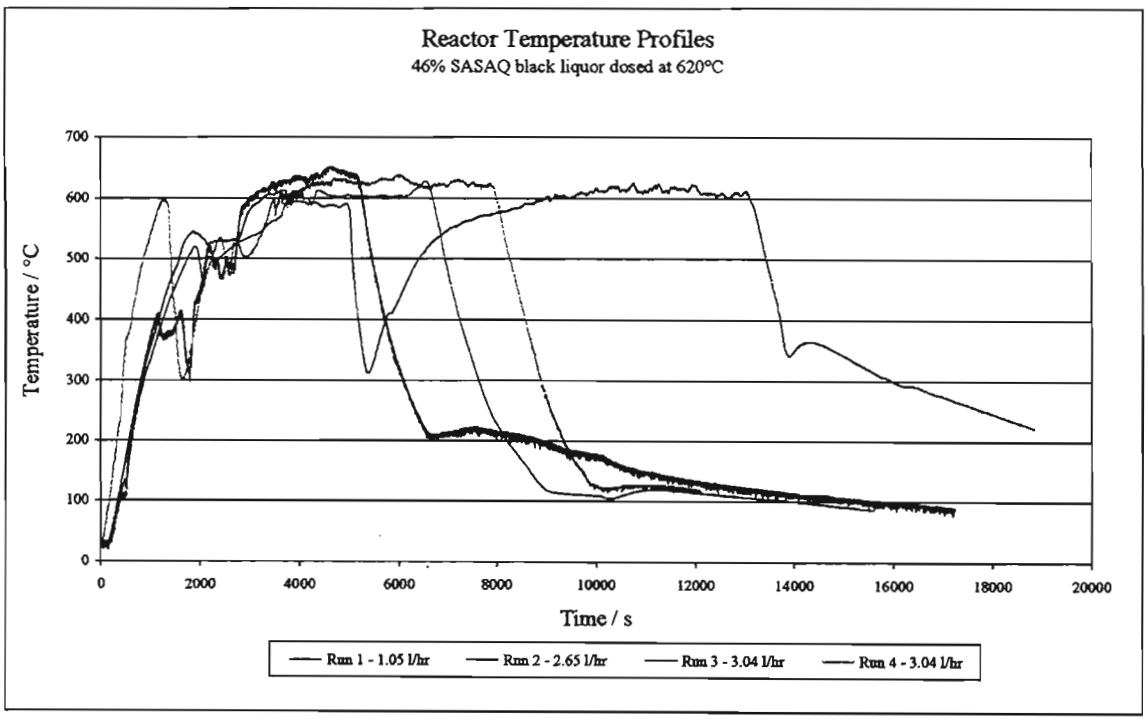

Figure 5.12: Hot zone temperatures for different runs at varying feed flow rates.

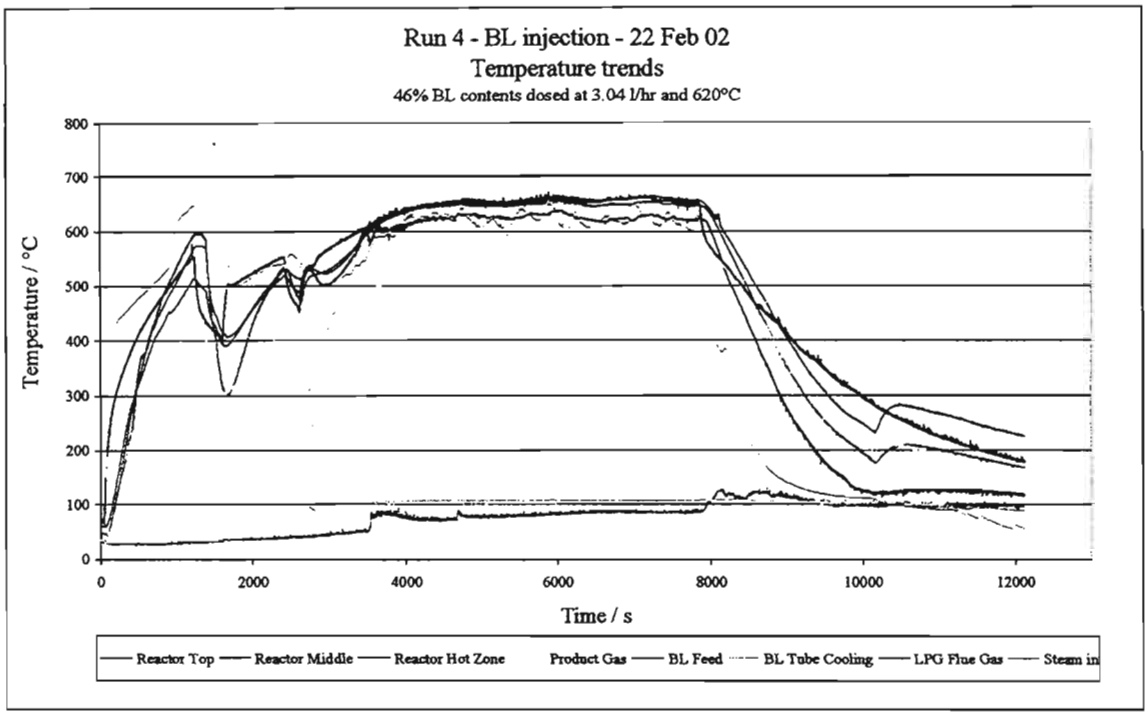

Figure 5.13: Temperature trends for Run 4 at 620°C and black liquor feed rate of 3.04L/hr

The reactor middle and top temperatures were almost the same temperature as the exiting flue gases. The data shows that they are also approximately 25°C higher than the reactor hot zone temperature. This phenomenon is attributed to the convective heat transfer effect that the exiting flue gases from the gas burner have on the reactor as it passes through the shell side of the reactor as discussed earlier.

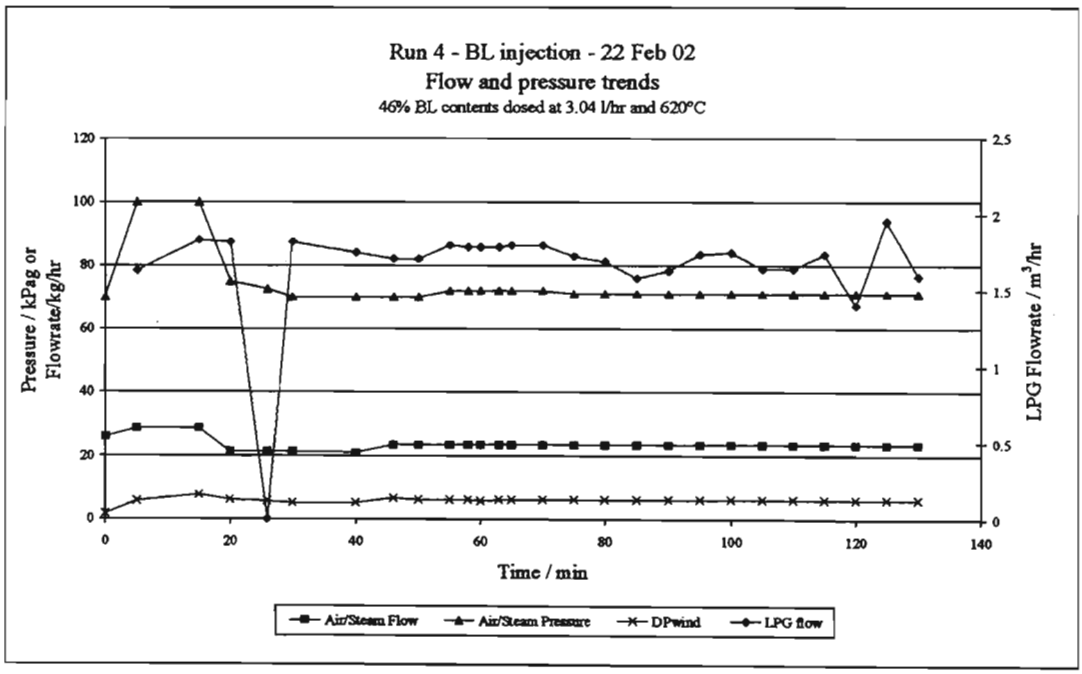

Figure 5.14: Flow and pressure trends for Run 4 at 620°C and black liquor feed rate of 3.04L/hr

The observed 30°C difference has been reduced to a 25°C difference, showing that some of the heat in the top section has been absorbed by the steam jacket on the black liquor injection tube. Clearly this still leaves an excess of energy still available at the top of the reactor which would be well utilized by the injection of black liquor into the top zone of the reactor. Perhaps a combination of injection into the bed as well as at the top would make for interesting observations and allow further up rating of the gasification capacity of the unit. This is worth noting for further improvements to the design. But it is clear that the heat duty available to the system allows for increased capacity and modifications to the design would be needed to harness this energy and transfer it into the hot zone of the bed where it is needed. It is probably this same system behavior that contributed to the development of the TRI/MTCI process [US Patent No. 5637192; US Patent No. 5059404] that uses pulsed heaters in the bed itself.

To verify that the hot zone temperature is in fact approximately 25°C lower that the middle and top zones of the reactor and not just an instrumentation error, the data was compared to the second thermocouple placed in the hot zone, TT-208. TT-208 is linked to the internal heating element HT-201 on temperature control loop TIC-201 as discussed in CHAPTER 4. Figure 5.15 below plots these two sets of data and confirms the reading taken by TT-203.

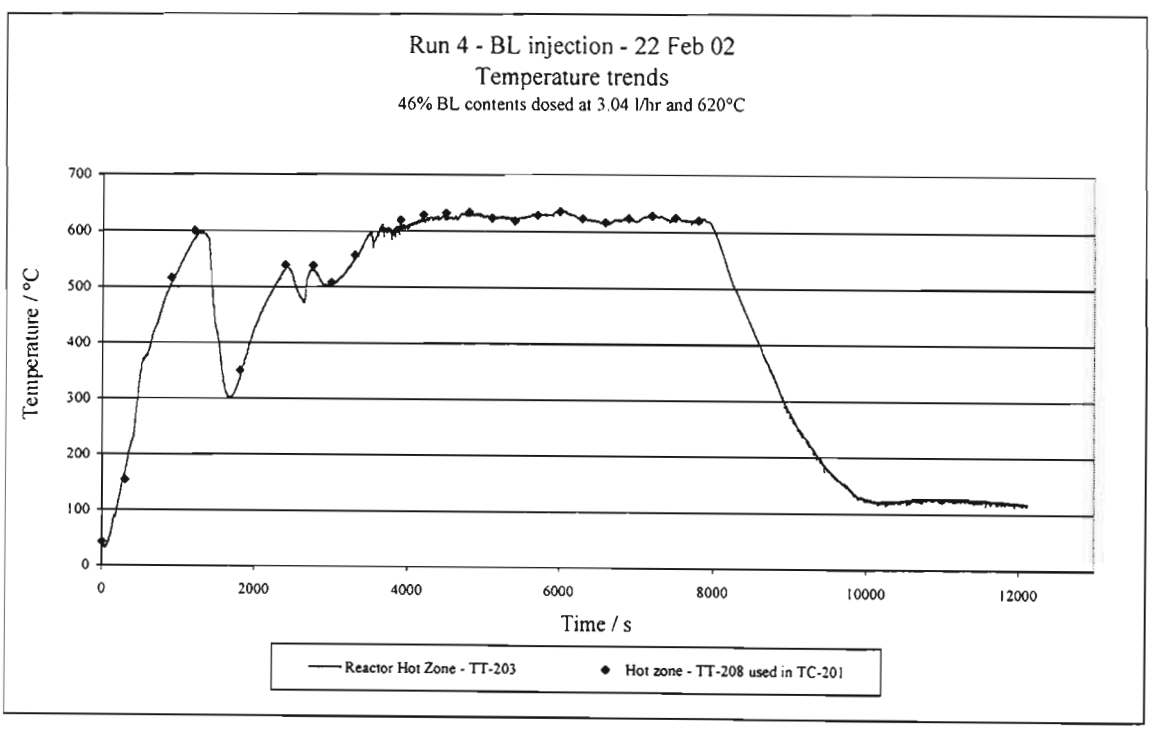

Figure 5.15: Comparison of temperatures recorded by TT-203 and TT-208 in reactor hot zone

Figure 5.16 below shows photos of bed material collected from the reactor before a run, and after the injection of black liquor.

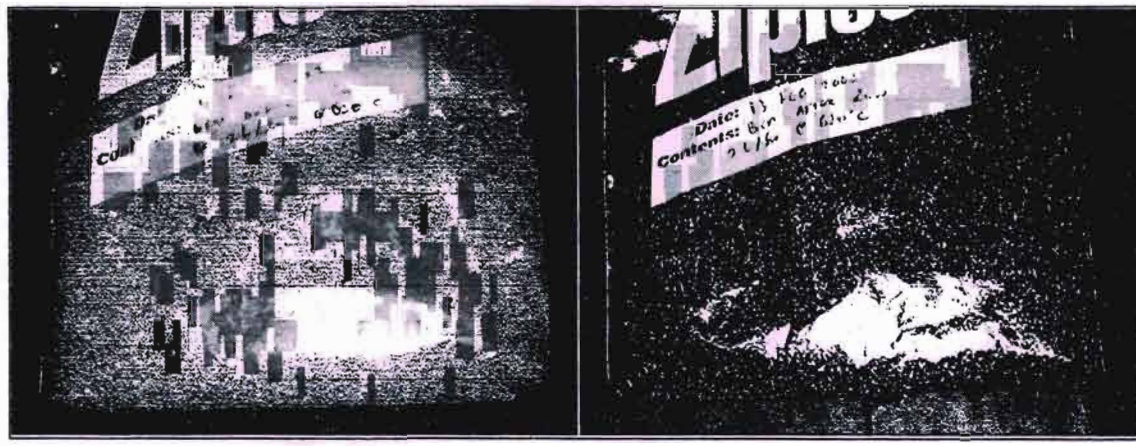

Figure 5.16: Photo of bed sample before a run (left) and after run (right)

The bed material was sampled at the start and end of each run and analyzed for ash, salt and silica content. Table 5.2 below presents the results from the analyses.

Table 5.2: Results of analyses on bed samples

Run number	**1**	**2**	**3**	**4**
Total mass / kg				
Bed in	6.500	6.500	5.600	5.500
Bed out	6.448	6.629	5.564	5.526
Change	-0.052	0.129	-0.036	0.026
wt% Cl anions				
Bed in	0.37	0.34	0.34	0.43
Bed out	0.33	0.32	0.31	0.37
Change	-0.04	-0.02	-0.03	-0.06
wt% SO4 anions				
Bed in	0.62	0.6	0.92	0.46
Bed out	0.59	0.75	0.88	0.62
Change	-0.03	0.15	-0.04	0.16
wt% Ash				
Bed in	99.7	99.7	99.7	98.1
Bed out	99.8	99.4	99.2	98.0
Change	0.1	-0.3	-0.5	-0.1
wt% Acid Insolubles				
Bed in	0.27	0.56	1.32	3.17
Bed out	0.25	0.53	1.76	3.03
Change	-0.02	-0.03	0.44	-0.14
wt% Sodium				
Bed in	39.18	38.85	37.81	36.01
Bed out	38.57	37.95	37.92	37.41
Change	-0.61	-0.90	0.11	1.40
wt% Potassium				
Bed in	0.088	0.102	0.092	0.010
Bed out	0.083	0.116	0.066	0.004
Change	-0.005	0.014	-0.026	-0.006
wt% Total silica				
Bed in	0.26	0.13	0.20	2.60
Bed out	0.08	0.16	0.29	1.94
Change	-0.18	0.03	0.09	-0.66
wt% Soluble Silica				
Bed in	0.15	0.14	0.24	1.99
Bed out	0.00	0.17	0.24	1.59
Change	-0.15	0.03	0.00	-0.40
wt% Insoluble Silica				
Bed in	0.11	0.00	0.00	0.62
Bed out	0.08	0.20	0.05	0.35
Change	-0.03	0.20	0.05	-0.27

Theoretically the bed mass should increase with the injection of the black liquor. The actual rate of bed deposition will depend on the gasification reaction rates, the solids content of the black liquor, and the feed rate at which it is injected into the reactor. We can see an increase in bed volumes in runs 2 and 4 whilst a bed loss in runs 1 and 3. These bed losses could be attributed to procedural errors in vacuuming and collecting the bed material after the run. More trial runs for a longer duration would deliver more definite results to this regard.

Runs 1 and 4 show some degree of silicate reduction from the soluble SiO_3^{2-} group to the insoluble SiO_2 salt. A further experimental plan is needed in this area as it is one of the important parameters for the paper mill. Silicates are a problem unique to non-wood based pulping processes. The only exit for these silicates is in the black liquor recovery system and one would need to study the efficiency of the silicate reduction further to establish relationships between the process variables. A possible route would be to use an alumina bed and dose with black liquor to specifically analyze for SiO_3^{2-} to SiO_2 conversions.

Apart from Run 1, the ash % of the bed decreases slightly. The increased carbon content in the bed and can also be clearly seen in photos of the bed samples shown in figure 5.16 above. Per given unit mass of bed material, if the carbon content increases; the ash content by weight percentage will decreased per unit mass of bed material. However since there are several inaccuracies in the sampling procedur and taking into considerations the loss of bed material through the top and very short run durations, it cannot be stated for sure based on this analysis that the carbon content of the bed increases. However visually it can be verified that there is some carbon buildup in the bed.

By increasing the bed operating temperatures, the gasification reaction rates can be increased. Optimizing the bed temperature and black liquor feed rates would allow for the net carbon content of the bed to remain unchanged. This would mean a perfect energy match between the heat transferred into the bed to gasify the carbon contained in the black liquor that is injected. This is not a simple matter in practice and one would normally exceed this minimum energy required due to heat transfer efficiency losses. However for such a system it is possible that a corresponding energy required could be matched with the black liquor feed rate.

Anion and cation changes within the bed are not well represented by the data. This is thought to be due to the short duration of the gasification runs and some of the light bed material leaving with the product gas out the top of the reactor. Given the low salt concentrations in the black liquor feed itself, one would need to gasify a considerable amount of black liquor before any substantial relationship between anion and cation contents in the bed can be established. This was not undertaken during this project as time did not permit any further testing. The addition of a cyclone to the top of the reactor to treat the exiting gas would return any entrained fines back to the bed as well. This work would be best suited to a further study.

Gas readings on the max 5 were taken shortly after the injection of black liquor. The values were out of the range of the MAX5 analyzer. Due to the nature of the system as discussed earlier, the diluent nitrogen was unsuccessful in assisting to obtain compositional values from the MAX5 gas analyzer. However the MAX5 did confirm that a combustible rich syn gas was produced during each run by monitoring the increase in the combustibles concentration till the upper limit of its range.

The four test runs successfully displayed the unit's capacity to gasify a viscous black liquor feed up to 3.04 L/hr. Spray patterns in the bed were satisfactory as indicated by the well coated bed particles sampled from the bed at the completion of the test runs. The experimental runs indicate potential for improvements in the thermal design to increase the gasification capacity of the unit.

5.6 Problems experienced

To highlight some of the problems not discussed elsewhere in this chapter, attention is drawn to the following problems experienced during the design and commissioning stages of the project.

- Plenum flange sealing gasket
- Poor distribution of steam – smelt formation
- Black liquor tank TK-101 surface skinning
- Heat damage of TI-202 recording steam inlet temperatures and signal fluctuations
- Smelt formation on internal electrical heater element HT-201

5.6.1 Plenum flange sealing gasket

It is important that the flange at the plenum chamber is sealed securely. Any leakage at this point deprived the bed of fluidizing medium and led to unsatisfactory fluidization. The probability of the formation of localized hot spots increased and this ultimately led to smelt formation.

Finding a suitable material for the plenum flange gasket proved quite a challenge. The harsh environment proved quite demanding on the gasket requirements and several novel options were attempted.

Initial trials with an asbestos gasket proved unsuccessful. The high temperature rendered the gasket brittle and it broke into pieces during operation causing a leakage of steam from the plenum flange.

The application of the next material attempted was Holts Gun Gum. This material is used for sealing leaks in exhaust manifolds and is well suited to the high temperature environment that the flange is in. It is supplied as a paste that dries to a hard solid material. The main component in Gun Gum is once again an asbestos based compound. This material worked well until the reactor needed to be washed and cleaned out. The material dissolved in the wash water, once again causing leaks in the flange.

A third attempt was made using a gasket made from asbestos tape in the department workshop. This tape is commonly used for insulation of high temperature surfaces but didn't prove to be suitable as a gasket material with leaks developing very early during operation.

Finally a suitable proprietary material specifically engineered for high temperature insulation applications was procured. Isoplan 1100 is a proprietary insulation material composed of bio-degradable mineral fibers with fillers and some organic binders capable of withstanding up to 1100°C. It is commonly used in the furnace and drying industry where its application has been well proven. A gasket constructed from Isoplan 1100 proved to provide good sealing of the flange and withstood the high temperature environment extremely well.

5.6.2 Poor distribution of steam

The poor distribution of steam experienced during the design and development of the distributor plate led to the formation of hot spots within the reactor. These hot spots were primarily at the reactor wall surfaces and the distributor plate itself. When the fluidizing medium failed to mix the bed material effectively, conduction through the wall surfaces and in particular the distributor plate meant that they were often at a higher temperature than the bed itself. Such conditions eventually gave rise to smelt formation within the bed. Figure 5.17 below shows photographs of smelt formed during one of such occasions.

Figure 5.17: Photo of smelt formed during initial testing of sieve distributor plate.

One area that did not improve with the introduction of bubble caps is that the distributor plate still remained a source of heat. The reason for this might be the restriction created by the plenum flange and the inner insulating shell. The flue gas velocity increases in this small annular region marked in red in figure 5.18 below.

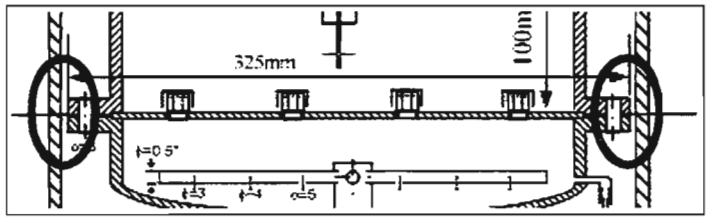

Figure 5.18: Sketch depicting constriction between plenum flange and inner insulating shell indicated by red rings.

This behavior causes turbulent conditions in the flue gases at this region which promotes high heat transfer to the flange and the distributor plate. This is not necessarily a drawback, just as long as the fluidizing medium is equally distributed by the plate and is able to transfer this heat into the bed. However it does mean that in the event of poor distribution, the distributor plate will become the first area where local hotspots are created and smelt will be formed.

5.6.3 Surface skin formation on TK-101

The black liquor storage tank TK-101 was initially unstirred. The intent was that the convection currents from the internal electrical heater would be sufficient to create movement within the bulk of the liquor. However this was not the case and it necessitated the use of a stirrer.

The formation of a skin layer on the surface of the liquid proved problematic. Particles in the black liquor settled out due to the lower temperatures at the surface of the liquor. This caused downstream problems in the blocking of the feed pump and the delivery lines to the reactor.

The installation of the stirrer AG-101 eliminated these problems.

5.6.4 Heat damage to TI-202 – steam inlet temperature

Initially thermocouple TI-202 recording the steam inlet temperature was only encased in a ¼" thermowell with a ½" stainless steel insulating shield as protection from the direct flame of the gas burner. The thermocouple wire itself is individually insulated with a silicone based insulating layer.

This proved to be insufficient protection and necessitated frequent replacement of the thermocouple due to a breakdown of the silicon insulation layer on the thermocouple wires. As a result of this, contact with the stainless steel structure of the reactor unit occurred. This relayed interference to the PC card used for the recording of the temperatures and caused huge fluctuations in temperature recordings of all thermocouples connected to the PC card.

The problem was finally solved by encasing the entire thermowell and ½" stainless steel insulation shield in a layer of fireclay cement. A mould was constructed around the thermowell to hold the fireclay cement during curing. The insulation layer worked exceptionally well and no further problems were experienced around the thermocouple measurements.

5.6.5 Smelt formation on internal electrical heating element HT-201

The temperature control on loop TIC-201 uses a solid state relay to regulate the operation of the internal heating element HT-201. This is controlled by the CB100 digital temperature controller which uses a "bang-bang' control philosophy. If the heater is switched on too early whilst the bed is not yet at operating temperature, this then means that the heater will have to add the extra duty to bring the bed up to temperature. As a result the element glows red hot which is indicative of surface temperatures in excess of 900°C, well beyond the smelt formation temperature.

This may be acceptable in the gasification of a solid carbon fuel. However with a sodium carbonate bed present this practice leads to a layer of smelt building up on the element surface. This is the reason why the timing of switching on the element was crucial and was done very close to injection of the black liquor. The gasification reactions consumed this heat and prevented the element from glowing.

The ability of the pilot plant to gasify a liquid feed with in a fluidized sodium carbonate bed at temperatures in the 600 – 630°C range has been successfully verified and it can be stated that the design objective has been achieved.

The next chapter concludes the findings of this work and lays out the recommendations and opportunities for further development of the pilot plant.

CHAPTER 6

CONCLUSION AND RECOMMENDATIONS

The aims of this project was to design, construct and commission a gasification pilot plant capable of gasifying a black liquor liquid feed in a fluidized bed reactor. The intention was to gain an understanding of specific areas of concern when scaling up from a bench scale unit and understand the problems around the operation of a fluidized bed gasifier with the intent of averting these areas of concern when a larger scale unit needs to be built.

Key elements of this project were:

- Design of a fluidized bed reactor
- Upstream and downstream process development
- Instrumentation requirements
- Construction, commission and operation of the pilot plant.

6.1 Design of a fluidized bed

A 10" 1.2m tall fluidized bed reactor was designed and constructed from stainless steel. Much effort was spent on the design of the distributor plate for even distribution of the fluidizing medium. This called for the use of bubble caps which proved to work well in this application. An internal electrical heater was designed to provide energy for the endothermic gasification reactions. The design was presented in CHAPTER 4.

6.2 Upstream and downstream process development

An overall pilot plant flow scheme was developed and detail design was done on the upstream and down stream processes. The approach used and outcomes were presented in CHAPTER 4.

For the upstream processes, an 8.5L/hr piston diaphragm dosing pump was selected to deliver a black liquor feed into the reactor. Attention was paid to the design of the black liquor injection tube and the black liquor delivery lines.

Detailed design of the feed system, the steam super heater, which utilized a forced draft gas burner, and the gas analysis train was completed and construction undertaken. A novel design approach saw the combination of the steam super heater and reactor in a single unit that featured heat integration between the super heater and the reactor. However this innovative integrated design proved to create more problems by complicating the operation and inter-dependence between the reactor and the steam superheater.

6.3 Instrumentation requirements

The instrumentation required for the operation of the gas burner was identified, sourced and installed. Logging of data was achieved through the use of an Eagle Technologies PC-73-T computer card and a program written in Microsoft Visual Basic. Pressure gauges were installed at critical points in the system to monitor system pressures.

6.4 Construction, commissioning and operation

Commissioning of the pilot plant led to design modifications of several reactor components and to the feed and gas sampling systems including the distributor plate, the gas sampling condenser and the thermocouples. Trial runs showed the steam super heaters capacity to produce 30 kg/hr of super heated steam at 700°C and 0.6 bar(g).

Preliminary experimental runs showed the successful gasification of both solid and liquid carbon sources and displayed stable operation and control of process conditions.

Up to 3.05l/hr of black liquor was able to be treated in the reactor with opportunities identified for future increases in throughput. The black liquor injector proved to function well as was indicated by uniform well coated bed particles removed from the reactor after experimental runs.

This research has achieved the project objectives and addressed crucial issues around the design and operation of such a unit. It has set the stage for further development of the technology by establishing a base unit capable of gasifying a 46% solid content Soda or synthesized SASAQ black liquor feed in a fluidized bed reactor with a sodium carbonate bed up to temperatures of 620°C. With further development of the technology key scale-up concern areas can be identified for consideration when building a full scale operating unit.

6.5 Recommendations

- The use of a gas chromatograph for analysis of the syn-gas is essential for optimization of operating conditions. The next step in the development of the technology must include a gas chromatograph before further advancements can be made.

- The distributor design utilizing the 12 bubble caps worked well as a first attempt. There is still place for optimization of the number of bubble caps and the general feel is that the more the number of bubble caps, the less the chance of a misdistribution of the fluidizing medium. It is recommended that a smaller size but greater number of bubble caps be utilized in a new distributor plate design. The construction effort involved in making each bubble cap is tedious and time consuming. Perhaps the purchase of bubble caps from a suitable vendor would be more appropriate with this approach.

- The inner insulation shell surrounding the plenum flange should be constructed so as to allow an even cross sectional area in the annular space between the reactor shell and the insulation shell. Currently the restriction at this point enhances heat transfer to the flange and the distributor plate. It's for this reason that the distributor plate is the first point of smelt formation in the event of a distribution problem. Should the construction of the insulation shell be too difficult to achieve this characteristic, then an alternative would be to increase the insulation shell diameter to reduce the effect of the restriction around the plenum flange.

- Fluidizing steam pressures should be increased to the region of 1.5-2 bar(g). This would ensure sufficient driving force to enhance vigorous mixing of the bed.

- The condenser in the gas sampling system needs to be supplied with a continuous cooling system on the shell side of the cooling coils. It is thought that the use of a

refrigerated system would prove ideal for this application due to the high reactor discharge temperature.

- The addition of a gas cyclone to the reactor gas outlet would help prevent the entrainment of fines in the outlet gas and return these particles to the bed. This would prevent inaccuracy in the mass balance.

- Investigate the possibility and feasibility of directing the flue gas from the gas burner through horizontal or vertical tubes in the reactor. This can be done by installing baffles on the reactor shell side and tubes through the reactor bed area.

- Source an alternative pump for the black liquor feed pump. A peristaltic pump would work well if a correct tube for the application can be sourced.

- Include a thermocouple on the surface of the internal heating element HT-201. This measurement must be used to control the bed temperature or activate an alarm to assist in preventing the surface of the element from overheating and leading to smelt formation on the element.

- Replacement of pressure switch PS-201 with a Bailey & Mackey adjustable pressure switch from Instralec cc. The current switch used is an oil pressure switch from a motor vehicle and is clearly not suited to the steam environment. Constant failure in service confirmed this.

- Study the effect of varying black liquor injection height in an effort of up rating the capacity of the reactor.

- Install a larger black liquor storage tank to facilitate longer runs.

- The novel integration of the reactor with the steam superheater caused more problems than anticipated. A separation of the two would mean easier control and operation of the reactor.

- More experimental runs particularly with SASAQ liquor with an increased solids concentration of 60% and at higher temperatures like 700°C.

REFERENCES

Abrahamsen, A.R. & Geldart, D; Behavior of gas-fluidized beds of fine powders part I. Homogeneous expansion ,*Powder Technology*, Vol 26, 1980, pp. 35-46

Agarwal, J.C., Davis, W.L. & King, D.T.; *Chem. Eng. Prog.*, Vol 58, 1962, pp. 85

Aghamohammadi, B.; Mansour, M.N.; Durai-Swamy,K; Steedman, W.; Rockvam, L.N.;

Ahlroth, M & Svedberg, G.; Case study on simultaneous gasification of black liquor and biomass in a pulp mill, *Transactions of the ASME*, 1998, pp. 98-GT-350

Bennington, C.P.J. & Kerekes, R.J.; *TAPPI 1985 International Chemical Recovery Conference Proceedings*, TAPPI Press, pp. 345

Berglin, N. & Berntsson, T; CHP in the pulp industry using black liquor gasification: Thermodynamic analysis; *Applied Thermal Engineering*, Vol 18, 1998, pp. 947-961

Berglin, N., Persson, L. & Berntsson, T.; Energy systems options with black liquor gasification; *Pulp & Paper Canada*, Vol. 97, No. 5, 1996, pp. 19-23

Braunstein, R; Pulping and bleaching of SAS-AQ bagasse pulps; *TAPPSA Journal*, March 2004

Brown, C.A. & Hunter, W.D.; Operating experience at North America's first commercial black liquor gasification plant; *TAPPI Proceedings, International Chemical Recovery Conference*, 1998, pp. 655-662

Cantrell, J; Simulation of Kraft black liquor gasification – A comparative look at performance and economics; *TAPPI Journal Peer Reviewed Paper*, Vol 84 No. 6, 2001

Consonni, S., Larson, E.D. & Berglin, N., "Black liquor-gasifier/gas turbine cogeneration", *American Society of Mechanical Engineers Paper*, 1997, P97-GT-273

Coulson & Richardson, Chemical Engineering, Vol 2- Particle Technology and Seperation Processes, Butterworth Heinmann, 1997, Chapter 6

Dow, W.M. & Jakob, M., Heat transfer between a vertical tube and a fluidized air-solid mixture; *Chem Eng Progr.*, vol 47, 1951, pp. 637

Eleftheriades, C.M., Design and operation of a multistage pressurized fluidized bed combustor; *PhD Thesis*, University of Natal, 1981

Empie, H.J., Lien, S.J., Yang, W. & Adams, T.N.; Spraying characteristics of commercial black liquor nozzles; *TAPPI Journal*, Vol. 78, No. 1; 1995, pp. 121-128

Energy Statistics Yearbook: 1993, New York: United Nations, 1995

Erickson, D. & Brown, C.; Operating experience with a gasification pilot project; *TAPPI Journal*, Vol. 82, No. 9, 1999, pp. 48-50

Finchem, K.J.; Black liquor gasification research yields recovery options for future; *Pulp & Paper*, Nov 1995. pp. 49-53

Fogelholm, C.J. & McKeogh, P.J., Black liquor as a fuel for combined cycles; *ASME Cogen-Turbo 6*, 1991, pp.307-312

Frederick, J; How integrated gasification will impact Kraft pulping and chemical recovery; *TAPPI Journal*, Vol 82, No.9, 1999, pp. 45-47

Galtung, F.L. & Williams, T.J., Model control Kraft prod. sys. pulp production; *Process Symposium.*, 1975, pp. 131-147

Gea, G., Murillo, M.B., Arauzo, J. & Frederick, W.J.; Swelling behavior of black liquor from Soda pulping of wheat straw; *Energy and Fuels*, Vol 17, pp. 46-53

Geldart D, The effect of particle size and size distribution on the behavior of gas- fluidized beds; *Powder Technology*, Vol 6, 1971, pp. 201

Geldart, D. - *Gas Fluidization Technology*, Wiley Interscience, 1986.

Grace, T.M.; Bring on the gasifiers, *Pima Magazine*, April 1996, pp. 42-43

Grace, T.M. & Timmer, W.M.; A comparison of alternative black liquor recovery technologies; *TAPPI Proceedings, International Chemical Recovery Conference*; 1995, pp. B269-B-275

Harriz, J.T.; Black liquor gasification: A comprehensive update; *TAPPI Journal*, Vol. 82, No. 9, 1999, pp. 43-44

Helpio, T.E.J. & Kankkunen, A.E.P.; The effect of black liquor firing temperature on atomization performance; *TAPPI Journal*, Vol. 79, No. 9, 1996, pp. 158-163

Howard, D; Anthraquinone and Polysulfide - Applicability for use in pulp mill operations; *TAPPI Pulping Conference Proceedings*, 1996

Hunt, N; Review of PIRA non-wood fibre conference; *TAPPSA Journal*, March 2003

Hupa, M., Solin P. & Hyoty P., Combustion behavior of black liquor droplets; *Journal of Pulp and Paper Science*, Vol 13, 1987, pp. J67-J72

Ihren, N.C. & Svedberg, G.; Simulation of combined cycles with black liquor gasification; *Transactions of the ASME*, 1994, pp. 94-GT-447

Khan, A.R. & Richardson, J.F., Fluid-particle interactions and flow characteristics of fluidized beds and settling suspensions of spherical particles; *Chem. Eng. Commun.*, vol 78, 1989, pp. 111

Kreutz, T.G., Larson, E.D. & Consonni, S.; Performance and preliminary economics of black liquor gasification combined cycles for a range of Kraft pulp mill sizes; *TAPPI Proceedings, International Chemical Recovery Conference*, 1998, pp. 675-692

Krishna, R & van Baten, J.M.; Using CFD for scaling up gas–solid bubbling fluidized bed reactors with Geldart A powders; *Chemical Engineering Journal,* Vol 82 ,2001, pp. 247–257

Kunii, D. and Levenspiel, O. - *Fluidization Engineering*, J. Wiley and Sons, 1969.

Larson, E.D. & Raymond, D.R.; Commercializing black liquor and biomass gasifier/gas turbine technology; *TAPPI Journal*, vol 80, No. 12, 1997, pp. 50-57

Larson, E.D., Consonni, S. & Kreutz, T.G.; Preliminary economics of black liquor gasifier/gas turbine cogeneration at pulp and paper mills; *Transactions of the ASME*, 1998, pp. 98-GT-346

Larson, E.D., Kreutz, T.G & Consonni, S.; Combined biomass and black liquor gasifier/gas turbine cogeneration at pulp and paper mills; *Transactions of the ASME*, Vol. 121, July 1999, pp. 394-400

Larson, E.D., Kreutz, T.G & Consonni, S.; Combined biomass and black liquor gasifier/gas turbine cogeneration at pulp and paper mills; *Transactions of the ASME*, 1998, pp. 98-GT-339

Larson, E.D., McDonald, G.W., Yang, W., Frederick, W.J., Iisa, K., Kreutz, T.G., Malcolm, E.W. & Brown, C.A.; A cost benefit assessment of black liquor gasifier/combined cycle technology integrated into a Kraft pulp mill; *TAPPI Proceedings, International Chemical Recovery Conference*, 1998, pp. 1-18

Larson, E.D., McDonald, G.W., Yang, W., Frederick, W.J., Iisa, K., Kreutz, T.G., Malcolm, E.W. & Brown, C.A.; A cost benefit assessment of BLGCC technology; *TAPPI Journal,* Vol. 83, No.6, 2000, pp. 57

Leva, M., *Fluidisation*, McGraw-Hill Book Company, New York, 1959

Li, J.& Heiningen A.R.P.; "The rate process of H_2S Emission during steam gasification of black liquor char"; *Chemical Engineering Science*, Vol 49: No. 24, 1995, pp. 4143-4151

Lombardi,G., Pagliuso, J.D., Goldstein Jr., L.; Performance of a tuyere gas distributor; *Powder Technology,* v94 – 1997, pg 5-14

Marshall, B. & Ropers, H.; Fluidized bed reactor offers incremental capacity option; *Pulp & Paper*, Nov 1995, pp. 67-69

McDonald, C; DNCH4ET1 - Chemical Engineering Topics: Paper and Pulp course notes, University of Natal Durban, 1998

McKeough, P; Research on black liquor conversion at the technical research institute of Finland; Bioresource Technology, Vol 46, 1993, pp. 135-143

Monaghan, M.T. & Siddall, R.G.; The combustion of single drops of waste sulphite liquor – A preliminary investigation, *TAPPI Journal*, 1963

Näsholm, A & Westermark, M.; Energy studies of different cogeneration systems for black liquor gasification; *Energy Convers. Mgmt*, Vol 38, No 15-17, 1997, pp. 1655-1663

Oscarsson, B.; Lessons learned from gasifier operating experience; *TAPPI Journal*, Vol. 82, No. 10, 1999, pp. 46-48

Perry & Green, *Perry's chemical engineers handbook*, McGraw-Hill Book Company, 1997,1999. Chapters 5, 11,17

Qureshi, A.E. & Creasy, D.E; Fluidized bed gas distributors; *Powder Technology*, Vol 22, 1979, pp. 113-119

Richard, A., Davies, C., D'Agostino, D., DuPlooy, A., Kerr, I.; Steam explosion pulping of bagasse for fine paper production; *TAPPI Pulping Conference Proceedings*; 1998

Rockvam, L.N., Tenore, F., Spent liquor steam reforming and recovery; *TAPPI Proceedings Engineering Conference*, 1996, pp. 269-272

Salmenoja, K; Black liquor gasification: theoretical and experimental studies; *Bioresource Technology*, Vol 46, 1993, pp. 167-171

Sharma, N.K., Bhargava, K.S. & Sharma, S.K.; A good recovery for FBR technology; *PPI*, June 1998, pp. 69-71

Spielbauer, T.N., Adams, T.N., Monacelli, J.E. & Bailey, R.T.; *CPPA 1989 International Chemical Recovery Conference, Technical Section CPPA*, 1989, pp. 119

Stigsson, L, "Pressurised black liquor gasification – future technology for bio-electric power production and recovery of pulping and bleaching chemicals"; *TAPPI Pulping Conference*, 1994

Stigsson, L; Chemrec™ Black liquor gasification; *TAPPI Proceedings, International Chemical Recovery Conference*, 1998, pp. 663-674

Verrill, C.L. & Van Heiningen, A.R.P.; Calcuim bases sulphur recovery process for Kraft black liquor gasification – proof of concept; *TAPPI Journal*, Vol. 83, No. 7,2000, pp. 71

Verrill, C.L.; Kitto, J.B. & Dickson, J.A.; Development and evaluation of a low temperature gasification process for chemical recovery from Kraft black liquor; *TAPPI Proceedings of International Chemical Recovery Conference*, 1998, pp. 1067-1078

Vreedenberg, HA, Heat transfer between fluidized beds and vertically inserted tubes, *J. Applied Chem*, Vol 2, 1952, pp. S26

Wen, C.Y. & Yu, Y.H., A Generalized method for predicting minimum fluidizing velocity, *AIChe Journal*, Vol. 12, 1966, pp. 610

Wessel, R.A., Parker,K.L., Verrill, C.L.; Three-dimensional kraft recovery furnace model: implementation and results of improved black-liquor combustion models; *TAPPI Journal*; Vol 80, No 10, 1997. pp. 207-220

Whitehead, A.B. & Dent, D.C.; Behavior of multiple tuyere assemblies in large fluidized beds, *International Symposium on Fluidization, Endhaven Conference*, 1967, pp. 802-820

Whitehead, A.B.; Gartside, G. & Dent, D.C., Flow and pressure multidistribution at the distributer level of a gas-solid fluidized bed; *Chem. Eng. Journal*, Vol 1, 1970, pp. 175-185

Whitty, K, Backman, R., Forssen, M., Hupa, M., Raino, J. & Sorvari, V.; Liquor-to-liquor differences in combustion and gasification processes: Pyrolysis behavior and char reactivity; *Journal of Pulp and Paper Science*, Vol. 23, No. 3, 1997, pp. J119-J128

Zenz, F.A.; Bubble formation and grid design; *Tripartite Chemical Engineering Conference Syumposium Series*, Vol. 30, 1968, pp. 136-139

BIBLIOGRAPHY

The following literature were consulted:

Brown, C; Smith, P.; Large scale pilot testing of the MTCI/Thermochem black liquor steam reformer; *TAPPI Proceedings, International Chemical Recovery Conference*, 1995, pp. B297-B-301

Coulson & Richardson, Chemical Engineering, Vol 6- Chemical Engineering Design, Butterworth Heinmann, 1996

Frederick, W.J., Wag, K.J. & Hupa, M.M.; Rate and mechanism of black liquor char gasification with CO_2 at elevated pressures; *Ind. Eng.Chem. Res.*, Vol. 32, 1993, pp. 1747-1753

Ghalke, S.N. & Veeramani, H; Viscosity of bamboo, bagasse and Eucalyptus black liquors; *TAPPI Progress Report No.8*, 1977

Jahnke, F; Commercial success of gasification technology; *TAPPI Journal*, Vol 82, No. 12, 1999, pp. 49-53

Meadows, D.G.; The pulp mill of the future: 2005 and beyond; *TAPPI Journal*, Vol. 78. No. 10, 1995, pp. 55-60

Mullen, T. & Mayotte, L.G.; Effects of black liquor oxidation on overloaded evaporators; *Pulp & Paper Canada*, Vol. 89. No. 5, 1988, pp. T159-T163

Rita, T, Mathur, R.M., Kulkarni, A.G. & Rao, N.J.; Chemical recovery options for agro based pulp and paper mills; *IPPTA*, Vol 8, No.3, 1996, pp. 31-36

Zeng, L. & Van Heiningen, A.R.P.; Sulphur distribution during air gasification of Kraft black liquor solids in a fluidized bed of TiO_2 particles; *Pulp & Paper Canada*, Vol 100, No. 6, 1999, pp. 58-63

The following websites were consulted:

1. www.babcock.com

2. www.chemrec.se

3. http://www.energysolutionscenter.org/supercenter/GTMagazine/PDFs/GT_W02_SteamReforming.pdf

4. http://etcpitea.se/blg/

5. Marklund, M., "Black Liquor Recovery : How does it work?", http://etcpitea.se/blg/document/PBLG_or_RB.pdf

6. http://www.cartonboard.com.au/SchoolProjects/History.htm

7. http://www.ieer.org/ensec/no-1/glbnrg.html

8. http://www.tri-inc.net/

9. http://www.tri-inc.net/TRI%20Attachment%201%20(White%20Paper).pdf

APPENDIX A

PROCESS FLOW DIAGRAMS FOR BLACK LIQUOR GASIFICATION PILOT UNIT

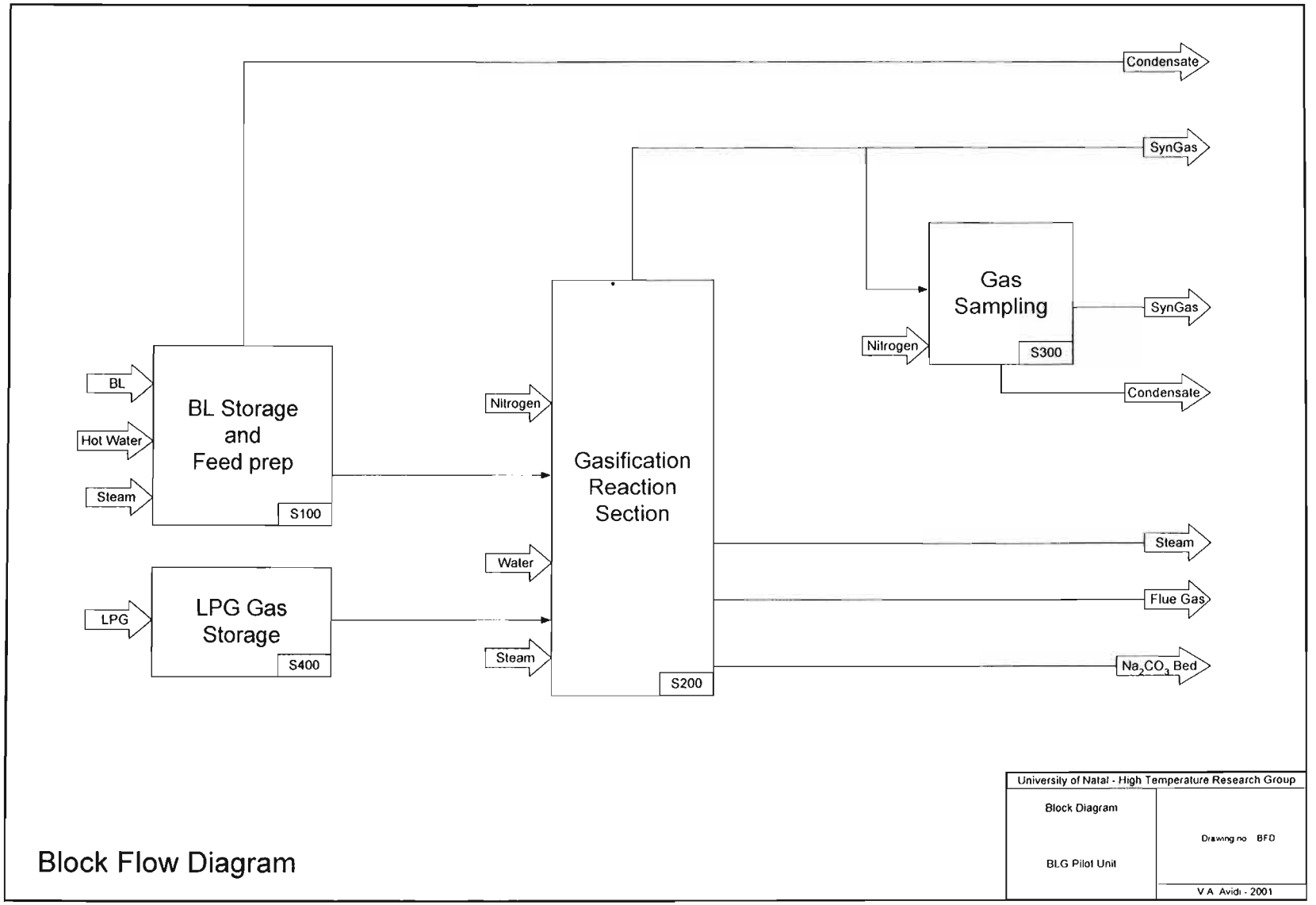
Condensate
SynGas
Gas
Sampling
S300
SynGas
Nitrogen
Condensate
BL
Hot Water
Steam
BL Storage
and
Feed prep
S100
Nitrogen
Gasification
Reaction
Section
Water
Steam
S200
Steam
Flue Gas
Na_2CO_3 Bed
LPG
LPG Gas
Storage
S400
Block Flow Diagram
University of Natal - High Temperature Research Group
Block Diagram
BLG Pilot Unit
Drawing no BFD
V A Avidi - 2001

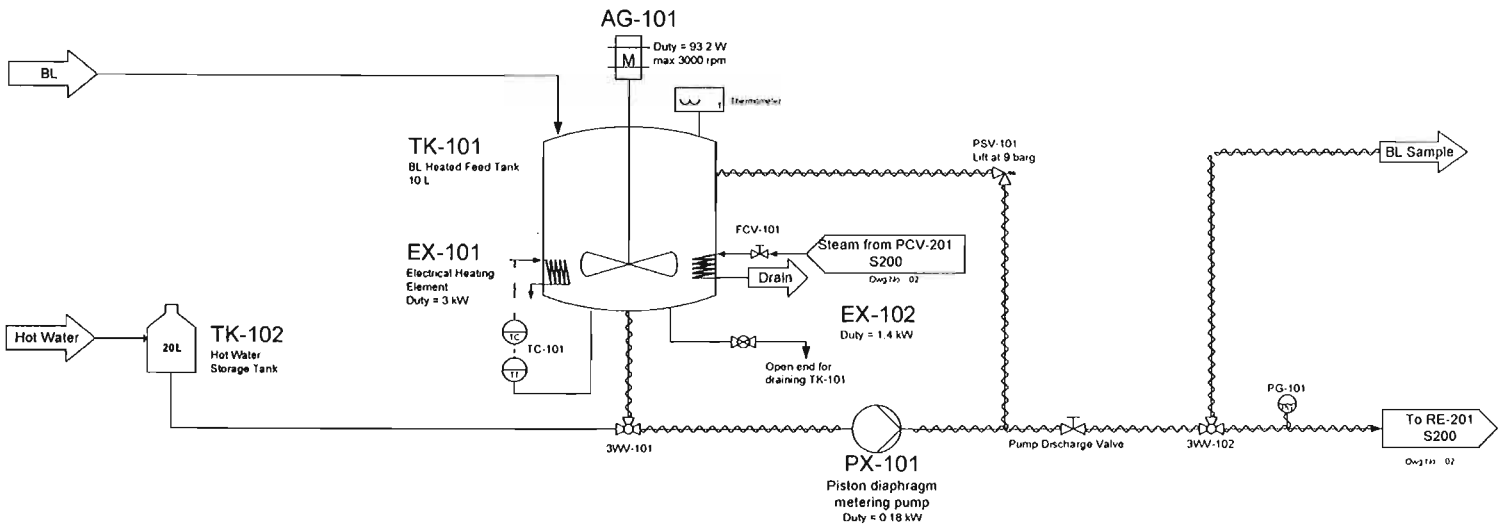

S100 - Black Liquor Storage and Feed Preparation

University of Natal - High Temperature Research Group	
Process Flow Diagram S100 Black Liquor Gasification BL Storage and Feed Prep.	Drawing no : 01
	V.A Avidi - 2001

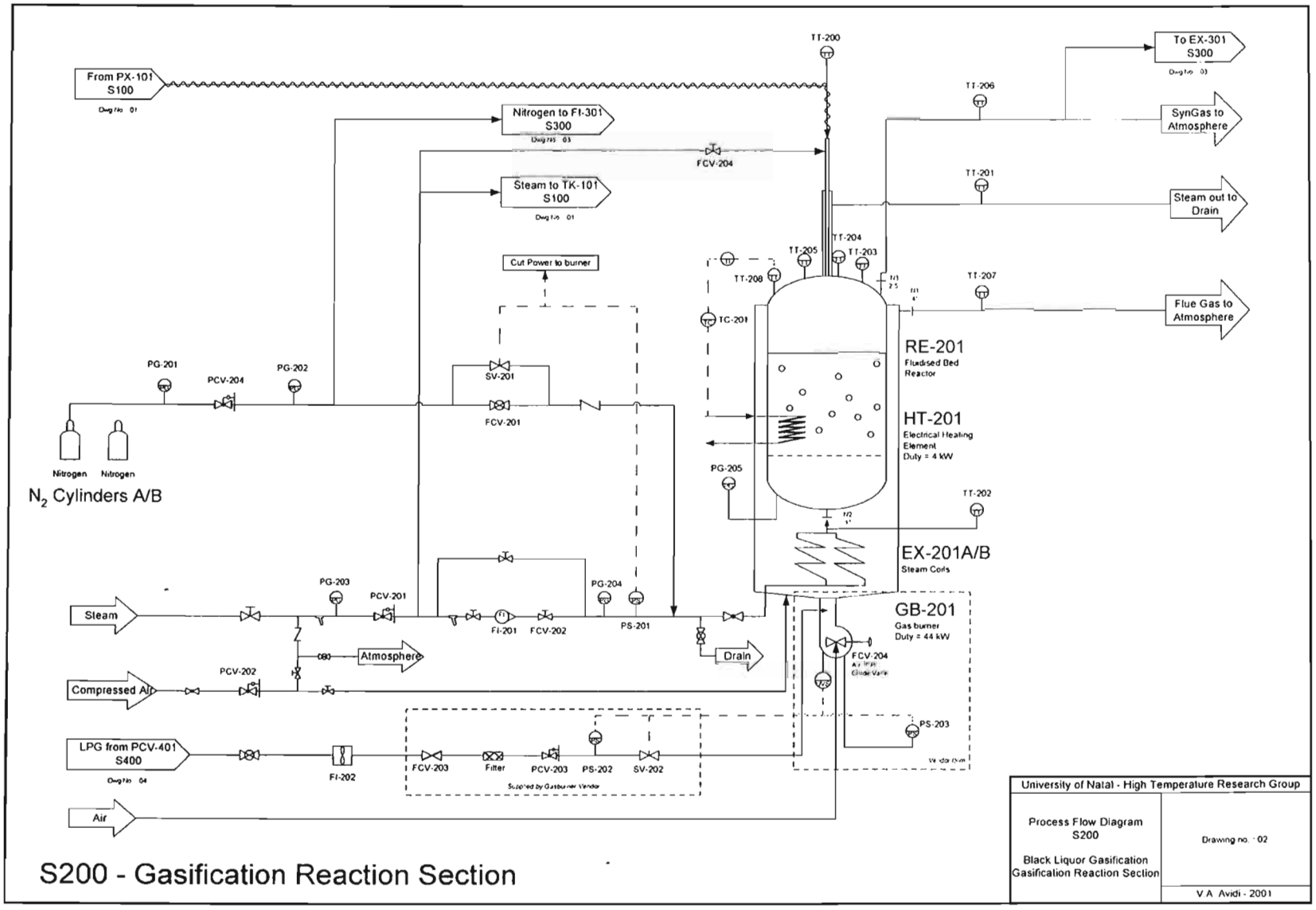

S200 - Gasification Reaction Section

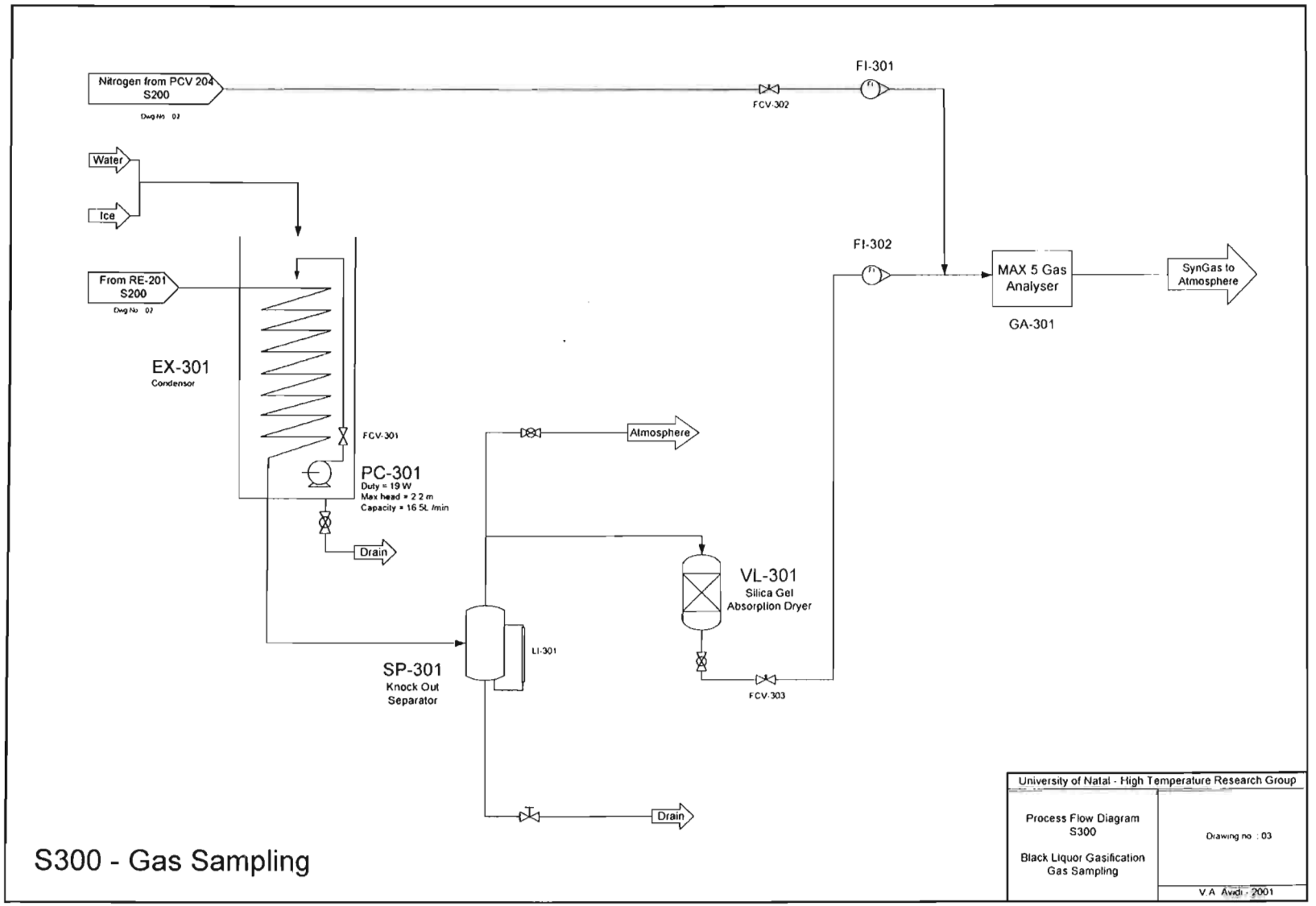
Nitrogen from PCV 204
S200
Dwg No 02
FCV-302
FI-301
Water
Ice
From RE-201
S200
Dwg No 02
EX-301
Condensor
FCV-301
PC-301
Duty = 19 W
Max head = 2.2 m
Capacity = 16.5L /min
Drain
Atmosphere
VL-301
Silica Gel
Absorption Dryer
LI-301
SP-301
Knock Out
Separator
FCV-303
FI-302
MAX 5 Gas
Analyser
GA-301
SynGas to
Atmosphere
Drain
S300 - Gas Sampling
University of Natal - High Temperature Research Group
Process Flow Diagram
S300
Black Liquor Gasification
Gas Sampling
Drawing no : 03
V.A Avidi - 2001

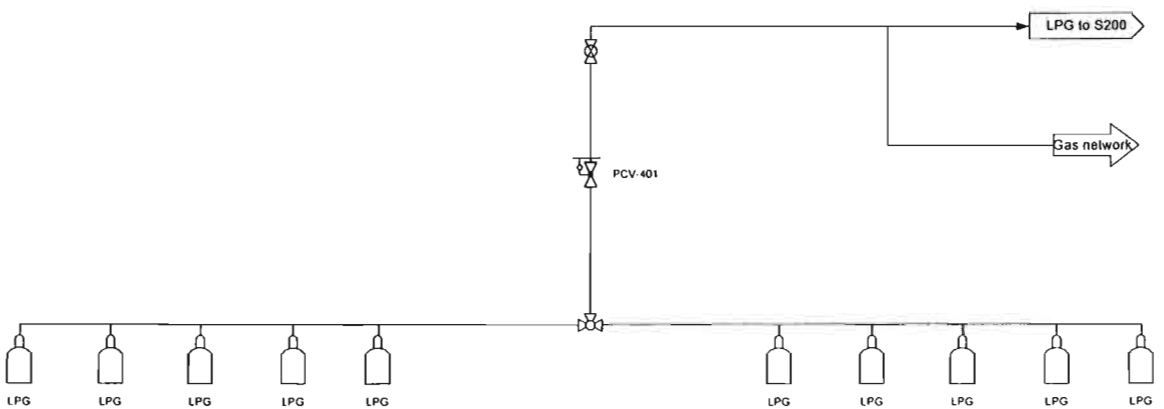

University of Natal - High Temperature Research Group	
Process Flow Diagram S400 Black Liquor Gasification LPG Gas Storage	Drawing no. : 04 V.A. Avidi - 2001

S400 - LPG Gas Storage

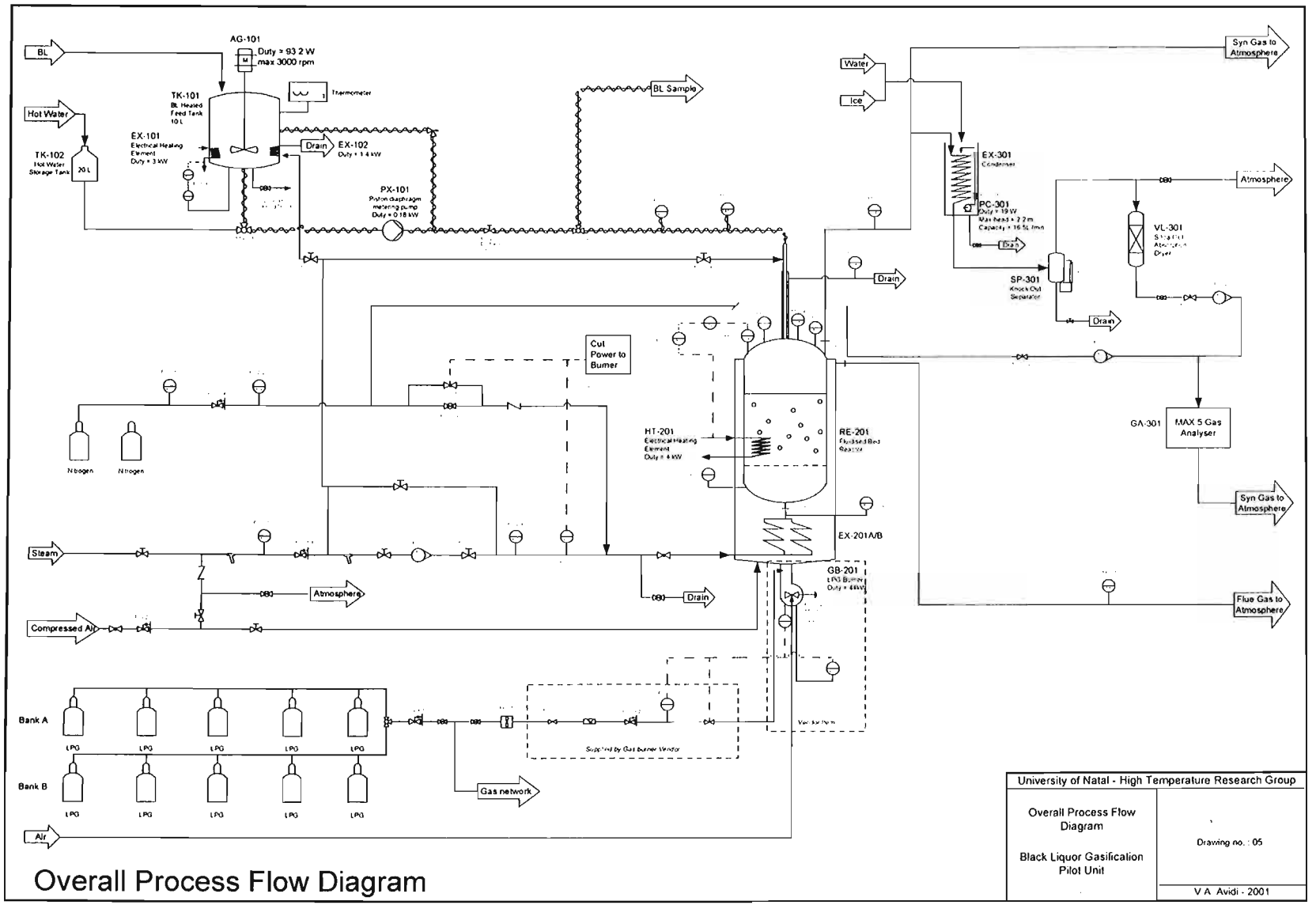
BL
AG-101
Duty = 93.2 W
max 3000 rpm
TK-101
BL Heated Feed Tank 10 L
Thermometer
BL Sample
Hot Water
TK-102
Hot Water Storage Tank
30 L
EX-101
Electrical Heating Element
Duty = 3 kW
Drain
EX-102
Duty = 1.4 kW
PX-101
Piston diaphragm metering pump
Duty = 0.18 kW
Water
Ice
Syn Gas to Atmosphere
EX-301
Condenser
PC-301
Duty = 19 W
Max head = 2.2 m
Capacity = 16.5 L/min
Drain
Atmosphere
VL-301
SP-301
Knock Out Separator
Drain
Drain
Cut Power to Burner
HT-201
Electrical Heating Element
Duty = 6 kW
RE-201
Fluidised Bed Reactor
GA-301
MAX 5 Gas Analyser
Syn Gas to Atmosphere
Nitrogen
Nitrogen
EX-201A/B
Steam
GB-201
LPG Burner
Duty = 48kW
Atmosphere
Drain
Compressed Air
Flue Gas to Atmosphere
Bank A
LPG
LPG
LPG
LPG
LPG
Supplied By Gas Burner Vendor
Bank B
LPG
LPG
LPG
LPG
LPG
Gas network
Air
Overall Process Flow Diagram
University of Natal - High Temperature Research Group
Overall Process Flow Diagram
Black Liquor Gasification Pilot Unit
Drawing no. : 05
V A Avidi - 2001

APPENDIX B

Appendix B1 – Black liquor delivery pump PX-101 datasheet and inspection certificate

Appendix B2 – Relief valve PSV-101 test certificate

Appendix B3 – Black liquor delivery pump PX-101 calibration curve

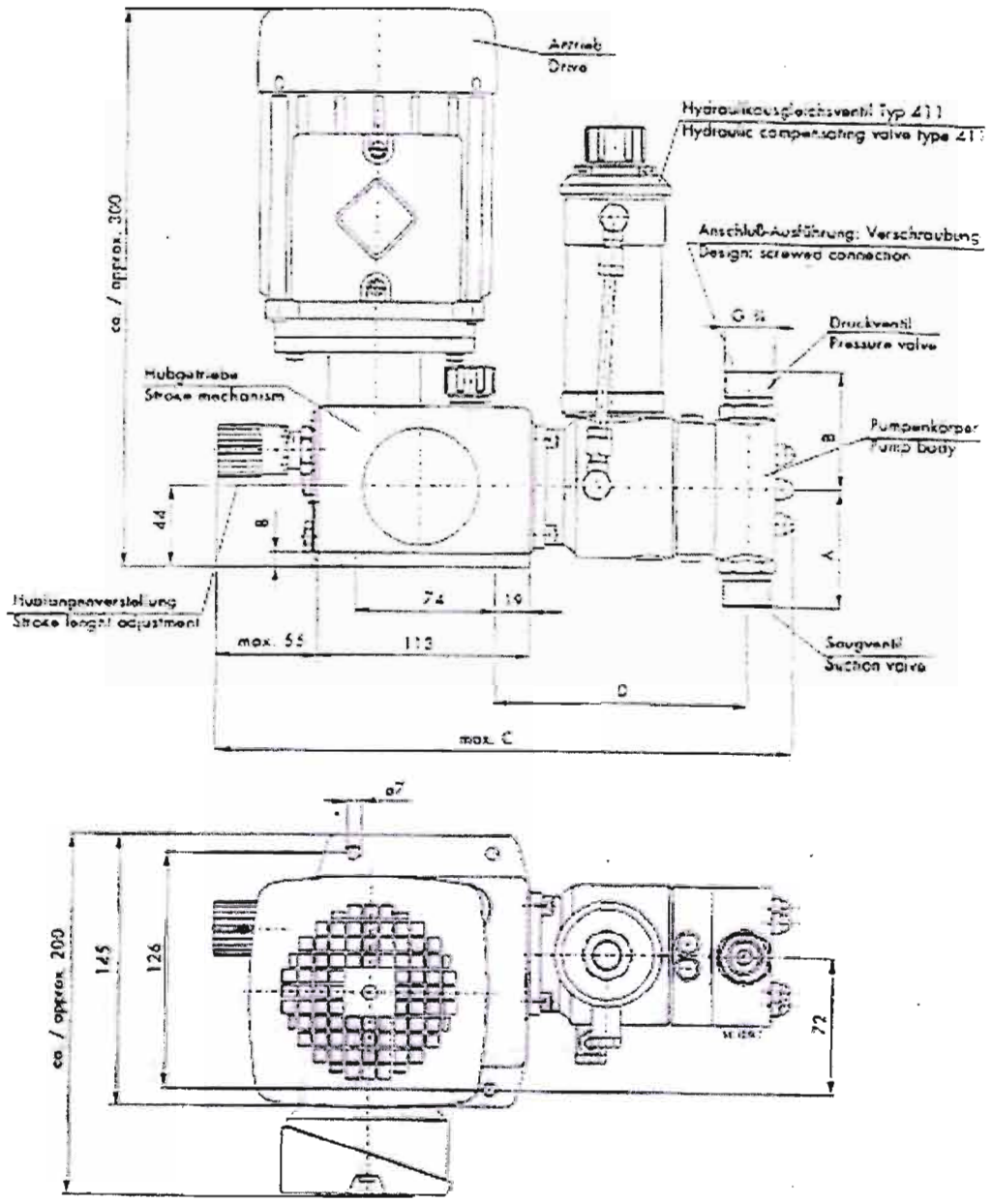
Antrieb
Drive
Hydraulikausgleichsventil Typ 411
Hydraulic compensating valve type 411
Anschluß-Ausführung: Verschraubung
Design: screwed connection
G ¾
Druckventil
Pressure valve
Hubgetriebe
Stroke mechanism
Pumpenkörper
Pump body
ca. / approx. 300
44
8
A
74
19
max. 55
113
D
max. C
Hublängenverstellung
Stroke length adjustment
Saugventil
Suction valve
ø7
145
126
ca. / approx. 200
72

Kolben(doppel-)membranpumpe
Piston (double) diaphragm pump
R 409.1- ... K|D|M/14
R 409.1- ... K|D|M/20

sera
Dosieren
Fördern
Verdichten

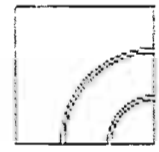

Maßtabelle / Dimensions

Typ Type	C	D	A Kammerventile/ Chamber valves	A Doppelventile/ Double valves	B Kammerventile/ Chamber valves	B Doppelventile/ Double valves
			1.4571 PVC	PP-GFK, PVDF-GFK PP-FRP, PVDF-FRP	1.4571 PVC	PP-GFK, PVDF-GFK PP-FRP, PVDF-FRP
R 409.1- 8.5 KM/14	290	114	62	62	62	62
R 409.1- 8.5 KDM/14	310	134				
R 409.1- 11 KM/14	290	114	62	62	62	62
R 409.1- 11 KDM/14	310	134				
R 409.1- 17 KM/20	290	114	62	62	62	62
R 409.1- 17 KDM/20	310	134				
R 409.1- 23 KM/20	290	114	62	62	62	62
R 409.1- 23 KDM/20	310	134				

Technische Daten / Technical data

Typ Type	Pumpenleistung / Pump data: Q_N bei / at P_2 max		P_1 max	P_2 max	h_s max m WS	CN	n_N 1/min 50Hz	60Hz	h_s (0) mm	Motorleistung / Motor data: P_N kW	U V	f Hz	I A
	50Hz l/h	60Hz l/h	bar	bar									
R 409.1- 8.5KM/14	8,5	10,2	10	0,2/6	2	B	100	120	10	0,18	346-440	50	0,56
R 409.1- 8.5KDM/14											346-480	60	0,54
R 409.1- 11 KM/14	11	13	10	0,2/6	2	B	134	160	10	0,18	346-440	50	0,56
R 409.1- 11 KDM/14											346-480	60	0,54
R 409.1- 17 KM/20	17	20	10	0,2/6	2	B	100	120	10	0,37	346-440	50	0,94
R 409.1- 17 KDM/20											346-480	60	1,01
R 409.1- 23 KM/20	23	27	10	0,2/6	2	B	134	160	10	0,37	346-440	50	0,94
R 409.1- 23 KDM/20											346-480	60	1,01

Gewicht/weight: 17 kg

* Linearität gemäß TA-012/01 / linearity acc. to TA-012/01

Pumpenkörper und Ventile aus Kunststoff nur bis P_2 max = 10 bar einsetzbar.
Mögliche Anschlußteile nach Übersichtsblatt TA-015.
Die elektrischen Daten gelten für Antriebsmotor in Standardausführung. Bei Sonderausführungen sind die Daten der Werksbescheinigung über Pumpenprüfung zu entnehmen.

Pump bodies and valves made of plastics can be used only up to a pressure of P_2 max = 10 bar.
Possible connections as per data sheet TA-015.
The electrical data are valid for the standard motor. In case of special design show these form the certificate of compliance of the pump.

Technische Änderungen vorbehalten! Subject to technical modifications!

Seybert & Kaiser GmbH + Co. Betriebs KG · Jahnstraße 1 · D-34376 Immenhausen · Telefon (05673) 9992 · Telefax (05673) 99 91 55

Seybert & Kahler GmbH + Co.Betriebs-KG Sera-Str. 34376 Immenhausen

Inspection Certificate EN 10204 / 3.1 B covering pump test QS 285-01

Datatrol Systems (PTY)LTD
P.O.Box 70589
Bendywood 2144

ZA - Sandton / SOUTH AFRIC

Customers No. 1128707
Date 12.02.01
Order conf. No. 9231860
Your order
SR245

Piston diaphragm pump
S 409.1 - 8.5 KM/14
Serial No.: 255967

Pump body:	1.4571
Chamber valves:	1.4571, DN 5
Valve balls:	1.4401
Diaphragm:	waved PTFE
Valve sealings:	FEP-covered
Connection thread:	G 3/4
Nominal capacity:	0 - 8,5 l/h(QN) at 50 Hz
Suction head:	afflux
Manometric pressure:	10 bar (P2max)
Hydraulic fluid:	55 ccm silicone oil
Nom. no. of strokes:	100 1/min at 50 Hz
Medium:	Black liquor, free of solids, up to 100° C, max. 500 mPas

Drive
80180125 3-PHASE MOTOR / SIZE 63 0,180 KW
230/400V 50 Hz 0,88/ 0,51 A 55 IP Iso-Class F
2790 RPM Execut. V18

Test report from 12.02.01 Tester-No. 0003
Responsible: Mr. Bremme

Capacity C:

S.-No. 255967: K1/ 50 Hz = 9,50 L/H
Static pressure test: test pressure 1,3 · pn (1 min.)

Please observe the enclosed technical instructions
'Mounting notes, Commissioning, safety precautions'

In case of spare parts order please always indicate
Pump type and serial-number.

This declaration was made out with a computer and is valid without signature!

DLM

Flow Measurement, Over Pressure Protection & Control
55 Forge Road, Spartan,
Kempton Park, 1619
PO Box 756, Isando, 1600
Tel 27 11 - 975 1171
Fax 27 11 - 975 7762
Web:protea.co.za/dlm

15 MARCH 2001

UNIVERSITY OF NATAL.

CERTIFICATE OF PRESSURE SETTING

This is to certify that one valve supplied against

Your order number	MC9852/1
Our delivery note number	20572

Has been pneumatically set to relieve at 900 KPAG

Make of valve	BIRKEET SAFETY VALVE
Figure Number	716ASL
Inlet	20mm BSP SCREWED FEMALE
Outlet	32mm BSP SCREWED FEMALE
SAF No.	N/A

FRASER CLARK
WORKSHOP MANAGER

MARTIN ELS
QUALITY ASSURANCE MANAGER

Divisional Executive: BL Bamberger (Managing), SD Buchanan, GK Durge
Protea Data Systems (Pty) Ltd Directors: GD Johnston (Managing), BL Bamberger, L Fisher, B Shingler (British).
Protea Data Systems (Pty) Ltd. Registration No. 81/09419/07
Cape Town (021) 551 6727; East London (043) 736 2227; Pinetown (031) 701 8585;
Rustenburg (014) 538 1057; Vereeniging (016) 421 4586; Welkom (057) 355 3081

Pump PX-101 calibration data

Pump calibration carried out with water at 80°C

Time/s	Volume/ml	Pump dial reading	Flowrate / l/hr
37.94	9.2	10	0.873
16.69	8.7	20	1.877
11.87	9.4	30	2.851
7.88	8.7	40	3.975
62.87	64	40	3.665
7.18	9.5	50	4.763
60.59	80	50	4.753
52.91	85	60	5.783
46.46	87.5	70	6.780
39.4	84.5	80	7.721
34.81	83.5	90	8.635
29.47	80	100	9.773

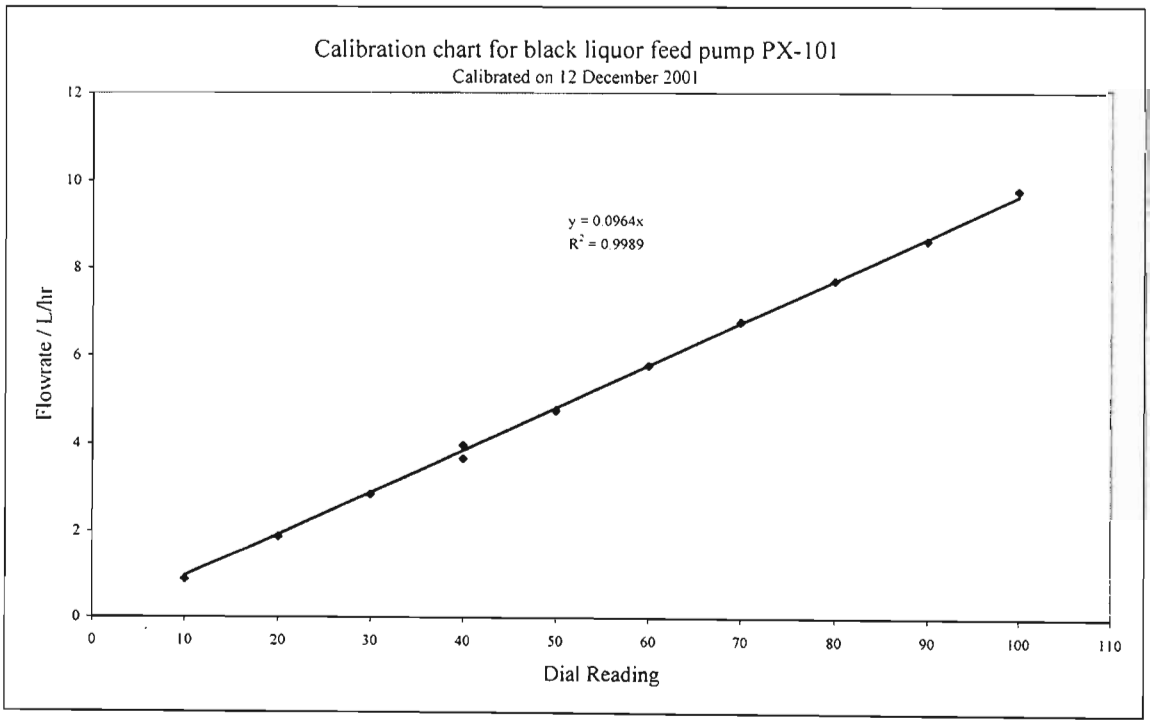

APPENDIX C

HAZOP STUDY

Report Back on BLG HAZOP Study held on 22 September 2000

High Temperature Processing Group

School of Chemical Engineering
University of Natal - Durban
South Africa
4041
Ph : +27 31 260 3132
Cell : +27 (0)82 797 8831
Fax : + 27 31 260 1118
e-mail : Avidiv@nu.ac.za

Hazop Team : Jon Buzzard – Chairman
Dave Arnold
Brian Loveday
Brian Ravno
Ken Jack
Kelly Robertson
Prathisha Devnarain
Kleantha Pillay
Vernon Avidi – Project Student

Date : 6 December 2000

Refer to Hazop Flowsheet Figure 1 on pg. C4

1. Item : Black Liquor Storage Tank

Contents : Black Liquor Temp : 85-90 °C

Keyword	Deviation	Cause	Consequences & Action	By whom
None	Flow	Tank Empty Outlet tube blocked	Likely that the pump P-01 will suck in air through it's seals. Air will enter the reactor - lead to combustion in reactor - Undiserable. **Action :** Use a float level indicator in the black liquor tank.	Workshop Staff - Ken Jack

2. Line Nos : 1,3,8

Contents : Black Liquor Temp : 85-90 °C Pressure : 500-600 kPag

Keyword	Deviation	Cause	Consequences & Action	By whom
None	Flow	Valve V-01 Blocks	Pump P-01 sucks in Air - Combustion in Reactor. **Action :** Fit a strainer on Black Liquor Tank so that solids are removed when filling tank up.	Workshop Staff
	Temp	Lines Cold	Black Liquor solidifies in lines. Blocks Lines. Pump sucks in Air - Combustion in Reactor. **Action :** Use Line 2 (steam) to heat up lines at start-up. Increase Lines 1,3,11 from ¼" to ½" and chase them with line 9 (hot water @ 90°C) and insulate.	Workshop Staff Ken Jack

3. Line No : 9

We agreed at the meeting that the use of Hot water instead of steam to cool the Black liquor as it enters the reactor is an alternative and indeed it was considered during the design stages. The option was chosen to remain open and so the route we have opted for now is to start up with hot water and change over to steam if necessary.

Contents : Hot Water Temp : 90-95 °C

Keyword	Deviation	Cause	Consequences & Action	By whom
None	Flow	V-05 Blocked	Black Liquor tube over heats. Nozzles blocks. No Hazard but need to shutdown and remove and clean tube manually. **Action :** Moniter Steam outlet from line 10. Install a pressure gauge (PG-04) after V-05 to moniter flow into the jacketed tube itself.	V.A. Avidi Workshop Staff

4. Line No : 11

Contents : Black Liquor Temp : 85-90 °C Pressure : 600-700 kPag

Keyword	Deviation	Cause	Consequences & Action	By whom
None	Flow	V-02 blocked Nozzle Blocked	No hazard but need to shutdown and physically clean out lines. **Action :** Fit Storage tank with strainer. Monitor steam outlet on line 10.	Workshop V.A.Avidi
More of	Flow	No Control or indication of flow while in operation so should V-02 be increased by someone.	Higher capacity than what can be gasified enters the reactor. Build up of solids in the reactor & possible mud ball formation leading to poor fluidisation. **Action :** Feed flow is key parameter to be controlled so rather use a cheaper centrifugal pump and spend more on a on-line flowmeter which can be used to control V-02 (either automatically or manually) during runs. This would replace the bucket & stopwatch method initially chosen.	V.A. Avidi D. Dhavaraj Workshop Staff
Less of	Flow	No Control or indication of flow while in operation so should V-02 be decreased by someone.	Inaccurate measure of feed flow to the reactor. **Action :** Use an on-line flowmeter. (As above)	V.A. Avidi D. Dhavaraj Workshop Staff
	Pressure	Pump inefficiency	Poor spraying of Black liquor into reactor. Formation of mud balls in reator. Poor fluidisation. **Action :** Include Pressure Gauge (PG-05) to just before line 11 enters tube.	Workshop Staff

5. Line No : 12

Contents : Low Pressure Steam Temp : 600-700 °C Pressure : 100-200 kPag

Keyword	Deviation	Cause	Consequences & Action	By whom
None	Flow	V-06 Blocks	Fluidisation stops. Pump P-01 continues pumping black liquor into reactor. Gas burner overheats coil - possibly melt coil. **Action :** Install Presure Switch PS-01 in line 5 after V-07. If flow of steam fails switch off burner, pump. Operator to open V-01 to flush line out with steam and open V-06 to purge/fluidise bed with Nitrogen.	D.Dhavaraj Workshop Staff V.A. Avidi
More of	Flow	Valve V-07 Opened full	Transportation of Bed. **Action :** Need to moniter degree of fluidisation in bed. Install PG-06 at base of reactor and observe pressure drop across bed.	V.A. Avidi Workshop Staff
Less of	Flow	Valve V-07 not open to desired limit	Poor Fluidisation. Poor heat and mass transfer » Hot zones - Smelt formation. **Action :** Install PG-06 at base of reactor and observe pressure drop across bed.	V.A. Avidi Workshop Staff

6. Points of Interest raised at the HAZOP Meeting

Steam Generator :

The schools boiler has a capacity of vapourising 325kg/hr on Low Fire. Bear in mind that this is currently half of design capacity as 2 of the 4 heating coils have been removed. So if we draw of a steam flow rate of between 10-15kg/hr we would be drawing between 3-5% of the boiler's total capacity on Low Fire.

Action : We will start the gasifier up on steam from the big boiler to determine the amount of fluidising steam required. Once this has been determined we will utilise a separate smaller boiler unit. This option needs further investigation.

LPG Autoignition Temperature :

This point was raised due to the hazard of the jacket side of the reactor filling with LPG in the combined events of both a flame out and the built in safety devices of the gas burner failing. The probability of both these events occuring at the same time to produce the hazard is small and can be neglected.

Autoignition Temperature : ± 450 °C

Flammability in Air : 2.2 - 9.5%

H_2S Autoignition Temperature :

This point was raised to determine the possibility of a H_2S flare for the product gases. It was agreed that after the first trial run, a mini HAZOP on the sampling and H_2S emmision problems be done.

Autoignition Temperature : ± 260°C

Flammable Limits : 4.3 - 46% v/v [LEL - UEL]

Health Hazard : At low concentrations (0.02 - 0.03 ppm) "rotten egg" smeel changing to "sickening sweet odor" as levels rise above 50-200 ppm. Exposure above 100 ppm may rapidly deaden sense of smell in as little as 2-15 minutes, particularly at higher concentrations. Above 200 ppm loss of smell is very rapid.

Safety Health and Environment Requirments

Proper safety gear is to be used when operating the unit. This includes long sleep jackets, safety shoes, safety goggles and heat resistant gloves. And dust masks.
Copies of the chemical MSDS is to be kept at the unit.
Post warning signs around equipment regarding high temperature surfaces and flammable gasses in the area.
Discarded bed material and black liquor to be disposed off appropriately.
H2S is in low concentrations in the reactor gas outlet and diluted with steam - not a concern with emmission concentration
It is envisaged that the unit is not run continously at high rates so intermittent emmissions to the atmosphere is acceptable.

Figure 1 : Pilot Plant Flowsheet

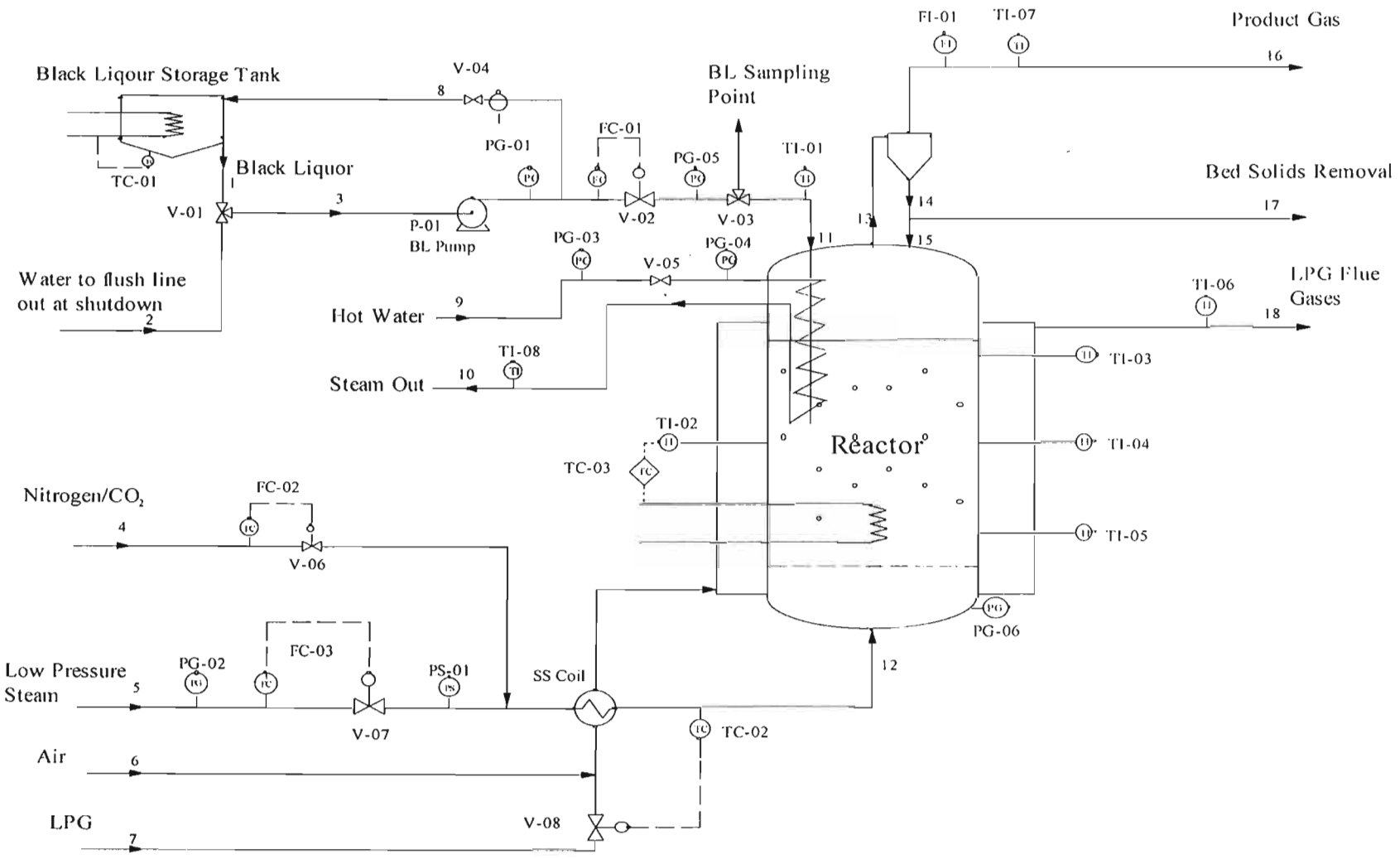

APPENDIX D

START-UP AND SHUT DOWN PROCEDURE

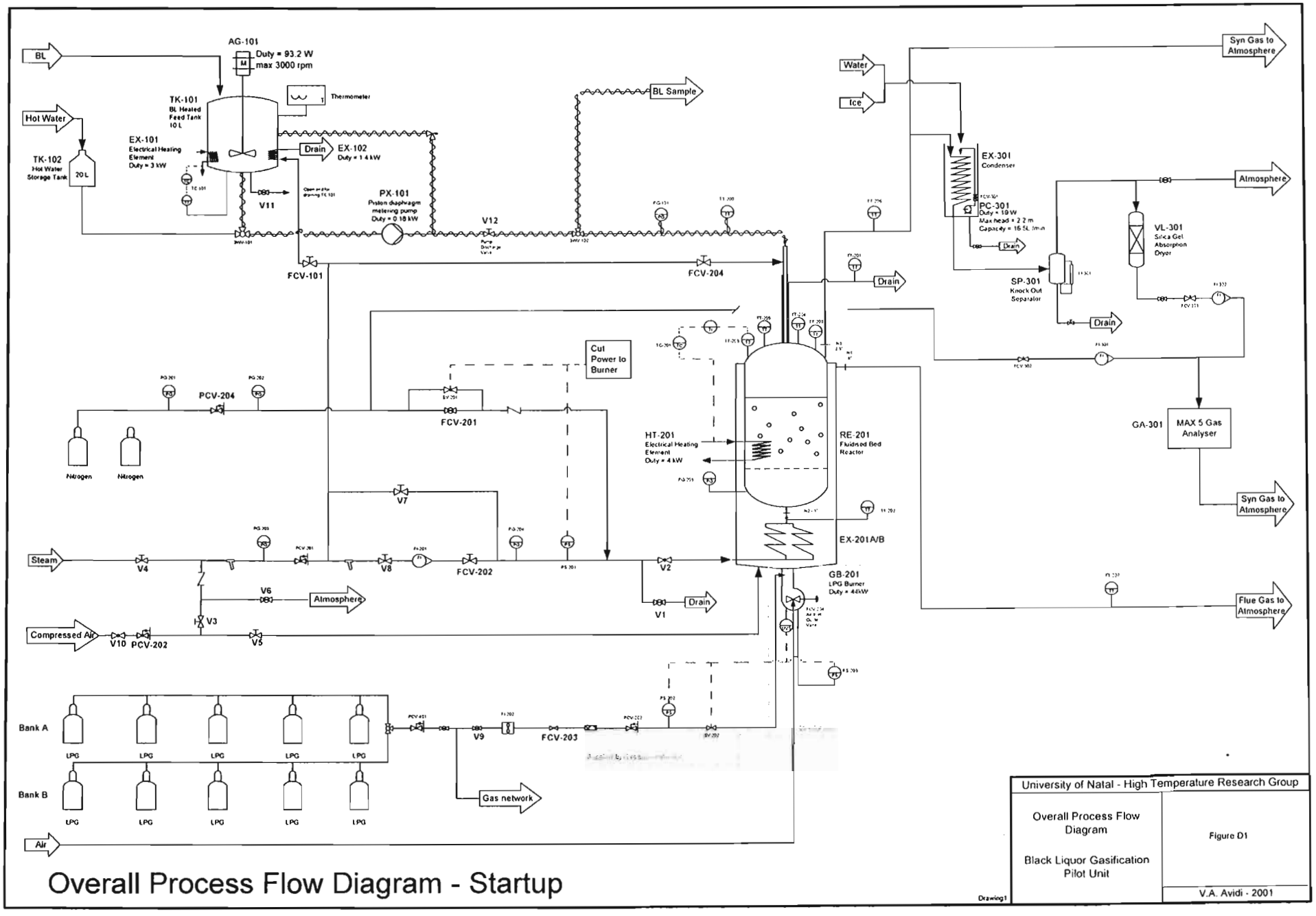
BL
AG-101
Duty = 93.2 W
max 3000 rpm
Thermometer
TK-101
BL Heated Feed Tank 10 L
BL Sample
Hot Water
TK-102
Hot Water Storage Tank
20 L
EX-101
Electrical Heating Element
Duty = 3 kW
Drain
EX-102
Duty = 1.4 kW
V11
PX-101
Piston diaphragm metering pump
Duty = 0.18 kW
V12
FCV-101
FCV-204
Water
Ice
Syn Gas to Atmosphere
EX-301
Condenser
PC-301
Duty = 18 W
Max head = 2.2 m
Capacity = 16.5 L/min
Atmosphere
VL-301
Silica Gel Absorption Dryer
SP-301
Knock Out Separator
Drain
Cut Power to Burner
PCV-204
FCV-201
Nitrogen
Nitrogen
HT-201
Electrical Heating Element
Duty = 4 kW
RE-201
Fluidised Bed Reactor
GA-301
MAX 5 Gas Analyser
V7
Steam
V4
V8
FCV-202
V2
EX-201A/B
GB-201
LPG Burner
Duty = 44kW
V6
Atmosphere
V3
V1
Drain
Compressed Air
V10
PCV-202
V5
Flue Gas to Atmosphere
Bank A
LPG
Bank B
LPG
V9
FCV-203
Gas network
Air
Overall Process Flow Diagram - Startup
University of Natal - High Temperature Research Group
Overall Process Flow Diagram
Black Liquor Gasification Pilot Unit
Figure D1
V.A. Avidi - 2001
Drawing1

Start up Procedure -

1. Switch computer on and run *BLG.exe* program on desktop. Select all temperature tags that are required for logging. Don't start logging now.
2. Switch on the variac to start heating the lines, set voltage to around 100V.
3. Open the nitrogen supply from the nitrogen gas cylinders and set the downstream pressure to 60kPa by adjusting the regulator PCV-204. Make sure you have sufficient nitrogen in the cylinder for a run.
4. Lock down the reactor lid with the chain and lock it.
5. Make sure valve FCV-101 controlling steam flow to EX-102 (steam coil in black liquor tank TK-101) is closed.
6. Open valve FCV-204 for BL steam supply to black liquor tube cooling
7. At bottom of the reactor RE-201 close water drain valve V1 and open steam/air valve V2 to the steam superheater coils EX-201A/B.
8. Switch extraction fans on over the unit.
9. Open air supply to piping with V10, PCV-202 and V3 and verify with pressure gauge PG-203 and that there is supply of air. NOTE: Valves V5, V6 and V7 must be closed.
10. Open V8
11. Open FCV-202 to supply air to into the steam coils EX-201A/B. Set air flow to 25-30 kg/hr.
12. Start the logging programme.
13. Open LPG isolation valve V9 to supply the gas burner with LPG.
14. Switch on burner with LPG flow to the burner set at 30% on FCV-203.
15. Monitor temperature profiles. The "Steam in" temperature profile should display a rapid increase almost immediately after starting the burner.
16. While heating up the reactor TK-101 should be filled with black liquor and the agitator AG-101 started.
17. Fill TK-102 the hot water from a domestic geyser. 20L is sufficient for a run.
18. Once the reactor has reached operating temperatures AND kept there for at least half an hour, the bed is ready to be charged to the reactor.
19. Switch the gas burner off.
20. Close off air supply to the reactor using FCV-202.
21. Remove one of the quartz sight glasses on the reactor lid and add the bed to the reactor using a metal funnel. Replace sight glass after bed has been loaded.
22. Reintroduce air into the reactor and turn on the burner, using the same LPG flow setting as before.

23. Monitor temperature profiles as the bed is heated up to operating temperatures. During this operation the bed is cleaned of any residual carbon by combustion with the fluidising air.
24. Regulate FCV-203 to obtain stable bed temperatures (620°C – 700°C) and maintain stable operation for 30 minutes.
25. Switch the burner off in preparation for changeover to steam.
26. Close air supply valve to reactor at the bottom of the reactor with V2
27. Close off air supply to feed train using V3.
28. Open valve V6.
29. Open drain valve V1 at the bottom of the steam coils EX-202.
30. Open up steam supply to piping train, the supply gauge PG-203 will rise to about 6-7 bar. (depending on the boiler pressure)
31. Open up steam supply to the reactor slowly using FCV-202 and the FI-201 bypass valve V7. No steam will enter the reactor but will pass through to drain.
32. Open up the valves FCV-204 and FCV-101 to allow bring the BL tube steam jacket and the steam coil EX-102 in TK-101 into commission. The coil in the urn is there to assist with even distribution of heat in the urn, so control accordingly with FCV-101.
33. When the piping is heated up (about 5 minutes) as indicated by steam flow to drain and no longer condensate, steam is ready to be introduced into the reactor.
34. Close the bypass valve V7 around FI-201.
35. Switch the burner on.
36. When the burner ignites, slowly open the steam supply valve at the bottom of the reactor to allow steam into the bed. When fully open, close off the drain valve V1 and then control steam flow using FCV-202 to fluidise the bed.
37. Switch on the internal heating element EX-202 and give TC-201 a set point of the desired operating conditions.
38. Set 3WV-102 to discharge to the black liquor sample line.
39. Open pump discharge valve V12.
40. Set 3WV-101 to take feed from TK-102.
41. While the bed is heating up, start the black liquor feed pump PX-101 to heat the pump by circulating hot water at 80% pump capacity from TK-102 through the pump and into a bucket through the black liquor sample line from 3WV-102.
42. When the bed is near operating temperature, reduce the pump flow to operating flow conditions using the pump dials and changeover 3WV-102 to pump hot water into the reactor.
43. Observe PG-101 on the BL delivery line to check if the line is blocked. The relief valve is set to discharge at 9barg.

44. When stable bed conditions are attained under these conditions, change the variac voltage to around 35V.
45. Black liquor can be introduced into the bed by changing 3WV-101 to feed PX-101 from TK-101. The bed temperatures should drop at first, but EX-202 will kick in and maintain bed temperatures at the set point.

Shutdown Procedure :

1. Switch from BL to hot water from TK-102 using 3WV-101 to flush out the pump and lines. The bed temperatures will increase at first and then drop. Continue flushing for 15 minutes.
2. Switch off the gas burner and EX-202 by feeding TC-201 a setpoint of 10°C.
3. Switch over 3WV-102 to discharge to a bucket through the BL sample line until flow out of line is clear.
4. Empty the BL tank contents via the tanks drain valve V11 and wash out the tank.
5. Fill the BL tank with water and flush out the drain line.
6. Open the air supply to the shell side purge of the reactor using valve V5.
7. When the reactor cools to around 150°C, close of the main steam supply using valve V4..
8. Close valve V6 on the line to atmosphere tying off from the line linking the air and steam systems.
9. Crack open the nitrogen valve FCV-201 at the nitrogen cylinders to allow nitrogen gas to purge the reactor. Turn the purge gas off when the reactor has cooled down to around 50°C.
10. When the reactor reaches 50°C, shut off the steam/air supply valve V2 at the bottom of the reactor.
11. Stop logging the data.
12. Copy the log files *blgdata.txt* and *blglabels.txt* from *c:\BLG\Temp Logger* to another folder and rename it accordingly as the file is overwritten the next time the program is run.

APPENDIX E

APPENDIX E – CALIBRATION CURVES FOR FI-301 AND FI-302

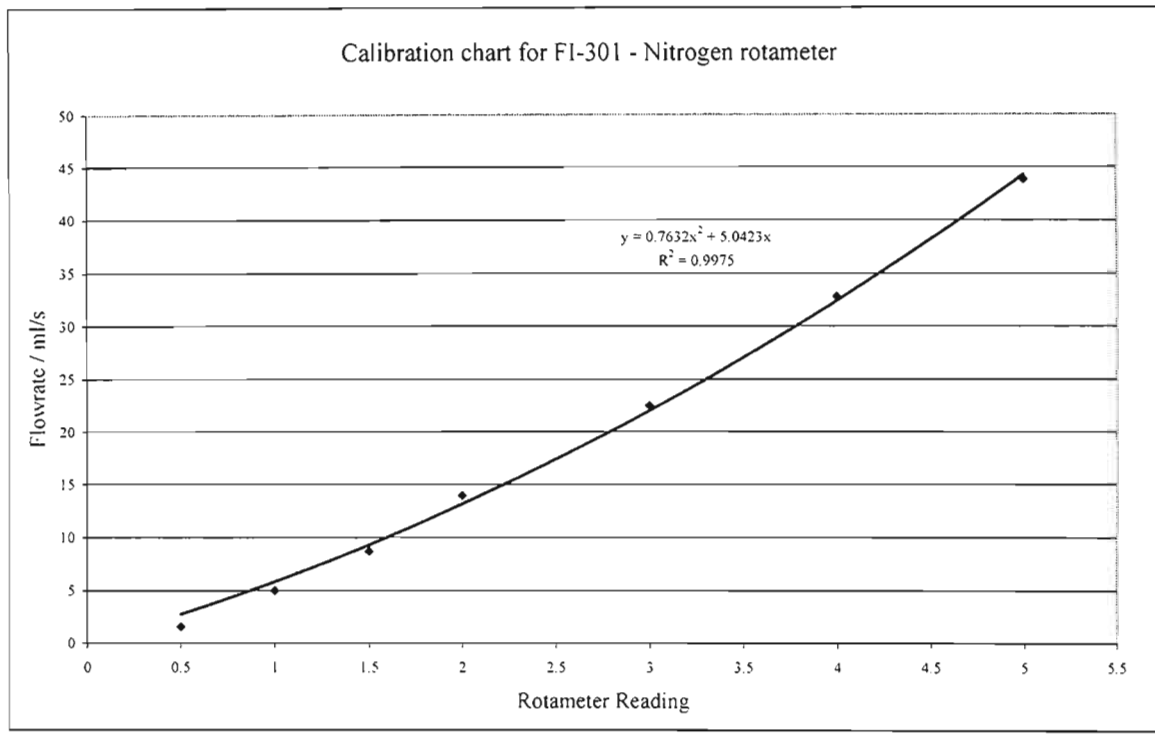
Calibration chart for FI-301 - Nitrogen rotameter
y = 0.7632x² + 5.0423x
R² = 0.9975
Flovrate / ml/s
Rotameter Reading
0
5
10
15
20
25
30
35
40
45
50
0
0.5
1
1.5
2
2.5
3
3.5
4
4.5
5
5.5

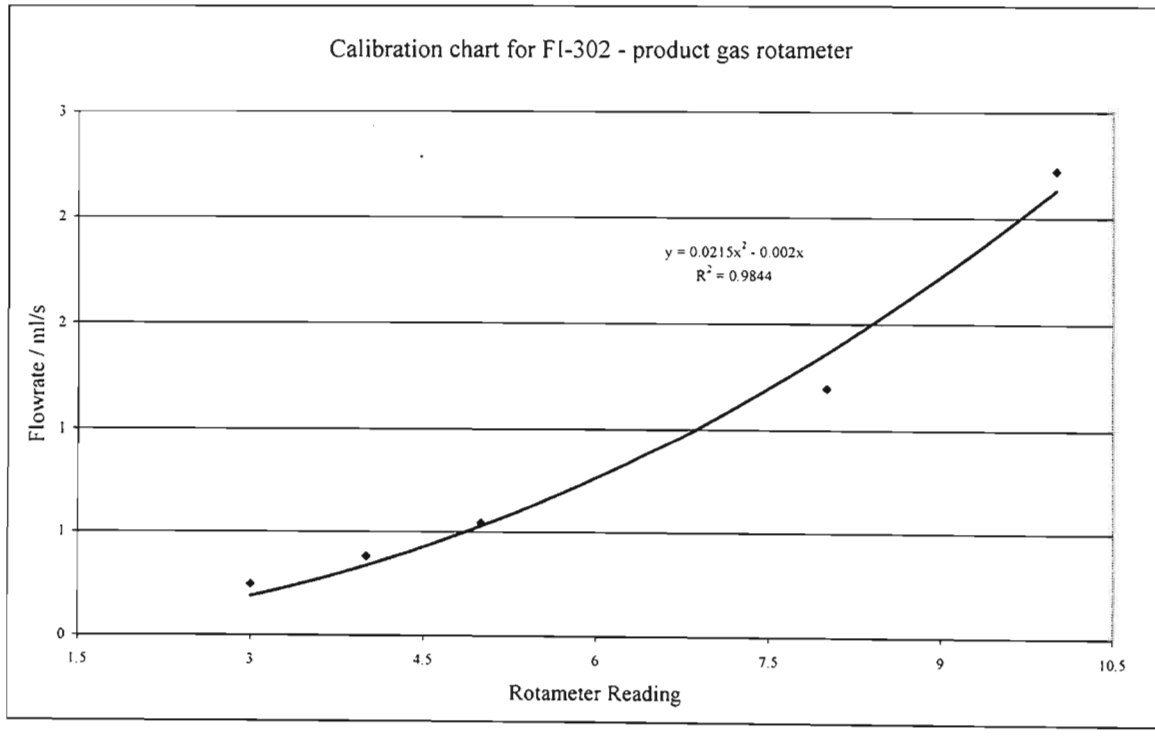
Calibration chart for FI-302 - product gas rotameter
y = 0.0215x² - 0.002x
R² = 0.9844
Flovrate / ml/s
Rotameter Reading
0
1
1
2
2
3
1.5
3
4.5
6
7.5
9
10.5

APPENDIX F

APPENDIX F – DATA LOGGING PROGRAM – MICROSOFT VISUAL BASIC 5.0

Main.frm

```
Option Explicit
Dim tcmc As Long
Dim GraphMaxed As Long
Dim total

Dim starttime As Single
Dim xold As Single, xnew As Single
Dim chanval(0 To 7) As Single
Dim oldchanval(0 To 7) As Single
Dim maxpoints As Integer
Dim started As Boolean
Private Sub DrawAxes()
 Dim i As Single

 picgraph.DrawStyle = 0

 picgraph.Line (-20, 0)-(HScroll.Max, 0)
 picgraph.Line (0, -50)-(0, 1000)

 'draw y grid lines
 picgraph.DrawStyle = 2

 For i = 0 To 1000 Step 100
  picgraph.Line (0, i)-(HScroll.Max, i), &HAFAFAF
 Next i

 For i = 0 To HScroll.Max Step 100
  picgraph.Line (i, 0)-(i, 1000), &HAFAFAF
  Call locate(i - 5, -20)
  picgraph.Print i
 Next i

End Sub

Private Sub locate(x As Single, y As Single)
 picgraph.CurrentX = x
```

```
 picgraph.CurrentY = y
End Sub

Private Sub showtitle()
 Call locate(HScroll.value + 550, -60)
 picgraph.Print "Time (s)"
End Sub
Private Sub Draw(xnew As Single, chanval() As Single)

 If chkChan(0).value = 1 Then
   picgraph.DrawStyle = 0
   picgraph.Line (xold, oldchanval(0))-(xnew, chanval(0)), &HFF
 End If

 If chkChan(1).value = 1 Then
   picgraph.DrawStyle = 0
   picgraph.Line (xold, oldchanval(1))-(xnew, chanval(1)), &H80
 End If

 If chkChan(2).value = 1 Then
   picgraph.DrawStyle = 0
   picgraph.Line (xold, oldchanval(2))-(xnew, chanval(2)), &HFF0000
 End If

 If chkChan(3).value = 1 Then
   picgraph.DrawStyle = 0
   picgraph.Line (xold, oldchanval(3))-(xnew, chanval(3)), &H0
 End If

 If chkChan(4).value = 1 Then
   picgraph.DrawStyle = 2
   picgraph.Line (xold, oldchanval(4))-(xnew, chanval(4)), &HC0C0&
 End If

 If chkChan(5).value = 1 Then
   picgraph.DrawStyle = 2
   picgraph.Line (xold, oldchanval(5))-(xnew, chanval(5)), &HFFFF00
```

```
End If

If chkChan(6).value = 1 Then
  picgraph.DrawStyle = 2
  picgraph.Line (xold, oldchanval(6))-(xnew, chanval(6)), &HFF00FF
End If

If chkChan(7).value = 1 Then
  picgraph.DrawStyle = 2
  picgraph.Line (xold, oldchanval(7))-(xnew, chanval(7)), &HC000&
End If


  xold = xnew
  oldchanval(0) = chanval(0)
  oldchanval(1) = chanval(1)
  oldchanval(2) = chanval(2)
  oldchanval(3) = chanval(3)
  oldchanval(4) = chanval(4)
  oldchanval(5) = chanval(5)
  oldchanval(6) = chanval(6)
  oldchanval(7) = chanval(7)

picgraph.DrawStyle = 0
End Sub
Private Sub readdata()
 Dim i As Integer

 Close #1

 Open "blgdata.txt" For Input As #1

 xold = 0

If (HScroll.value > 1) And (HScroll.value < (total - 2)) Then

For i = 1 To (HScroll.value - 1)
```

```
  Input #1, xnew, chanval(0), chanval(1), chanval(2), chanval(3), chanval(4), chanval(5),
chanval(6), chanval(7)
 Next i


 If (total - HScroll.value) < 1200 Then
  For i = HScroll.value To (total - 2)
  Input #1, xnew, chanval(0), chanval(1), chanval(2), chanval(3), chanval(4), chanval(5),
chanval(6), chanval(7)
  Call Draw(xnew, chanval())
  Next i
 Else
  For i = HScroll.value To (HScroll.value + 1198)
  Input #1, xnew, chanval(0), chanval(1), chanval(2), chanval(3), chanval(4), chanval(5),
chanval(6), chanval(7)
  Call Draw(xnew, chanval())
  Next i
  For i = (HScroll.value + 1199) To (total - 2)
   Input #1, xnew, chanval(0), chanval(1), chanval(2), chanval(3), chanval(4), chanval(5),
chanval(6), chanval(7)
  Next i
 End If

End If

 Close #1

 Open "blgdata.txt" For Append As #1

End Sub

Private Sub btnAbout_Click()
   About.Show 1
End Sub

Private Sub btnGo_Click()
   Dim i As Long
```

```
    ' Check interval
    i = Val(boxInt.Text) * 1000
    If i > 65000 Then
       MsgBox "Maximum interval is 65 seconds", 48
       Exit Sub
    End If
    ' Start sampling
    ready = 0
    logging = 1
    Timer1.Interval = i
    InitOtherControls

If Not started Then
   starttime = Timer
   Text1.Text = Time
   started = True
End If

Call HScroll_Change
End Sub


Private Sub btnStop_Click()
    ' Stop logging
    logging = 0
    ready = 1
    InitOtherControls
End Sub


Private Sub comBoard_Click()
    bh = comBoard.ItemData(comBoard.ListIndex)
    InitBoardControls
End Sub


Private Sub Form_Load()
```

```
Dim i As Long
Dim s As String
Dim e As Long
Dim t As Long
Dim c As Long

logging = 0
ready = 1

' Set the captions of all the chkChan's
For i = 0 To 7
   chkChan(i).Caption = Format$(i)
Next i

' Fill the board combo
comBoard.Clear
c = 0
bh = 0
For i = 1 To 8
   e = EDR_GetBoardType(i, t)
   If e = EDR_OK Then
      s = Space$(80)
      EDR_StrBoardType t, s
      s = RTrimZ(s)
      comBoard.AddItem Format(i) & " " & s
      comBoard.ItemData(c) = i
      If bh = 0 Then
         bh = i
         comBoard.ListIndex = c
      End If
      c = c + 1
   End If
Next i

' Init controls etc based on this setup
chkChan(0).value = 1
InitBoardControls
```

```
  InitOtherControls

 total = 2
 xold = 0
 xnew = 0

 oldchanval(0) = 0
 oldchanval(1) = 0
 oldchanval(2) = 0
 oldchanval(3) = 0
 oldchanval(4) = 0
 oldchanval(5) = 0
 oldchanval(6) = 0
 oldchanval(7) = 0

 Open "blgdata.txt" For Output As #1  'create file to store data

 Open "blglabels.txt" For Output As #2  'create file to store labels
 Write #2, "Time", "BL Feed", "BL Tube Cooling", "Steam in", "Reactor Top", "Reactor
Middle", "Reactor Hot Zone ", "Product Gas", "LPG Flue Gas" 'write to file
 Close #2

 started = False
 starttime = Timer

End Sub

Private Sub InitBoardControls()
   ' Looks to see what board we have etc
   ' and hides/grays controls that do not
   ' apply and so on
   Dim bt As Long
   Dim i As Long, n As Long, a As Long
   Dim s As String

   btnStop.Enabled = False
```

```
    ' Copy the board type into bt
    i = EDR_GetBoardType(bh, bt)

    ' First check how many A/D chans we have
    i = EDR_GetADInType(bt, 0, a)
    n = EDR_NumADInputs(bt, a)
    For i = 0 To 7
        chkChan(i).Enabled = True
    Next i

        ' Hide the go button if no chans
    If n = 0 Then
        btnGo.Enabled = False
        ready = 0
    Else
        ready = 1
        btnGo.Enabled = True
    End If

End Sub

Private Sub InitOtherControls()
    ' This gets called when sampling is started,
    ' stopped, finishes etc. It enables/disables
    ' controls not done by InitBoardControls.
    If ready = 1 Then
        ' We can start sampling
        btnGo.Enabled = True
        btnStop.Enabled = False
        comBoard.Enabled = True
    Else
        ' We may not start sampling
        btnGo.Enabled = False
        ' Check if we are busy sampling
        If logging Then
            ' Sampling so stop=on setup=off
            btnStop.Enabled = True
```

```
        comBoard.Enabled = False
      Else
        ' Not sampling so stop=off setup=on
        btnStop.Enabled = False
        comBoard.Enabled = True
      End If
   End If
End Sub



Private Sub HScroll_Change()
 picgraph.Scale (HScroll.value - 50, 1000)-(HScroll.value + 1150, -100)

 If HScroll.value > HScroll.Max - 1200 Then
   HScroll.Max = HScroll.Max + 100
 End If


 picgraph.Cls
 Call DrawAxes
 Call showtitle
Call readdata

End Sub

Private Sub Timer1_Timer()
   ' Sample all the checked channels and print
   ' the data into the log control
   Dim v As Single, i As Long, j As Long, k As Long
   Dim c As Long

   Dim uv As Long
   Dim ambient As Long
   Dim temp As Long
   Dim ret  As Integer
   Dim tc As Integer
```

```
Dim bin As Integer
Dim chanval(0 To 7) As Single
Dim txnew As Single

tc = 1

For i = 0 To 7
 chanval(i) = 0
Next i



If logging Then
   c = 0
   total = total + 1
'**************
j = EDR_ADInBinOneSample(1, 8, bin)
uv = bin
ambient = uv * 100

'***************
   For i = 0 To 7
      If chkChan(i).value = 1 Then
  '*
         j = EDR_ADInBinOneSample(bh, i, bin)
         uv = bin
          If j < 0 Then
             ErrorBox j
             Exit Sub
          End If
  '**************
         uv = uv * 10
         v = uv

         j = EDR_CalcTCmC(tc, uv, ambient, temp)

         v = temp
```

```
        '***************
          v = v / 1000
          chanval(i) = v    'save channel temperatures

        End If

      Next i



      picLog.Cls
       For k = 0 To 7
        If chkChan(k).value = 1 Then
       'Labels and temperatures

         Select Case k
         Case 0
            picLog.ForeColor = &HFF
            picLog.Print "0 BL Feed       = " & Format$(chanval(k), "#0.000") & Chr$(9);
         Case 1
            picLog.ForeColor = &H80
            picLog.Print "1 BL Tube Cooling   = " & Format$(chanval(k), "#0.000") &
Chr$(9);
         Case 2
            picLog.ForeColor = &HFF0000
            picLog.Print "2 Steam in      = " & Format$(chanval(k), "#0.000") & Chr$(9);
         Case 3
            picLog.ForeColor = &H0
            picLog.Print "3 Reactor Top     = " & Format$(chanval(k), "#0.000") & Chr$(9);
         Case 4
            picLog.ForeColor = &HC0C0&
            picLog.Print "4 Reactor Middle = " & Format$(chanval(k), "#0.000") & Chr$(9);
         Case 5
            picLog.ForeColor = &HFFFF00
            picLog.Print "5 Reactor Hot Zone = " & Format$(chanval(k), "#0.000") &
Chr$(9);
```

```
        Case 6
            picLog.ForeColor = &HFF00FF
            picLog.Print "6 Product Gas    = " & Format$(chanval(k), "#0.000") & Chr$(9);
        Case 7
            picLog.ForeColor = &HC000&
            picLog.Print "7 LPG Flue Gas    = " & Format$(chanval(k), "#0.000") & Chr$(9);
       End Select

        c = c + 1
        If c = 2 Then
          c = 0
          picLog.Print
        End If
      End If
     Next k

'***********Graph***********

 xnew = Timer - starttime
 txnew = Format(xnew, "#####0.0")
 Write #1, txnew, chanval(0), chanval(1), chanval(2), chanval(3), chanval(4), chanval(5),
chanval(6), chanval(7) 'write to file

'****************************
  Call Draw(txnew, chanval())
'****************************

   End If
Text2.Text = Time
End Sub
```

Globals.bas

```
Option Explicit

' Global variables for adindemo

Global bh As Long     ' Our board handle
Global logging As Long  ' Logging flag
Global ready As Long  ' Ready to log flag

Sub ErrorBox(e As Long)
   ' Converts error code e to a string and
   ' displays this in a message box
   Dim s As String
   s = Space$(80)
   EDR_StrError e, s
   MsgBox s, 16, "EDR error message"
End Sub
```

By Nelson Naidoo & Vernon Avidi, University of Natal, 2001

Edr32.bas

Interface program was supplied by Eagle Technology for their PC-73C-T card.

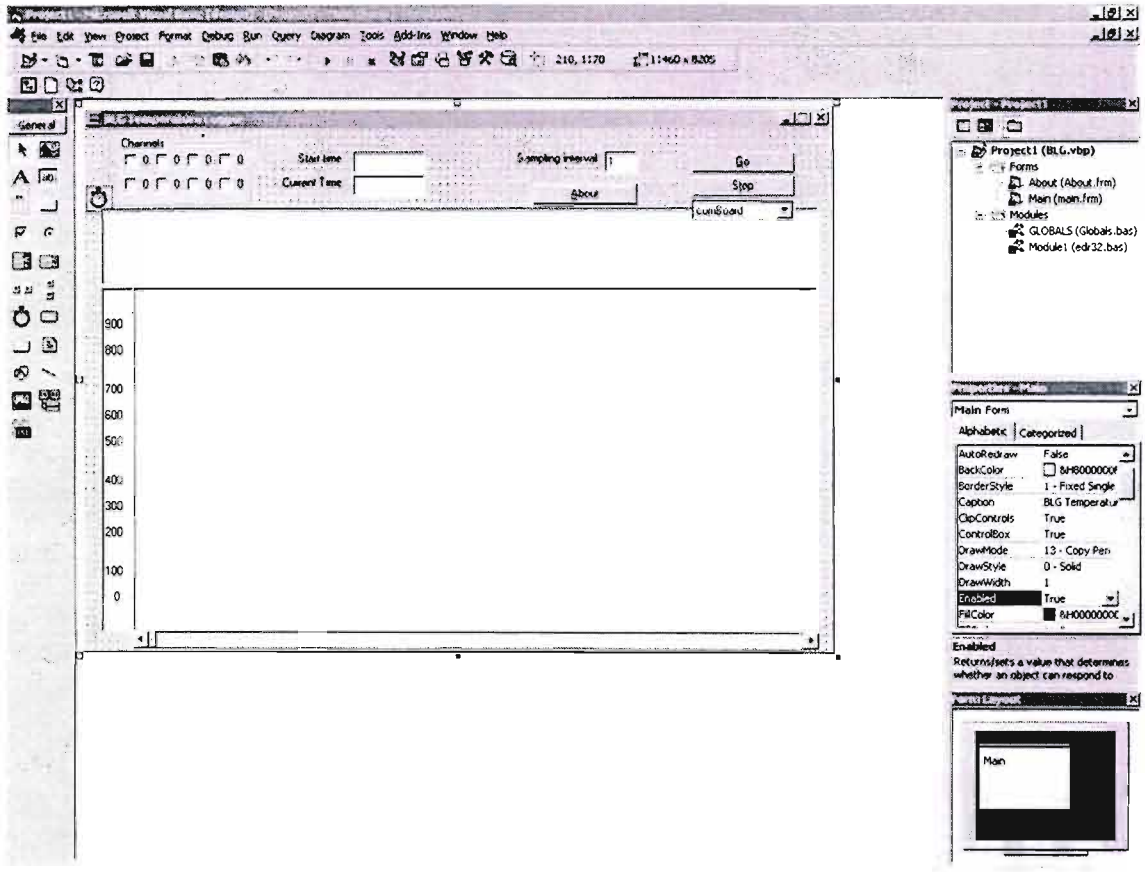
File Edit View Project Format Debug Run Query Diagram Tools Add-Ins Window Help
General
Channels
Start time
Current Time
Sampling interval
Go
Stop
About
comBoard
900
800
700
600
500
400
300
200
100
0
Project1 (BLG.vbp)
Forms
About (About.frm)
Main (main.frm)
Modules
GLOBALS (Globals.bas)
Module1 (edr32.bas)
Main Form
Alphabetic
Categorized
AutoRedraw
BackColor
BorderStyle
Caption
ClipControls
ControlBox
DrawMode
DrawStyle
DrawWidth
Enabled
FillColor
False
&H8000000F
1 - Fixed Single
BLG Temperatur
True
True
13 - Copy Pen
0 - Solid
1
True
&H00000000
Enabled
Returns/sets a value that determines whether an object can respond to
Main

APPENDIX G

APPENDIX G – DESIGN CALCULATIONS

1. Design of a Fluidised Bed Reactor

Choose Diameter = 0.254 m ie. 10" diameter pipe
For a 10" schedule 40S pipe, Stainless Steel 316L

D_i =	0.254508	m	S =	0.050873634	m^2
D_o =	0.27305	m	2 x S =	0.101747267	m^2

Design Temperature : 700 °C
Design Pressure : 1 Bar

D_i at 2 x S = 0.359928665 m
14.17041989 inch

1.1 Minimum Fluidising Velocity, u_{mf} :

Fluidising Na_2CO_3 :

d_p:

Size Range µm	Average size d_i - µm	Mass g	Mass % x_i	x_i / d_i
+425	450	60.8	14.1%	0.00031283
425/300	362.5	168	38.9%	0.001073045
300/180	240	161.4	37.4%	0.001557073
180/150	165	0.8	0.2%	1.12259E-05
150/75	112.5	38.3	8.9%	0.000788248
-75	50	2.6	0.6%	0.000120398
Total		431.9	100.0%	0.003862821

$$d_p = \frac{1}{\sum \frac{x_i}{d_i}}$$ .....Equation 1.1, Reference 2, Pg 17-4

Substituting into Equation 1.1 for d_p :

d_p = 0.000258878 m d_p/D_i = 0.001017171
0.000632119 Mondi - Piet Retief

ρ_s = 2532 kg/m^3 .....Health and Safety data sheet.
e_{mf} = 0.4
g = 9.8 m^2/s
ρ = 0.22272 kg/m^3 1 bar steam at 700°C - Reference 3, Pg 35
μ = 0.00003655 Pa.s 1 bar steam at 700°C - Reference 3, Pg 263

$$Ga = \frac{d_p^3 \rho(\rho_s - \rho)g}{\mu^2}$$ ..... Equation 1.2 - Reference 1, Pg 227

$$Re_{mf} = \frac{\rho u_{mf} d_p}{\mu^2}$$ ..... Equation 2 - Reference 1, Pg 227

Substituion into Equation 1.2 :

Ga = 71.766594

$$Ga = 150\frac{1-e_{mf}}{e_{mf}^3} Re_{mf} + \frac{1.75}{e_{mf}^3} Re_{mf}^2$$ ..... Equation 3 - Reference 1, Pg 227

$$Re'_{mf} = (1135.7 + 0.0408\ Ga)^{0.5} - 33.7$$ .....Equation 4 - Reference 2, Pg 17-4

Substitution into Equation 3 :

$$Ga = 1406.25\ Re'_{mf} + 27.34375\ Re'^{2}_{mf}$$

Solving for Re'_{mf}

Equation 3 :

$Re'_{mf} =$ 0.05098348

$u_{mf} =$ 0.032319319 m/s
$=$ 32.31931931 mm/s

Equation 4 :

$Re'_{mf} =$ 0.0435635

$u_{mf} =$ 0.0276157 m/s
$=$ 27.615658 mm/s

1.2 Steam Required at u_{mf}:

$Q_{mf} = u_{mf} \times S$ .....Equation 5

$Q_{mf,steam} =$ 0.0016442 m^3/s
$=$ 21.97179 g/min of steam
$=$ 1.3183074 kg/hr

S of 1/4" tube = 3.167E-05 m^2
u = 51.917961 m/s

1.3 Terminal Falling Velocity of Particles, u_o :

Fluidisation takes place for $u_{mf} < u < u_o$.

$$Re_o' = (2.33Ga^{0.018} - 1.53\ Ga^{-0.016})^{13.3}$$ .....Equation 6 - Reference 1, Pg 228

Substituting:

$Re_o' =$ 3.0483971
$u_o' =$ 1.9324322 m/s
$=$ 1932.4322 mm/s

1.4 Steam Required at u_o:

$Q_o =$ 0.0983098 m^3/s
$=$ 1313.7342 g/min of steam
$=$ 78.824051 kg/hr

1.4.1 Steam Baffle :

4 x 5mm holes
4 x 4mm holes
4 x 3mm holes

Diameter / m	area/m^2
0.005	1.963E-05
0.004	1.257E-05
0.003	7.069E-06

Sum = 3.927E-05
x 4 = 0.0001571 m^2

S of 1/2" tube = 0.000196037 m^2
2 x 1/2" Tube S = 0.000392074 m^2

S of 1/4" tube = 3.16692E-05 m^2
u = 3104.271507 m/s

d tube = 0.880947139
S of reqd tube = 0.000393239 m^2
u = 250.0000046 m/s
Re = 1342028.389

1.5 Heating Requirments :

1.5.1 Heat required to heat up the Steel.

$C_{p,steel}$ = 0.12 kcal/kg°C = 0.50208 kJ/kg°C .....Reference 2, Pg 2-186

$q = m \times C_p \times (\Delta T)$

Volume of steel :

D_i = 0.254508 m
D_o = 0.27305 m

Area of annulus = $\Pi/4 \times (D_o^2 - D_i^2)$ = 0.0076827 m^2

Set height of reactor = 0.8 m

Volume of steel = 0.0061462 m^3

Density of steel = 7830 kg/m^3 .....Reference 2, Pg 2-119

Mass of steel cylinder= 48.12 kg

T_o = 25 °C
T = 700 °C

q = 16309.7 kJ

To heat up in say 1 hour
= 3600 s

Power = 4.53 kW

Losses = 30%
Inlet & Outlet piping & distributer : 10%

Need **6.34** kW

1.5.2 Heat required to heat up the Bed of Na_2CO_3.

Say height of bed is 20% of length of reactor with a static voidage of 0.4

Volume of $NaCO_3$ = 0.004069891 m^3

Bulk density of bed = 1519.2 kg/m^3

Mass of bed = 6.18 kg

$C_{p,bed}$ = 28.9 kcal/kmol°C Mr Na_2CO_3 = 106 kg/kmol
= 0.2726415 kcal/kg°C
= 1.1407321 kJ/kg°C

q = 4760.856843 kJ

To heat up in say	1	hour	
=	3600	s	
Power =	1.32	kW	
Losses =	30%		
Need	**1.72**	kW	

To heat up steel and Bed = 8.06 kW

1.5.3 Heat required to heat up Steam :

Say operating on edge of particulate fluidisation , maximum steam mass flowrate = 1313.7342 g/min of steam
= 0.0218956 kg/s
= 78.824051 kg/hr

$C_{p,ave}$ of steam at 1 bar and 700 °C = 2.1575 kJ/kgK .....Reference 3, Pg 229

To heat up from saturated steam at 1 bar : T_o = 100 oC
T = 700 oC

Power = 28.343815 kJ/s
= 28.34 kW

Losses = 30%

Power required = **36.85** kW 12.55

Heat transfer surface area :

Tube Velocity : Tube size : 0.674 inches (internal) - 1/2" 10S
Area = 0.0002302 m^2

Tube size : 0.84 inches (external)
= 0.021336 m

Max Q_o =	0.0983	m^3/s		Min Q_{mf} =	0.0016	m^3/s
Per coil :						
Max Q_o =	0.0492	m^3/s		Min Q_{mf} =	0.0008	m^3/s
Max u_{tube} =	213.55	m/s		Max u_{tube} =	3.571477017	m/s

$Q=UA\Delta T$ $A = \Pi d L$
$Q = U\Pi dL\Delta T$ $L = Q/U\Pi d\Delta T$

U = 30 $W/m^2/°C$
ΔT = 1300 oC

L = 14.1 m

Heat flux in Radiation section of fired heater is 30 kW/m^2

Need 36.85 kW

Therefore area required is 1.228 m^2

or in terms of tube length 18.324 m

Total Coil length as constructed = 6.24 m due to space restrictions and uncertainties in heat fluz and heat transfer co-efficients. Will be extended if required. May mean longer start up times

1.6 Bed Properties :

Bed weight = 6.18 kg

Area of Reactor = 0.050873634 m^2

g = 9.8 m/s^2

Force of bed = 60.564 N

Pressure Required to sustain Bed = 1190.4791 N/m^2 or Pa (P = F/A)

= 1.1904791 kPa

2. Sizing of Heating Element :

Heat of Reaction = 1500 BTU/LB of BLS as supplied by SAPPI

x 2.326 to convert to kJ/kg

= 3489 kJ/kg BLS

Say black liqour is 60% solids and density = 1400 kg/m^3

Therefore 1 kg black liqour has 0.6 kg BLS and 0.4 kg water

To treat **0.00122072** kg/s of BL from T_o = 85 °C to T = 112 °C

= 3.139 L/hr

Specific heat is probably in the region of 0.6 to 0.7 cal/(gm c) at 60% solids as supplied by Sappi:

Converting to SI this is 2.5 kJ/kg.K to 2.9 kJ/kg.K

Use Cp of 2.7 kJ/kg.K

Compare C_p of Cellulose = 0.32 cal/g°C ... Perry's pg 2-186

= 1.339 kJ/kg°C

ΔH = 2676 kJ/kg - Latent heat of Vapourisation of H_2O

$Q = mCp(T - To) + m\Delta H$ = 1.396 kJ/s to heat up BL from 85 to 112°C and vapourise water.

$Q_{reaction}$ = 2.5554449 kJ/s

Q_{tot} = 3.952 kJ/s

= **4** kW

BL Flow L/hr	Energy kW
6.278	8
3.139	4
1.569	2
0.7845	1
0.39225	0.5

For a 4 kW element

Flow = 3.13915055 L/min

3. Storage Tank Heat Input :

To heat up 8 kg of BL :

T = 20 °C T_o = 85 °C

$Q = mCp(T - T_o)$ = 1415.1384 kJ

Heating time of 7.862 min for a power input of = 3.000 kW

Internal steam coil:

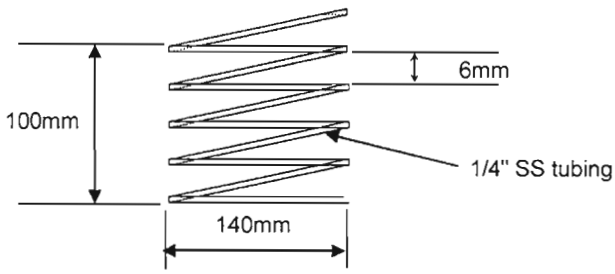

Tube Length :

diameter of tube =	6.35	mm
pitch =	6	mm
coil height =	100	mm
number of coils =	8.0972	
coil diameter =	140	mm
circumference =	439.8	mm
return length =	100	mm

Tube length = 3661.3196 mm

Area = 115951.13 mm2

= 0.1159511 m2

= 1.2480875 ft2

For steel steam coil in vegetable oil, U = 39 to 72 Btu/(h.ft^2.°F). Perrys pg 11-21

choose U = 55.5 Btu/(h.ft^2.°F)

BL starting temperature =	25	°C
BL end temperature =	100	°C
Steam Temperature =	113	°C

ΔT_{LM} = -39.21799 °C = 70.592389 oF

$Q = U \times A \times \Delta T_{LM}$ = 4889.854 BTU/hr

= 1.4318001 kW

3.1 Bed Turnover Rate

Flow of BLS = 2.6367445 kg/hr

Na_2CO_3 content = 6%

Rate of Na_2CO_3 deposited into bed = 0.1582047 kg/hr

Bed Mass = 6.00 kg

Time to replace bed = 37.93 hr!!!!

4.74 days of 8 hour operation!

4. Steam Requirements for Gasification Reactions:

$$H_2O + C \rightarrow CO + H_2$$

$$CO + H_2O \rightarrow CO_2 + H_2$$

ie. 1 mol C reacts with 2 Mols H_2O

Mass Flowrate of BLS = 2.6367445 kg/hr. This is how much the 4kW heating element can treat.
Carbon Content of BLS is about = 38% supplied by Sappi laboratories
Mass Flowrate of C = 1.00 kg/hr
Mr C = 12 kmol/kg
Molar Flowrate of C = 12.02 kmol/hr

∴ Molar flowrate of steam required for Gasification reactions is = 24.05 kmol/hr
Mr H_2O = 18 kmol/kg
Mass flowrate of Steam required = 1.34 kg/hr

Ratios for treating 60% BL :

Power		Vol/hr black Liqour		Mass/hr Steam
4	kW :	3.14	L/hr BL :	1.34 kg/hr Steam

or

1	kW :	0.79	L/hr BL :	0.34 kg/hr Steam

For 100 kg/hr steam we would need : 295.80 kW of power
and be able to treat 234.98 L/hr of BL at 60% BLS

We are limited by 8.5L/hr by the pump so all we would ever need is 10.70 kW
and 3.62 kg/hr steam
The calculations for total transport of the bed (250μm) comes out to 78kg/hr

Conclusion : Unlikely that the gasifier would require a flowrate greater than 100kg/hr steam. In the event it does, then a larger steam regulator would have to replace the current one. Should a flow greater than 50kg/hr be required then simply the float on the Metal tube flowmeter needs to be changed at a minimal cost (R200 - R300).

5. Black Liqour Tube Design

Hagen-Poiseuille Equation : $$\Delta P = \frac{32\mu u L}{D^2}$$

Black Liqour Properties :

ρ =	1400	kg/m^3
μ =	0.532	Pa.s
T =	112	°C
Q =	8.71939E-07	m^3/s
	3.139	L/hr

L = 1 m

Pipe size	Diameter/m	Area S / m^2	u / m/s	Re	ΔP / kPa
1.2mm id	0.0012	1.13097E-06	0.771	2.435	9112.966
1/8"	0.0068	3.66659E-05	0.024	0.428	8.670
1/4"	0.0092	6.71367E-05	0.013	0.316	2.586
3/8"	0.0125	0.000123155	0.007	0.233	0.769

Pipe Size 1.2mm I.d

Q / L/hr	u / m/s	Re	ΔP / kPa
2.2	0.540	1.707	6386.952
4.4	1.081	3.413	12773.905
6.6	1.621	5.120	19160.857
8.8	2.161	6.827	25547.810

Pipe Size 1/8"

Q / L/hr	u / m/s	Re	ΔP / kPa
2.2	0.017	0.300	6.077
4.4	0.033	0.599	12.154
6.6	0.050	0.899	18.230
8.8	0.067	1.199	24.307

Pipe Size 1/4"

Q / L/hr	u / m/s	Re	ΔP / kPa
2.2	0.009	0.222	1.813
4.4	0.018	0.443	3.625
6.6	0.027	0.665	5.438
8.8	0.036	0.886	7.250

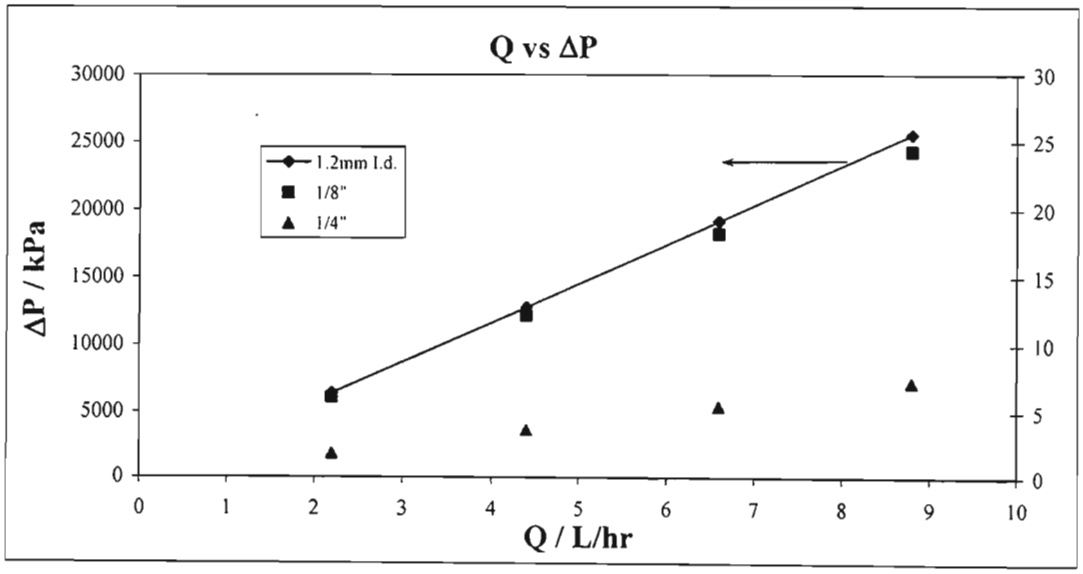

head/m	Pressure/ kPa
0.1	1.372
0.5	6.86
0.7	9.604
1	13.72

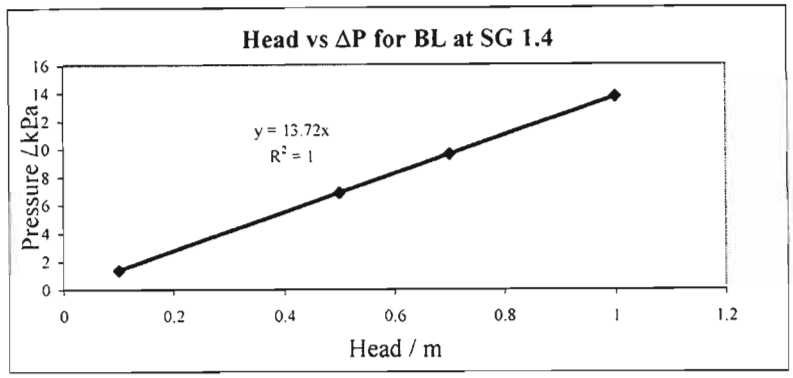

5.1 Pressure Drop across nozzle

No of holes: 3
Diameter holes = 0.001 m 1mm at first, later changed to 1.5 mm
Area per hole = 7.85398E-07 m2

Q per hole = 2.90646E-07 m3/s

u through hole = 0.37006254 m/s

DP = Kρu2/2
K for sudden exit = 1

DP = 95.86239864 Pa

For a 1/4 line and 3 hole nozzle, total pressure drop is :

Pipe Size	Q / L/hr	u / m/s	Re	ΔP_{line} / kPa	u_{nozzle} / m/s	ΔP_{nozzle} / kPa	ΔP_{Total} / kPa	ΔP_{Total} / Bar
1/4"	2.2	0.009	0.222	1.813	0.259	0.047	1.860	0.019
	4.4	0.018	0.443	3.625	0.519	188.355	191.980	1.920
	6.6	0.027	0.665	5.438	0.778	423.798	429.235	4.292
	8.8	0.036	0.886	7.250	1.037	753.418	760.668	7.607

References :

1. Coulson, J.M. and Richardson, J.F.; *Chemical Engineering Vol 2;* 4th Ed; Pergamon Press (1991), Ch 6.
2. R.H. Perry & D. Green, *Perry's Chemical Engineer's Handbook 7th Ed*, McGraw Hill Bk Company (1997), Ch 17
3. L. Haar, J.S. Gallagher, G.S. Kell; *NBS/NRC Steam Tables*; McGraw Hill Bk Company (1984)
4. Schmidt, E; *Properties of Water and Steam in SI Units*; Springer-Verlag Berlin Heidelberg New York R Oldenbourg Munich (1981)